SENSITIVITY OF FALLOUT PREDICTIONS TO INITIAL CONDITIONS AND MODEL ASSUMPTIONS

Joseph T. McGahan, et al

Science Applications, Incorporated

Prepared for:

Defense Nuclear Agency

December 1974

SECURITY CLASSIFICATION OF THIS PAGE (When Data Entered)

REPORT DOCUMENTATION PAGE	READ INSTRUCTIONS BEFORE COMPLETING FORM
1 REPORT NUMBER: DNA 3439F	2. GOVT ACCESSION NO.
	3. RECIPIENT'S CATALOG NUMBER: AD/A-002 469
4 TITLE (and Subtitle): SENSITIVITY OF FALLOUT PREDICTIONS TO INITIAL CONDITIONS AND MODEL ASSUMPTIONS	5. TYPE OF REPORT & PERIOD COVERED: Final Report 15 Nov. 1973 -15 June 1974
	6. PERFORMING ORG. REPORT NUMBER: SAI-74-548-WA
7 AUTHOR(s): Joseph T. McGahan, Edward J. Kownacki	8. CONTRACT OR GRANT NUMBER(s): DNA001-74-C-0096
9 PERFORMING ORGANIZATION NAME AND ADDRESS: Science Applications, Inc. 1651 Old Meadow Road McLean, Virginia 22101	10. PROGRAM ELEMENT, PROJECT, TASK AREA & WORK UNIT NUMBERS: NWE-D Subtask Code - W99QAXPD092. Work Unit Code 02
11. CONTROLLING OFFICE NAME AND ADDRESS: Defense Nuclear Agency Washington, D.C. 20305 (Radiation Physics Directorate)	12. REPORT DATE: December 1974
	13. NUMBER OF PAGES: 205
14 MONITORING AGENCY NAME & ADDRESS(if different from Controlling Office)	15. SECURITY CLASS. (of this report): UNCLASSIFIED
	15a. DECLASSIFICATION/DOWNGRADING SCHEDULE

16. DISTRIBUTION STATEMENT (of this Report)

Approved for public release; distribution unlimited.

17. DISTRIBUTION STATEMENT (of the abstract entered in Block 20, if different from Report)

18 SUPPLEMENTARY NOTES

19 KEY WORDS (Continue on reverse side if necessary and identify by block number)

Fallout, Dust, Neutron-Activitation, Height-of-Burst Effects, Fractionation, DELFIC, VORDUM, Crater, Soil Type

20 ABSTRACT (Continue on reverse side if necessary and identify by block number)

This report presents the results of an investigation into the effect of uncertainties in both initial conditions and model assumptions on fallout characteristics. The DELFIC code was used to provide baseline predictions. Among the specific areas considered are cloud rise, spatial distribution of dust, fractionation, dust size distribution, neutron activation, height-of-burst effects, and burst parameter uncertainties.

DD FORM 1 JAN 73 1473 EDITION OF 1 NOV 65 IS OBSOLETE

SECURITY CLASSIFICATION OF THIS PAGE (When Data Entered)

PREFACE

This report presents the results of Contract DNA001-74-C-0096 which was devoted to an analysis of the impact various types of uncertainties in models and input conditions have on fallout predictions. The program was sponsored by the Radiation Physics Directorate of the Defense Nuclear Agency whose technical representative was Captain John Phillips. The Principal Investigator was Dr. Joseph McGahan. Acknowledgements are due both to Captain Phillips for providing essential guidance and suggestions in the performance of the work and to Mr. David Rigotti and Mr. Joseph Maloney of the Ballistics Research Laboratory for their cooperation in execution of the DELFIC code.

TABLE OF CONTENTS

		Page
PREFACE		2
LIST OF FIGURES		5
LIST OF TABLES		12
Section 1	INTRODUCTION AND SUMMARY	13
1.1	Summary	14
Section 2	PROCEDURE	16
2.1	References	30
Section 3	SENSITIVITY TO BURST PARAMETERS	31
3.1	Objective	31
3.2	Baseline Calculations	31
3.3	Total Yield and Fission Fraction Sensitivity	34
3.4	Fission Type Sensitivity	50
3.5	Summary	56
3.6	References	56
Section 4	SIZE DISTRIBUTION SENSITIVITY	59
4.1	Sensitivity to Analytic Form of the Size Distribution	59
4.2	Height-of-Burst Effects on Fallout	73
4.3	References	91
Section 5	SENSITIVITY TO CLOUD MODEL ASSUMPTIONS DURING RISE	92
5.1	Nonuniform Mass Distribution	92
5.2	Sensitivity to Cloud Rise Dynamics	104
5.3	References	106

		Page
Section 6	SENSITIVITY TO ASSUMPTIONS IN THE PARTICLE ACTIVITY MODULE	112
6.1	Alternative Form of the Freiling Model	112
6.2	Comparison of Freiling Model with Simple Distributions	122
6.3	References	129
Section 7	SENSITIVITY TO UNCERTAINTIES IN INDUCED SOIL ACTIVATION	130
7.1	Comparison with Fission Activity	130
7.2	Soil Variation Effect on Induced Activity	137
7.3	Variable Water Content	141
7.4	Height-of-Burst Effects on Induced Activity	143
7.5	Size Distribution Effects on Induced Activity	147
7.6	References	150
APPENDIX A	USE OF THE STABILIZED CLOUD TAPE FROM SUBROUTINE RSXP IN THE CLOUD RISE MODULE	151
APPENDIX B	DISCREPANCIES IN THE GROUNDED PARTICLES TAPE	155
APPENDIX C	FORTRAN LISTING OF PROGRAM LINTAP	159
APPENDIX D	FORTRAN LISTING OF SIZE DISTRIBUTION CHANGE PROGRAM	201

LIST OF FIGURES

Figure		Page
2.1	Largest Particle in Main Cloud as Predicted with VORDUM	20
2.2	Schematic Representation of LINTAP Logic	26
2.3	Simplified Dose Calculation Within LINTAP	29
3.1	Normalized Dose Rate Along Angle (Deg) = 350; Yield = 30 kt	32
3.2	Integrated Dose Along Angle (Deg) = 350; Yield = 30 kt	33
3.3	Normalized Dose Rate Along Angle (Deg) = 347; Yield = 100 kt	35
3.4	Integrated Dose Along Angle (Deg) = 347; Yield = 100 kt	36
3.5	Normalized Dose Rate Along Angle (Deg) = 345; Yield = 300 kt	37
3.6	Integrated Dose Along Angle (Deg) = 345; Yield = 300 kt	38
3.7	Normalized Dose Rate Along Angle (Deg) = 345; Yield = 3 Mt	39
3.8	Integrated Dose Along Angle (Deg) = 345; Yield = 3 Mt	40
3.9	Normalized Dose Rate Along Angle (Deg) = 345; Yield = 10 Mt	41

Figure		Page
3.10	Integrated Dose Along Angle (Deg) = 345; Yield = 10 Mt	42
3.11	Maximum Hotline Extent as a Function of Yield for Two Levels of Integrated Dose (R)	43
3.12	Variations in Predicted Dose Rate Due to ± 10 Percent Uncertainties in Total Yield	44
3.13	Variation in Predicted Dose Rate Due to ± 10 Percent Uncertainties in Total Yield	46
3.14	Variations in Predicted Dose Rate Due to ± 10 Percent Uncertainties in Total Yield	47
3.15	Variations in Predicted Dose Rate Due to ± 10 Percent Uncertainties in Total Yield	48
3.16	Variations in Predicted Dose Rate Due to ± 10 Percent Uncertainties in Fusion Yield	49
3.17	Variations in Predicted Dose Rate Due to ± 10 Percent Uncertainties in Fusion Yield	51
3.18	Variations in Predicted Dose Rate Due to ± 10 Percent Uncertainties in Fission Yield	52
3.19	Variations in Predicted Dose Rate Due to ± 10 Percent Uncertainties in Fission Yield	53
3.20	Variations in Predicted Dose Rate Due to Three Fission Types for a 30 kt Device	54
3.21	Variations in Predicted Dose Rate Due to Three Fission Types for a 30 kt Device	55
3.22	Variations in Predicted Dose Rate Due to Three Fission Types for a 3 Mt Device	57

Figure		Page
3.23	Variations in Predicted Dose Rate Due to Three Fission Types for a 3 Mt Device	58
4.1	Comparison of Size Distributions	62
4.2	Schematic Representation of Generation of Hybrid Distribution	64
4.3	3 Mt Dose Rate Normalized to H+1 Hour Along "Hotline"	69
4.4	300 kt Dose Rate Normalized to H+1 Hour Along "Hotline"	71
4.5	30 kt Dose Rate Normalized to H+1 Hour Along "Hotline"	72
4.6	Schematic of Dust and Debris Sources	76
4.7	Comparison of Dust and Debris Regions for a Low Air Burst	77
4.8	Fraction of Debris Mixed with Dust (Less Than 0.025 cm) Versus HOB for 50 kt	79
4.9	Fraction of Debris Mixed with Dust (Less Than .025 cm) Versus HOB for 200 kt	80
4.10	Fraction of Debris Mixed with Dust (Less Than .025 cm) Versus HOB for 1 Mt	81
4.11	Fraction of Debris Mixed with Dust (0.5 cm) Versus HOB for 200 kt	83
4.12	Fraction of Debris Mixed with Dust (0.5 cm) Versus HOB for 1 Mt	84
4.13	Fraction of Debris Mixed with Dust (0.05 cm) Versus HOB for 50 kt	85

Figure		Page
4.14	Fraction of Debris Mixed with Dust (0.05 cm) Versus HOB for 200 kt	86
4.15	Fraction of Debris Mixed with Dust (0.05 cm) Versus HOB for 1 Mt	87
4.16	Fraction of Debris Mixed with Dust (0.1 cm) Versus HOB for 50 kt	88
4.17	Fraction of Debris Mixed with Dust (0.1 cm) Versus HOB for 200 kt	89
4.18	Fraction of Debris Mixed with Dust (0.1 cm) Versus HOB for 1 Mt	90
5.1	The VORDUM and DELFIC Clouds Compared at 848 Seconds	93
5.2	Comparison of Particle Positions Produced by VORDUM and DELFIC	95
5.3	Comparison of Particle Positions Produced by VORDUM and DELFIC	96
5.4	Comparison of Particle Positions Produced by VORDUM and DELFIC	97
5.5	Comparison of Particle Positions Produced by VORDUM and DELFIC	98
5.6	Pictorial Representation of Simplifying Assumptions	100
5.7	Comparison Between Uniform Density Wafers and VORDUM Mass Distribution Annuli Along the Cloud Hotline	101

Figure		Page
5.8	Comparison Between Uniform Density Wafers and VORDUM Mass Distribution Annuli Along the Cloud Hotline	102
5.9	Comparison Between Uniform Density Wafers and VORDUM Mass Distribution Annuli Along the Cloud Hotline	103
5.10	Comparison of Modified VORDUM Cloud with Standard VORDUM Cloud for W = 300 kt, at T = 4.75 Minutes	105
5.11	Comparison of Rise Parameters for 30 kt	107
5.12	Comparisons of Predicted Dose Rate on Cloud "Hotline" Normalized to H+1 Hour for a 30 kt Burst	108
5.13	Comparison of Rise Parameters for 300 kt	109
5.14	Comparisons of Predicted Dose Rate on Cloud "Hotline" Normalized to H+1 Hour for a 300 kt Burst	110
5.15	Comparisons of Predicted Dose Rate on Cloud "Hotline" Normalized to H+1 Hour for a 3 Mt Burst	111
6.1	Comparison of Activity Versus Size for Alternative Forms of Freiling Model	114
6.2	Comparison of Alternative Freiling Model Forms for 3 Mt Hotline Dose — Short Range	115
6.3	Comparison of Alternative Freiling Model Forms for 3 Mt Hotline Dose — Intermediate Range	116
6.4	Comparison of Alternative Freiling Model Forms for 30 kt Hotline Dose — Short Range	118

Figure		Page
6.5	Comparison of Alternative Freiling Model Forms for 30 kt Hotline Dose — Intermediate Range	119
6.6	Sensitivity of Hotline Integrated Dose to Crossover of Specific Activity (From Radial to Constant) for 3 Mt — Short Range	120
6.7	Sensitivity of Hotline Integrated Dose to Crossover of Specific Activity (From Radial to Constant) for 3 Mt — Intermediate Range	121
6.8	Sensitivity of Hotline Integrated Dose to Crossover of Specific Activity (From Radial to Constant) for 30 kt — Short Range	123
6.9	Sensitivity of Hotline Integrated Dose to Crossover of Specific Activity (From Radial to Constant) for 30 kt — Intermediate Range	124
6.10	Comparison of Freiling Model with Assumptions of Volatile and Refractory Radial Components for 3 Mt Hotline Dose — Short Range	125
6.11	Comparison of Freiling Model with Assumptions of Volatile and Refractory Radial Components for 3 Mt Hotline Dose — Intermediate Range	126
6.12	Comparison of Freiling Model with Assumptions of Volatile and Refractory Radial Components for 30 kt Hotline Dose — Short Range	127
6.13	Comparison of Freiling Model with Assumptions of Volatile and Refractory Radial Components for 30 kt Hotline Dose — Intermediate Range	128

Figure		Page
7.1	Schematic of Zones Used in Monte Carlo Calculations of Neutron Capture in Soil	132
7.2	Comparison of Fission and Neutron — Induced Soil Activity.	136
7.3	Soil Variation of Induced Activity	140
7.4	Dependence of Induced Activation in Soil of Water Content	144
7.5	HOB Correction Factor for Induced Activity . .	146
7.6	Comparison of Alternative Fractionation Assumptions for Induced Activity at Close-In Ranges	148
7.7	Comparison of Alternative Fractionation Assumptions for Induced Activity at Intermediate Ranges	149

LIST OF TABLES

Table		Page
2.1	Invariant DELFIC Input Parameters	17
2.2	Variant DELFIC Input Parameters	18
2.3	Inputs to LINTAP	23
2.4	Available Computation Codes	25
2.5	Integrated Dose Calculation Comparison	30
4.1	3 Mt Mass Fractions	65
4.2	300 kt Mass Fractions	66
4.3	30 kt Mass Fractions	67
7.1	Fraction of Neutrons Captured	131
7.2	Fraction of Neutrons Captured Within Apparent Crater	133
7.3	Fraction of Neutrons Activating the Soil Burden of the Stabilized Cloud	134
7.4	Weight Fractions for Representative Soils	138
7.5	Atomic Fractions for Representative Soils	139
A.1	Printout Explanation	151
A.2	RSXP Debug Printout for 3 Mt	153
B.1	Wind Field Data	155
B.2	Section of 3 Mt Tape IPOUT	156
B.3	Section of 3 Mt Tape IPOUT	157

Section 1

INTRODUCTION AND SUMMARY

The accurate prediction of the fallout hazard that results from a subsurface, surface, or low air burst is perhaps one of the most complex tasks that has faced military analysts. It encompasses many fields of technology ranging from radio-chemistry and thermodynamics to meteorology both micro-scale and synoptic. However, the mere fact that a component of the problem is difficult to understand and model does not necessarily mean that progression from a simple algorithm to a sophisticated computation changes the ultimate answer significantly. Hence, there is a continuing need for sensitivity analyses to indicate both how accurate a present code is and perhaps what might be important areas in need of improvement.

This report presents the results of a study on the sensitivity of fallout predictions to uncertainties associated first with the burst parameters (Section 3) and secondly with assumptions and models contained in the overall prediction. The basis for the study was the calculation of the DELFIC code (Department of Defense Land Fallout Prediction System). As will be discussed in Section 2, the Ballistics Research Laboratory made a series of runs with DELFIC. Science Applications, Inc., (SAI) with partial modifications, exercised the Particle Activity and Output Processor Modules.

In addition to uncertainties in burst parameters, several other areas were investigated. The first of these is the size distribution (Section 4) of the entrained dust for which different types of

distributions were analyzed. The effect of variations in heights of burst is also discussed. Section 5 deals with several aspects of the rise phase including time-dependent cloud dimensions and the internal distribution of dust. Section 6 is devoted to the Particle Activity Module with emphasis on fractionation. Finally, Section 7 reports on analysis of neutron-induced soil activation which may be significant under certain circumstances. The various appendices deal with several problems and inconsistencies found in DELFIC and provide a listing of a modified output processor.

1.1 SUMMARY

This section presents some important conclusions of the study.

a. Variations in the analytic form of the size distribution can result in changes in close-in dose of a factor of 20 and a factor of 5 for long-range dose levels (Section 4.1).

b. Present HOB algorithms overestimate dose levels close-in particularly for low yields (Section 4.2).

c. DELFIC predicts a larger and less dense cloud than does the analytic flow field model, VORDUM, and does not loft particles greater than 1 cm (at 300 kt). This plus the differences in the spatial distribution of the dust between VORDUM and DELFIC result in a discrepancy in the predicted dose of approximately a factor of 2 and in the predicted time of arrival of about 15 minutes (Section 5.1).

d. The differences in rise parameters between DELFIC and VORDUM (with semi-empirical equations) result in slightly under an order-of-magnitude discrepancy in the predicted dose rate for the 30 kt case. At higher yields, there is better agreement (Section 5.2).

e. An alternative formalism of the Freiling fractionation model changes the dose by about 50 percent (Section 6.1).

f. Assuming the debris to be purely refractory for all mass chains satisfactorily reproduces the more complex Freiling model, at least for a power law size distribution (Section 6.2).

g. The neutron energy spectra is an important parameter in determining the fraction of neutrons captured in crater material that is later entrained into the cloud (Section 7.1). The neutrons above 4 Mev are twice as efficient in contributing to the total activity of entrained dust as those below 4 Mev (Section 7.1).

h. A factor of 5 variation was noted in the induced activity between the various soil types examined (Section 7.2).

i. DELFIC overestimates the contribution of induced activity for heights of burst greater than a few feet (scaled to 1 kt) (Section 7.4).

j. DELFIC assumes the activated soil to be refractory in the fractionation scheme. If one assumes, with some justification, that it is volatile then for the burst configuration examined, the result is an order-of-magnitude decrease in the very close-in dose levels due to the activated soil component of the fallout (Section 7.5).

Section 2
PROCEDURE

The basic DELFIC runs were performed at the Ballistic Research Laboratories (BRL) and material in the form of data tapes and output were sent to SAI for further computation and analysis. A total of ten yields was included. These were 30 kt, 100 kt, 270 kt, 300 kt, 330 kt, 1 Mt, 2.7 Mt, 3 Mt, 3.3 Mt, and 10 Mt. The topographical and wind-field data were identical for all runs; the only input differences were yield-dependent parameters. Additionally, the 300 kt run was executed using the horizontal subdivision option in the cloud rise module; all other runs were performed with no horizontal cloud subdividing. Table 2.1 contains the invariant input parameters for all runs, while Table 2.2 contains the variant parameters.

A complete input deck for DELFIC contains many more parameters, some involving machine-related variables such as number of tape drives available, and others being standard variables such as atmospheric profiles. Since DELFIC is a growing program in the sense that its various modules are being continuously updated, no readily available operator's manual exists. The personnel at BRL, on consultation with SAI, provided the necessary input variables not listed in the following tables.

A critical input parameter is the specification of particle size distribution. Traditionally, users of DELFIC have assumed a log-normal distribution. However, as will be discussed in Section 4,

Table 2.1. Invariant DELFIC Input Parameters

Number of Particle Size Classes	40
Type of Size Distribution	$a^{-3.5}$ (power law)
Soil Specific Gravity	2.5
Soil Solidification Temperature	1673 ^{o}K
Height of Burst	0.0
Type of Atmosphere	Standard U.S. -45^{o} N July
Time Range of Interest	0 - 48 Hr
Type of Topography	Planar at MSL
Fission Type	U235 HE
Capture to Fission Ratio	0.0
Ground Roughness Factor	.5
Wind Hodograph Extending Over Complete Range of Interest	Winds for 60N - 20E Winter

Vector Altitude, ZV(J) (m)	VX(J) (m/sec)	VY(J) (m/sec)
0.00000	4.55700+00	-8.19000-01
3.04800+03	4.55700+00	-8.19000-01
6.09600+03	6.75800+00	-2.45800+00
9.14400+03	1.00860+01	-1.79200+00
1.21920+04	1.20320+01	-4.40300+00
1.52400+04	1.20320+01	-4.40300+00
1.82880+04	1.51040+01	-2.66200+00
2.13360+04	1.74080+01	-3.12300+00
2.43840+04	2.04800+01	0.00000
2.74320+04	2.30400+01	0.00000
3.04800+04	2.56000+01	0.00000

Table 2.2. Variant DELFIC Input Parameters

Yield (kt)	CAY	FW (kt)	KDI	EMITN	IRAD
30	7.26×10^{7}	30	30	1.5	0
100	2.11×10^{8}	100	30	1.5	0
270	5.29×10^{8}	270	40	1.5	0
300	5.29×10^{8}	300	40	1.5	3
330	5.29×10^{8}	330	40	1.5	0
1000	1.61×10^{9}	500	40	4.5	0
2700	4.25×10^{9}	1350	50	4.5	0
3000	4.25×10^{9}	1500	50	4.5	0
3300	4.25×10^{9}	1650	50	4.5	0
10000	1.23×10^{10}	5000	50	4.5	0

CAY = Mass Normalization Factor

FW = Fission Yield

KDI = Number of Wafers in Cloud Rise Module Per Size Class

EMITN = Number of Neutrons Per Fission

IRAD = Horizontal Wafer Subdivision Factor

there is conclusive evidence that the distribution for particles with diameters above a few hundred microns obeys a power law. Consequently, the base-line calculations generated by BRL, were performed with the distribution on particle size of the following form:

$$\frac{dn}{da} \propto a^{-3.5}$$

where a is diameter and dn/da is the number of particles per unit diameter. The normalization to the total mass burden, M, of the cloud is made through the input variable CAY as follows:

$$M = CAY \int_0^{10^4 \mu} \frac{\pi}{6} \rho \, a^3 \left(\frac{dn}{da}\right) da \; W$$

where ρ is the bulk density of the soil and the particles are assumed to be spherical. The limits on the integration were taken to be 0 and $10^4 \mu$. The total mass is expressed in grams. Table 2.2 lists the values of CAY for the various yields.

The first case exercised was for a yield of 300 kt. It was found that the DELFIC formalism for gravitational settling was invalid for particles greater than 1 cm. For yields in the kiloton and megaton range, particles of this size and larger are expected to be entrained. Using the VORDUM code[1], which describes the velocity field in and around the rising fireball, Figure 2.1 was generated for the largest particle entrained versus yield (for surface bursts only). DELFIC (in the RSXP subroutine) makes use of an approximate expression developed by Davies[2] for the drag coefficient as a function of Reynold's number that does not apply to large particles (greater than 1 cm). Because of this, the value of CAY for all subsequent runs was chosen so that the upper limit on particle size was 1 cm.

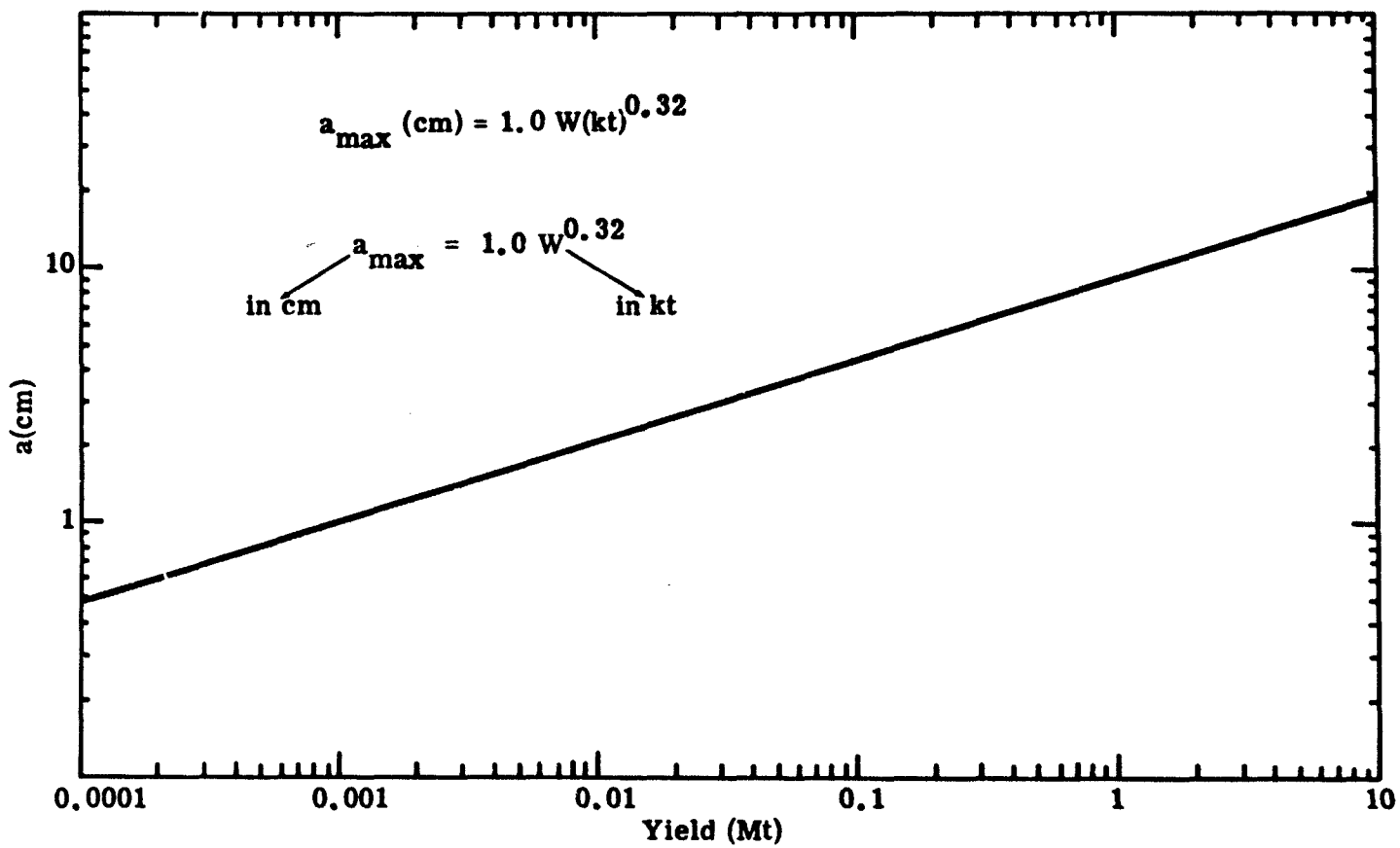

Figure 2.1. Largest Particle in Main Cloud as Predicted with VORDUM

The data sent to SAI for analysis and further computation were in the form of magnetic tapes and computer printouts. The data on the tapes were the stabilized cloud description from the Cloud Rise Module (option KRX = 1), and the grounded particles tape (tape IPOUT). Initially, tape difficulties due to machine inconsistencies arose, but all the necessary data were finally transmitted.

Additionally, a tape containing card images of the complete DELFIC code was brought to SAI. BRL uses a UNIVAC 1108, while SAI has access to a CDC 6400, so the DELFIC code had to be modified to take into account the different FORTRAN compilers. The Output Processor Module, with the associated PAM routines, was successfully run at SAI using the appropriate grounded particle tapes. The output produced was identical to that supplied by BRL, so the transfer of the Output Processor was successful.

The computer printout was also used to identify an appropriate "hotline" for the wind field used. It appeared that this "hotline" occurred along a line 345° to the positive x-axis for the larger yields. A line of 350° was used for the 30 kt case, and a line of 347° was used for the 100 kt case.

The form of the standard DELFIC output, a rectangular map, was inappropriate for purposes of a sensitivity study along the hotline and along lines parallel to the hotline but removed from ground zero by a stabilized cloud radius. For this reason, a program was written to produce the desired output along any specified line. This program is called LINTAP, and a listing of it appears in Appendix C. LINTAP uses all the associated PAM subroutines, as well as subroutine GETSET from the Output Processor. The functions that were performed by the rest of the Output Processor

are performed in subroutine LINOUT. The inputs to LINTAP are the grounded particles tape (IPOUT), as well as the inputs to the PAM module and a modified version of the inputs to the standard Output Processor. Table 2.3 is an explanation of the inputs to LINTAP, while Table 2.4 is an explanation of the various requests (variable NREQ). It was desired to keep modifications of the Output Processor to a minimum, which is the reason for the similarity of the input deck structures. The output of LINTAP is a tape suitable for input to a CALCOMP program, if requested (LDIS $\neq$ 0), and/or the values of any of the 16 quantities along the specified line. If a tape is requested, the information is written on Tape 4.

The logic of LINTAP is as follows. The grounded particles tape contains the X and Y coordinates of the center of the wafer when it hits the ground, as well as the particle diameter associated with the wafer, the time of impact, the mass per unit area, and a number (IRBZ) from which the radius of the wafer can be calculated. The standard Output Processor assumes rectangular wafers, where the Cloud Rise Module assumes cylindrical wafers. This is handled within the Output Processor by adjusting the wafer radii to conserve area (hence mass). In the standard Output Processor, a value of 886 for the variable IRBZ corresponds to a wafer which is as wide as the visible cloud. This value of 886 corresponds to $(\pi/4)^2$ x 1000, the diameter correction factor between circles and squares containing the same area. LINTAP assumes the wafers are cylinders, and the associated IRBZs are adjusted accordingly.

Figure 2.2 illustrates the actual program logic. The specification of XMIN, YMIN, ALPHA, RANMAX, and DGX totally specifies the line and points 1 through 24 on the line. The program then checks each wafer for intersection points. Wafer #1 does not

Table 2.3. Inputs to LINTAP

Tapes: Tape 3 = IPOUT		
Card	Description	Format
1	Run Identifier	12A6
2	Blank	
3*	IC(I), I = 1, 18	18I4
	IC(17) > 0 Stops after printing IPOUT	
	IC(17) = 0 Proceed with job	
	IC(18) > 0 Print IPOUT	
	IC(18) = 0 Do not print IPOUT	
4	DIFCON	F10.3
5	IH, IV	18I4
6	Run Identifier	12A6
7	Blank	
8	Blank	
9*	CAPFIS, EMITN	2F10.3
10*	FISSID	A6
11	LLL, LDIS	2I4
	LLL = No. of lines desired	
	LDIS > 0 Write tape, print output	
	LDIS = 0 Do not write tape, print output	
	LDIS < 0 Write tape, do not print output	

(Continued)

Table 2.3. Inputs to LINTAP (Continued)

Tapes: Tape 3 = IPOUT		
Card	Description	Format
12✱	XMIN, YMIN, ALPHA, RANMAX, DGX, GRUFF XMIN, YMIN = Starting point of line (m) ALPHA = Angle of line to horizontal (^{o}) RANMAX = Maximum range desired (m) DGX = Increment along line (m) GRUFF* = Ground roughness factor	6F10.4
13✱	KKK1 KKK1 = Number of output requests per line	I4
14✱+	NREQ, T1, T2, MASCHN	I4, 2F10.3, I4

NOTE: Cards 1 through 10 are identical to the cards required for the standard Output Processor.

* Signifies input in the first ten cards that is still utilized in LINTAP.

✱ Signifies cards within a loop defined by LLL, i.e., LINTAP requires LLL sets of these cards.

\+ Signifies cards within a loop defined by KKK1, i.e., LINTAP requires KKK1 cards I4.

Table 2.4. Available Computation Codes

Computation Code NREQ	Computation Type Description
1	Count of wafers covering each output point
2	Exposure rate normalized to time H + 1 hour
3	Exposure rate at time H + T1 hours
4	Integrated exposure, H + T1 to infinity accounting for time of arrival
5	Integrated exposure, H + T1 to H + T2 accounting for time of arrival
6	Total mass deposited
7	Total mass deposited from time H + T1 to H + T2
8	Integrated exposure, H + T1 to H + T2 assuming all particles have arrived by H + T1 hours
9	Same as 8 integrated to infinity
10	Concentration of an individual mass chain (curies/m^2)
11	Time of arrival of first fallout particle
12	Time of deposit of last fallout particle
13	Smallest particle size deposited
14	Largest particle size deposited
15	Mass from particles in size range T1 to T2
16	H + 1 hour "normalized" exposure rate resulting from particles in size range T1 to T2 microns

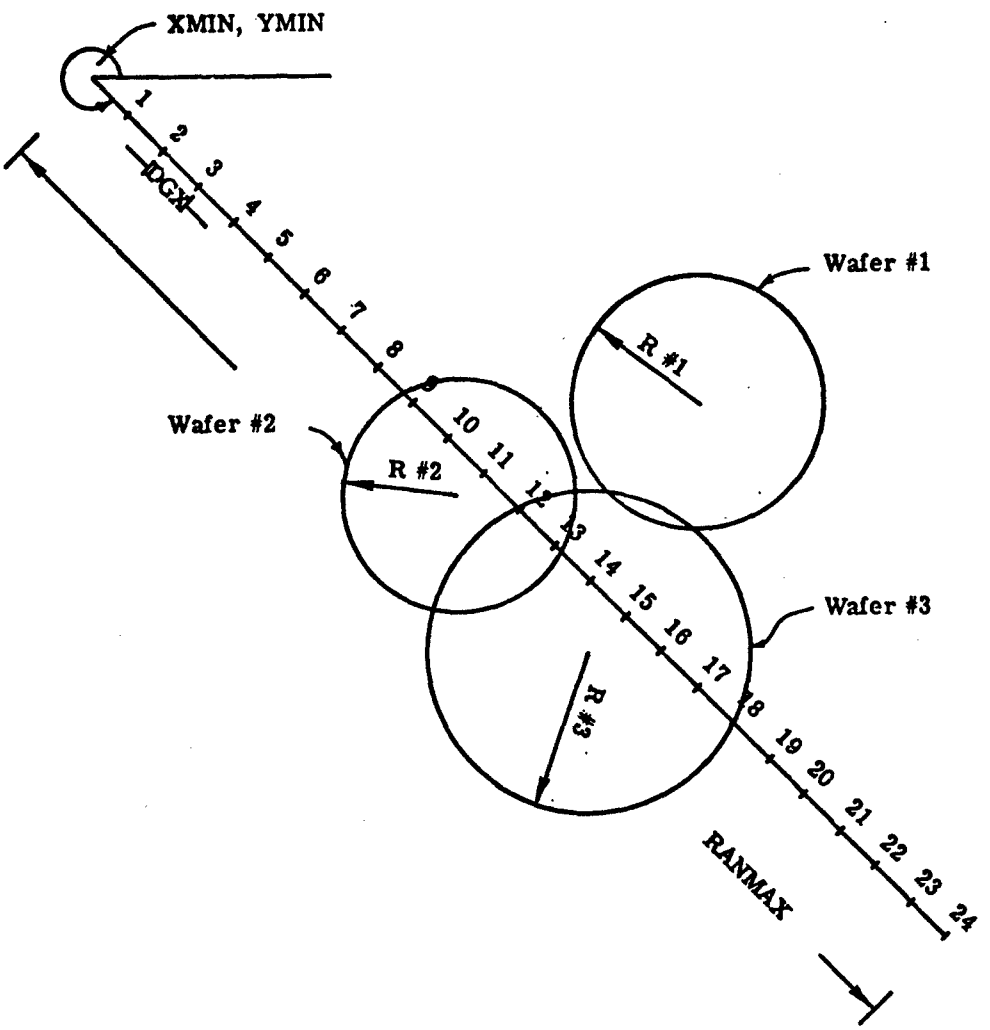

Figure 2.2 Schematic Representation of LINTAP Logic

intersect and is ignored while wafers #2 and #3 do intersect. Following the output processor logic, points 9 through 13 are incremented equally according to the mass (or time, etc.) associated with wafer #2, and points 12 through 18 are incremented equally according to the mass associated with wafer #3. This process is continued until all wafers have been tested, and the results, values at points 1 through 24, are then printed. If another request exists, the program rewinds the grounded particles tape and starts again.

The results from program LINTAP were compared with the maps produced by the Output Processor, and although a direct one-to-one comparison is not possible (because of the above-mentioned squares-circles logic), the differences are insignificant. LINTAP was used in all the sensitivity analyses.

When integrated dose (NREQ = 4 or 5) is requested of the Output Processor, the run almost always requires astronomical amounts of time. For example, a grounded particles tape of 34 particles needs 118 sec of CDC 6400 executive time. Most of the tapes used in this study contained approximately 2000 particles, so a faster method of calculation was developed for LINTAP. This long time is needed for integrated dose rates because each particle requires a call to PAM2 and its associated routines, while for all other requests, PAM2 is called once, if at all, and the data stored in array FP are used for all particles. In effect, the integrated doses are the only time-of-impact dependent requests. A modification to the Output Processor logic was made within LINTAP to increase the speed of execution of integrated dose requests, with little loss of accuracy.

PAM2 calculates the integrated dose for all particle sizes from time T1 to time T2 (either infinity or a specific value depending on NREQ = 4 or 5), and stores this information in array FP. The Output Processor sets T1 equal to the time of impact of the specific particle, calculates the integrated doses for all particle sizes, and then just uses the one value for the specific particle size. LINTAP calculates the integrated doses for all particle sizes at a number of specific times, and saves these values in array FCAN. The time of impact is then used as the parameter to interpolate between the various times without having to resort to PAM2. Figure 2.3 is a simplified sketch showing this process.

The times, in hours, at which the dose is calculated are 0, 0.25, 0.5, 0.75, 1, 2, 4, 6, etc., in two-hour increments until time of cessation or time requested (NREQ = 5) is reached. These times were chosen on the basis of the experimental evidence which showed that the dose from early fallout followed a $T^{-1.2}$ dependence, and from actual LINTAP development runs which showed that better than two-hour resolutions were needed for early times. Also, on the basis of the above-mentioned power-law dependence, the interpolation is done as a log-log procedure.

This process was checked using the 3 Mt grounded particles tape. Using the output received from BRL, regions of the map were identified which contained very few particles. A version of LINTAP was used which calculated the integrated dose from time of arrival to 48 hours after burst (NREQ = 5) according to the Output Processor procedure. The dose from these regions was also calculated using the above procedure. Table 2.5 summarizes the results of these comparisons. It can be seen that the doses are predicted by the Output

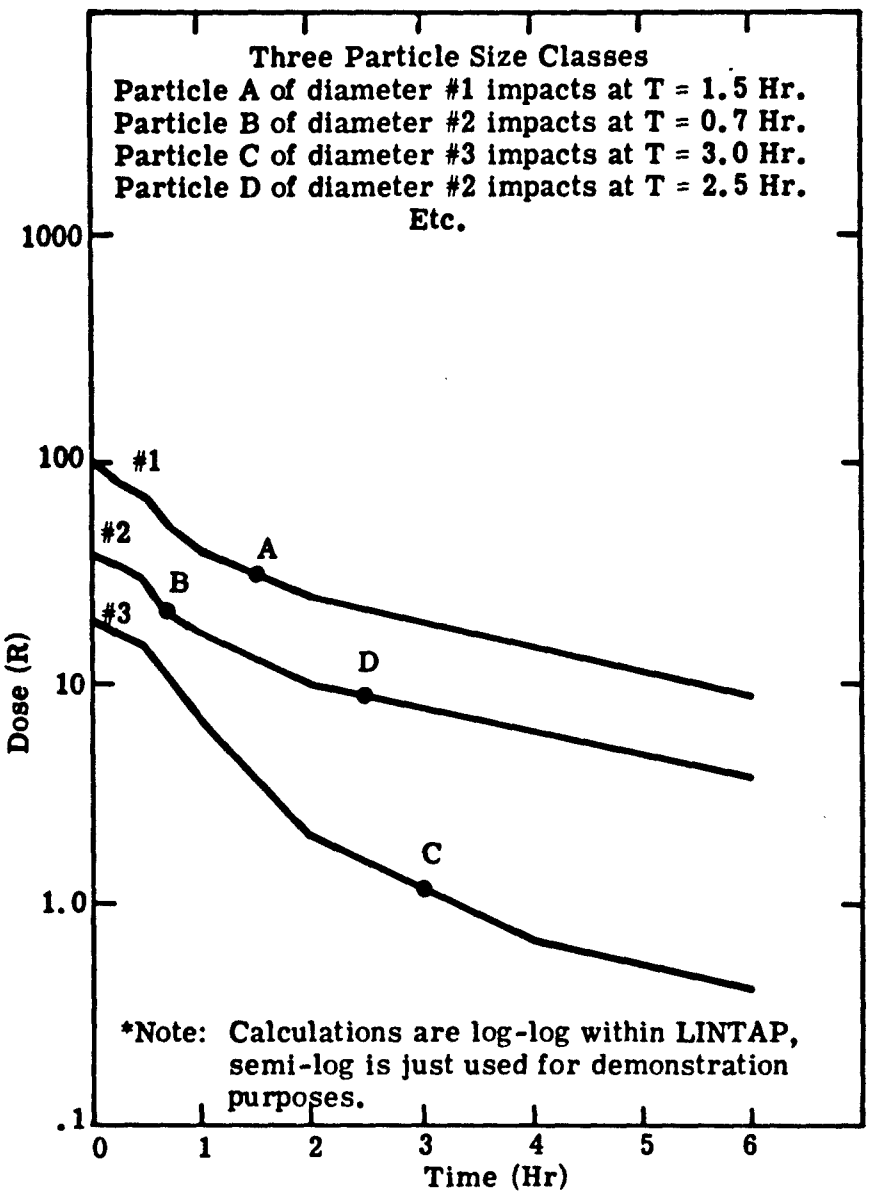

Figure 2.3. Simplified Dose Calculation Within LINTAP

Processor over a wide range of impact times. Further comparisons were not made because of the cost involved with generating the "standard" doses.

Table 2.5. Integrated Dose Calculation Comparison

Number of Particles	Time of Impact (Sec)	Standard Dose (R)	LINTAP Dose (R)
1	66970	.28625186	.28552985
2	2382 - 3689	5.53905285	5.524743

2.1 REFERENCES

1. J. A. Shannon, Science Applications, Inc., McLean, Virginia, Private communications, 1974.

2. Green and Lane, "Particulate Clouds: Dust, Smokes and Mists," 1964.

Section 3
SENSITIVITY TO BURST PARAMETERS

3.1 OBJECTIVE

Even in the most elaborately fielded nuclear test, there is some uncertainty in the total yield estimate, as well as the total fission and fusion yields. In an operational situation, these uncertainties in total yield, fission yield, and also fission type could be greatly magnified. This section investigates the effects of these uncertainties on the predicted fallout.

3.2 BASELINE CALCULATIONS

The dose rate and total dose for five yields spanning the range 30 kt to 10 Mt were determined along the downwind radial from ground zero, (the "hotline"), and along two lines parallel to the hotline but displaced from it by the visible cloud radius at stabilization. The five yields were 30 kt, 100 kt, 300 kt, 3 Mt, and 10 Mt.

Figures 3.1 and 3.2 are the dose rate normalized to H+1 hr and the total integrated dose 48 hours after burst, respectively, for the 30 kt device along the three lines. In these and subsequent figures in this subsection, the solid line corresponds to the hotline output, the "+'s" correspond to the parallel line displaced to the left of the hotline by the cloud radius at stabilization, and the "x's" correspond to the line one stabilized cloud radius to the right of the hotline. The run parameters listed in the preceding section were used for all the yields considered. (Note: The irregularity associated with all the

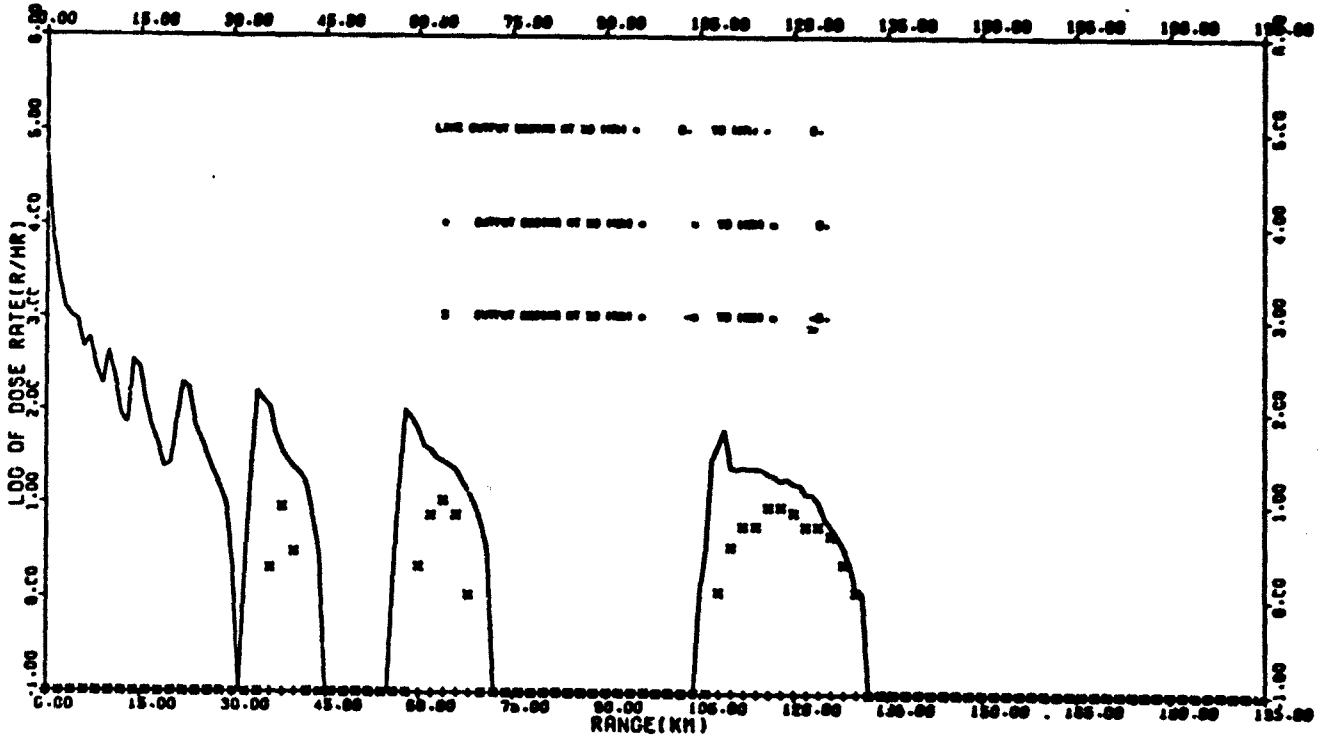

Figure 3.1. Normalized Dose Rate Along Angle (Deg) = 350; Yield = 30 kt

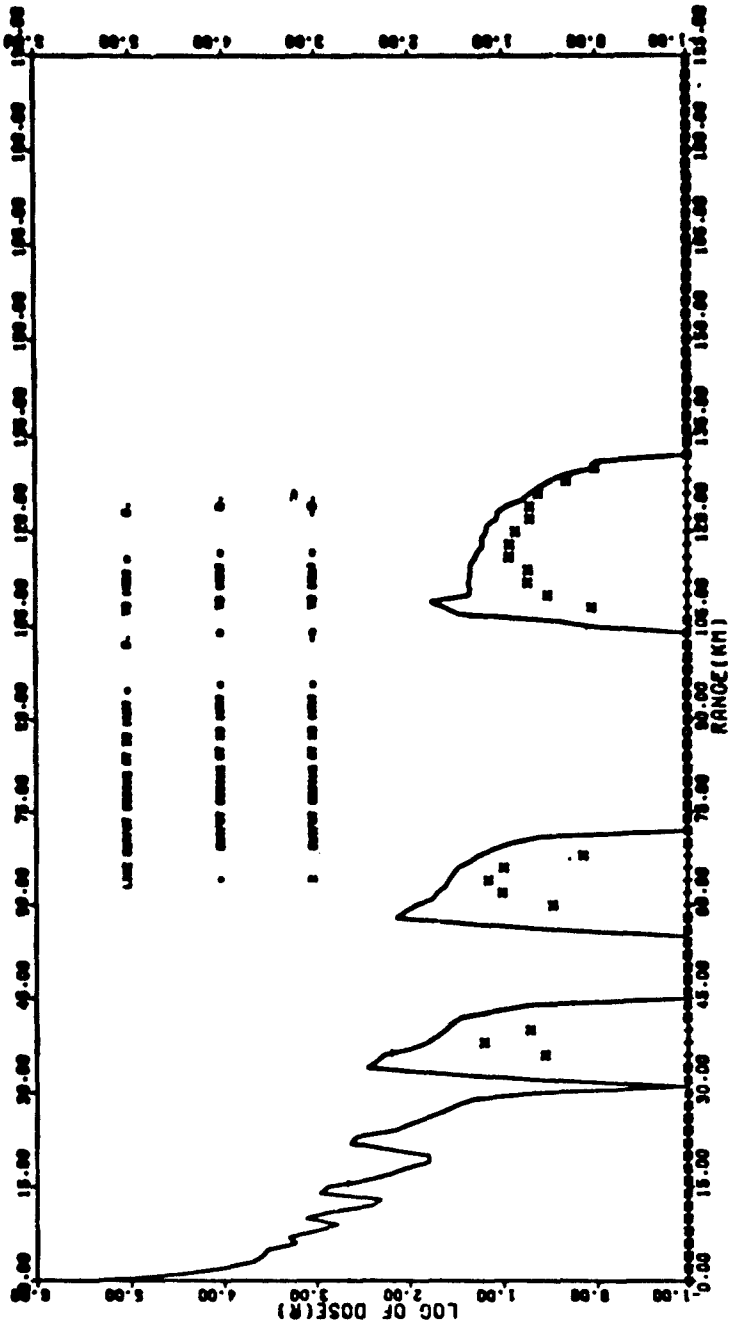

Figure 3.2. Integrated Dose Along Angle (Deg) = 350; Yield = 30 kt

LINTAP output is due to the division of the cloud into a finite number of wafers.)

Figures 3.3 and 3.4 are the dose rate and total integrated dose 48 hours after burst, respectively, for the 100 kt device along the three lines. Similarly, Figures 3.5 and 3.6 present the same information for 300 kt, while Figures 3.7 and 3.8 correspond to 3 Mt and Figures 3.9 and 3.10 correspond to 10 Mt.

As expected, the above figures show that the downwind projection of the cloud outline, the cloud "shadow," is the only area that need be considered. Figure 3.11 is a plot of the maximum downwind extent of two dose levels 48 hours after burst as a function of yield. The dose levels considered are 150 R (the mid-burdening dose), and 450R (the mid-lethal dose). For these two levels, at least, the maximum downwind extent is not a linear function of yield, which means, for example, that doubling the total yield will not double the downwind extent of these levels. Rather the range for either dose level is proportional to W^P where W is the yield and P is approximately 0.22.

3.3 TOTAL YIELD AND FISSION FRACTION SENSITIVITY

This subsection investigates the fallout variations due to uncertainties in the total yield and fission yield on the order of ±10 percent which are the approximate variations that could be expected when the designed yield of the device is known. The two specific yields investigated were 300 kt and 3 Mt.

The first effect studied was total yield sensitivity. Figure 3.12 is a plot of dose rate along the hotline normalized to

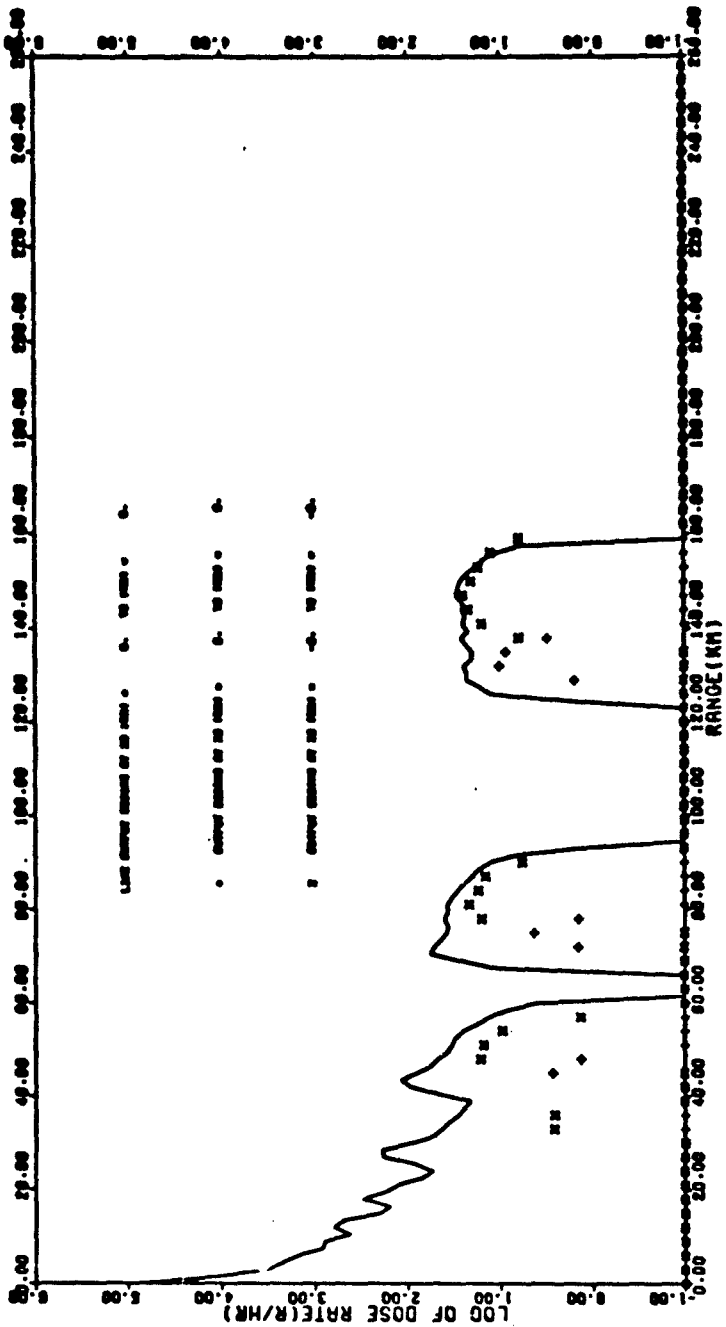

Figure 3.3. Normalized Dose Rate Along Angle (Deg) = 347; Yield = 100 kt

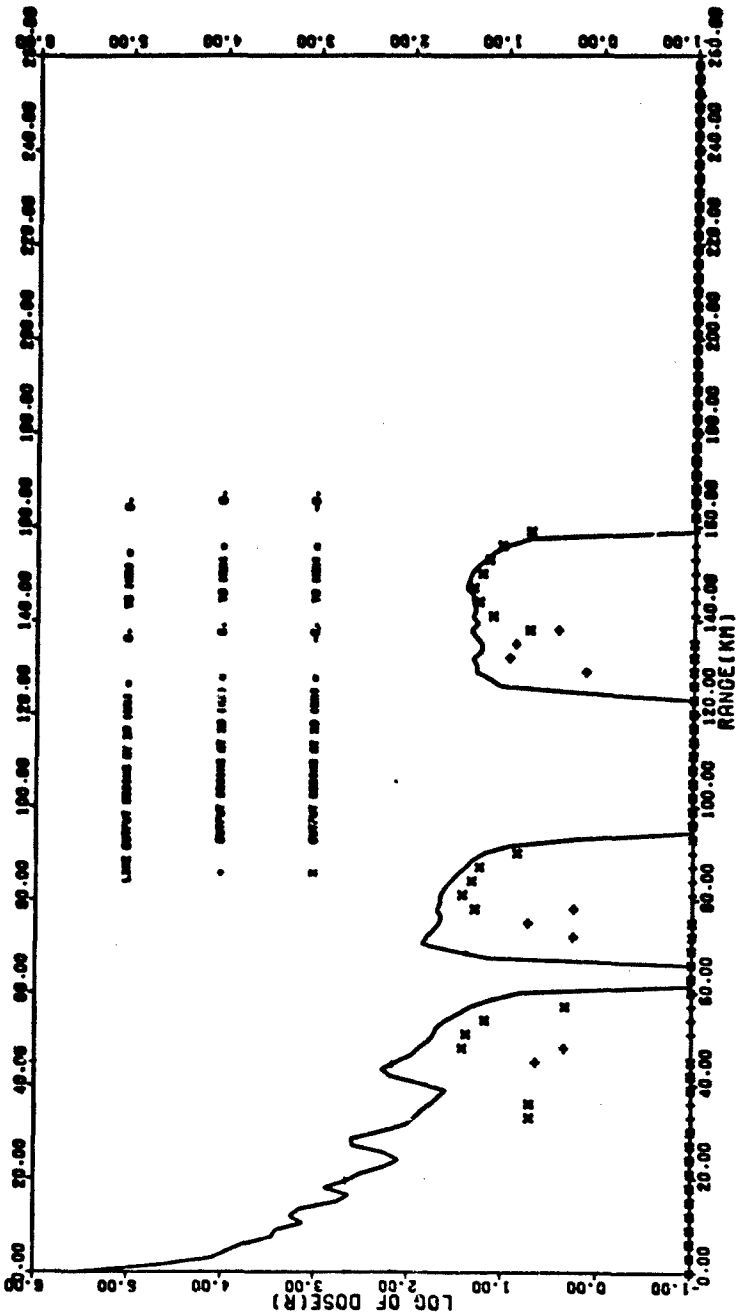

Figure 3.4. Integrated Dose Along Angle (Deg) = 347; Yield = 100 kt

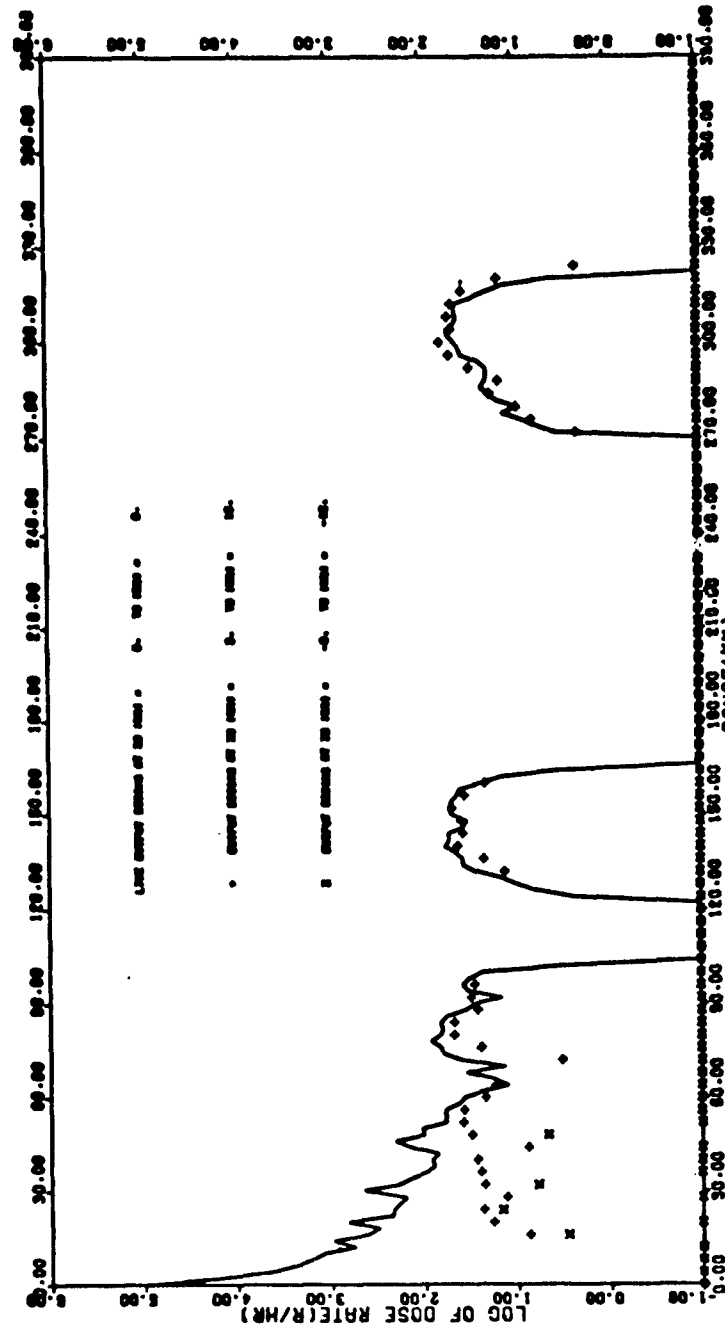

Figure 3.5. Normalized Dose Rate Along Angle (Deg) = 345; Yield = 300 kt

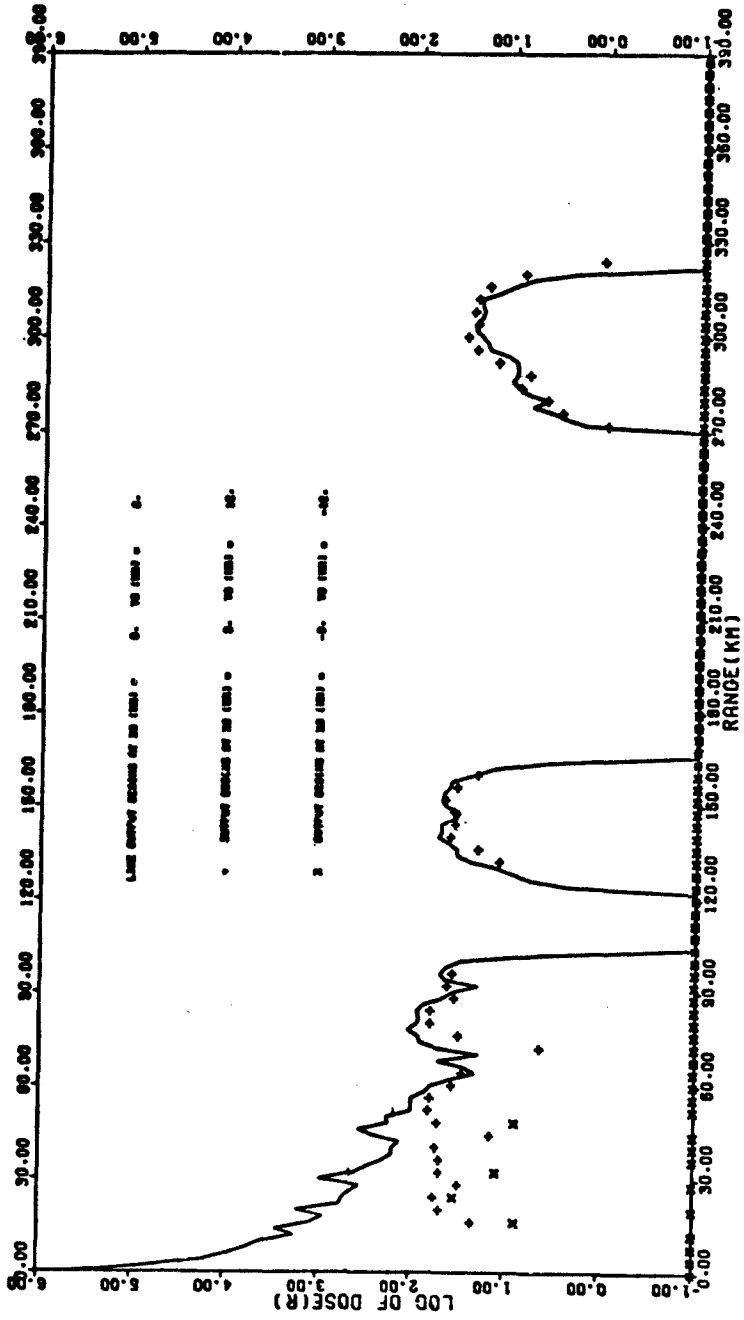

Figure 3.6. Integrated Dose Along Angle (Deg) = 345; Yield = 300 kt

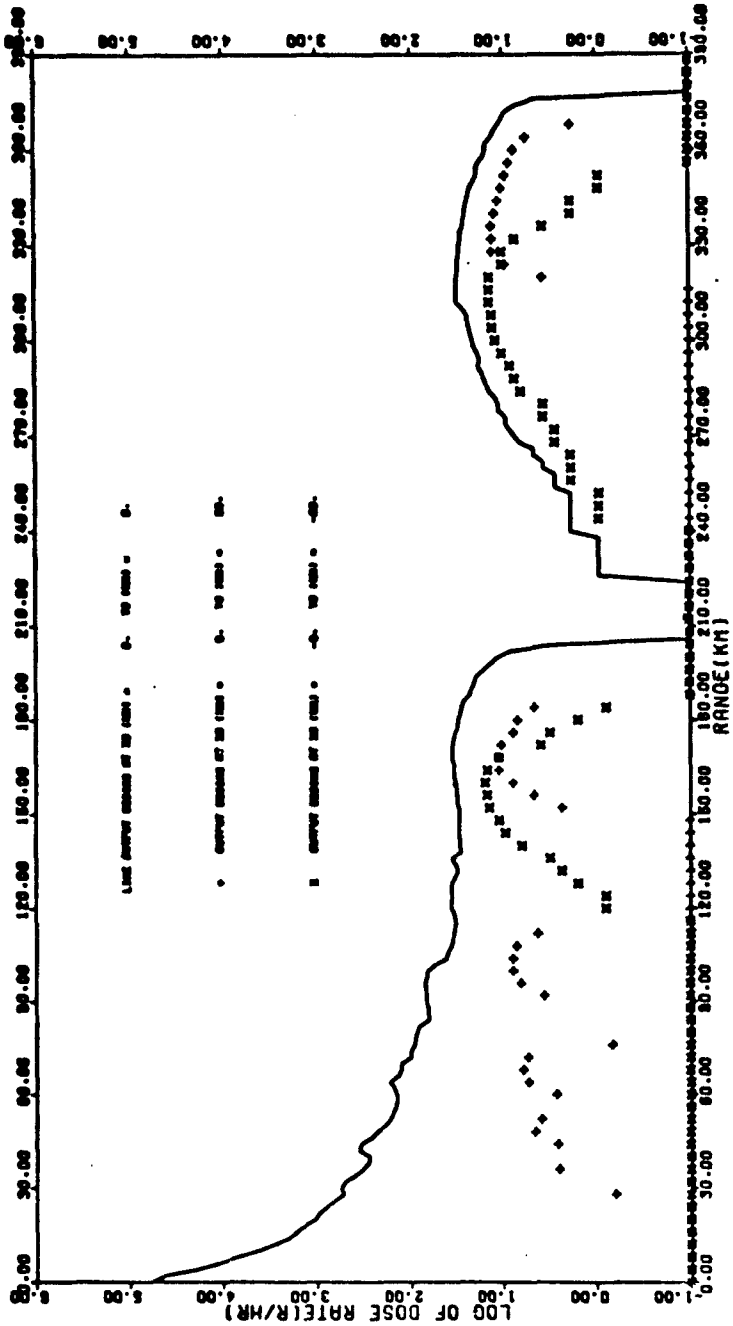

Figure 3.7. Normalized Dose Rate Along Angle (Deg) = 345; Yield = 3 Mt

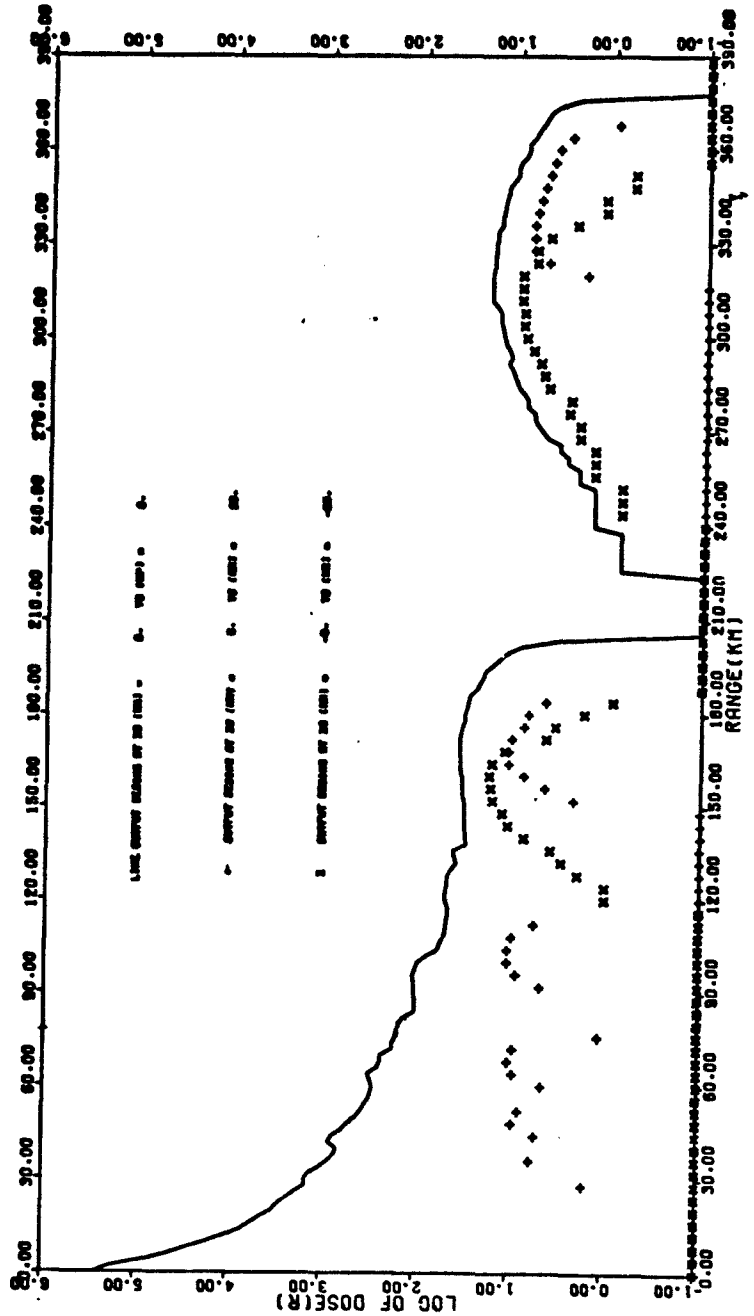

Figure 3.8. Integrated Dose Along Angle (Deg) = 345; Yield = 3 Mt

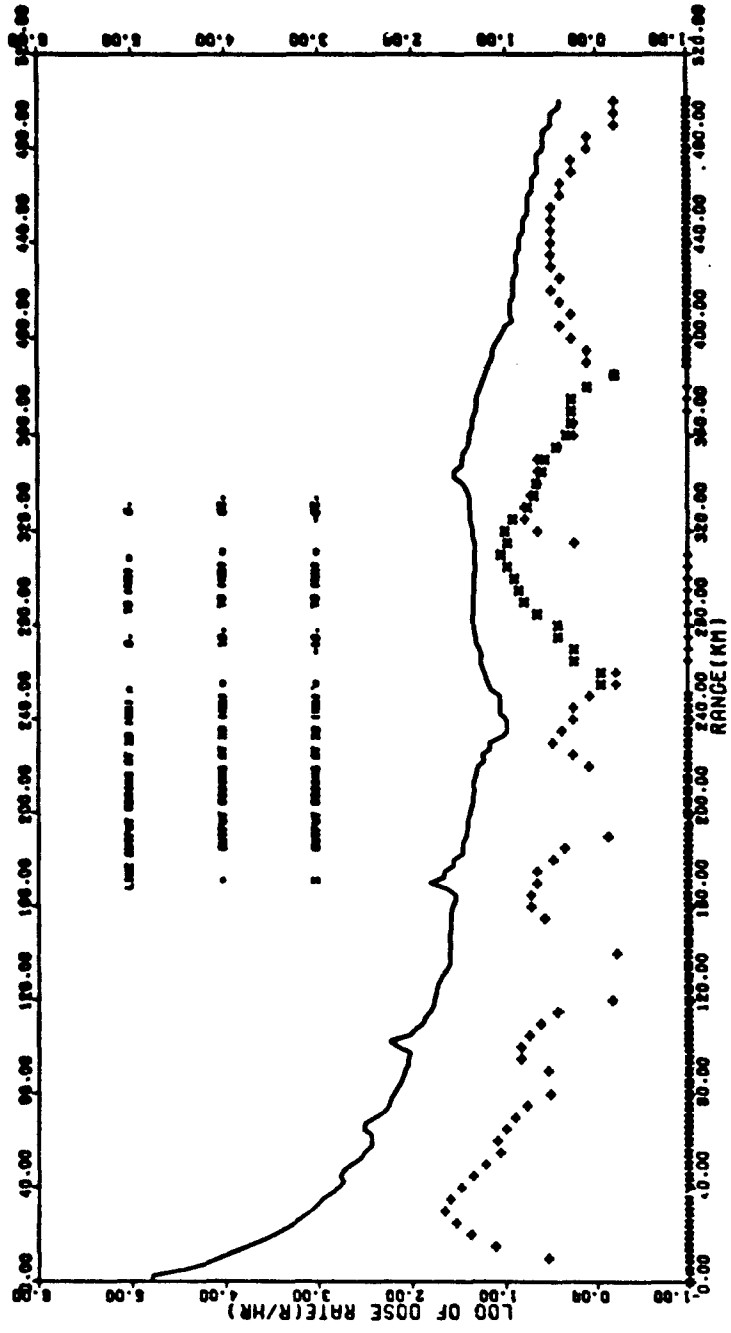

Figure 3.9. Normalized Dose Rate Along Angle (Deg) = 345; Yield = 10 Mt

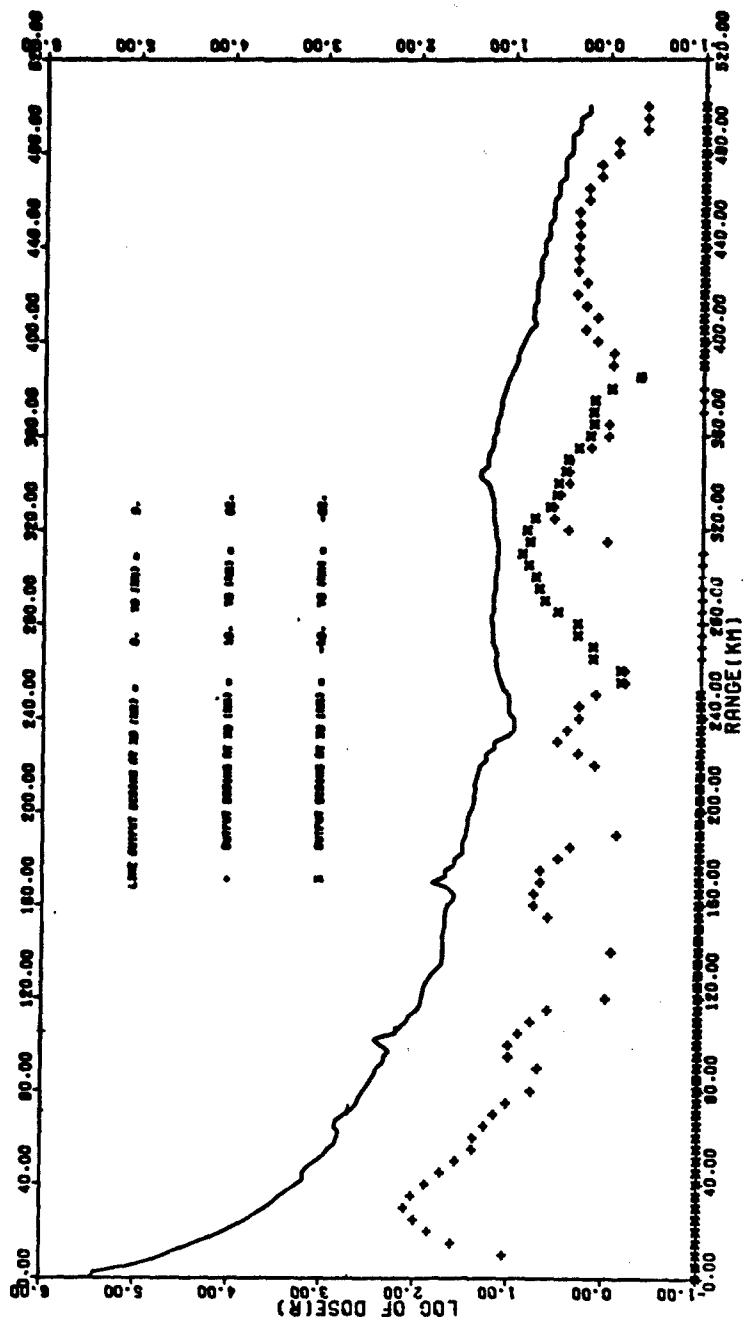

Figure 3.10. Integrated Dose Along Angle (Deg) = 345; Yield = 10 Mt

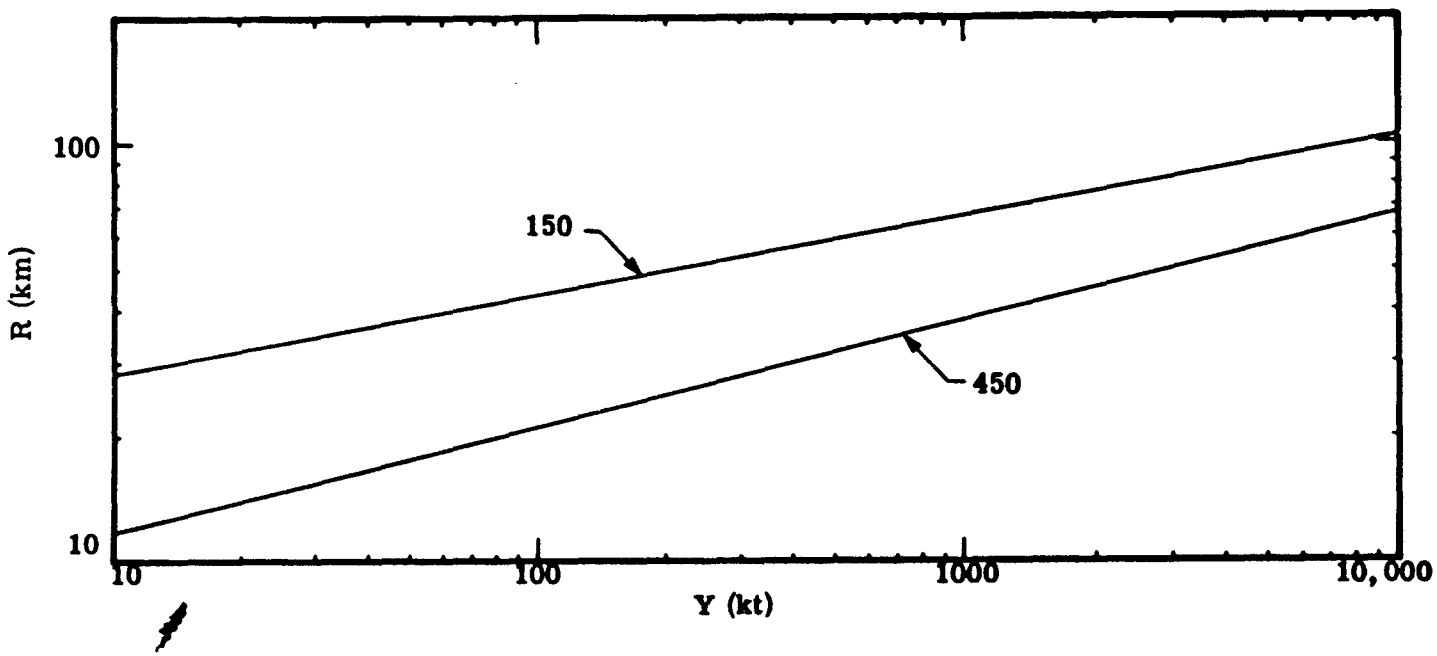

Figure 3.11. Maximum Hotline Extent as a Function of Yield for Two Levels of Integrated Dose (R)

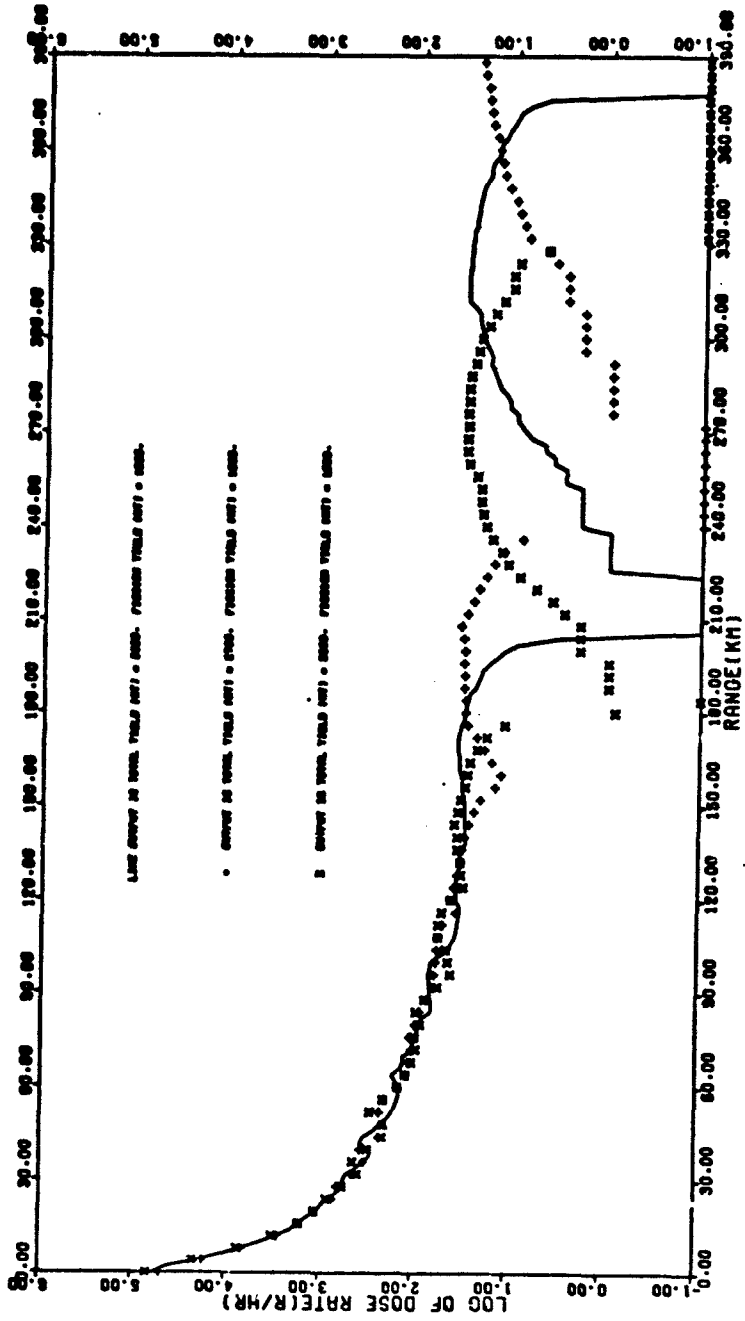

Figure 3.12. Variations in Predicted Dose Rate Due to ±10 Percent Uncertainties in Total Yield

H+1 hour for three yields, 2.7 Mt, 3.0 Mt, and 3.3 Mt, where both the fission yield and total yield have been varied proportionally (±10 percent around the 3 Mt baseline case). Figure 3.13 is the hotline total integrated dose 48 hours after burst for the same three yields. The doses and dose rates for the three devices are labeled by yield on the plot itself. It can be seen from these figures that the close-in fallout at any specific range varies at most by ±10 percent with yield, and that the long-range fallout appears to vary by a greater amount, but that this latter effect is most probably caused by the limited number of cloud wafers used in the DELFIC formulism, and thus not be greater than the close-in variation if a greater number of small particle wafers were used.

Similarly, Figures 3.14 and 3.15 are the respective H+1 hr normalized hotline dose rates and total integrated doses 48 hours after burst for the 270 kt, 300 kt, and 330 kt devices. The variations of the close-in fallout are again within ±10 percent, and the same conclusions regarding the long-range fallout can also be made.

An important conclusion regarding the future execution of the DELFIC code can be made from these figures. To accurately describe the long-range fallout, many more small particle wafers should be included in the run. Perhaps an option of specifying the number of wafers as a function of particle size could be incorporated in the code.

The next effect investigated corresponded to a hypothetical case of a device which detonates with its designed fission yield but with improper fusion yield. The three total yields considered were 2.7 Mt, 3.0 Mt, and 3.3 Mt, each with a fission yield of 1.5 Mt. Figure 3.16 is the H+1 hr normalized dose rate along the hotline for

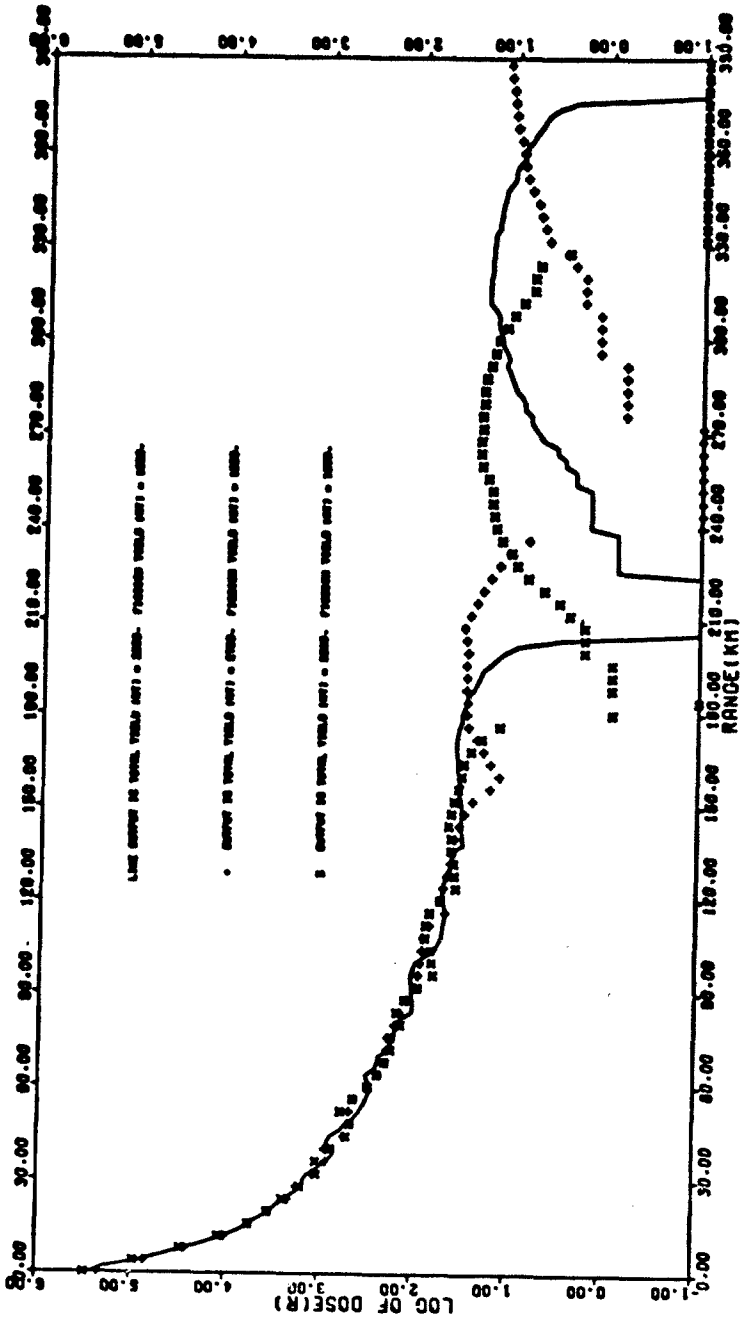

Figure 3.13. Variations in Predicted Dose Rate Due to ±10 Percent Uncertainties in Total Yield

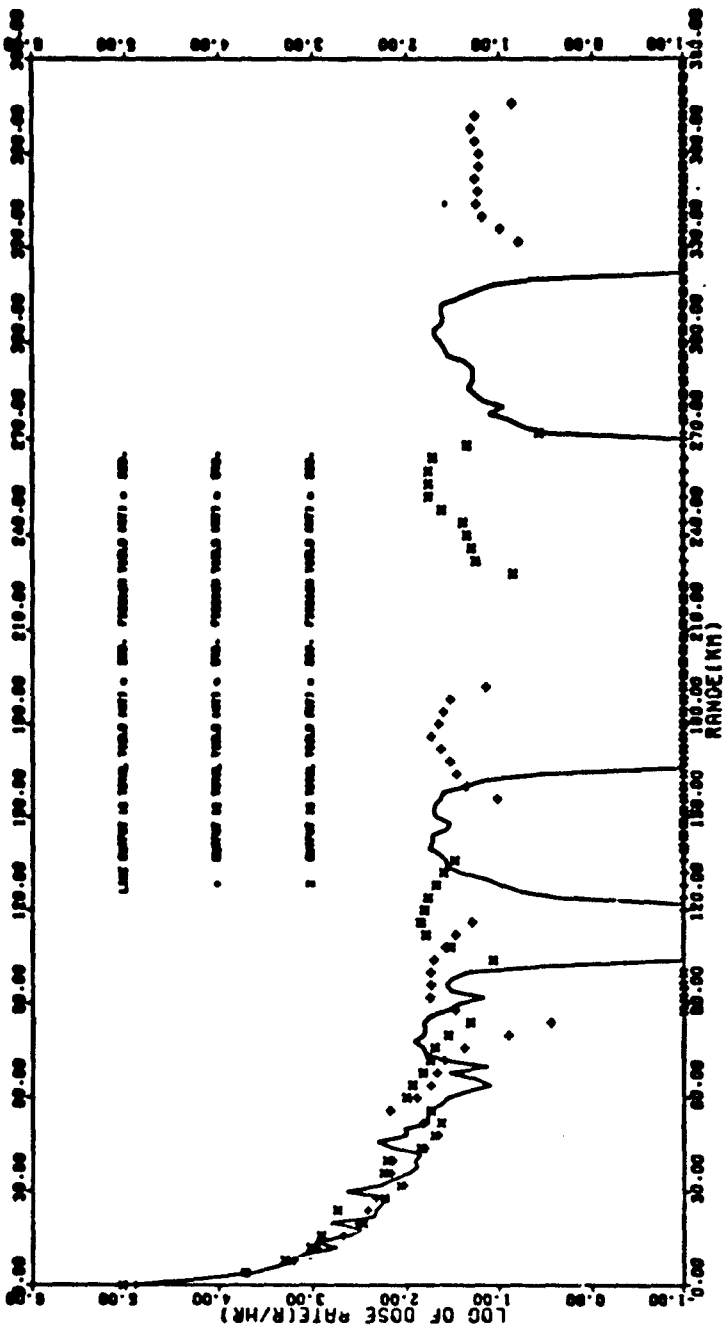

Figure 3.14. Variations in Predicted Dose Rate Due to ±10 Percent Uncertainties in Total Yield

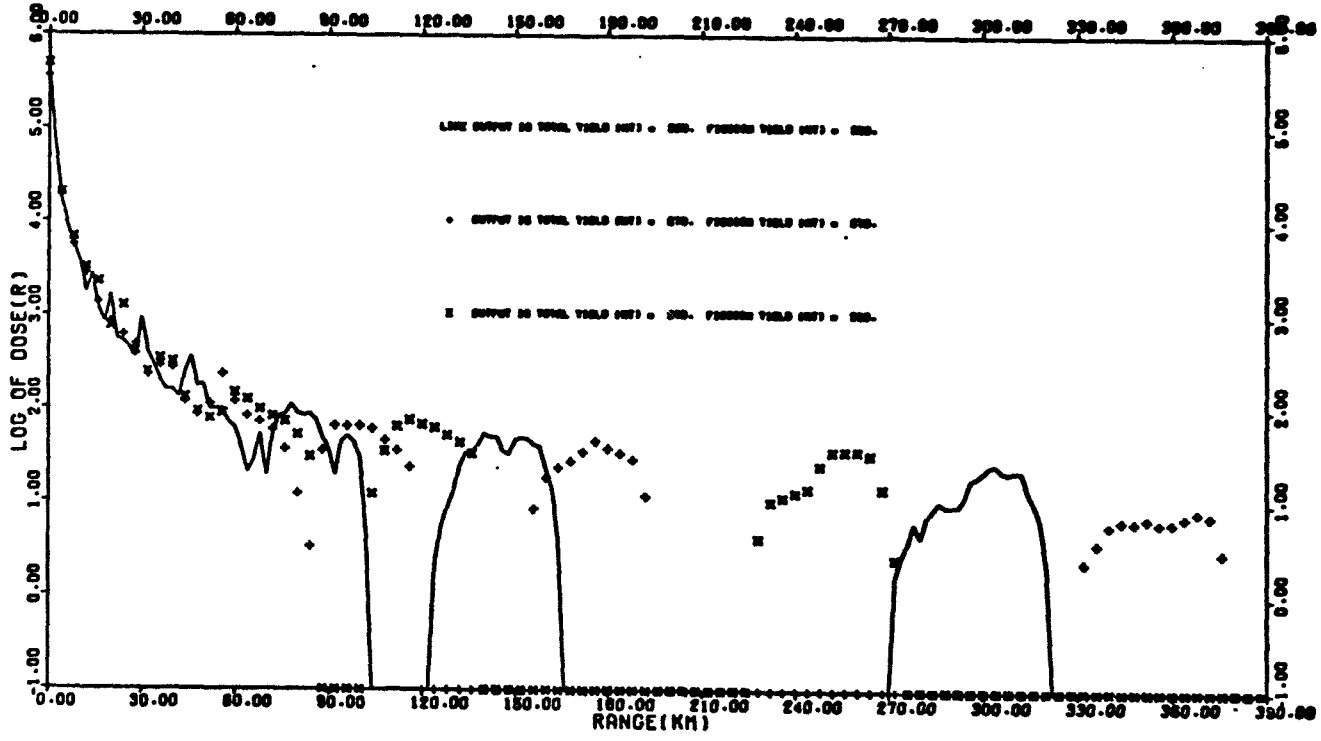

Figure 3. 15. Variations in Predicted Dose Rate Due to ±10 Percent Uncertainties in Total Yield

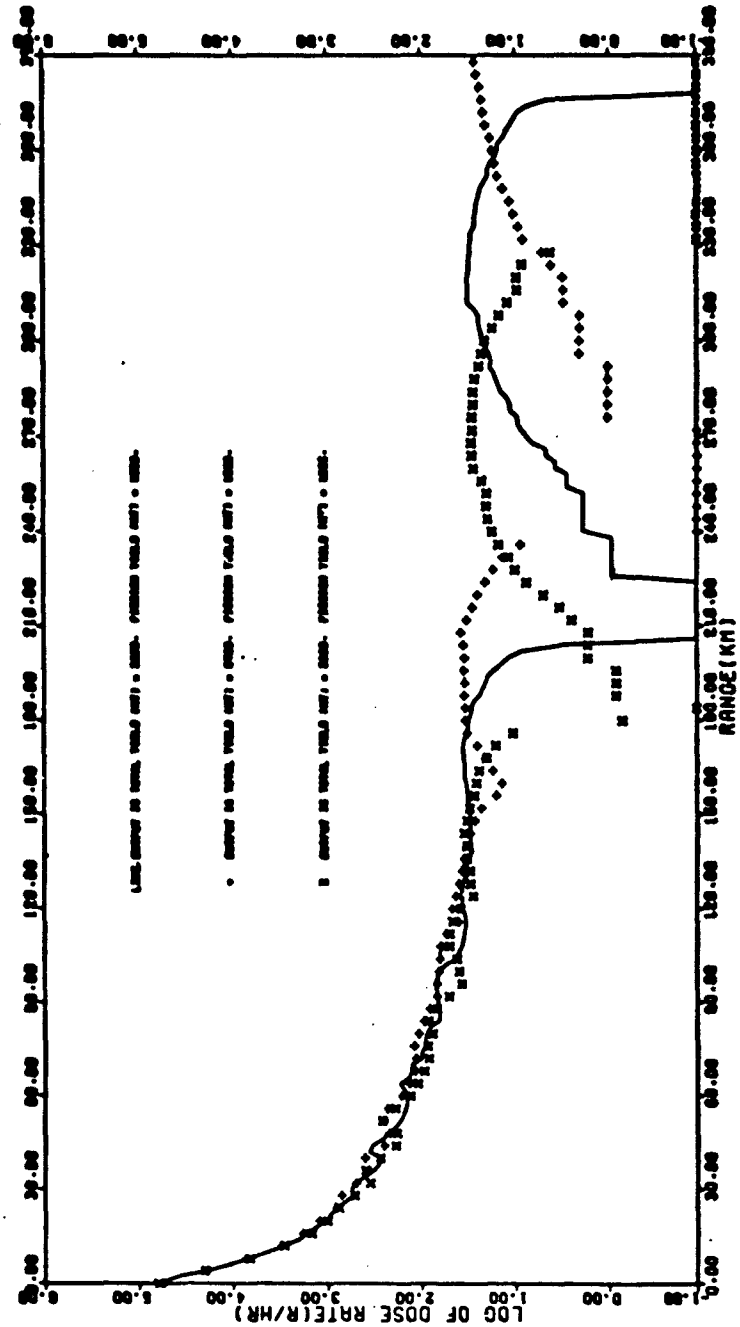

Figure 3.16. Variations in Predicted Dose Rate Due to ±10 Percent Uncertainties in Fusion Yield

the three devices, and Figure 3.17 is the total integrated hotline dose 48 hours after burst for the same devices. Again, a maximum ±10 percent variation is evident.

Finally, the hypothetical case of a device exploding with its designed fusion yield, but not its fission yield, was investigated. A fusion yield of 1.5 Mt and fission yields of 1.2 Mt, 1.5 Mt, and 1.8 Mt were used in this investigation. Figure 3.18 is a plot of H+1 hr normalized dose rate for the three devices along the hotline, and Figure 3.19 is a plot of total integrated dose 48 hours after burst along the hotline for the same devices. Again, a maximum ±10 percent variation is observed.

These calculations have shown that uncertainties in the total yield and fission and fusion fractions can lead to uncertainties of the same order of magnitude in the predicted dose rates and doses at specific downwind ranges.

3.4 FISSION TYPE SENSITIVITY

All the runs discussed in this report were performed using ^{235}U high energy (U235HE) as the device fission type. The sensitivity of the results to fission type are investigated in this section. Tompkins (Reference 1) performed a sensitivity analysis of the Particle Activity Module in which he found that ^{235}U fission spectrum (U235FI) and ^{239}Pu high energy (P239HE) were the two fission types which bound the K-factor as a function of particle size results. The K-factor relates exposure rate to debris deposition density.

Two yields were investigated, 30 kt and 3 Mt. Figure 3.20 is the 30 kt dose rate along the hotline normalized to H+1 hr for the three fission types while Figure 3.21 is the 30 kt total integrated dose

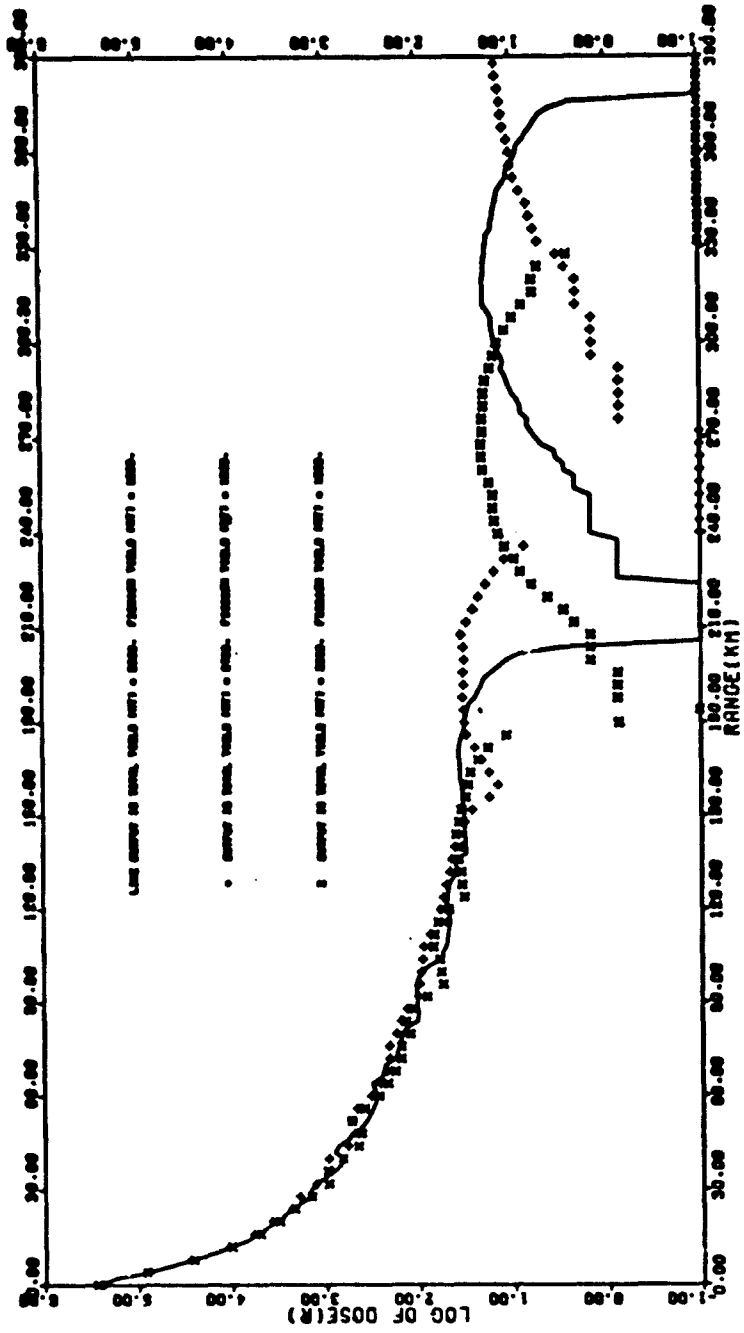

Figure 3.17. Variations in Predicted Dose Due to ±10 Percent Uncertainties in Fusion Yield

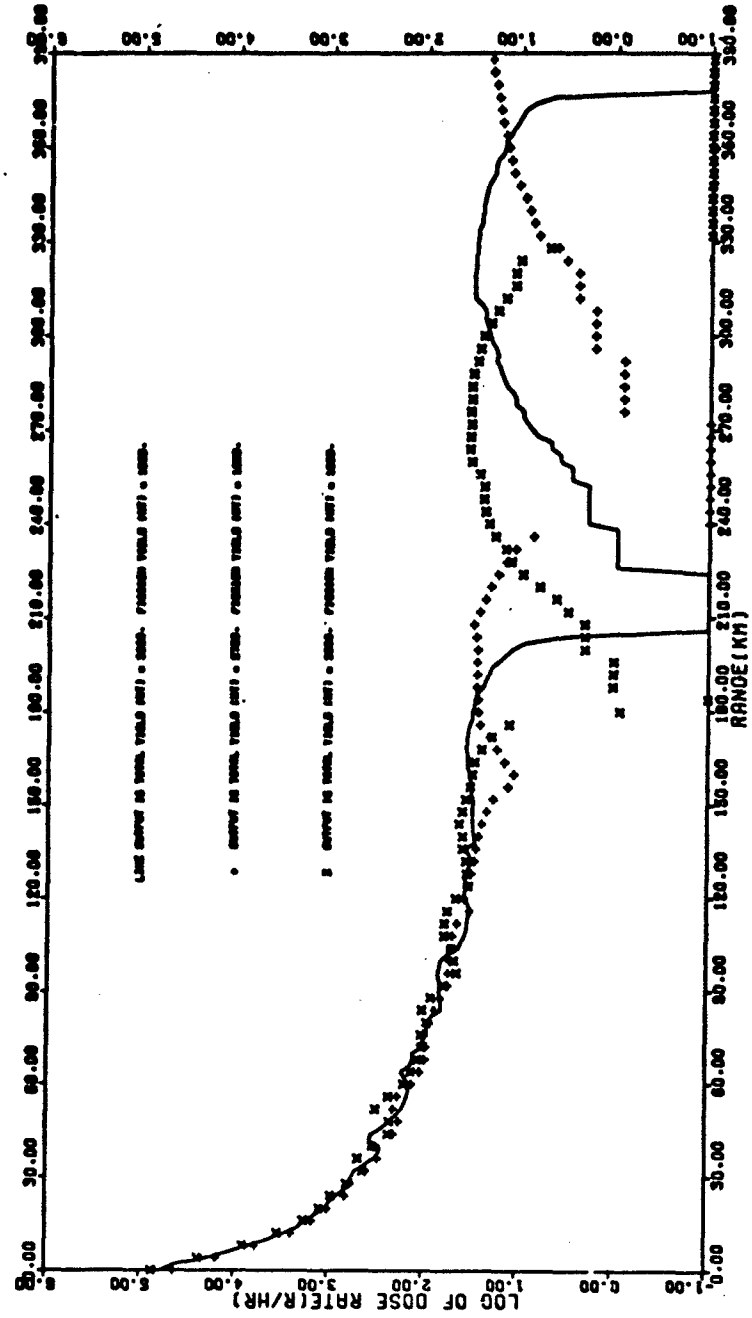

Figure 3.18. Variations in Predicted Dose Rate Due to ±10 Percent Uncertainties in Fission Yield

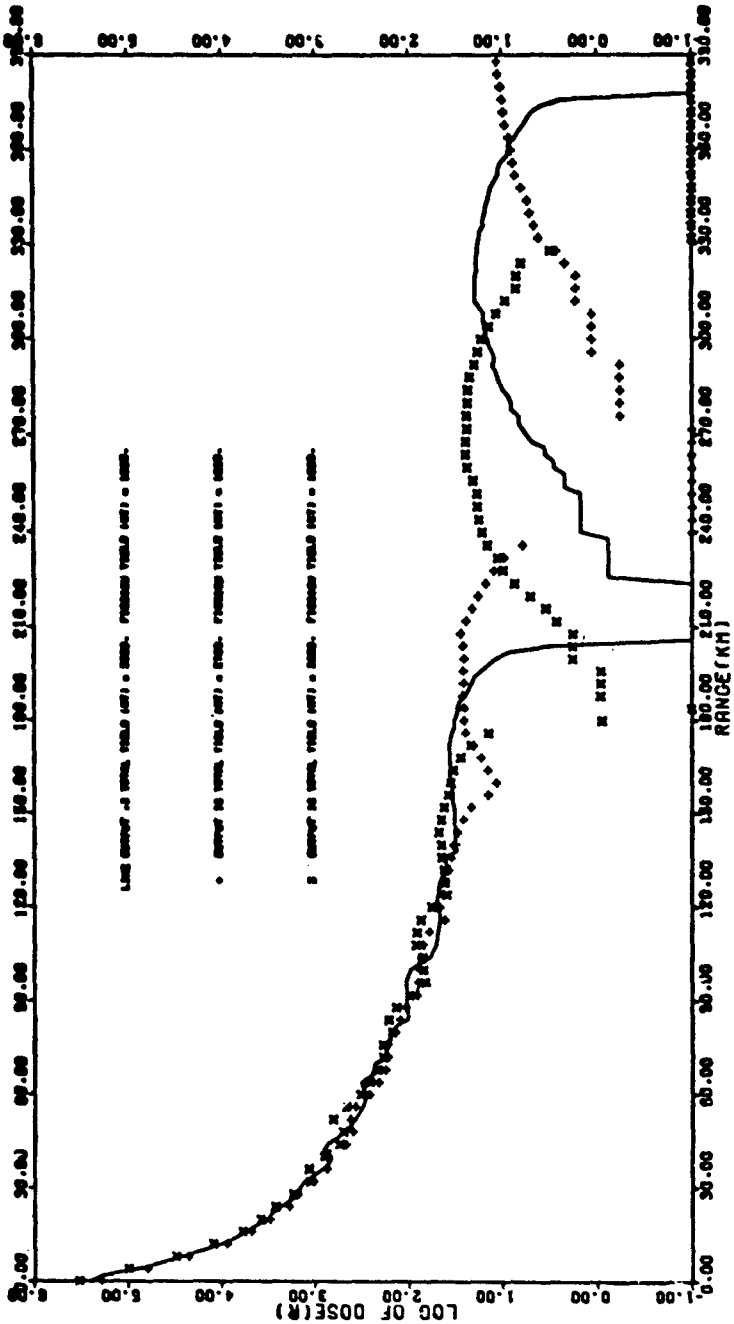

Figure 3.19. Variations in Predicted Dose Due to ±10 Percent Uncertainties in Fission Yield

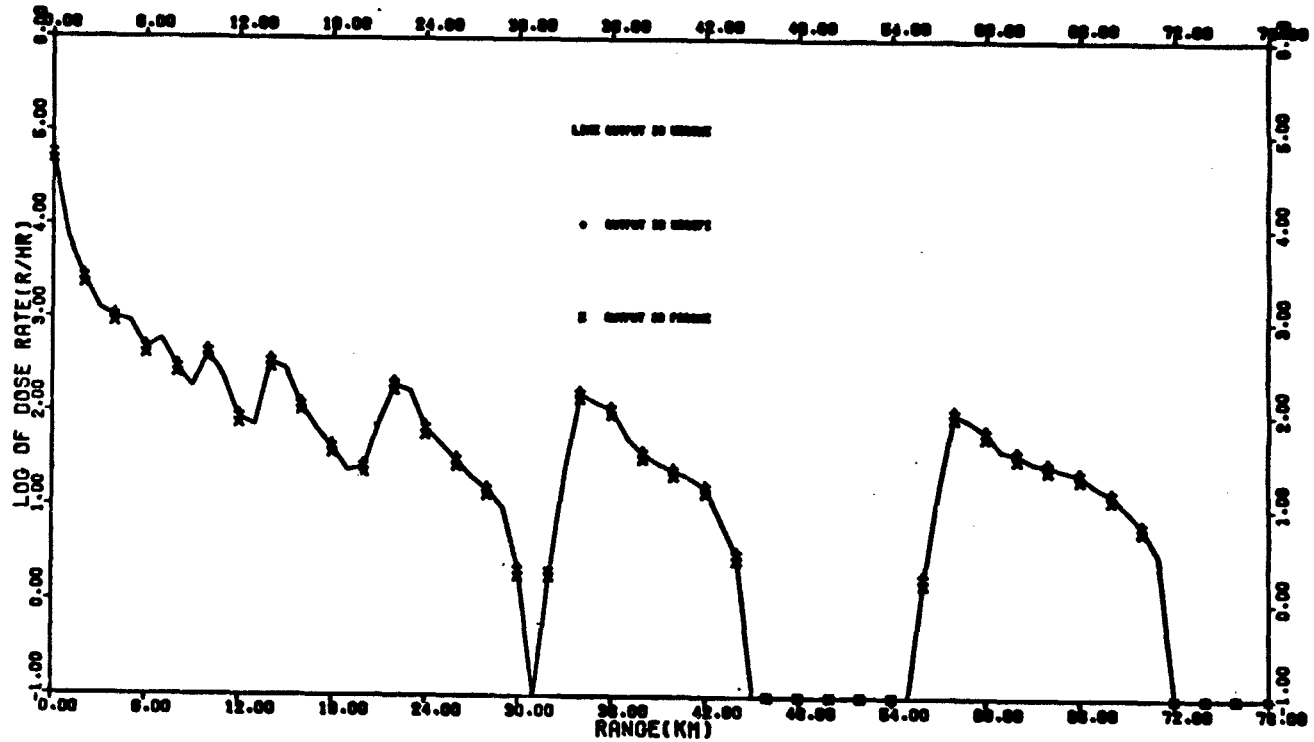

Figure 3.20. Variations in Predicted Dose Rate Due to Three Fission Types for a 30 kt Device

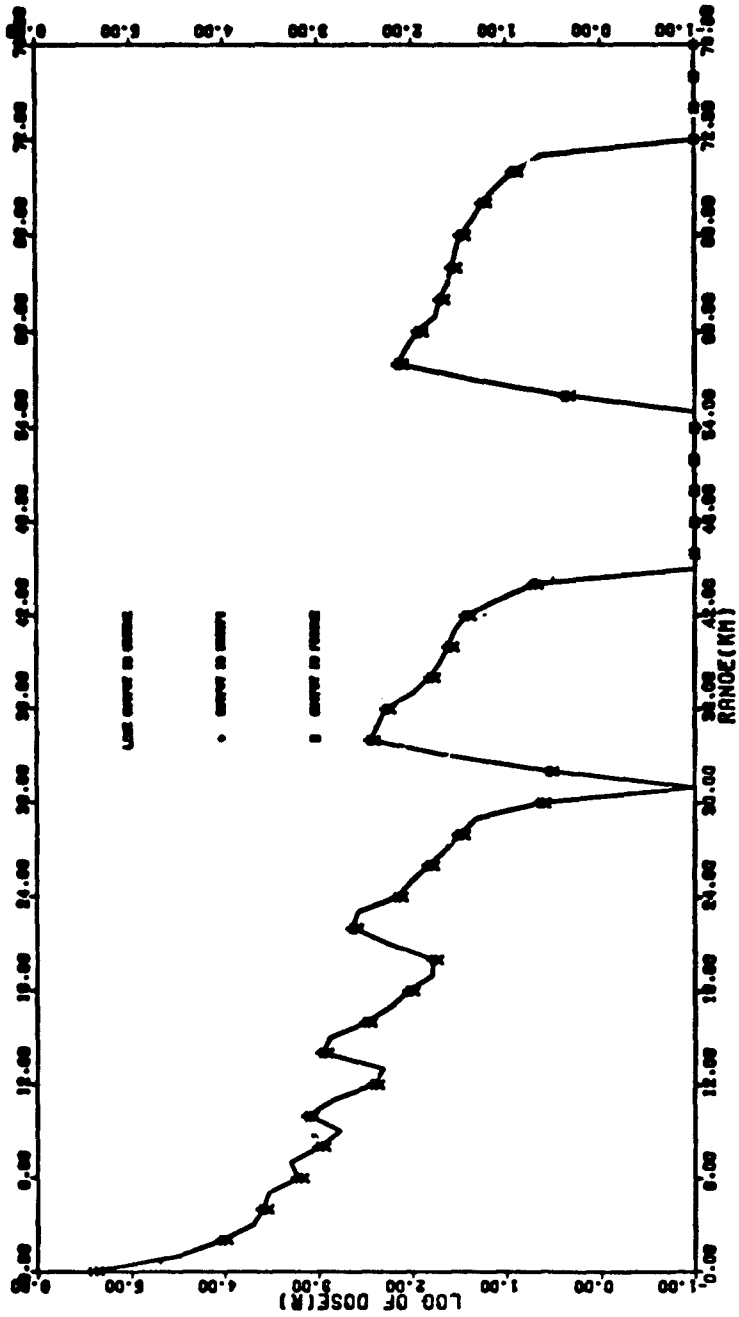

Figure 3.21. Variations in Predicted Dose Due to Three Fission Types for a 30 kt Device

48 hours after burst for the same three fission types. Figures 3.22 and 3.23 are the respective 3 Mt hotline dose rates and integrated doses for the three fission types. It can be seen that the variations due to fission type are at most on the order of ±10 percent.

3.5 SUMMARY

The sensitivity of fallout predictions to variations in total yield, fusion yield, fission yield, and fission type were investigated. Four significant conclusions were reached as a result of this investigation.

First, variations in total yield, fission yield and fusion yield are directly reflected in variations of predicted dose rate and total dose of the same order of magnitude along the hotline.

Second, changes in fission type can affect dose rate and dose predictions by no more than ±10 percent.

Third, the maximum downwind extent of significant dose levels is not a linear function of yield.

And last, to more accurately describe long-range fallout, many small particle DELFIC cloud wafers should be used.

3.6 REFERENCES

1. R. C. Tompkins, "Sensitivity Analysis of the DELFIC Particle Activity Module," BRL Report 1523, January 1971.

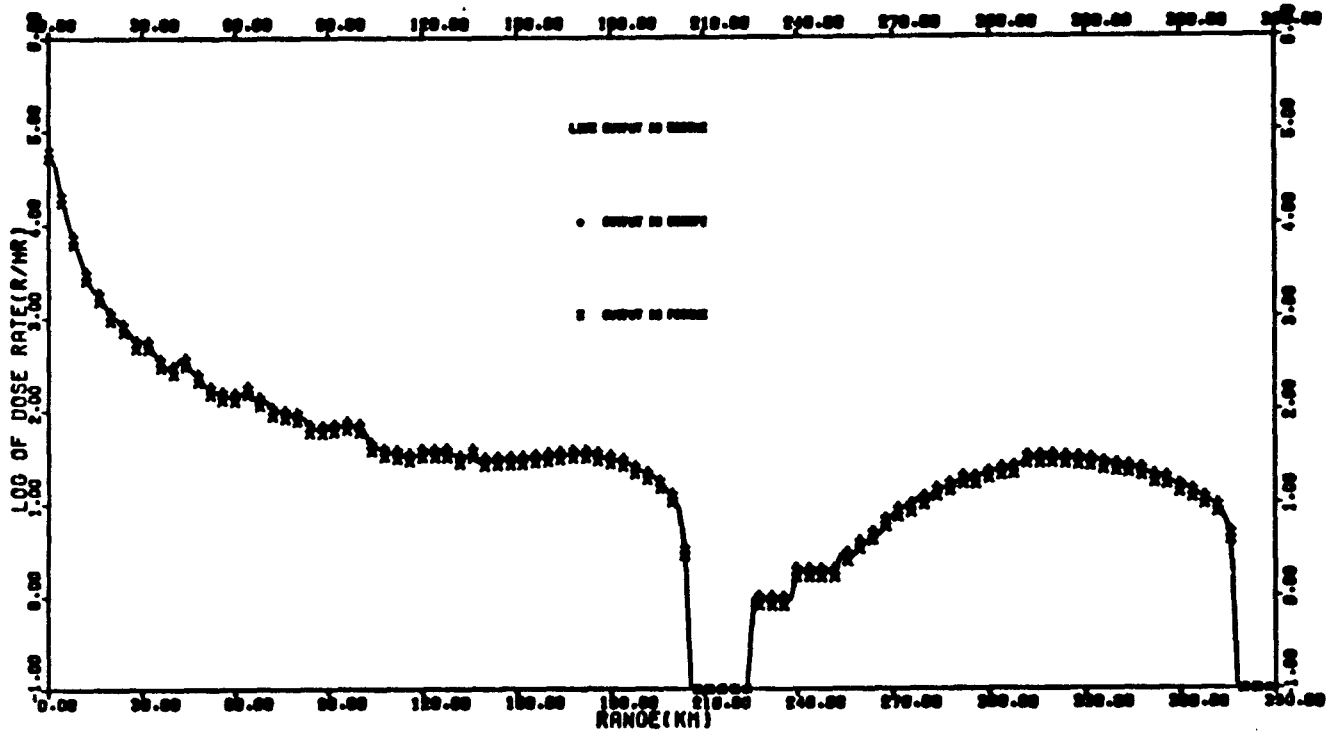

Figure 3.22. Variations in Predicted Dose Rate Due to Three Fission Types for a 3 Mt Device

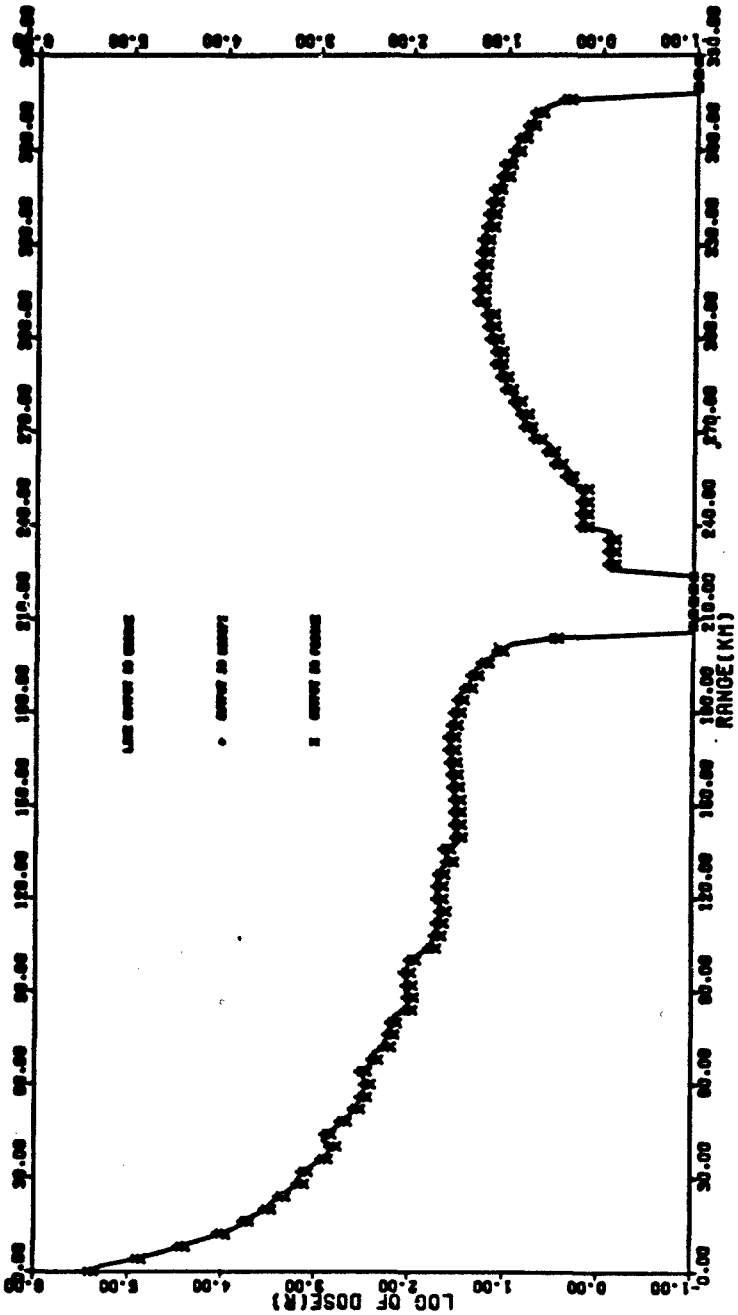

Figure 3.23. Variations in Predicted Dose Rate Due to Three Fission Types for a 3 Mt Device

Section 4

SIZE DISTRIBUTION SENSITIVITY

The subject of this section is the size distribution of the entrained soil material. Two specific aspects are addressed. The first is to show how different analytic forms of the distribution affect fallout predictions for a surface burst. Secondly, the height-of-burst dependence is discussed.

4.1 SENSITIVITY TO ANALYTIC FORM OF THE SIZE DISTRIBUTION

In the discussion to follow, the size distribution will be expressed as cumulative mass fraction versus particle size. In this form the dependent variable is the fraction of the total soil burden in the cloud with particles smaller than a specified diameter. The distribution refers to the total amount of soil that initially is in the cloud and hence does not include a time-dependence due to fallout. Section 6 presents the results of an investigation into the uncertainties associated with size-dependence of specific activity (defined as the activity of a particle divided by its weight). Together, the two distributions determine the relative sizes and positions and shapes of iso-dose contours on the ground.

Three size distributions were chosen for comparison. The first two have analytic forms that are power-law, and log-normal. The third is a hybrid with the low end of the size spectrum having log-normal behavior while the larger particles follow a power-law

distribution; the motivation for choosing these distributions is based on the following comments. Fallout calculations using DELFIC and other codes have traditionally employed the log-normal distribution. The experimental basis for such a choice is found in the analysis (Reference 1) of cloud and fallout samples obtained at late times (several hours after burst). Because of gravitational settling, the particles in the samples tend to have diameters less than a few hundred microns. The log-normal size distribution is given by

$$CM_1(a) = K \int_{-\infty}^{x} \frac{dx}{\sqrt{2\pi}\sigma} \exp\left(\frac{[x - x_o - 3 \ln 10\sigma^2]^2}{2\sigma^2} \right)$$

where

CM = cumulative mass fraction
K = a normalization constant
$x = \log_{10} a$
$x_o = \log_{10} \bar{a}$
σ = standard deviation of the distribution
a = particle diameter
$\bar{a}$ = median diameter.

Based on an analysis[2] of data from shot SMALL BOY, DELFIC uses the following values for $\bar{a}$ and σ unless the user specifies his own distribution

$$\bar{a} = 0.407\mu$$
$$\sigma = \log_{10}(4.0)$$

for this choice of parameters, 50 percent of the mass is associated with particles below 130μ.

Complementing the studies of late-time cloud and fallout samples have been investigations into the characteristics of soil material ejected from the craters of various tests. Here the particle sizes typically ranged from millimeters to meters. An analysis[3] of the size distribution of the crater ejecta indicated a power-law behavior, i.e.,

$$CM_2(a) = K\, a^{-P}.$$

It was found in reference 3 that the various data indicated P to be about 0.5 for cohesive soils and rock.

In spite of the apparent disagreement between the log-normal and power-law distributions, it is important to note that they were based on different segments of the overall spectrum of particle sizes that are initially in the cloud. In fact, a compromise can be reached by creating a hybrid distribution, i.e., log-normal on the low end and power law on the high end. There are data to support this hypothesis[4]. The analytic form of this distribution is

$$CM_3(a) = CM_1(a) \quad a < a_t$$

$$= CM_1(a_t) + K'(a^P - a_t^P) \quad a > a_t$$

where a_t is diameter where the transition occurs, $CM_1(a)$ is given above and K' provides continuity at a_t. Not explicitly shown is an overall normalization. For this investigation, the transition diameter was taken to be upper limit on the 30th size class with a value of 756μ. Shown in Figure 4.1 are the three distributions as used for the 300 kt case. Note that the log-normal, the hybrid, and the

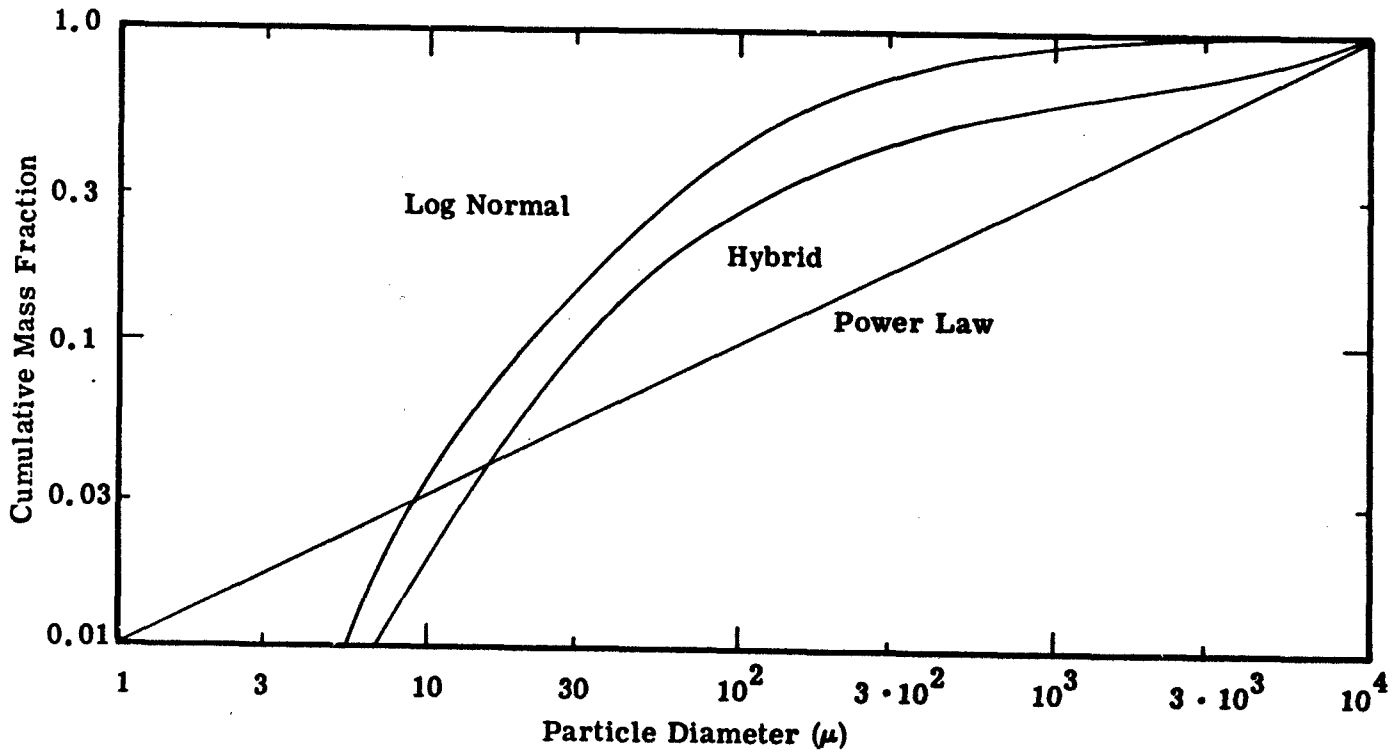

Figure 4.1. Comparison of Size Distributions

power-law cumulative mass fractions attain 50 percent by 130μ, 460μ and 2500μ respectively.

As described in previous sections, the base line DELFIC runs were performed with a power-law size distribution. The logic of the Initial Conditions Module sets up the particle size classes so that each size class contains an equal percentage of the total mass. In all the DELFIC runs, 40 size classes were chosen, so that the mass fraction in each size class was 0.025. The procedure developed to investigate the dependency of the analytic form of the size distribution made use of the grounded particles tape and the logic of the Initial Conditions Module to create new grounded particle tapes with different size distribution. Program DIAM, listed in Appendix D, was developed to create a grounded particles tape with a log-normal distribution from one with a power-law distribution. A modification of this program was used to create a tape with a hybrid distribution, part log-normal, part power-law.

The hybrid distribution was created with the constraint that the transition from log-normal to power law be continuous. Figure 4.2 is a schematic representation of the process used. The mass fractions generated by the log-normal distribution for the 11 smallest size classes were used in the hybrid distribution for all yields along with a mass fraction of 0.025 for the remaining 29 classes. These distributions were then normalized to produce the corrected hybrid distributions. Tables 4.1, 4.2, and 4.3 are the mass fractions in each size class generated by the power-law, the log-normal, and the hybrid distributions for the 3 Mt, 300 kt, and 30 kt yields, respectively. It can be seen from these tables that the log-normal distribution contains approximately 50 percent of the

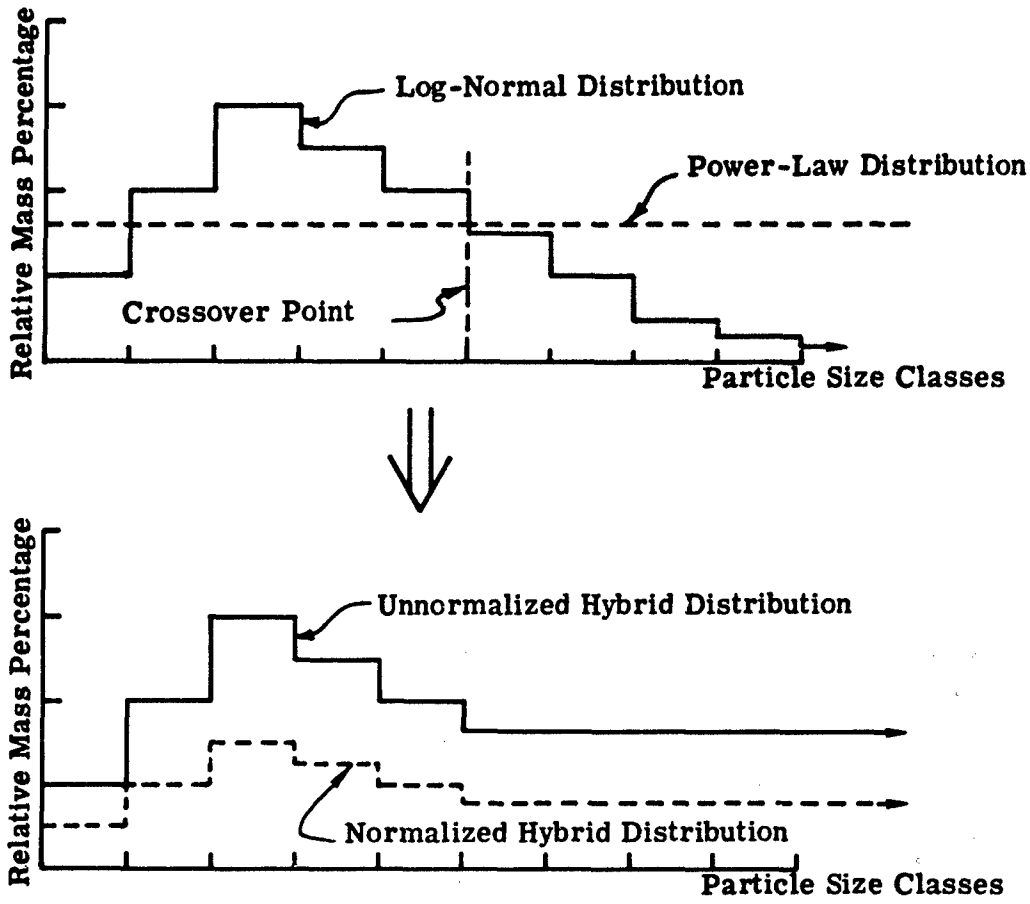

Figure 4.2. Schematic Representation of Generation of Hybrid Distribution

Table 4.1. 3 Mt Mass Fractions

Size Class	Particle Diameter (μm)	Power Law	Log-Normal	Hybrid
1	47[illegible]2.93[illegible]	.025	.00014377	.01552743
2	8343.7[illegible]		.00016495	.01552743
3	7915.90[illegible]		.00018967	.01552743
4	7499.2741		.00021859	.01552743
5	7093.90[illegible]		.00025251	.01552743
6	6699.80[illegible]		.00029242	.01552743
7	6316.9562		.00033949	.01552743
8	5945.3705		.00039518	.01552743
9	5585.0430		.00046128	.01552743
10	5235.9747		.00053947	.01552743
11	4898.1745		.00063397	.01552743
12	4571.6295		.00074665	.01552743
13	4256.3408		.00088220	.01552743
14	3952.3201		.00104549	.01552743
15	3659.5557		.00124433	.01552743
16	3378.0514		.00148549	.01552743
17	3107.8073		.00178119	.01552743
18	2848.8234		.00214381	.01552743
19	2601.0995		.00259115	.01552743
20	2364.6358		.00314571	.01552743
21	2139.4320		.00383663	.01552743
22	1925.4883		.00470197	.01552743
23	1722.8045		.00579165	.01552743
24	1531.3803		.00717149	.01552743
25	1351.2160		.00892874	.01552743
26	1182.3116		.01117957	.01552743
27	1024.6670		.01407910	.01552743
28	878.2824		.01783441	.01552743
29	743.1713		.02272369	.01552743
30	619.3094		.02911244	.01808190
31	506.7077		.03748041	.02327898
32	405.3662		.04842621	.03007739
33	315.2848		.06264205	.03890680
34	236.4636		.08076251	.05016138
35	168.9026		.10289625	.06390854
36	112.6017		.12735212	.07909805
37	67.5610		.14750870	.09161729
38	33.7805		.14562549	.09044759
39	11.2602		.09145241	.05680085
40	1.4075		.01179466	.00732565

Table 4.2. 300 kt Mass Fractions

Size Class	Particle Diameter (μm)	Power Law	Log-Normal	Hybrid
1	9745.4125	.025	.00011411	.01539562
2	9258.1420		.00013129	.01539562
3	8783.3654		.00015139	.01539562
4	8321.0830		.00017499	.01539562
5	7871.2947		.00020275	.01539562
6	7434.0006		.00023552	.01539562
7	7009.2006		.00027431	.01539562
8	6596.8947		.00032035	.01539562
9	6197.0828		.00037520	.01539562
10	5809.7651		.00044075	.01539562
11	5434.9416		.00051934	.01539562
12	5072.6122		.00061393	.01539562
13	4722.7768		.00072821	.01539562
14	4385.4356		.00086679	.01539562
15	4060.5885		.00103556	.01539562
16	3748.2356		.00124196	.01539562
17	3448.3767		.00149552	.01539562
18	3161.0120		.00180848	.01539562
19	2886.1414		.00219664	.01539562
20	2623.7649		.00268057	.01539562
21	2373.8825		.00328709	.01539562
22	2136.4943		.00405154	.01539562
23	1911.6002		.00502063	.01539562
24	1699.2001		.00625657	.01539562
25	1499.2942		.00784263	.01539562
26	1311.8824		.00989094	.01539562
27	1136.9648		.01255319	.01539562
28	974.5413		.01603518	.01539562
29	824.6118		.02061645	.01539562
30	687.1765		.02667523	.01642727
31	562.2353		.03471743	.02137986
32	449.7883		.04540152	.02795939
33	349.8353		.05953363	.03666229
34	262.3765		.07795817	.04800858
35	187.4118		.10114348	.06228667
36	124.9412		.12794149	.07878956
37	74.9647		.15228020	.09377794
38	37.4824		.15584745	.09597474
39	12.4941		.10303699	.06345274
40	1.5618		.01430255	.00880787

Table 4.3. 30 kt Mass Fractions

Size Class	Particle Diameter (μm)	Power Law	Log-Normal	Hybrid
1	8945.9185	.025	.00014153	.01551792
2	8403.6226	↓	.00016241	.01551792
3	7972.6675		.00018679	.01551792
4	7553.0535		.00021531	.01551792
5	7144.7804		.00024878	.01551792
6	6747.8481		.00028815	.01551792
7	6362.2568		.00033461	.01551792
8	5988.0064		.00038959	.01551792
9	5625.0969		.00045486	.01551792
10	5273.5284		.00053258	.01551792
11	4933.3007		.00062545	.01551792
12	4604.4140		.00073680	.01551792
13	4286.8682		.00087080	.01551792
14	3980.6634		.00103266	.01551792
15	3685.7994		.00122894	.01551792
16	3402.2764		.00146795	.01551792
17	3130.0942		.00176023	.01551792
18	2869.2531		.00211927	.01551792
19	2619.7528		.00256236	.01551792
20	2381.5934		.00311186	.01551792
21	2154.7750		.00379676	.01551792
22	1939.2975		.00465494	.01551792
23	1735.1609		.00573609	.01551792
24	1542.3653		.00710581	.01551792
25	1360.9105		.00885110	.01551792
26	1190.7967		.01108785	.01551792
27	1032.0238		.01397104	.01551792
28	884.5919		.01770808	.01551792
29	748.5008		.02257624	.01551792
30	623.7507		.02894357	.01796575
31	510.3414		.03729033	.02314672
32	408.2732		.04822063	.02993135
33	317.5458		.06243442	.03875409
34	238.1593		.08058091	.05001791
35	170.1138		.10279304	.06380535
36	113.4092		.12741502	.07908862
37	68.0455		.14785776	.09177777
38	34.0228		.14633127	.09083025
39	11.3409		.09222029	.05724266
40	1.4176		.01195390	.00741998

mass in the five smallest size classes, and that the normalization of the hybrid distribution results in there being approximately 60 percent of the mass in each class with respect to the "parent" distributions. These changes in the relative mass distributions directly affect the dose rates predicted on the ground.

Figure 4.3 presents the 3 Mt, H+1 hr normalized dose rate for the three distributions along a line 345^{o} from the horizontal (the chosen "hotline") as a function of range. The interpretation of these curves is quite simple in terms of aerodynamics. The smaller particles will be raised higher by the buoyant cloud, will fall slower through a viscous atmosphere, and consequently, will impact the ground later and farther along the downwind axis than the larger particles. Impact time and distance along the downwind axis are directly related to particle diameter.

The higher dose rates predicted in the vicinity of ground zero by the power-law distribution are caused because of the greater percentage of mass allocated to the larger particles. That this dose rate is directly proportional to this mass fraction can be seen from a comparison of the fractions in the large particle sizes for the power-law and hybrid distributions. The power-law fractions are almost one and a half times the hybrid fractions, and this is the ratio of the two dose rates for approximately the first 20 km downwind. In the same way, it can be readily observed that the particles impacting from approximately 30 km downwind and further are in the 11 smallest size classes since the hybrid curve values are two-thirds of the log-normal values in this region.

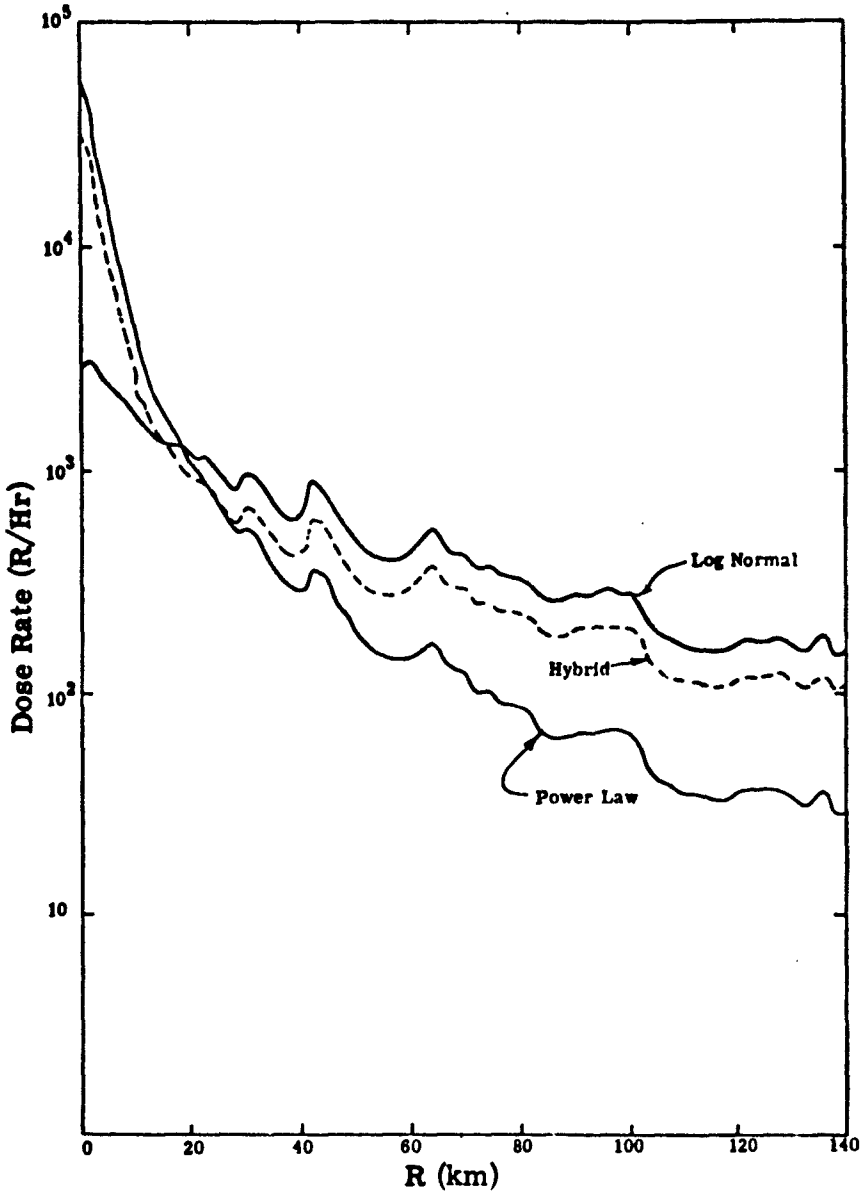

Figure 4.3. 3 Mt Dose Rate Normalized to H+1 Hour Along "Hotline"

These curves show that variations in the size (and therefore mass) distributions can cause variations in the predicted dose on the order of a factor of 20 near ground zero, and a factor of 5 at larger ranges. Data are only shown along the hotline to 140 km because past this range the probability of single wafer impact is greater, and the effects will then be proportional to mass fractions in individual size classes and not to overall size distributions.

Figure 4.4 presents the 300 kt, H+1 hr normalized dose rate for the three distributions along a line 345^{o} from the horizontal as a function of range. The same conclusions that were drawn from the 3 Mt curves can also be drawn here, the only difference being that the larger particles do not travel as far as in the 3 Mt case. This was the only yield for which the horizontal wafer subdivision option was used, which explains the relative roughness of this curve. However, the factor of 20 difference near ground zero and the factor of 5 difference further downwind are still clearly defined for the power-law and log-normal distributions.

Figure 4.5 presents the 30 kt, H+1 hr normalized dose rate for the three distributions along a line 350^{o} from the horizontal as a function of range. Again, the same effects that were seen for the larger yields are also shown here.

This investigation of the fallout sensitivity to the analytic form of the size distribution of dust has shown that the overall variation of the predicted dose rate can be as large as a factor of 20 near ground zero and as large as a factor of 5 further downwind for two reasonable forms of the size distribution. This occurs because the predicted dose is proportional to the relative amounts of mass in each size class, and the particle impact positions are dependent on particle diameter, not total amount of mass at that diameter.

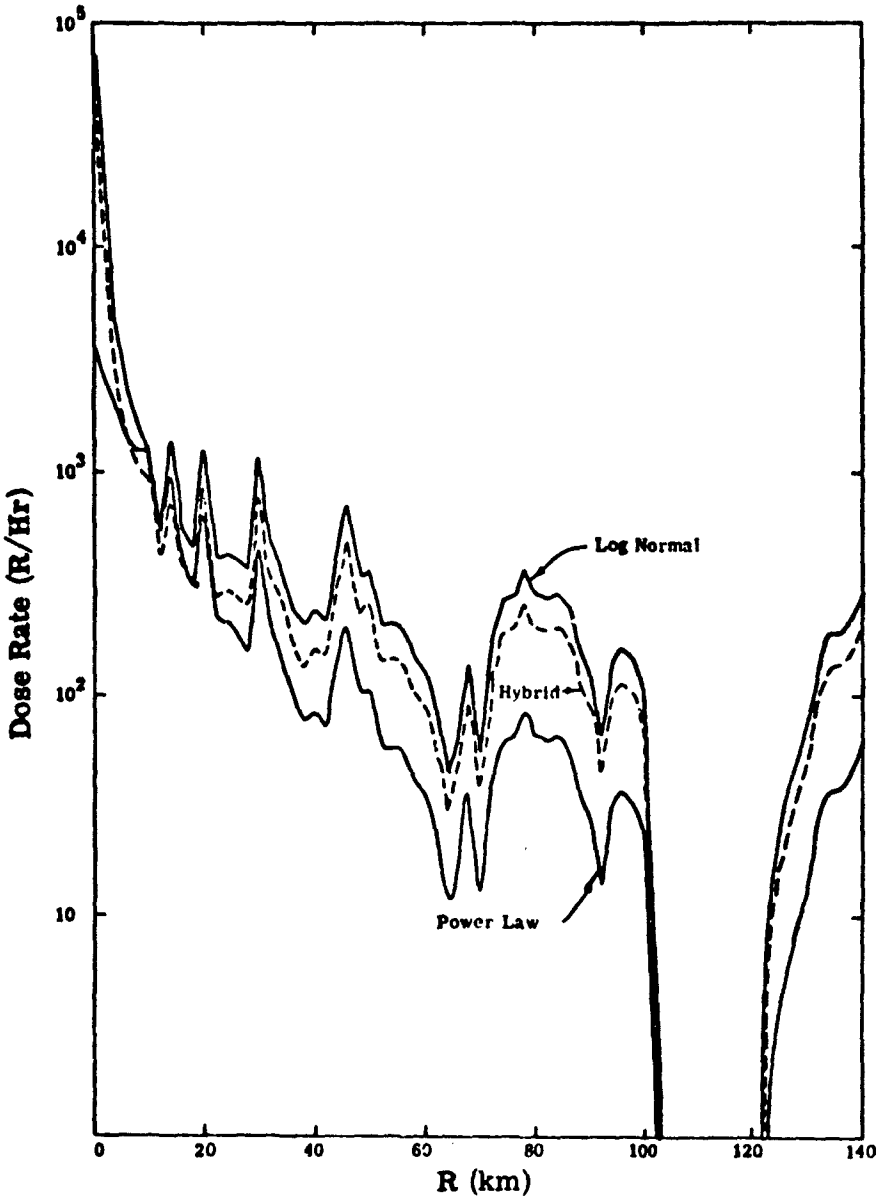

Figure 4.4. 300 kt Dose Rate Normalized to H+1 Hour Along "Hotline"

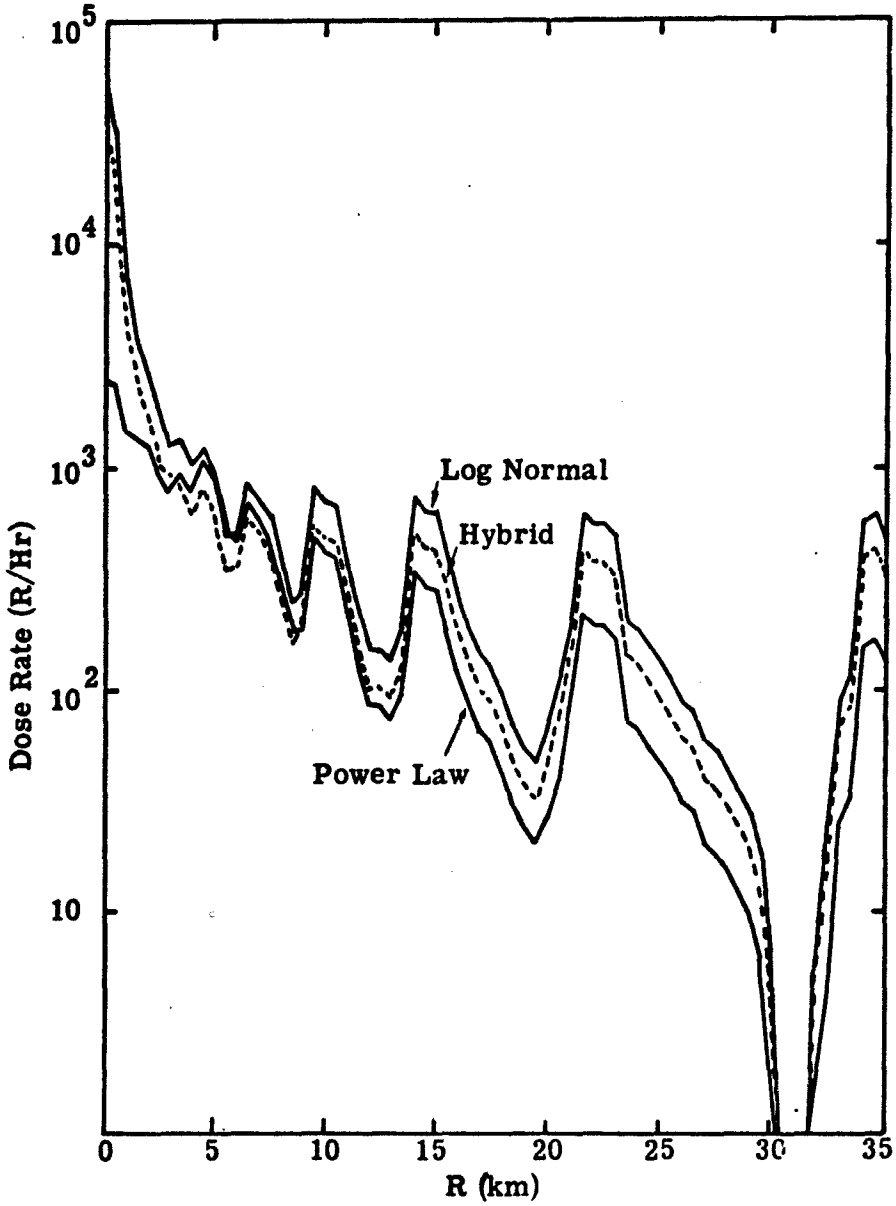

Figure 4.5. 30 kt Dose Rate Normalized to H+1 Hour Along "Hotline"

4.2 HEIGHT-OF-BURST EFFECTS ON FALLOUT

This section deals with the height-of-burst (HOB) dependence on that part of the fallout hazard that is attributed to fission debris. The variation with HOB of the neutron-activated soil is discussed in Section 7.

There are presently two algorithms for predicting the change in the fallout pattern for a low-air burst versus a surface burst. Both determine a correction factor versus HOB that is to be applied uniformly over the entire fallout pattern of a surface burst. The first correction factor is a fit to empirical data. For a number of U.S. tests at varying heights of burst, an integration was performed over the fallout pattern to determine the total activity brought down in the so-called "close-in fallout" (which usually implies times of arrival up to H+24 hrs). The form of this correction factor[5] is

$$F_1 = \exp(-.01238\,\lambda)$$

where

λ, is the scaled HOB, given by

$$\lambda = \mathrm{HOB} \cdot W^{-1/3}$$

with the HOB in feet and W, the yeild, in kt. There is a large scatter in the data on which the fit is based so that the uncertainty varies from ±50 percent at λ = 50 feet to ± an order of magnitude at λ = 300 feet.

The second correction factor[6] is based on the volume of intersection between a sphere and the ground. The radius of the sphere is given by

$$R = 180W^{0.4}$$

where R is in feet. The form of the correction factor is

$$F_2 = 0.5\,(1 - HOB/R)^2\,(2 + HOB/R).$$

Models such as these omit potentially significant effects that change the size distribution of the radioactive soil and thus result in a fallout pattern that cannot be related to that of a surface burst by a simple correction factor.

In the case of a surface burst, most of the dust is crater material ejected into the fireball before rise begins and there is probably homogeneous mixing between debris vapor and dust, part of which may itself be melted or vaporized. (Further research would be required to confirm this observation, however.) As the HOB increases, however, two changes occur which make the estimation of fallout dose levels more difficult. First, at a low HOB (approximately 15 feet for a 1 kt yield), the ejection crater disappears although compaction might still occur. At HOBs above the crater-formation cutoff, the one remaining source of dust is the thermally generated surface layer. Entrainment of this material is not instantaneous. Depending on the HOB, it may occur after the debris has cooled and condensed onto whatever nucleation sites are normally available in the atmosphere. Furthermore, the spatial distribution of the debris is changing from symmetrical to toroidal.

The approach taken to examine HOB effects employed the VORDUM code described elsewhere in this report to determine the fraction of the debris mass that was co-located with dust of various sizes at several times. The source of the dust is the surface layer.

The bomb debris was modeled as flow field trace particles distributed in a uniform density cylinder with radius equal to 0.5 the fireball radius. The vertical cylinder was fixed so that its volume equaled that of a sphere with a radius half the fireball radius. These assumptions are based on the best current estimation for describing the bomb debris. There is, however, continuing controversy about the radial extent of the debris at the time of pressure equilibrium. One-dimensional radiation hydrocodes predict the debris to be within 0.1 fireball radii of the burst point while photographic evidence indicates 0.5 radii. Currently it is the feeling of some researchers in this area that the hydrocode calculations are incomplete in that turbulence is not included. Figure 4.6 is a schematic of the two sources for a typical configuration.

Because the time at which fission debris condenses varies depending on the volatility of each mass chain, a range of times was selected for examination — 5 to 30 seconds. No attempt is made in this study to model the temperature history of the debris.

In the VORDUM calculation, the debris and the dust are represented as sets of trace particles. Associated with each trace particle is a fraction of the total debris or dust mass. The dust trace particles are tracked through the flow field and at several times a snapshot of their positions is obtained which defines a two-dimensional envelope of the dust region. The debris trace particles are tracked through the same flow field. At each snapshot time, their individual locations are examined to determine which (if any) are within the dust region. If a particular debris trace particle is within the dust, then the fraction of total debris which it represents is defined to be mixed with the dust. Shown in Figure 4.7 is a

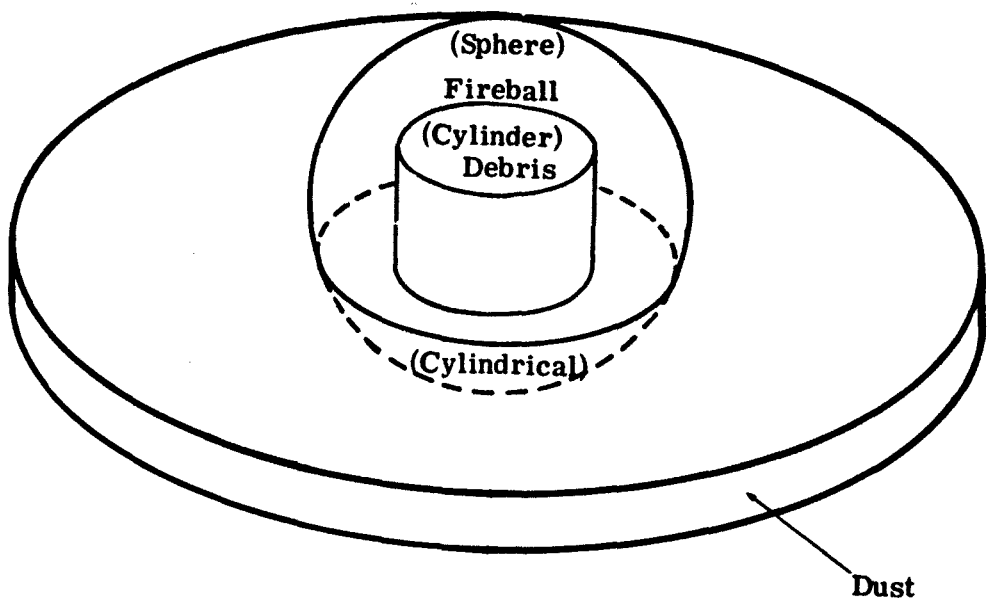

Figure 4.6. Schematic of Dust and Debris Sources

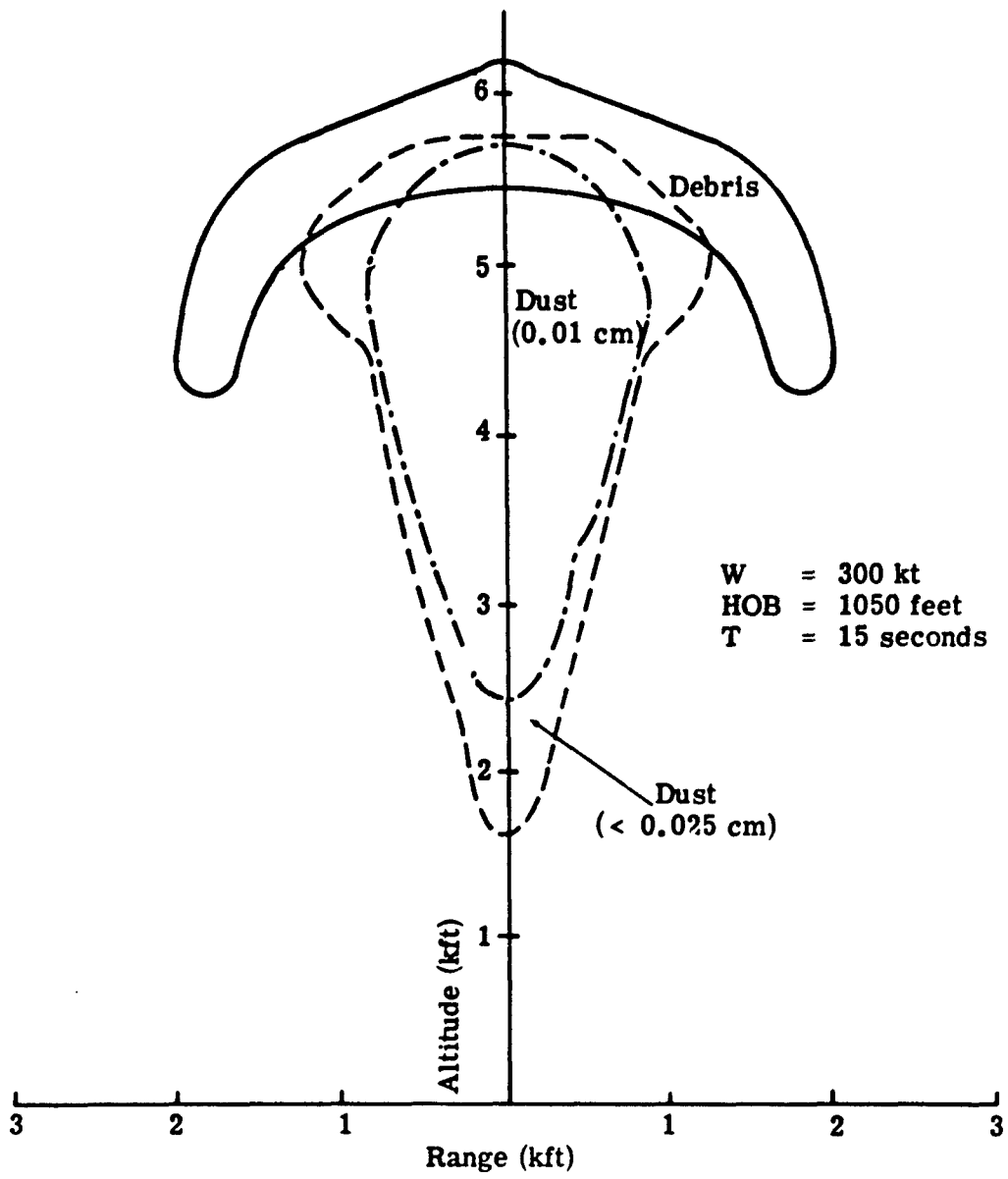

Figure 4.7. Comparison of Dust and Debris Regions for a Low Air Burst

typical output from VORDUM using the two sources described above. The parameters were a 300 kt burst at 1050 feet and the time at 15 seconds. The solid contour outlines the debris region while the two dashed contours correspond to dust particles with diameter of 0.025 cm and 0.1 cm respectively. The significance of this figure is that if 15 seconds is the time at which the debris condenses, then a prediction can be made about the fraction of the total debris that is not co-located with dust particles of a particular size. In this way, an upper limit can be obtained for the fraction of the debris that condenses onto dust particles as a function of size and HOB. Determination of such an upper limit avoids difficulties related to the condensation process itself as well as fractionation over the size spectrum of the dust. Hence, this analysis provides only a partial answer to the determination of HOB effects. As will be seen below, significant differences exist between these upper limits and the algorithms presently used in fallout codes and discussed above.

Three yields were investigated, 50 kt, 200 kt and 1 Mt. The VORDUM code was run for each at several heights of burst ranging from 96 feet (scaled to 1 kt by the cube root of the yield) up to 275 feet. No runs were made for cratering bursts. Four particle sizes were used — 0.025 cm, 0.050 cm, 0.1 cm, and 0.5 cm. The smallest of these is run in VORDUM with the assumptions of infinite drag coefficient and zero gravity so that the flow field is tracked perfectly. Consequently the 0.025 cm trace particles represent particles smaller than this size. Figures 4.8 - 4.10 show the HOB (scaled to 1 kt) dependence, of the fraction of debris mixed with dust (up to 0.025 cm) for the three yields respectively. Also, indicated on each figure are the two algorithms — F_1 is a fit to test data and F_2 is based on sphere-ground intersectio... In the 50 kt case, it is

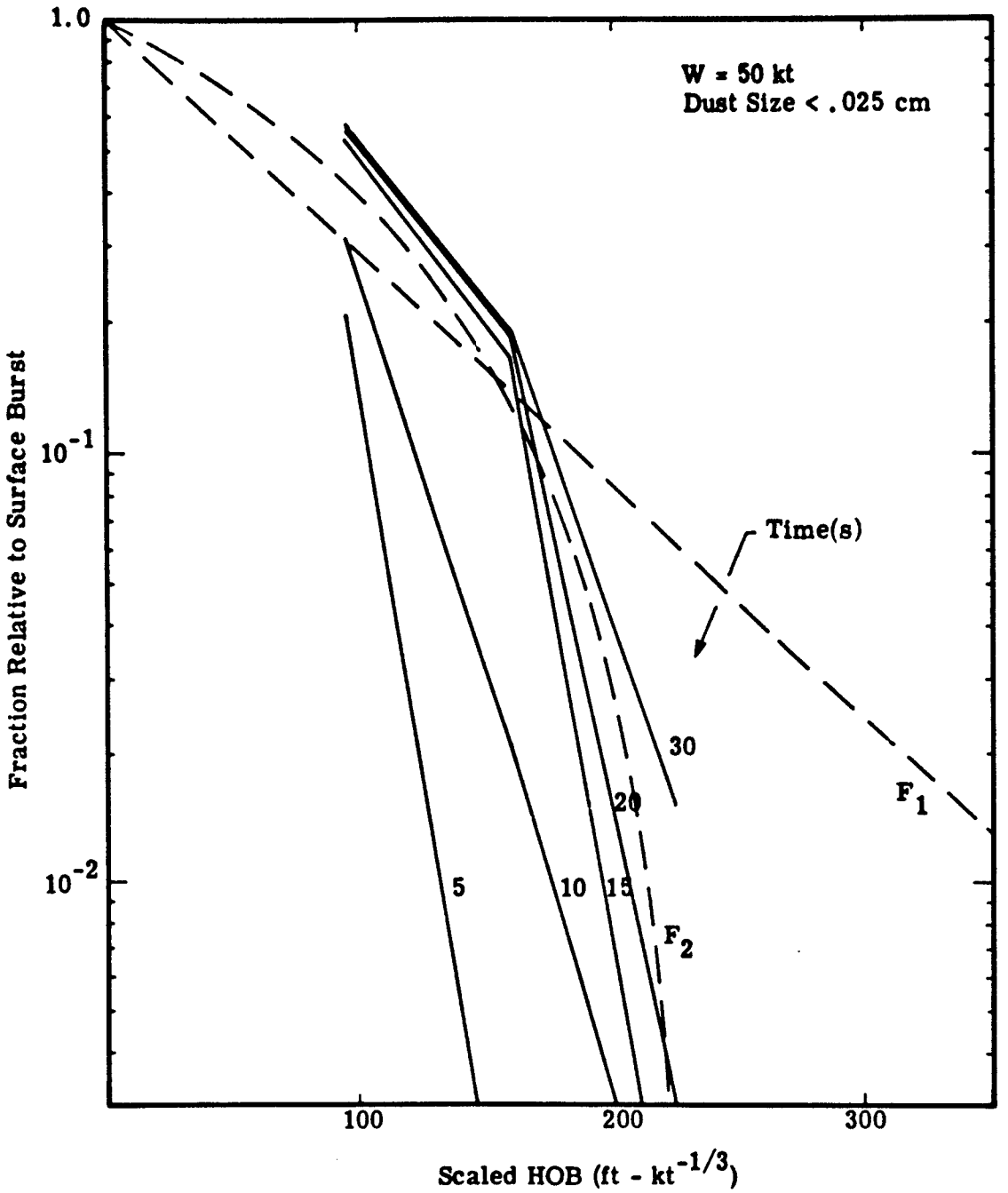

Figure 4.8. Fraction of Debris Mixed with Dust (Less Than .025 cm) Versus HOB for 50 kt

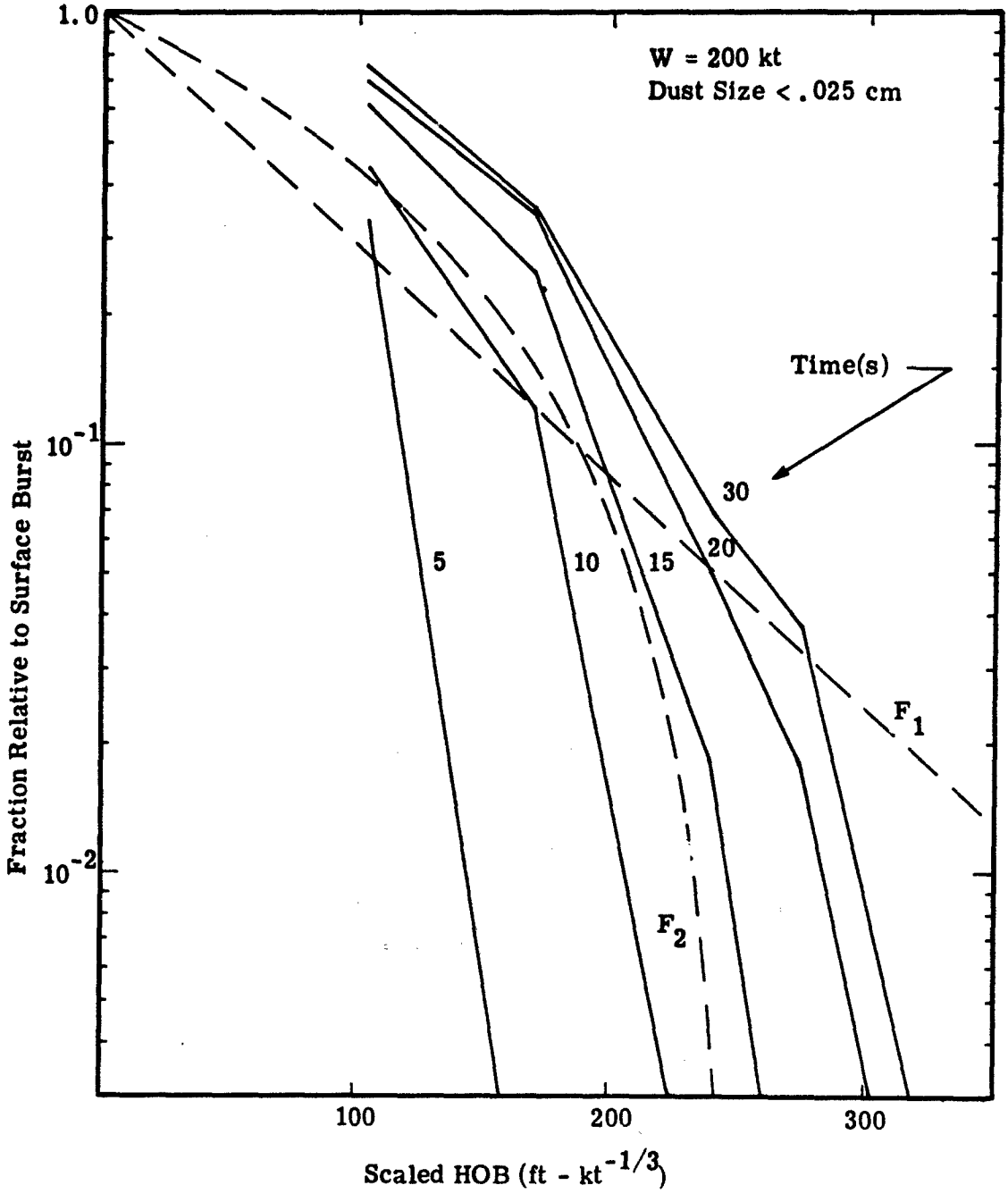

Figure 4.9. Fraction of Debris Mixed with Dust (Less Than .025 cm) Versus HOB for 200 kt

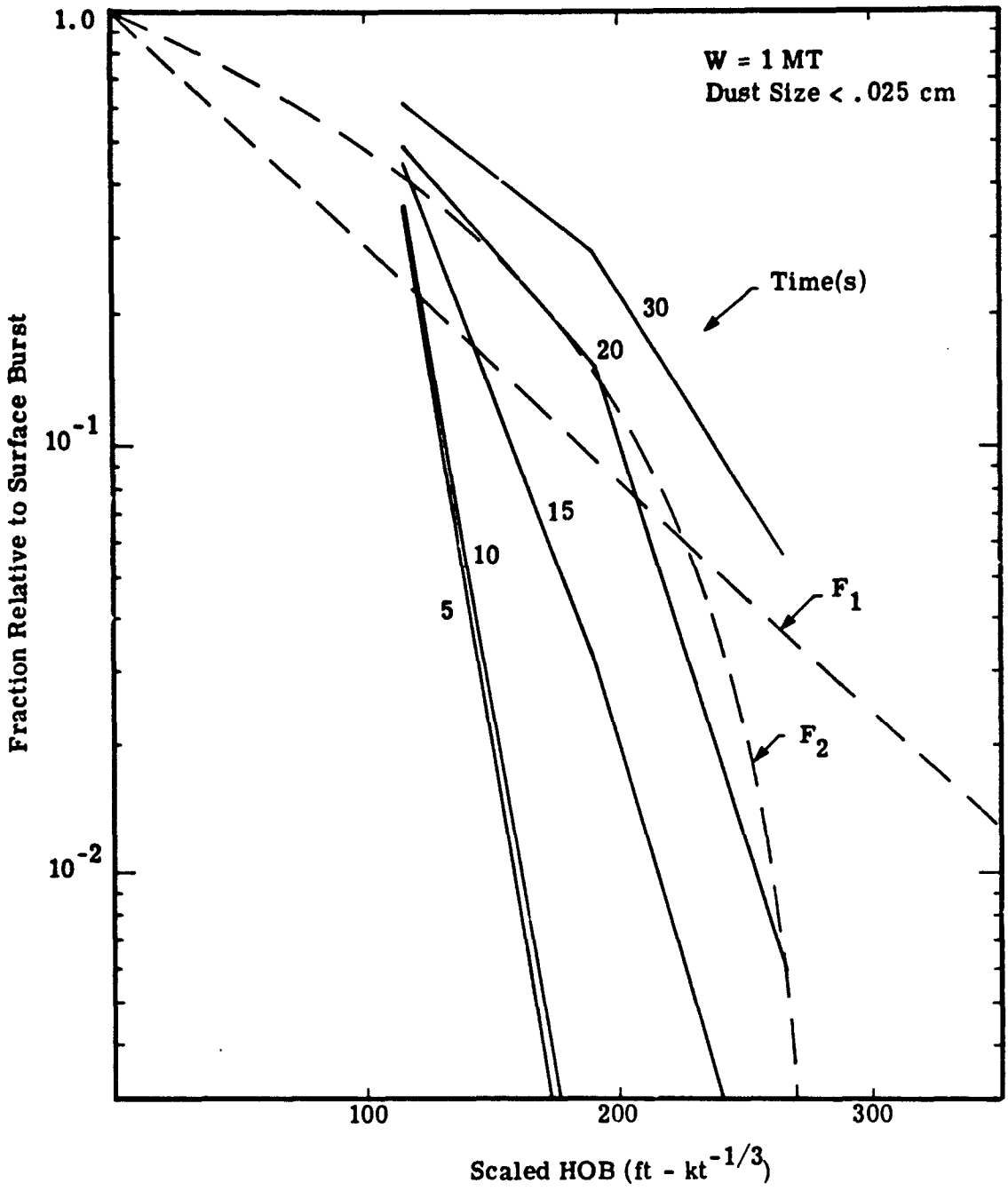

Figure 4.10. Fraction of Debris Mixed with Dust (Less Than .025 cm) Versus HOB for 1 Mt

apparent that F_1 is overestimating the fallout activity for scaled HOBs above 200 feet. The present calculations tend to support the F_2 curve for times greater than 15 seconds. However, if debris condensation and attachment to the dust is occurring much earlier (e.g., 5 sec), then F_2 is also an overestimate. Comparison at 200 kt again indicates F_1 to be higher than either F_2 or the calculations above a scaled HOB of 275 feet. At 1 Mt a similar comparison can be made.

Figures 4.11 through 4.18 depict F_1, F_2 and the calculations of dust-debris mixing for the three yields, but for dust particle diameters from 0.05 cm to 0.5 cm. The dust trace particles used for these sizes were subject to finite drag and gravity. The fraction of debris mixed with dust decreases with increasing size. For example Figures 4.11 and 4.14 show, in contrast with the small dust sizes (Figure 4.8) that for 50 kt, both the F_1 and F_2 algorithms are too high for scaled HOBs above 100 feet. However, this size effect has a yield dependence as can be seen from Figures 4.13, 4.16 and 4.18.

An important observation on the calculations is the HOB above which there is no mixing by 30 seconds. Although not shown on the figures, all yields were examined for the HOB such that the fireball just touches the ground. In no case was there any mixing of dust (of any size) and debris.

The above analysis is incomplete in the sense that the condensation of the fission debris is not modeled. However, the results do indicate that for yields above 200 kt, the F_2 algorithm is more realistic than F_1 for scaled heights of burst above 200 feet.

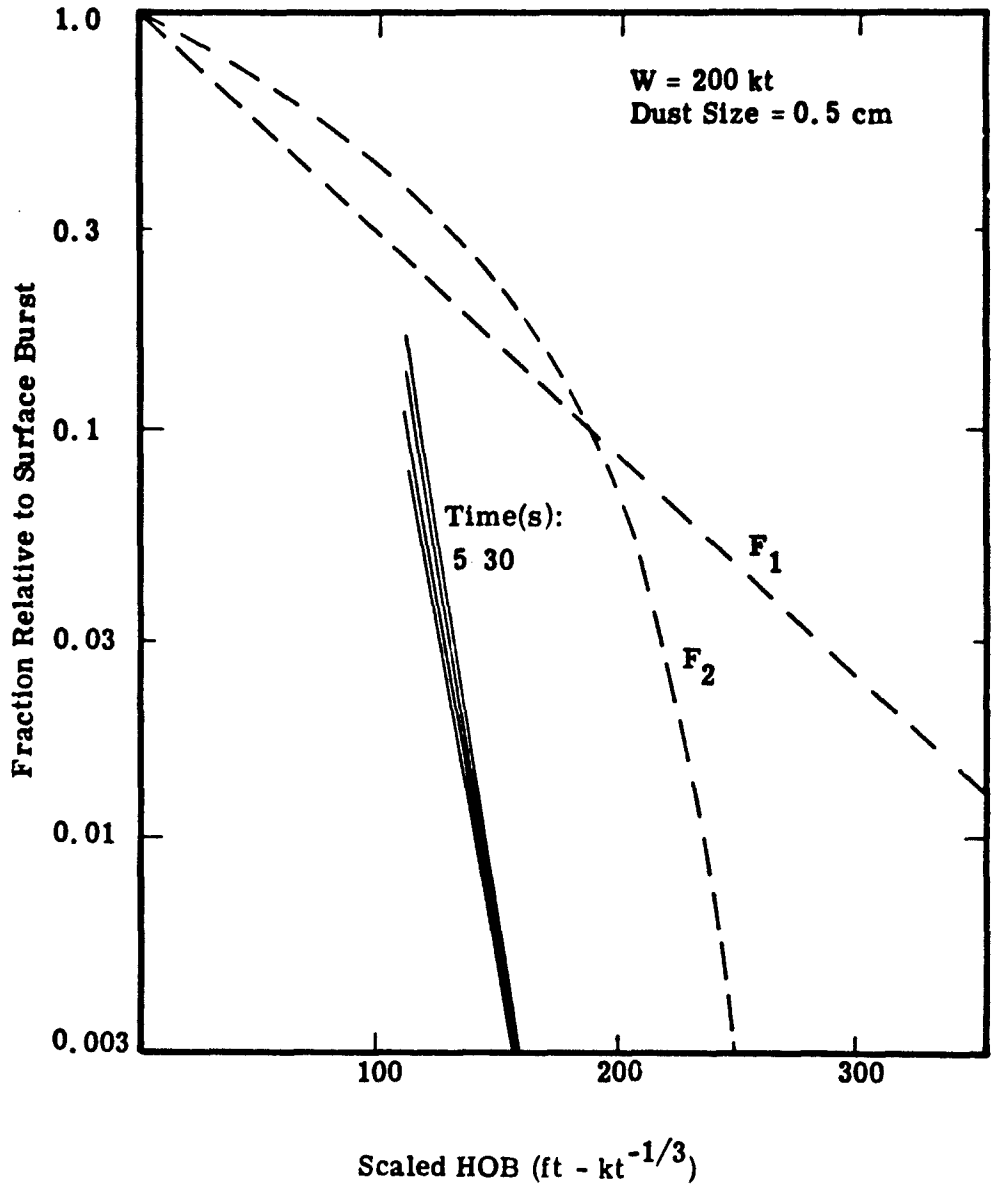

Figure 4.11. Fraction of Debris Mixed with Dust (0.5 cm) Versus HOB for 200 kt

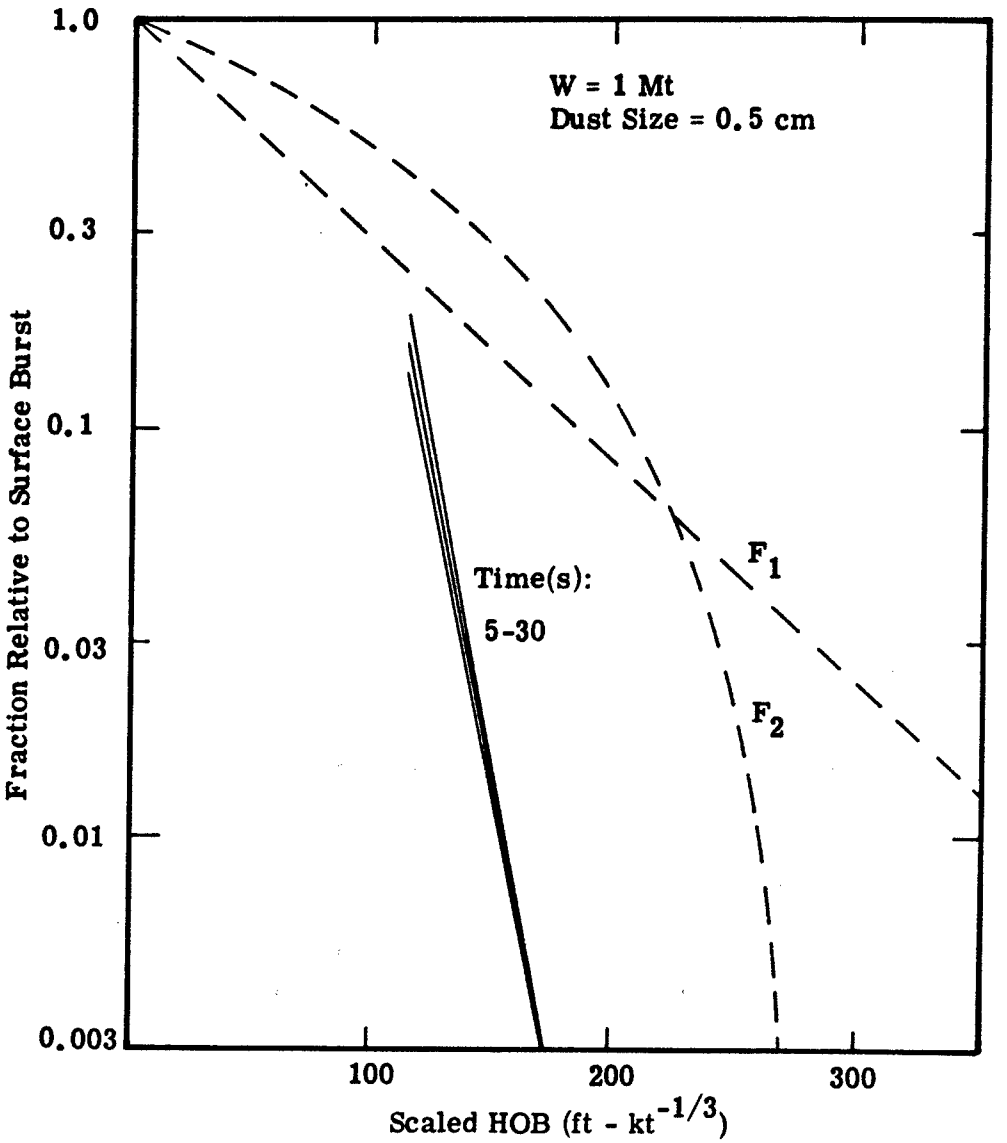

Figure 4.12. Fraction of Debris Mixed with Dust (0.5 cm) Versus HOB for 1 Mt

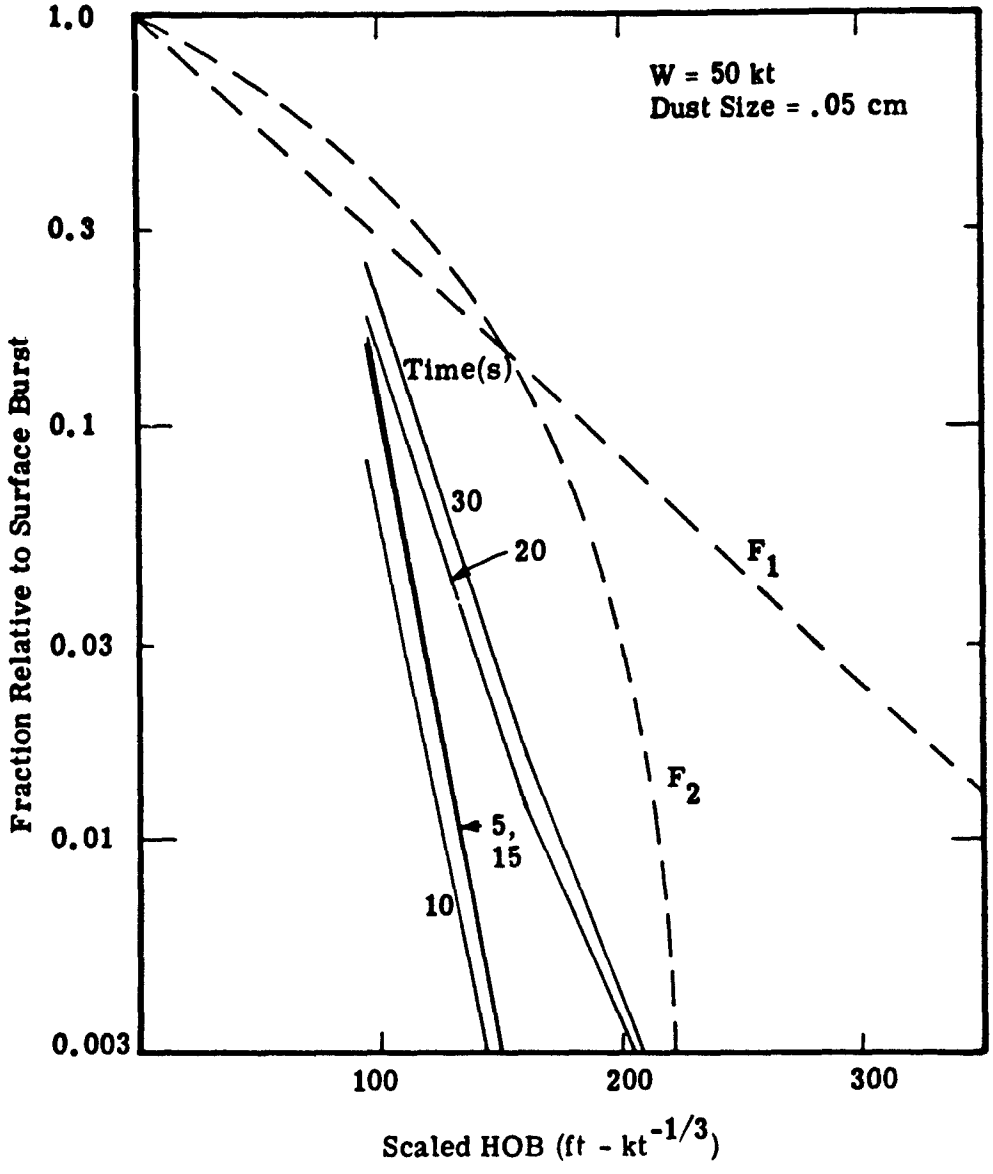

Figure 4.13. Fraction of Debris Mixed with Dust (0.05 cm) Versus HOB for 50 kt

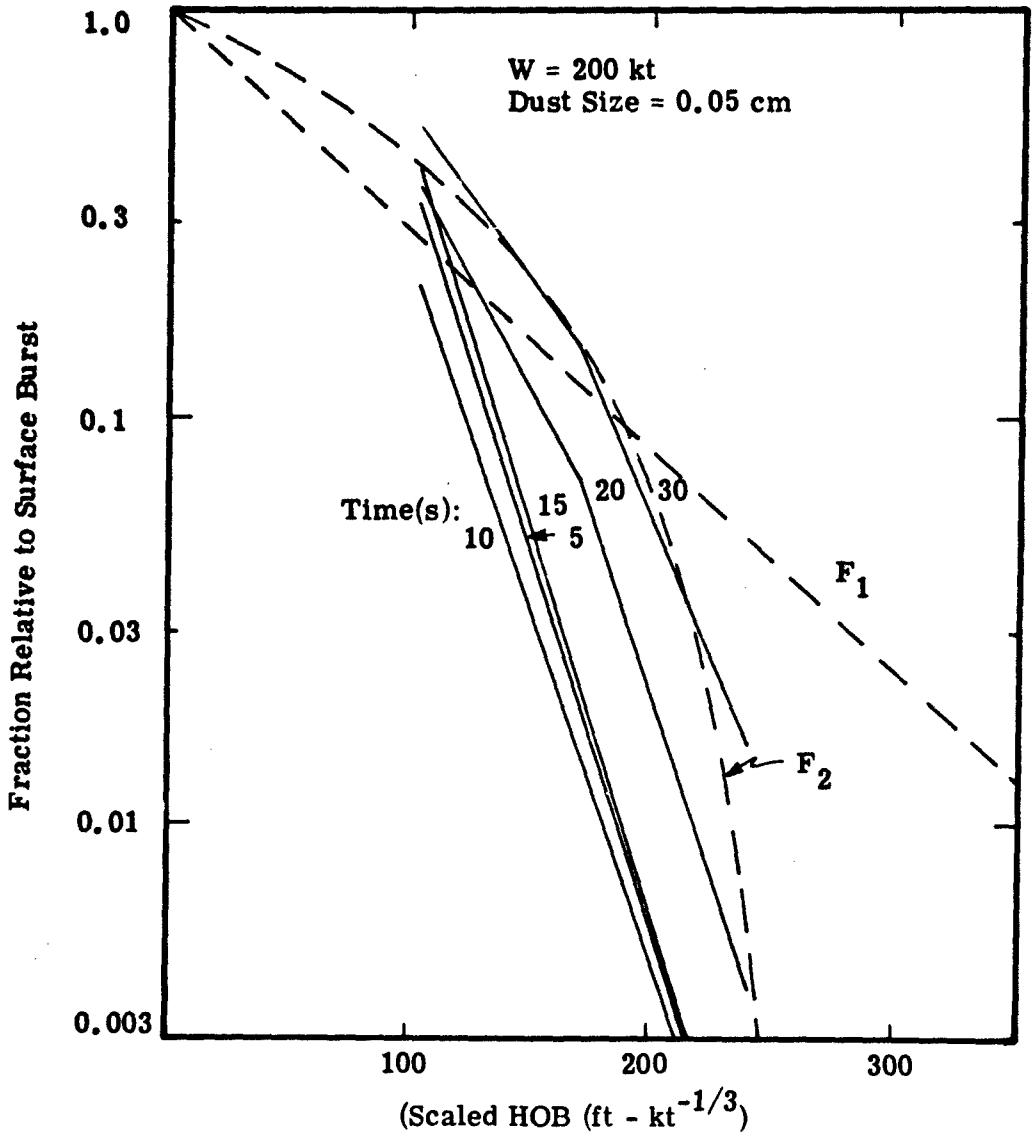

Figure 4.14. Fraction of Debris Mixed with Dust (0.05 cm) Versus HOB for 200 kt

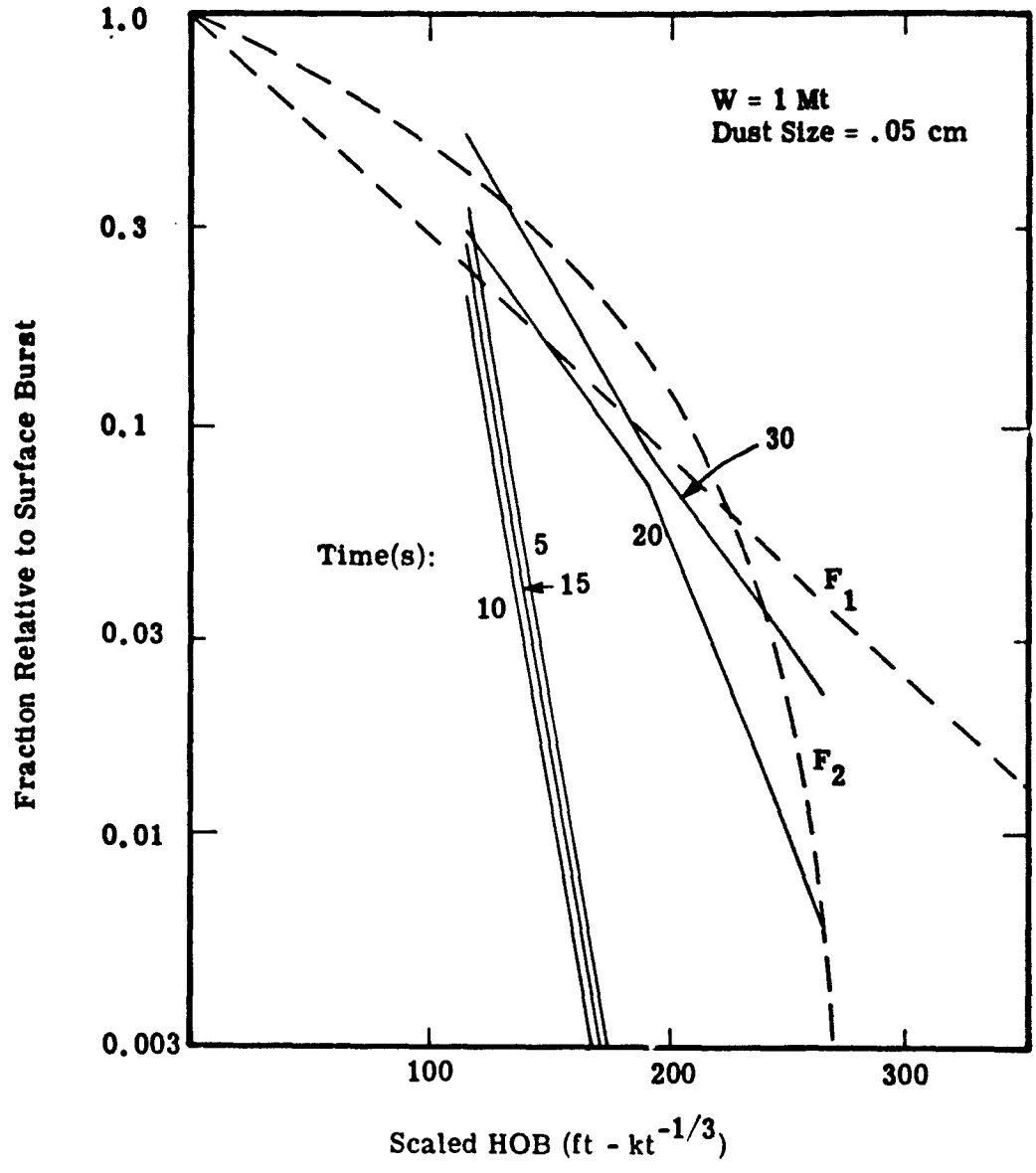

Figure 4.15. Fraction of Debris Mixed with Dust (.05 cm) Versus HOB for 1 Mt

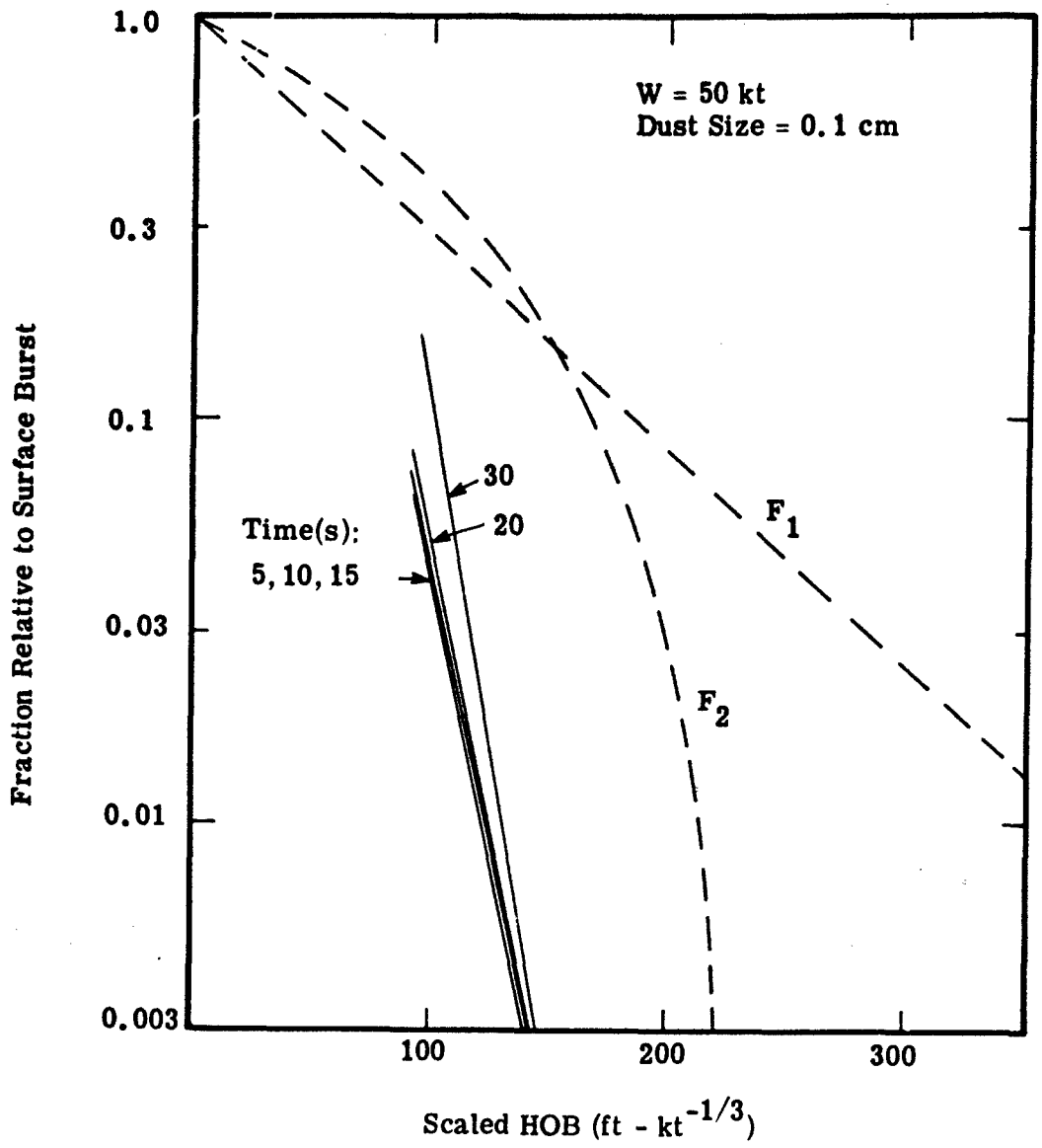

Figure 4.16. Fraction of Debris Mixed with Dust (0.1 cm) Versus HOB for 50 kt

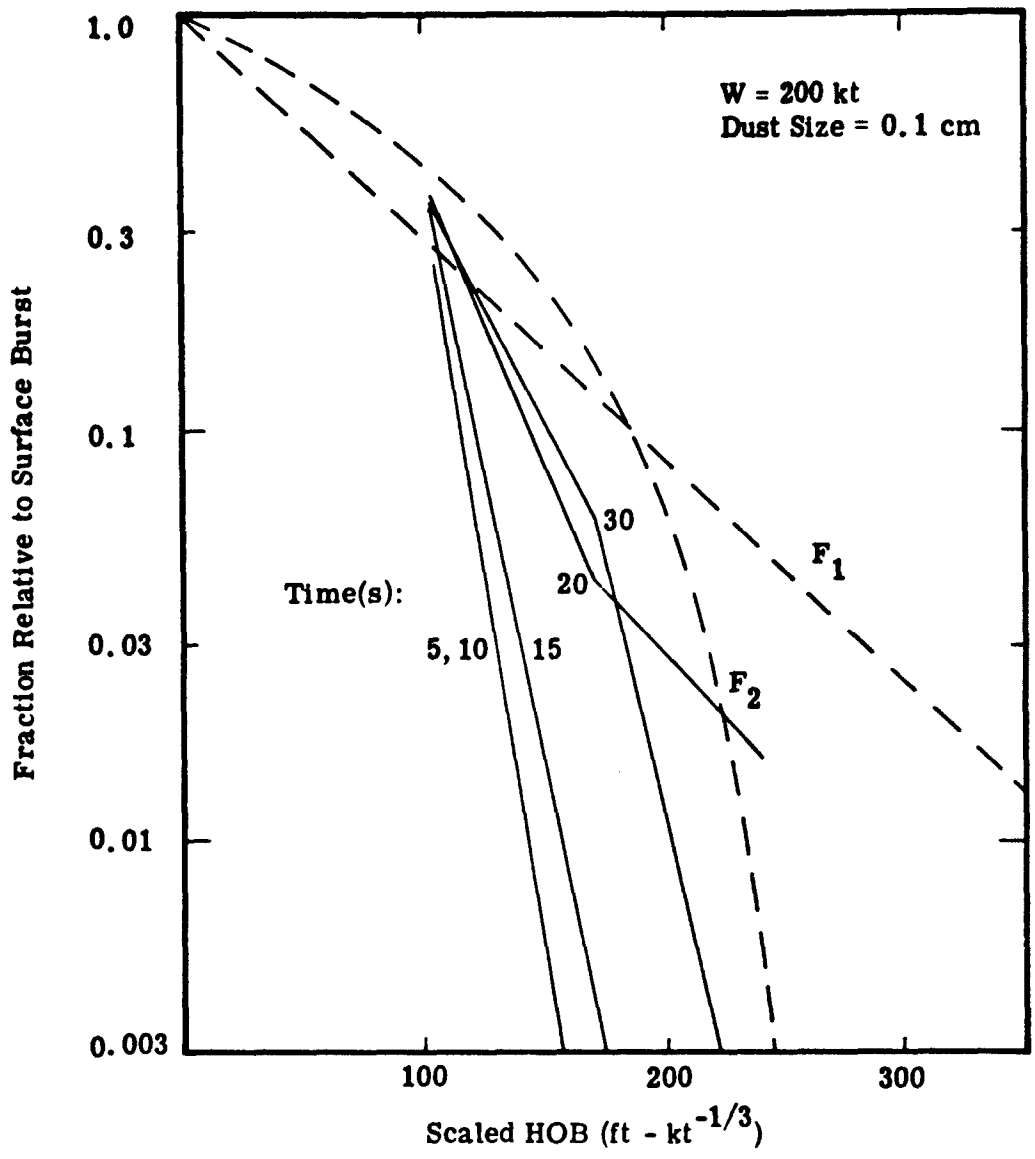

Figure 4.17. Fraction of Debris Mixed with Dust (0.1 cm) Versus HOB for 200 kt

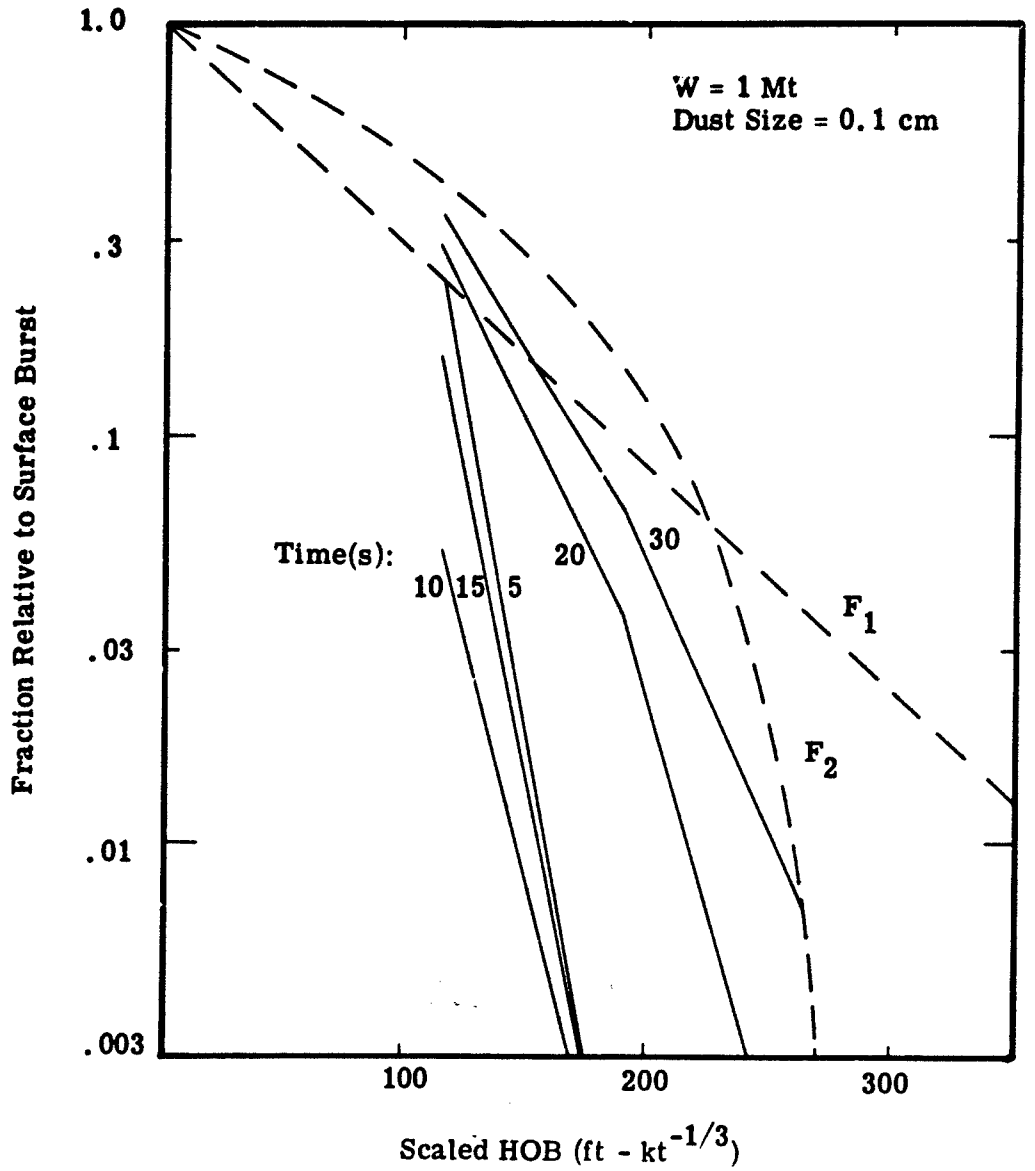

Figure 4.18. Fraction of Debris Mixed with Dust (0.1 cm) Versus HOB for 1 Mt

Both of these prescriptions overestimate by approximately an order of magnitude. The very close-in fallout (due to dust larger than 0.05 cm which will have times of arrival up to an hour) from low yield (e.g., 50 kt) weapons burst above 150 scaled feet.

4.3 REFERENCES

1. R. Heft, "The Characterization of Radioactive Particles from Nuclear Weapons Tests," UCRL-70790, Lawrence Livermore Laboratory, University of California, Livermore, California, 1968.

2. J. Maloney, Ballistic Research Laboratories, U.S. Army, Aberdeen Research and Development Center, Aberdeen, Maryland, private communication, 1974.

3. W. M. Layson, Science Applications, Inc., McLean, Virginia, Private communications, 1974.

4. M. Tobriner, et al., "Technology Support for Environmental Defense — Second Bimonthly Progress Report," SAI-74-561-WA, Science Applications, Inc., McLean, Virginia, 1974.

5. R. L. Showers, "Improvements to the PROFET Fallout Prediction Program," BRL Memorandum Report 2095, (AD-883-280), Ballistic Research Laboratories, U. S. Army Aberdeen Research and Development Center, Aberdeen, Maryland, February, 1971.

6. Draft, Effects of Nuclear Weapons, October, 1973.

Section 5

SENSITIVITY TO CLOUD MODEL ASSUMPTIONS DURING RISE

5.1 NONUNIFORM MASS DISTRIBUTION

The sensitivity of the fallout predictions to the DELFIC assumption of uniform density mass wafers was investigated using the output from a 3 Mt VORDUM run. VORDUM is an analytic model which has been developed to describe the air and dust/debris motion inside and around a nuclear cloud. Inside the cloud the air motion takes the form of a spheroidal vortex which persists as the cloud rises, while the motion outside the cloud is that induced by a spheroid moving through an inviscid fluid. The model uses empirical equations for rise velocity and radial expansion.

The procedure followed in making comparisons was to first insert the DELFIC rise and expansion equations into VORDUM. A total of 1656 trace particles, representing the same particle size class range that was used for DELFIC, was run in VORDUM until stabilization time. The cloud defined by these particles was then radially expanded according to the DELFIC equations until 848 seconds after burst, the time at which the Cloud Rise Module ends. Figure 5.1 is a comparison of the two clouds at this time. Since both VORDUM and DELFIC produce cylindrically symmetric clouds, this figure consists of cloud contours in the R and Z coordinate system. Shown are the maximum cloud extents and the average densities within the clouds. The DELFIC cloud is larger radially and contains less mass than the VORDUM cloud, and is consequently less dense. The VORDUM cloud also contains larger particles.

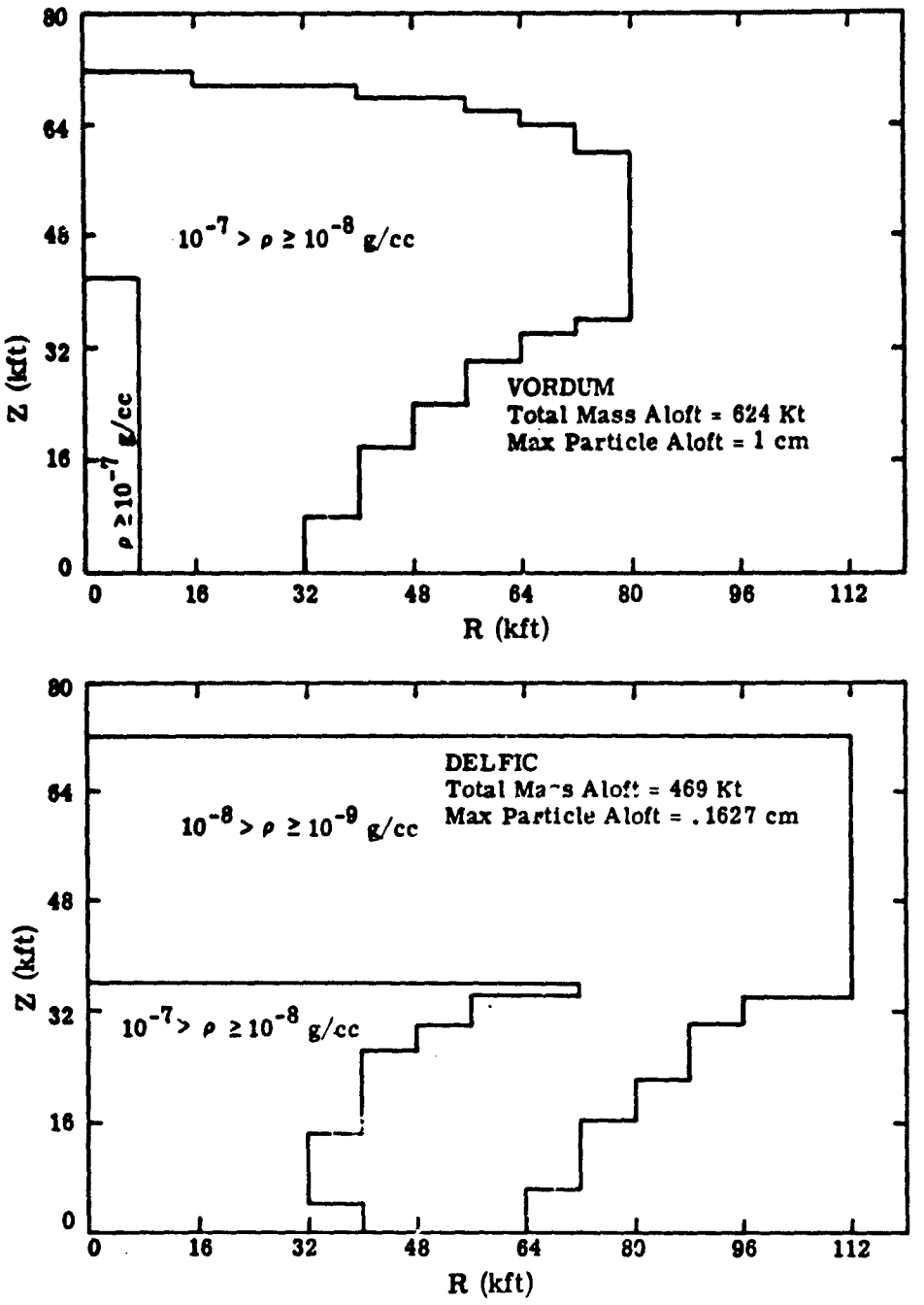

Figure 5.1. The VORDUM and DELFIC Clouds Compared at 848 Seconds

A comment on the generation of the above cloud contours is in order. VORDUM has associated with it a density program which outputs mass and number densities, as well as radar reflectivity and attenuation information. No such program exists with DELFIC. Subroutine RSXP has the option of printing the pertinent information for each wafer, and this information was used in producing the desired contours. However, an examination of the output showed certain discrepancies, and modifications had to be made to produce meaningful results. Appendix A contains an explanation of these discrepancies and the methods used to correct them.

Comparisons between the particle positions predicted by the two codes were made using the procedures discussed above. Figures 5.2 through 5.5 show the volumes of space occupied by the specified particles transported through the two codes. It can be seen that overlapping volumes exist only for particles smaller than 0.1441 cm.

Discrepancies in the grounded particles tape, discussed in Appendix B, as well as the large non-overlapping regions of the two clouds, make a meaningful comparison of the fallout from the two models extremely difficult. The following simplifying assumptions were made to reduce the degree of difficulty:

a. Only wafers aloft at 848 seconds were considered.

b. Only wafers co-located with similar VORDUM particles were considered.

c. The mass in each wafer was constant, but the density was changed to reflect the generally smaller VORDUM particle occupied regions.

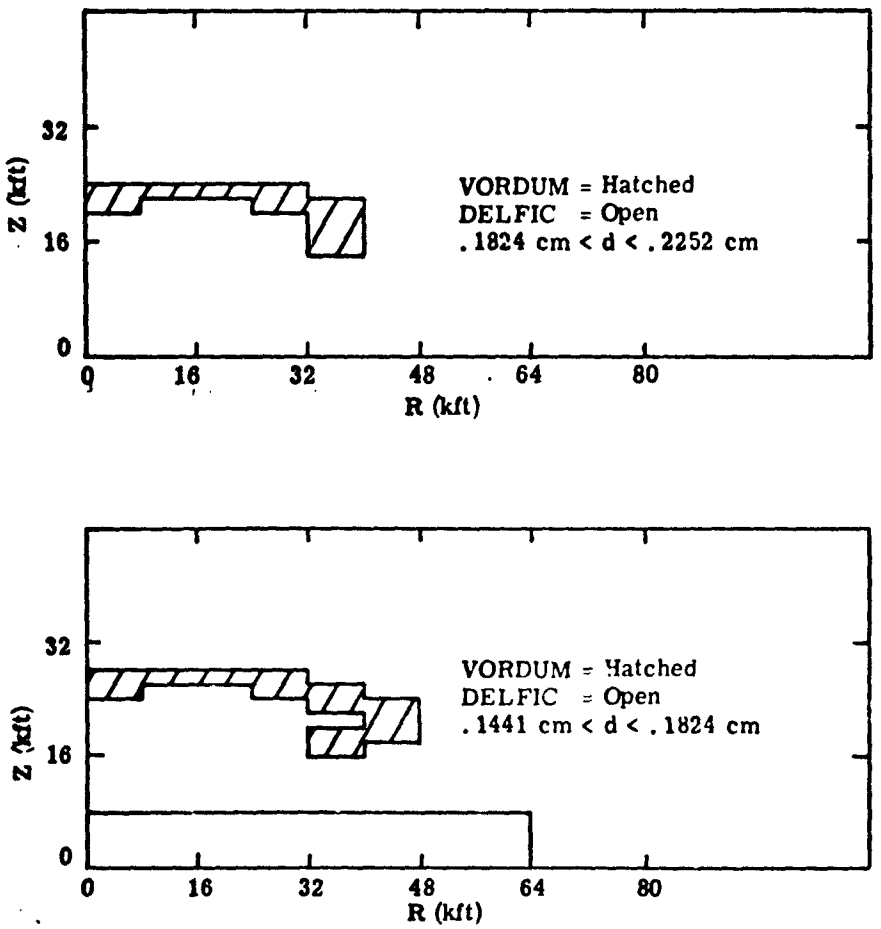

Figure 5.2. Comparison of Particle Positions Produced by VORDUM and DELFIC

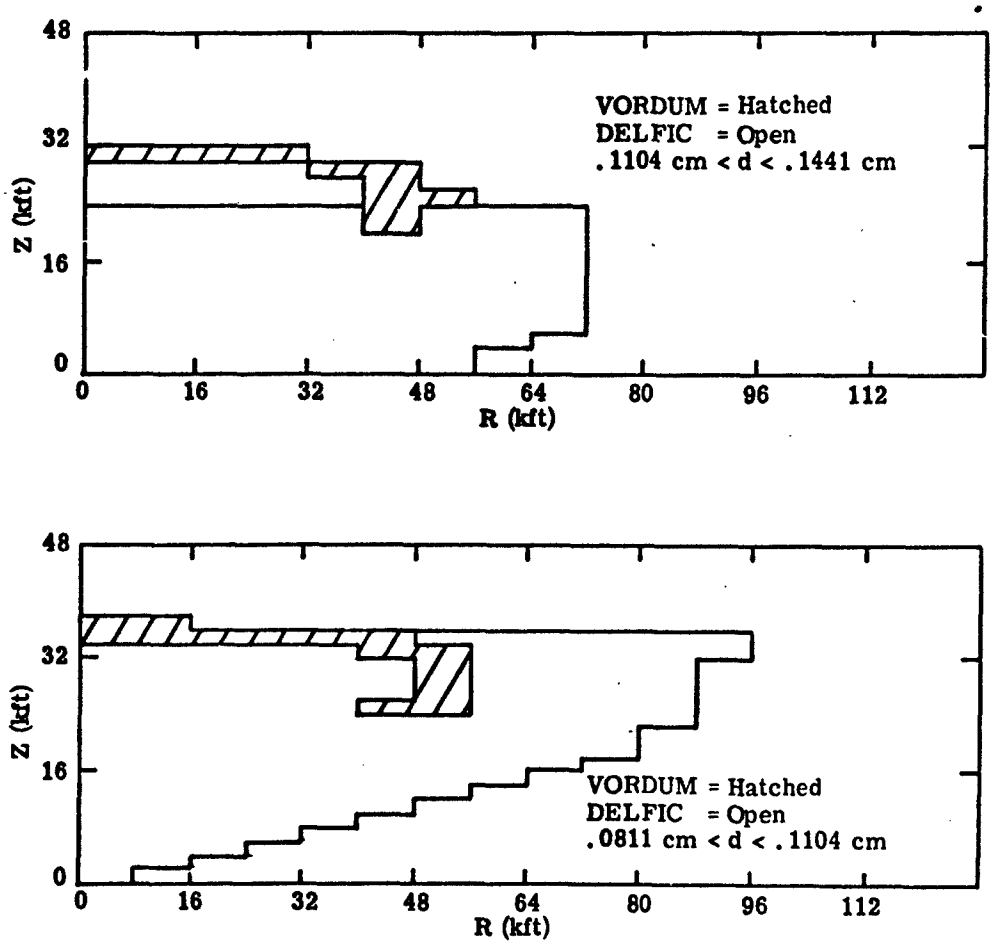

Figure 5.3. Comparison of Particle Positions Produced by VORDUM and DELFIC

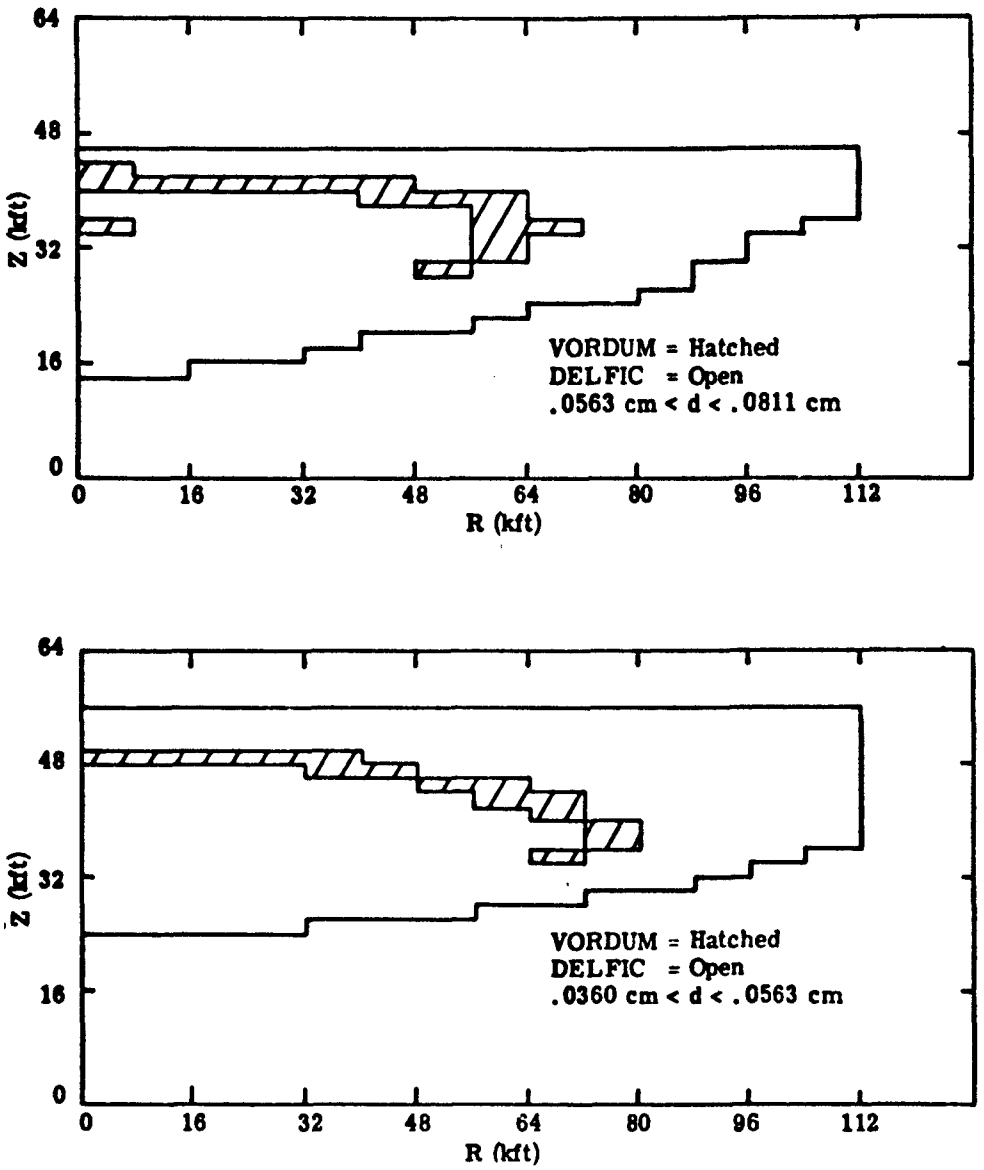

Figure 5.4. Comparison of Particle Positions Produced by VORDUM and DELFIC

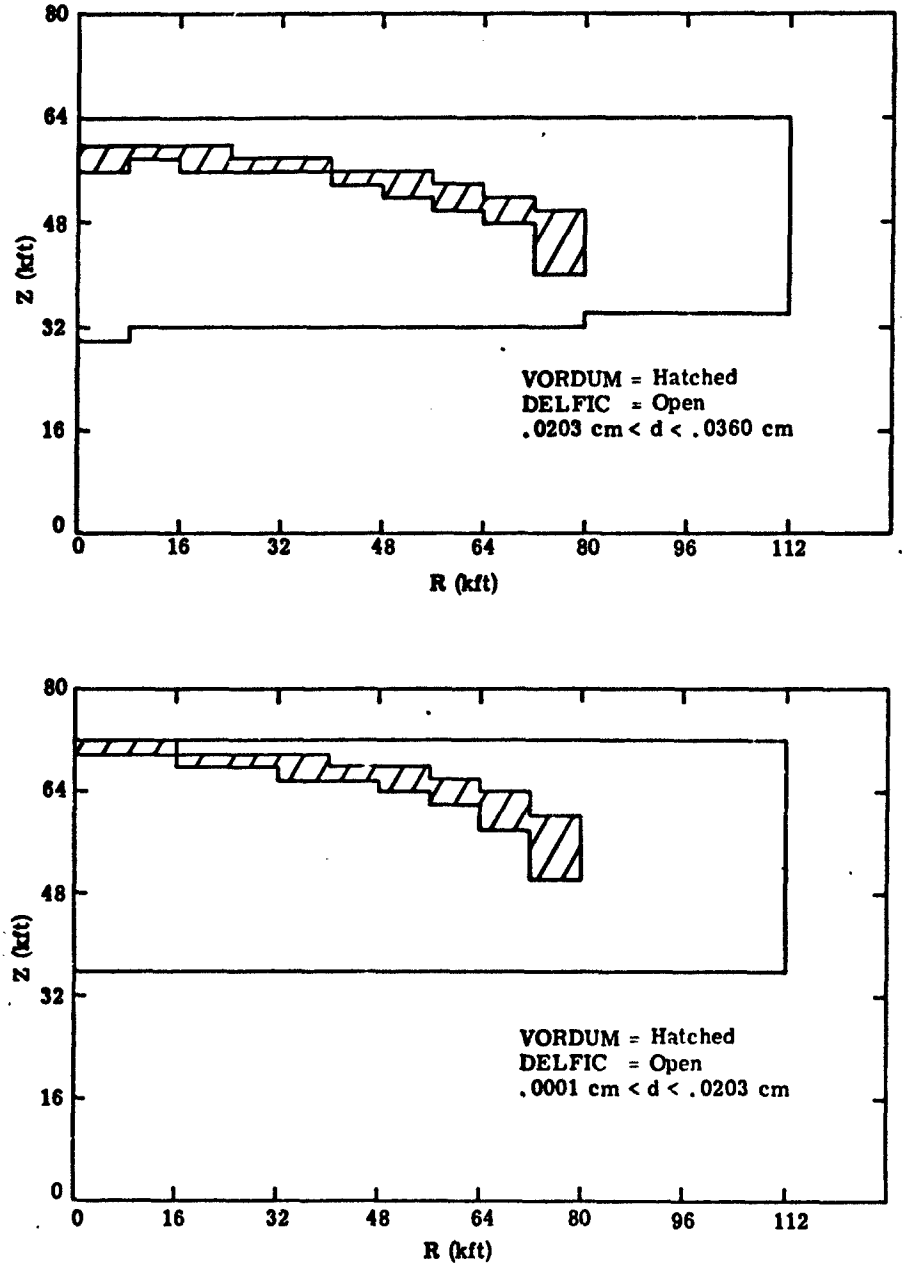

Figure 5.5. Comparison of Particle Positions Produced by VORDUM and DELFIC

d. Only VORDUM particle positions were important, not relative density.

e. The modified DELFIC wafer mass was still uniformly distributed over the annuli.

Figure 5.6 is a simplistic example of the procedure used in generating a new grounded particle tape. The 3 Mt DELFIC tape, which contained 1987 particles, was modified to one of 323 particles. These particles represent most of the long range fallout particles. A modified version of LINTAP (discussed in Section 2) was produced to predict fallout from the annuli created from the wafers so that one-to-one comparisons could be made.

Figures 5.7 through 5.9 are dose rate normalized to H+1 hour, integrated dose, and time of arrival, respectively, of the fallout predicted from both clouds along a line 345° to the horizontal, the chosen "hotline." These curves can be interpreted quite easily by reference to Figure 5.1. The radius of the VORDUM cloud is approximately two-thirds that of the DELFIC cloud, so if the densities in each wafer were changed to reflect just this fact, the dose rate, which is proportional to the density, should be higher by a factor of 2 for the VORDUM density cloud. Also, since the VORDUM modified wafers are generally smaller than the standard wafers, they do not extend as far along the hotline, and consequently, the time of arrival more closely reflects the wafers which fell earlier uprange and extend over a wide area.

In summary, it appears that the assumptions of uniform density mass wafers can vary the predicted fallout by a factor of 2, and the time of arrival calculations can be 1000 seconds early.

1) Volumes Occupied by VORDUM and DELFIC Particles of Diameter d, at 848 seconds after burst.

2) Only Wafers 1, 2, 3, and 4 retained.

3) Total Mass Aloft = $Mass_{\#1} + Mass_{\#2} + Mass_{\#3} + Mass_{\#4}$

4) New Wafer Radii

#1 = 0 to 16
#2 = 16 to 32
#3 = 16 to 56
#4 = 24 to 56

5) New Mass in Wafer 2 = Old Mass in Wafer 2

$$\text{New Mass Density in Wafer 2} = \frac{(\text{Old Mass Density in Wafer 2}) \times 80^2}{32^2 - 16^2}$$

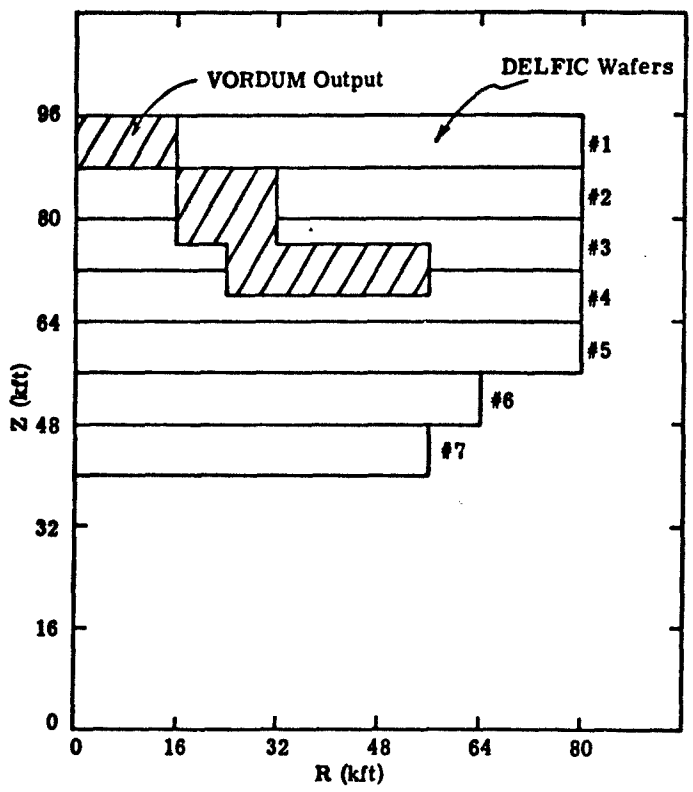

Figure 5.6. Pictorial Representation of Simplifying Assumptions

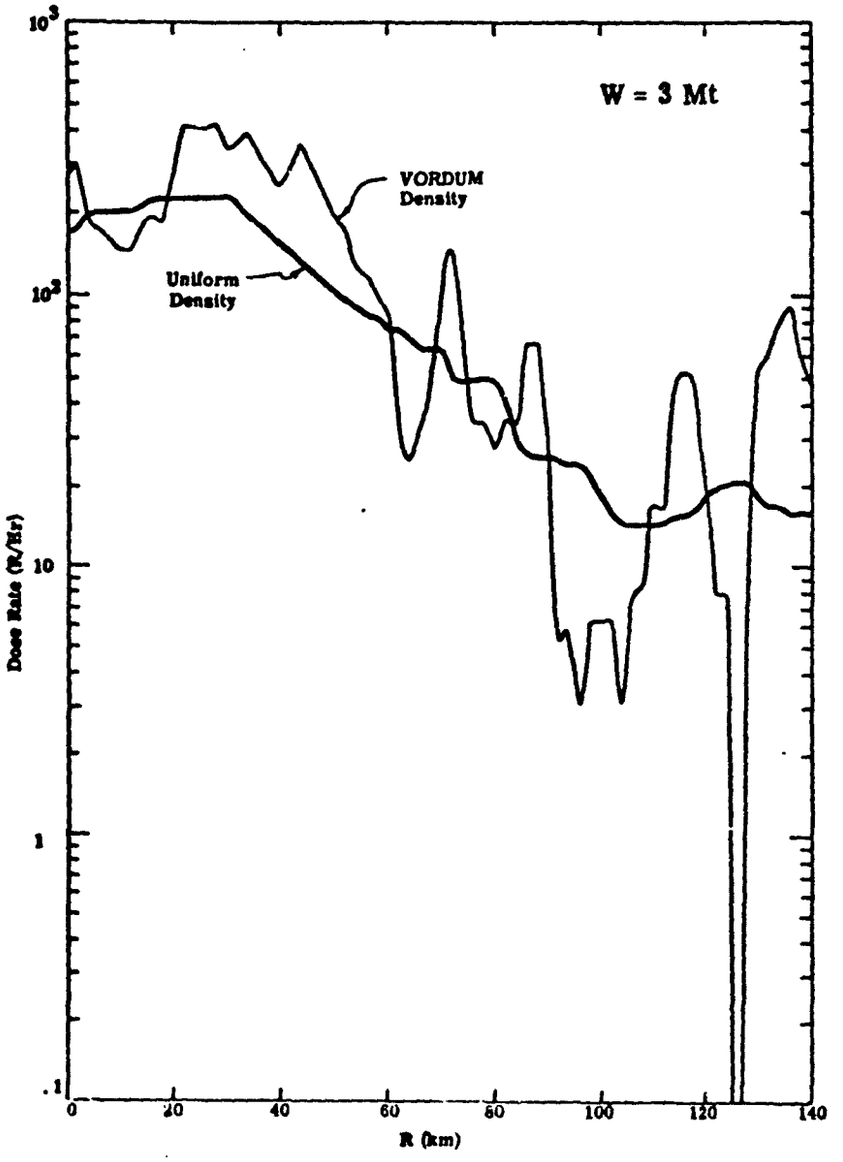

Figure 5.7. Comparison Between Uniform Density Wafers and VORDUM Mass Distribution Annuli Along the Cloud Hotline

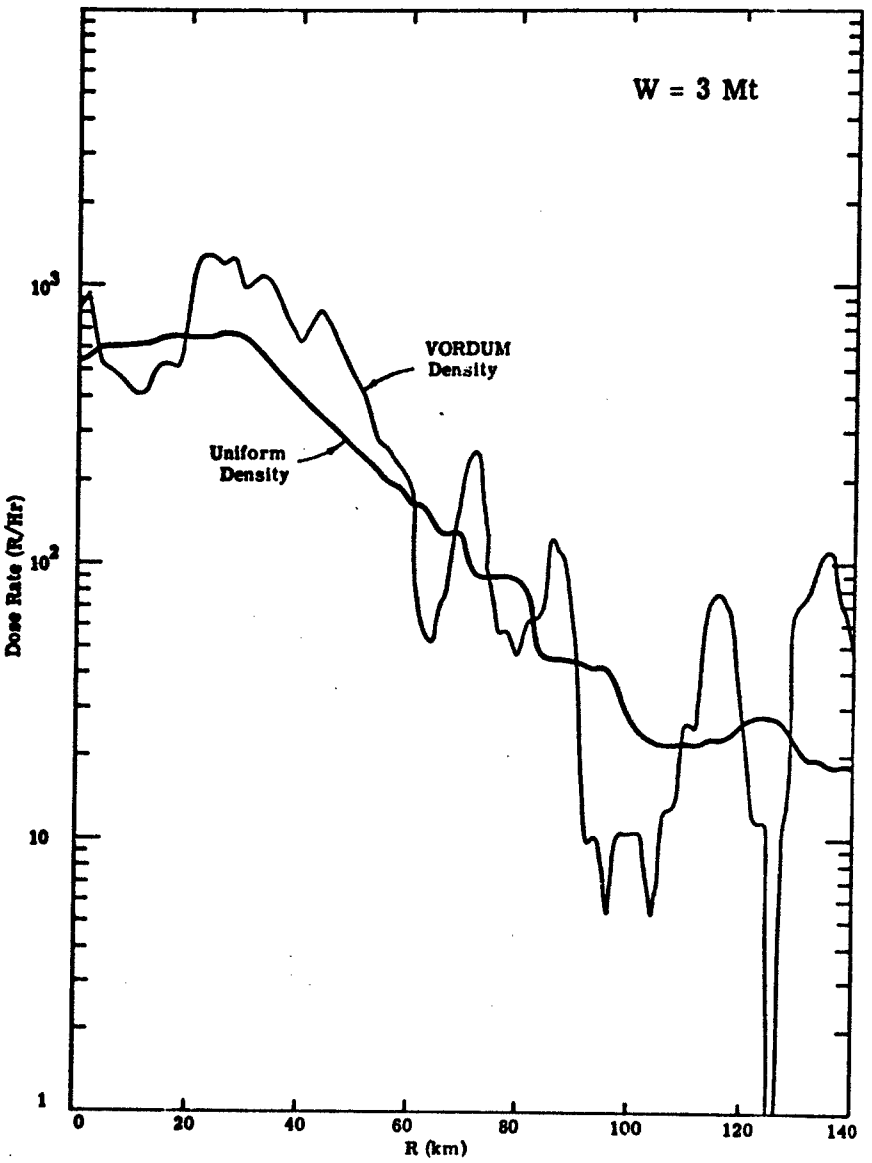

Figure 5.8. Comparison Between Uniform Density Wafers and VORDUM Mass Distribution Annuli Along the Cloud Hotline

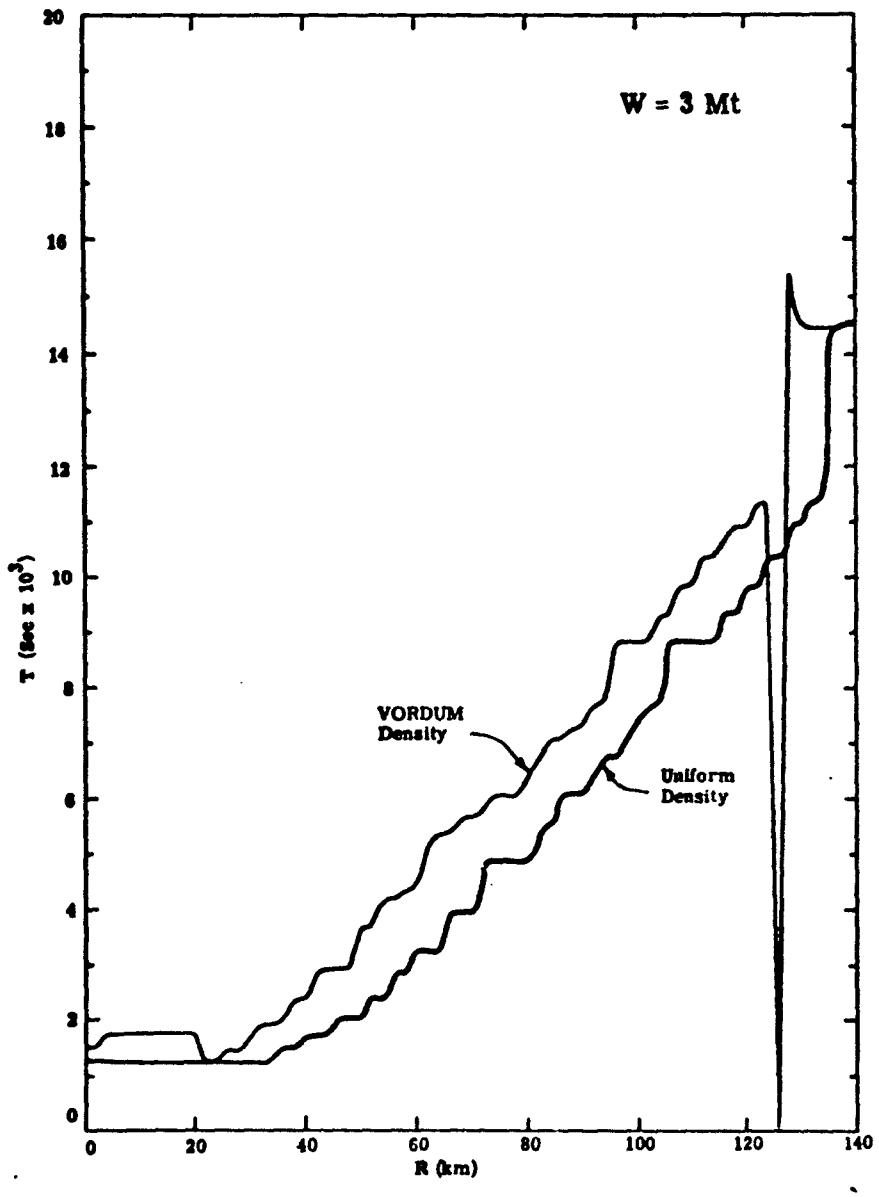

Figure 5.9. Comparison Between Uniform Density Wafers and VORDUM Mass Distribution Annuli Along the Cloud Hotline

5.2 SENSITIVITY TO CLOUD RISE DYNAMICS

DELFIC calculates the rise history of the cloud thermodynamically including the effects, for example, of latent heat release as the entrained atmospheric water vapor in the cloud condenses. The principal drawback of this approach is that some parameters must be predetermined since there is at least one more unknown than constraining equations. In particular, the cloud's horizontal radius is obtained from the volume and vertical thickness assuming an oblate spheroidal shape. VORDUM, on the other hand, uses empirically determined equations for rise velocity, radius, and cloud top. At high yields, the standard deviation on fits to these parameters is typically on the order of 10 percent. In the low-kiloton range, however, there is significantly higher uncertainty since atmospheric conditions especially the lapse rate play a more significant role.

In the course of this study, it was found that the DELFIC and VORDUM rise parameters differed significantly. To determine the effect this has on the fallout calculations, VORDUM was exercised for three yields – 30 kt, 300 kt, and 3 Mt, using both the standard VORDUM equations for rise and expansion and the DELFIC predictions for these parameters. Figure 5.10 is a comparison of cloud shapes and densities for the standard VORDUM and the special case with DELFIC rise parameters at 4.75 minutes for the 300 kt case. It can be seen that the standard VORDUM lofts the dust higher but the two clouds are similar in shape and structure.

To make a comparison on the basis of fallout dose levels, the VORDUM program was modified to include the same wind field used in DELFIC for this study. In addition, VORDUM was extended in time to calculate the time and position of grounding for the trace

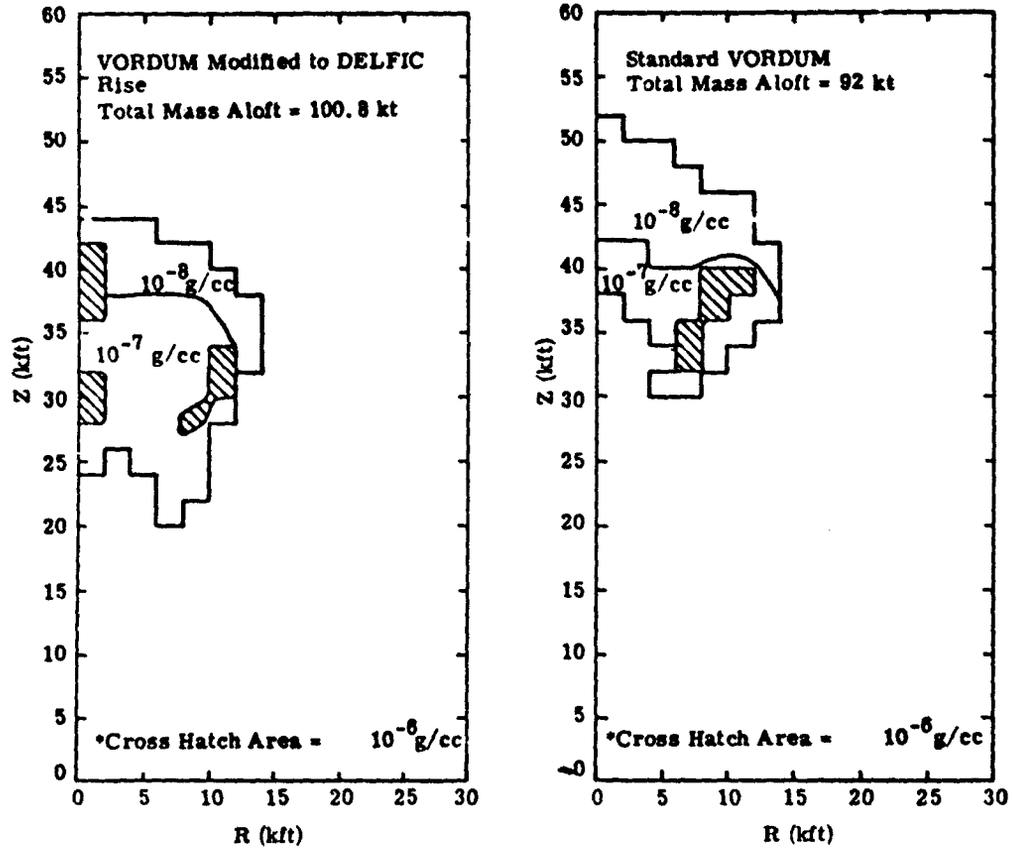

Figure 5.10. Comparison of Modified VORDUM Cloud with Standard VORDUM Cloud for W = 300 kt, at T = 4.75 Minutes

particles. A modified version of LINTAP was created to calculate the predicted dose rates for the two sets of VORDUM trace particles at each of the three yields. The major modification was the assignment of mass to annuli rather than to disks. A grounded particles tape was created for input to this modified LINTAP.

Figure 5.11 compares the standard VORDUM rise with that predicted by the Cloud Rise Module for 30 kt. The cloud bottom predicted by VORDUM stabilizes later and much higher than DELFIC would predict (8.7 km versus 5 km). Figure 5.12 shows the dose rate (normalized to H+1 hr) that results using the two rise formalisms in VORDUM. The irregularity in the curves is due to the limited number of trace particles used in the VORDUM runs but it would appear that the average deviation for the range 0 to 8 km is on the order of a factor of 5 to 10. However, local variations can be several orders of magnitude.

At higher yields, the discrepancy in rise is not quite so severe. Figure 5.13 depicts the cloud bottom and radius for the 300 kt case and Figure 5.14 compares the dose rate at H+1 hr for the standard and the DELFIC-modified cases. As can be seen, there is significantly better agreement here than at lower yields. Figure 5.15 shows the comparison for 3 Mt and confirms this observation.

5.3 REFERENCES

1. J. Shannon, Science Applications, Inc., McLean, Virginia, Private communication, 1974.

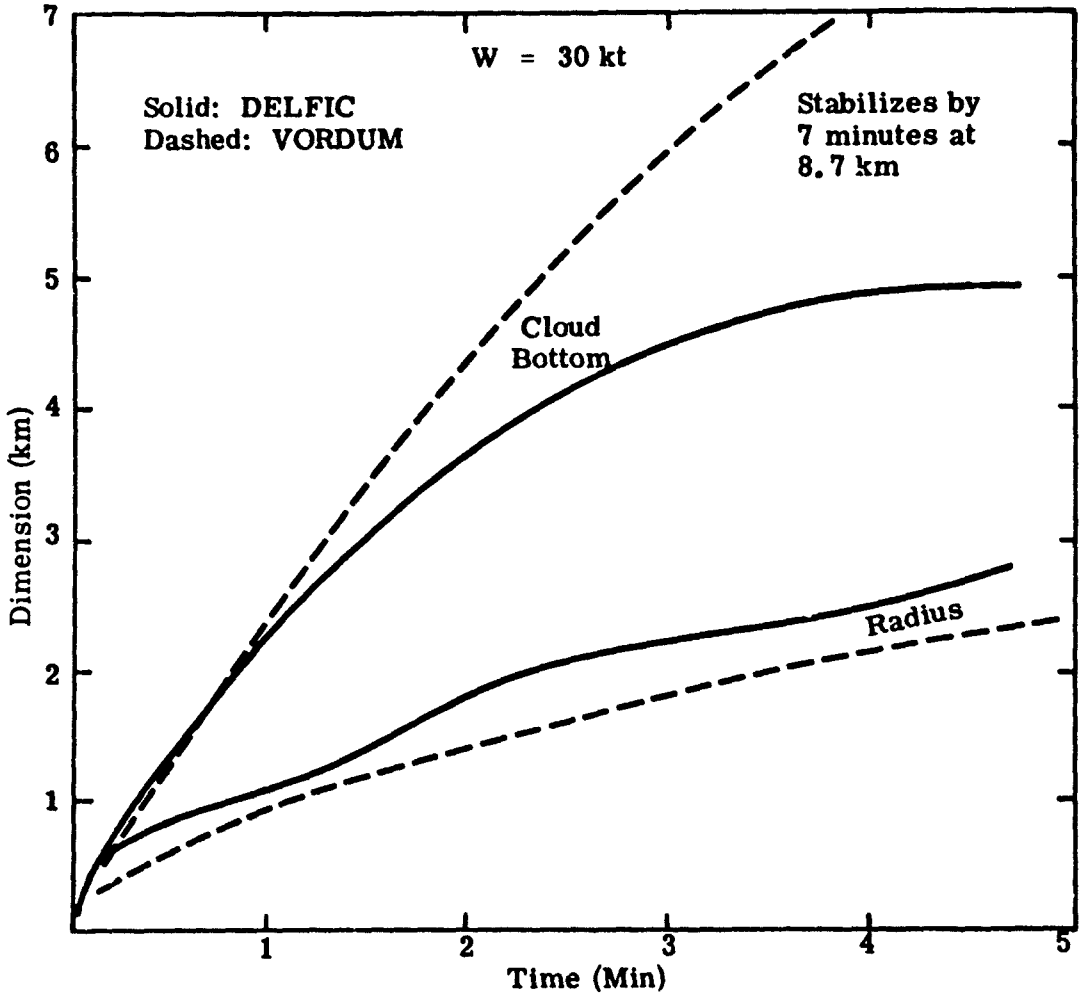

Figure 5.11. Comparison of Rise Parameters for 30 kt

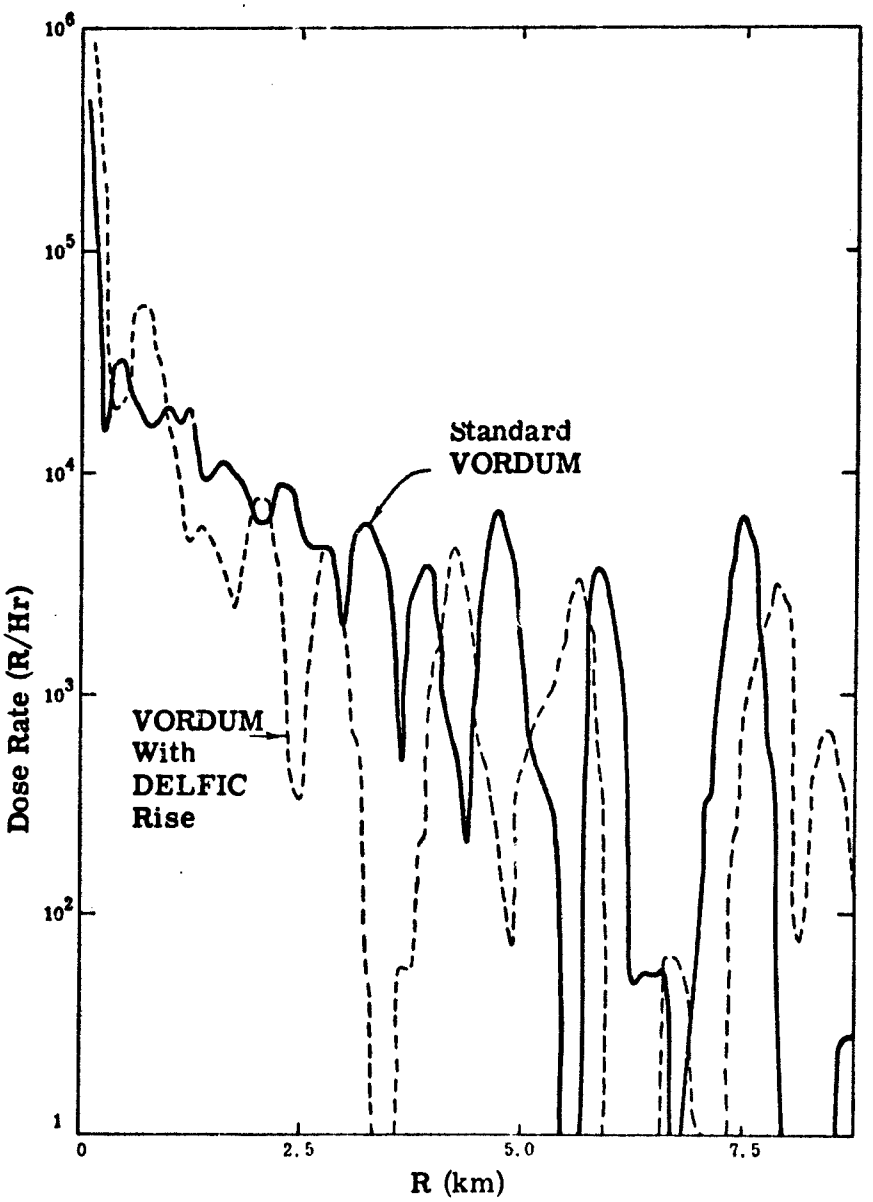

Figure 5.12. Comparisons of Predicted Dose Rate on Cloud "Hotline" Normalized to H+1 Hour for a 30 kt Burst

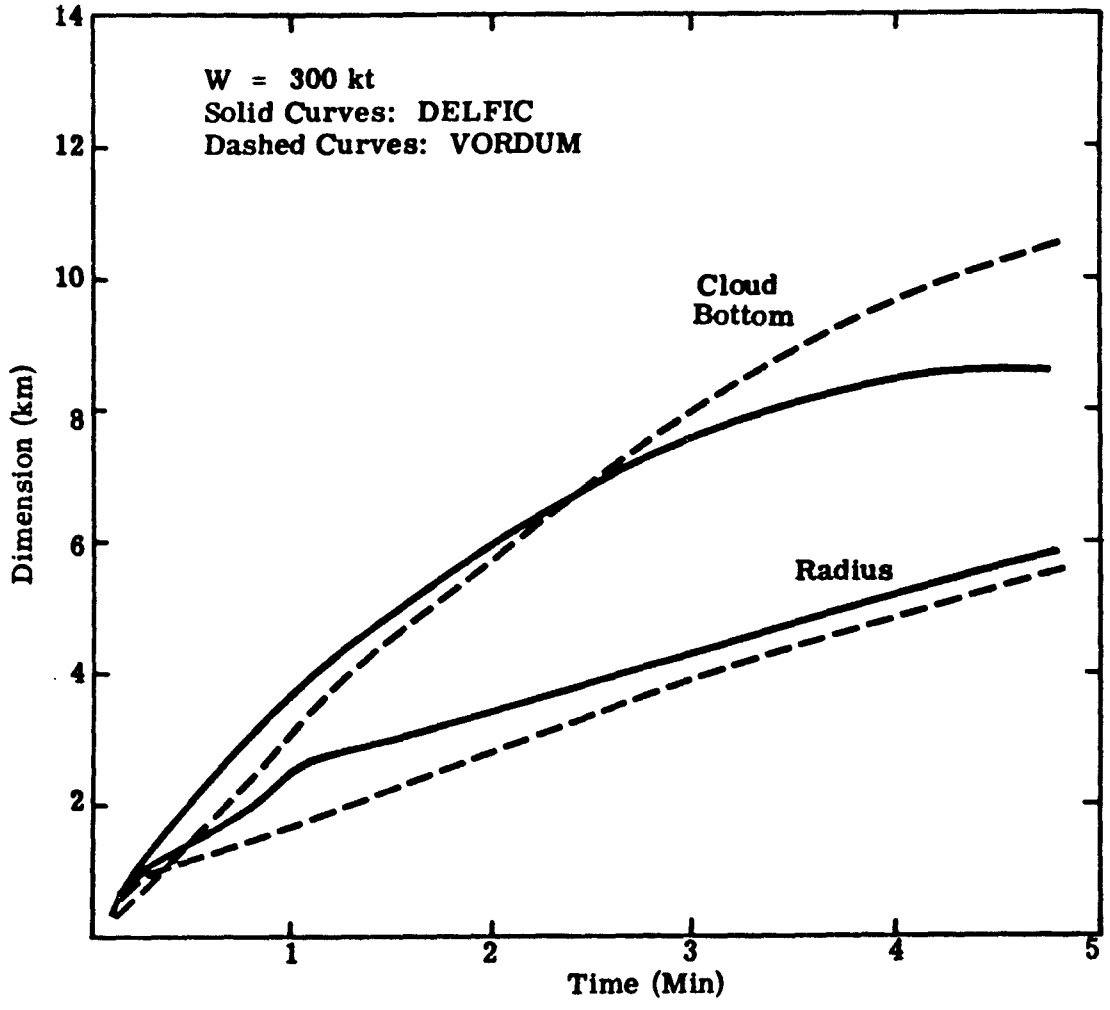

Figure 5.13. Comparison of Rise Parameters for 300 kt

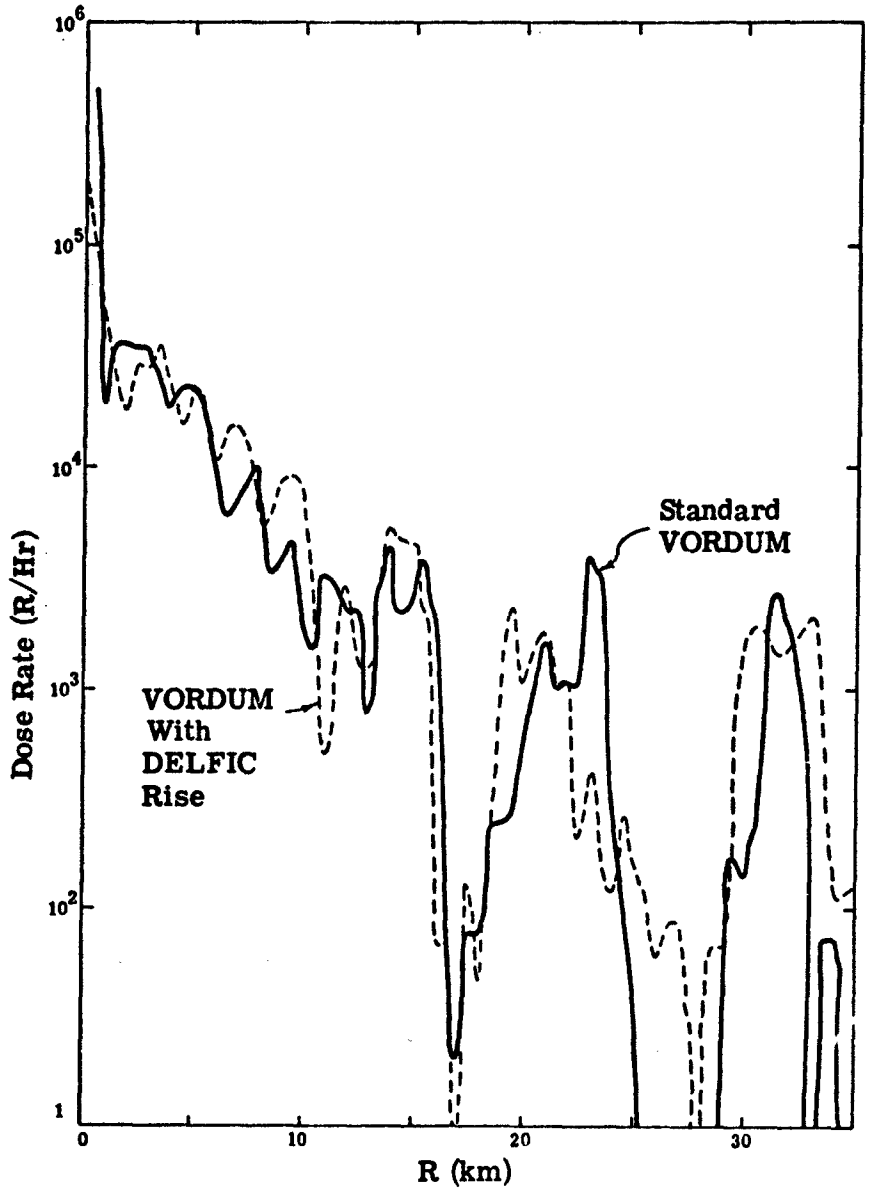

Figure 5.14. Comparisons of Predicted Dose Rate on Cloud "Hotline" Normalized to H+1 Hour for a 300 kt Burst

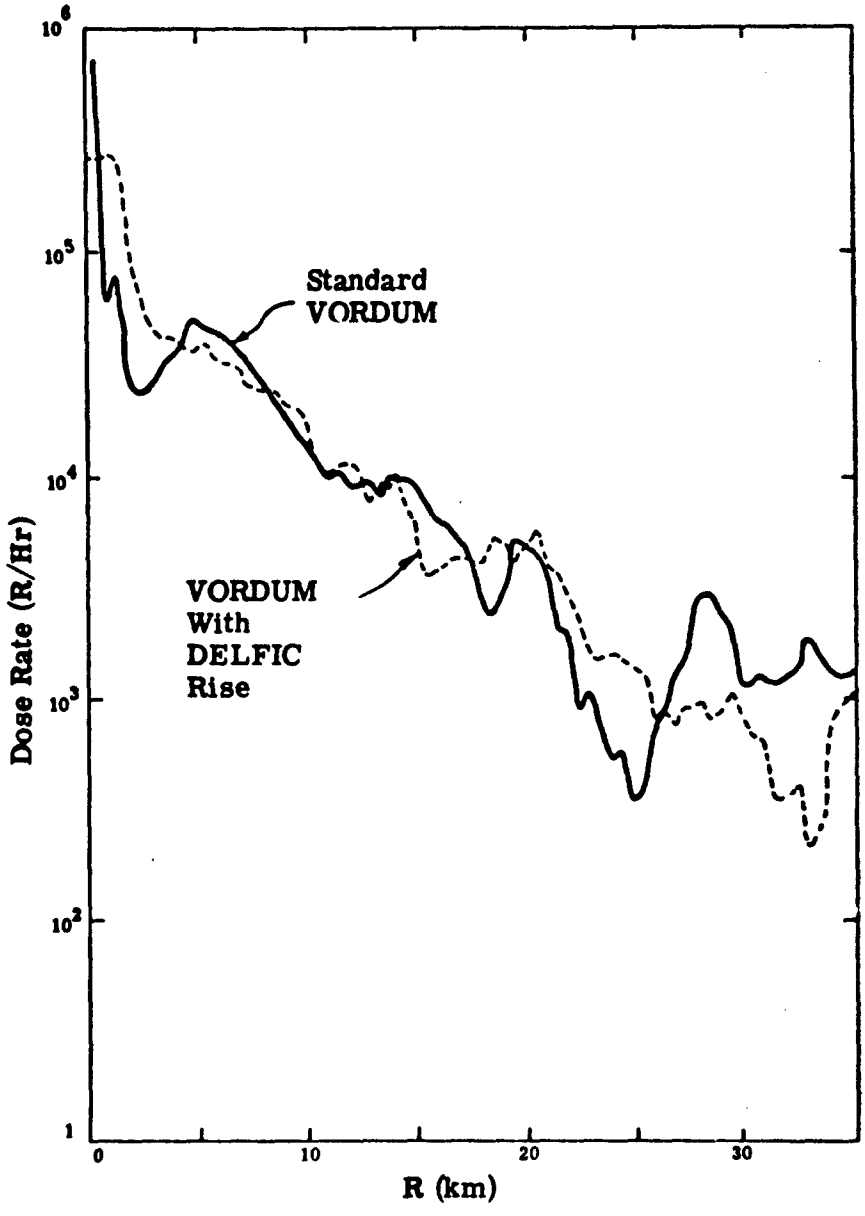

Figure 5.15. Comparisons of Predicted Dose Rate on Cloud "Hotline" Normalized to H+1 Hour for a 3 Mt Burst

Section 6

SENSITIVITY TO ASSUMPTIONS IN THE PARTICLE ACTIVITY MODULE

The subject of this section is the assignment of fission activity to the dust particles. The Particle Activity Module[1] uses the radial-distribution model of Freiling modified to account for an observed trend to constant specific activity for particles above a few hundred microns.

For a given mass chain, the Freiling ratio, FR, is defined as the fraction of its membership that has a higher melting temperature than the entrained soil and hence is considered refractory. The specific activity (activity per unit mass) is then assumed to be proportional to the $(b_i - 1)$ power of the particle size where b_i is the square root of FR for the i^{th} mass chain. The reader is referred to Reference 1 for a comprehensive discussion of the Freiling model.

6.1 ALTERNATIVE FORM OF THE FREILING MODEL

A more exact formalism of the Freiling model was examined for its effect. In this alternative approach, the refractory and volatile elements of each mass chain are separate. The number of equivalent fissions of mass chain i in size class k is given by

$$F_i(dk) = FT \cdot Y_i \cdot f_m(dk) \left[FR + \frac{(1 - FR)\, dk^{-1}}{\sum_k f_i(dk)\, dk^{-1}} \right]$$

where FT is the total number of fissions in all size classes, Y_i is the fission yield of the i^{th} mass chain, $f_m(dk)$ is the fraction of fissions in the k^{th} size class for a perfectly refractory mass chain and dk is the mean diameter of the k^{th} size class. This equation. however, has to be modified to account for the experimental evidence that $F_i(dk)$ becomes constant for large particles. Following the same procedure described in Reference 1, then,

$$F_i(dk) = FT\, Y_i\, f_m(dk) \left[1.0 - R_i(1 - FR) \cdot \left(1 - \frac{dk^{-1}}{\sum f_m(dk)\, dk^{-1}}\right)\right]$$

where R_i is the fraction of fissions in the i^{th} mass chain that follows the radial distribution; it is determined as in the present version by that particle diameter, D, where the radial and the constant specific activity components cross (see, for example, Figure 2.1 of Reference 1). The fraction, R_i, is thus determined to be

$$R_i = \left(1.0 + FR + (1 - FR)\frac{D^{-1}}{\sum_k f_m(dk)\, dk^{-1}}\right)^{-1} .$$

Currently D is 100μ in the PAM. Shown in Figure 6.1 is a comparison of the activity distribution with size for the current formalism (labeled PAM) and that described above for a 3 Mt surface burst. The significance of the comparison is that the exact form predicts the activity associated with particles greater than a few hundred microns to be about 50 percent lower than the current formalism while the activity on the very small particles (less than 10μ) is proportionally higher. Figures 6.2 and 6.3 show the integrated dose along the hotline for

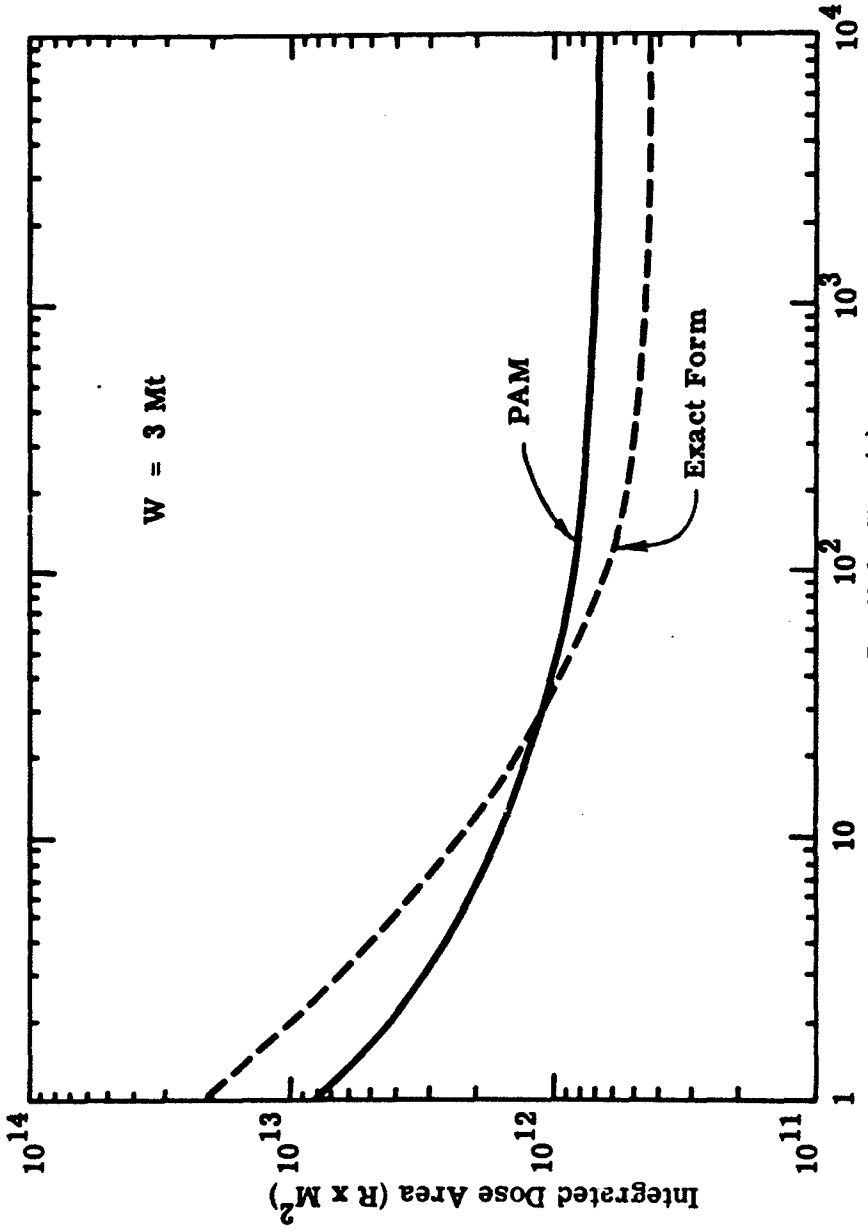

Figure 6.1. Comparison of Activity Versus Size for Alternative Forms of Freiling Model

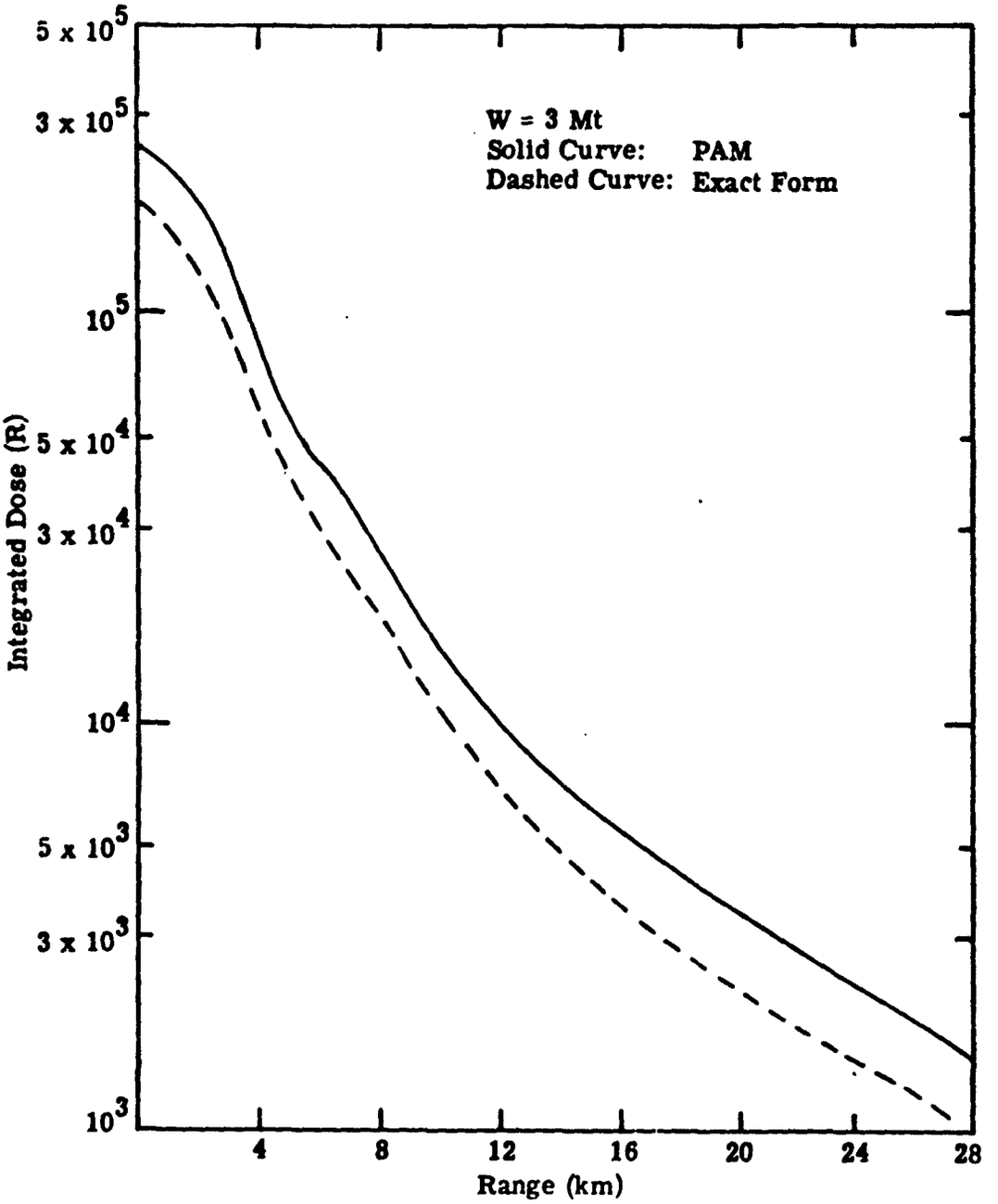

Figure 6.2. Comparison of Alternative Freiling Model Forms for 3 Mt Hotline Dose – Short Range

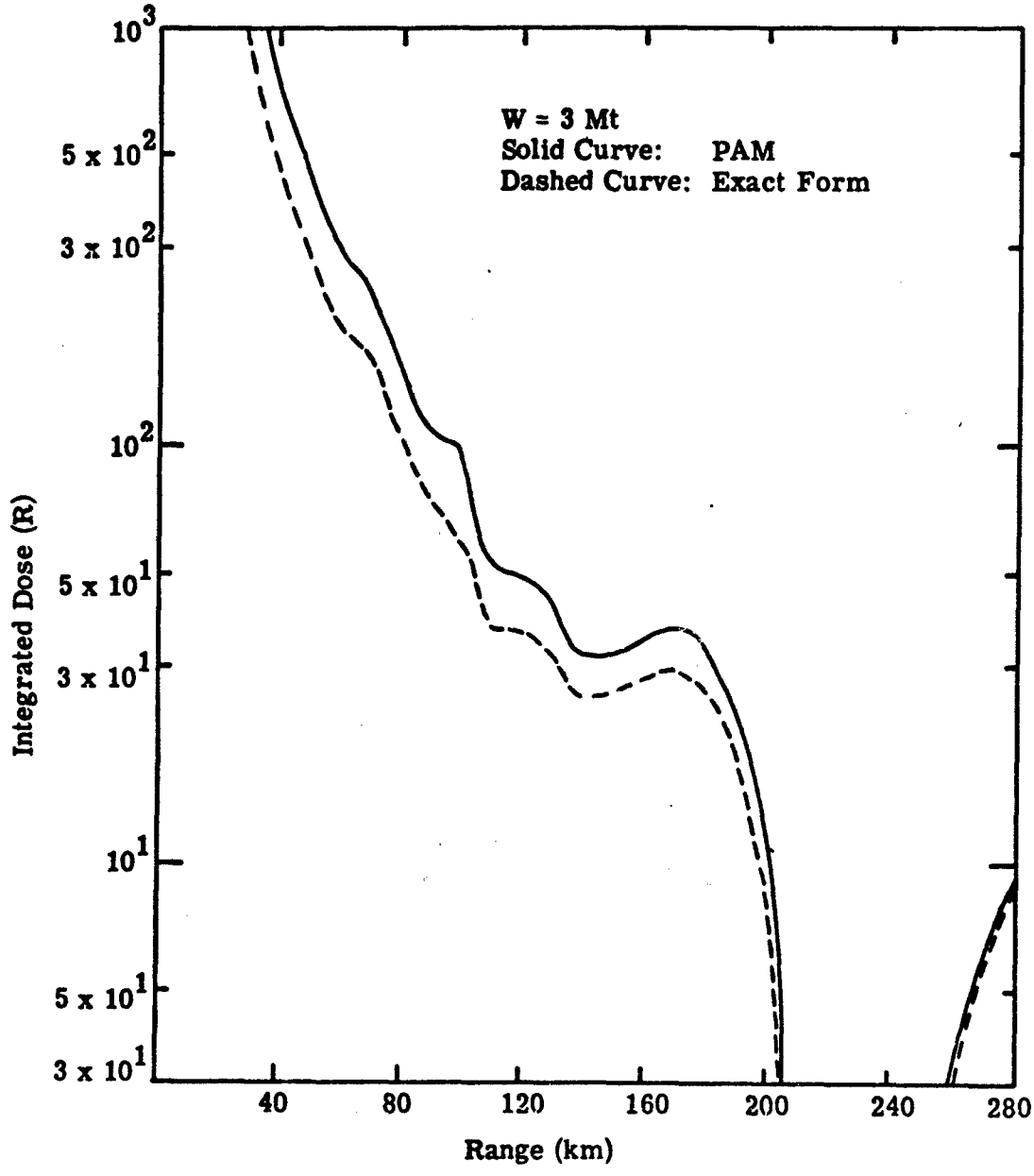

Figure 6.3. Comparison of Alternative Freiling Model Forms for 3 Mt Hotline Dose – Intermediate Range

this yield in two range regimes, the first extending to 28 km and the second to 280 km. The dose predicted by the standard formalism is always larger typically by 30 to 50 percent, but the two become comparable past 160 km. Not shown, are the long range fallout, where, as indicated by the comparison shown on Figure 6.1, the alternative form of the Freiling model would predict higher dose levels. However, at these distances, the dose is small enough that 50 percent effects are unimportant.

A comparable situation is manifest at other yields. As shown in Figures 6.4 and 6.5 for 30 kt, the alternative form of the Freiling model results in a lower dose out to 70 km, but only between 5 and 7 km is the difference more than a factor of 50 percent. The conclusion to be reached is that while the present coding is not the most exact, it overestimates the integrated dose by factors less than 50 percent for particles above 20-30 microns (i.e., for close-in fallout).

In addition to establishing the sensitivity to alternative forms of the Freiling model, the effect of variations in the crossover diameter, D, was also investigated. This is the diameter at which the radially dependent and constant components of the specific activity cross. Presently, it is set at 100μ. Shown in Figures 6.6 and 6.7 are the standard curve for integrated dose along the hot-line for 3 Mt as well as the curves that result when D is set to 20μ and 500μ. As is indicated on these figures, there is very little sensitivity to variations in this parameter with the two extreme values of D resulting in an average variation on the dose of about plus or minus 10 percent. Up to a range of 200 km, the 20μ curve is higher than the standard and the 500μ curve, but past 260 km, it

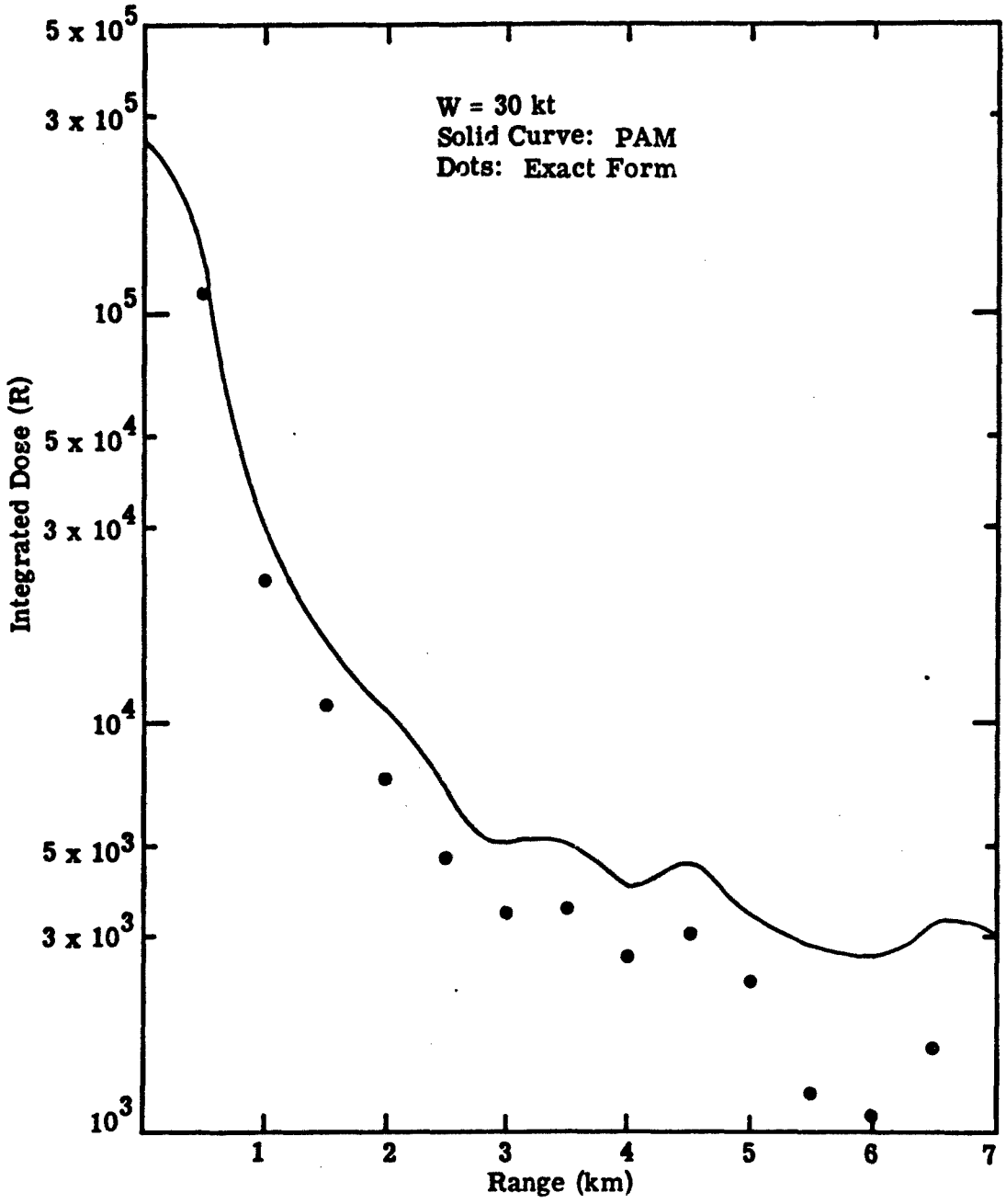

Figure 6.4. Comparison of Alternative Freiling Model Forms for 30 kt Hotline Dose – Short Range

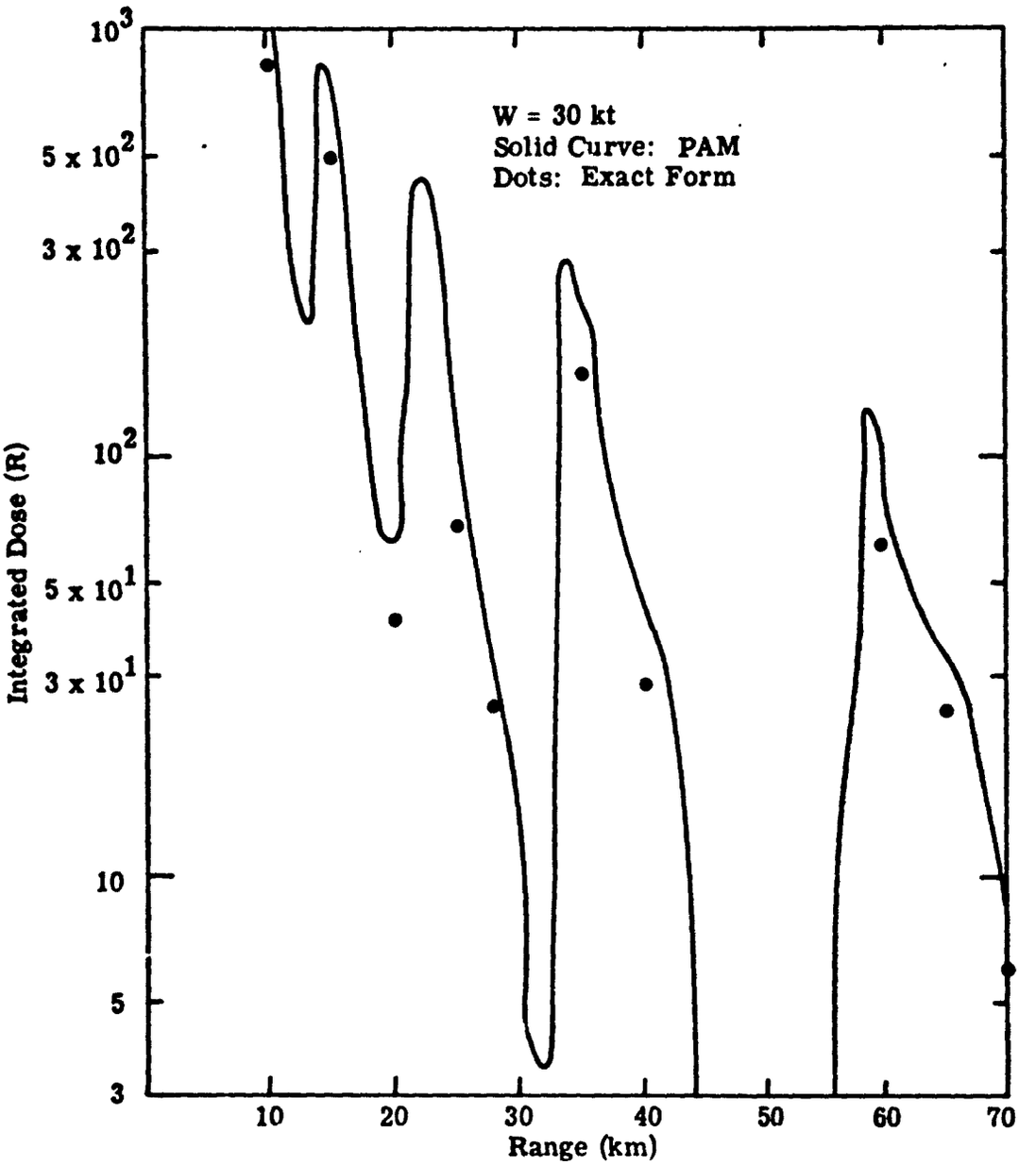

Figure 6.5. Comparison of Alternative Freiling Model Forms for 30 kt Hotline Dose – Intermediate Range

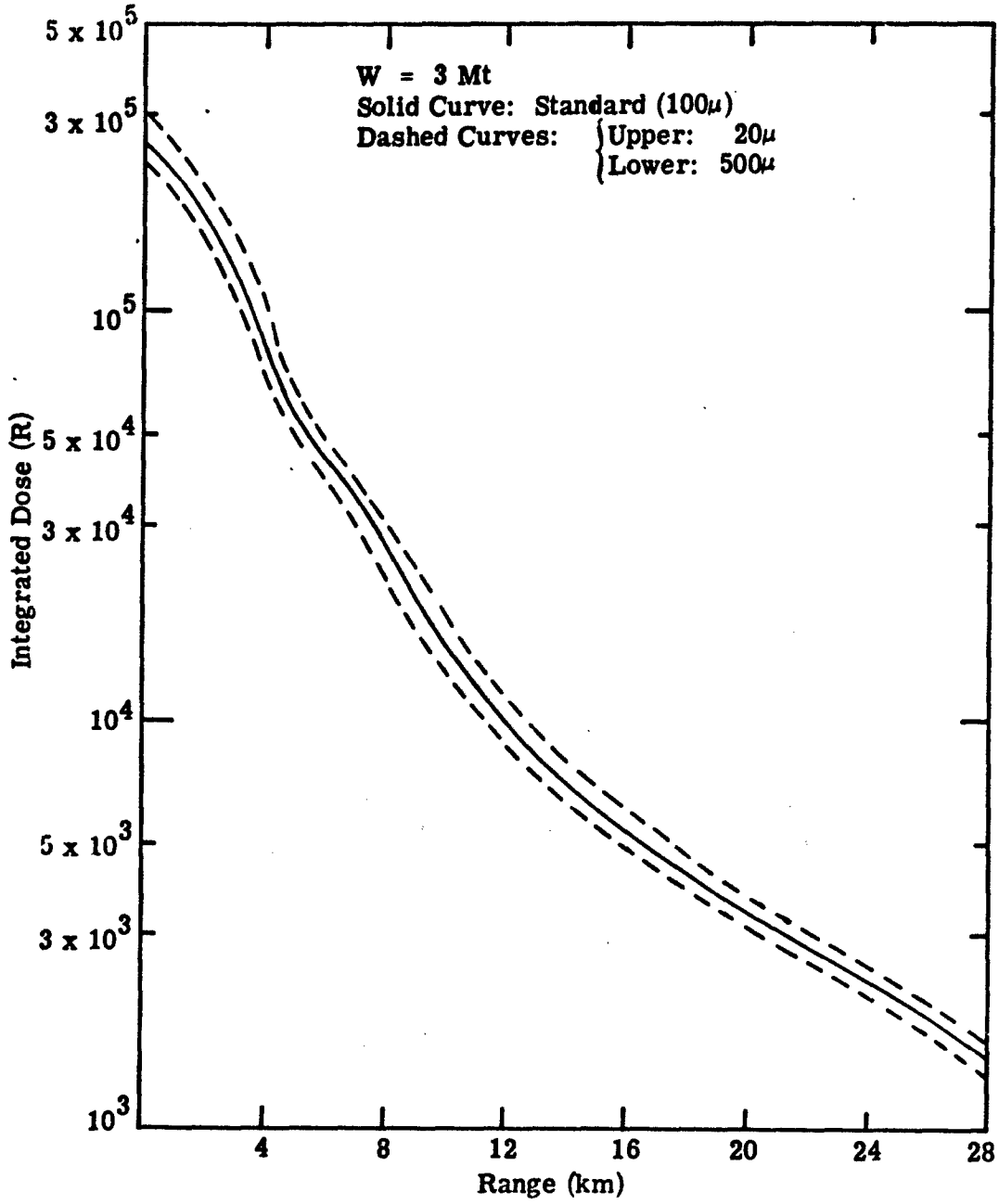

Figure 6.6. Sensitivity of Hotline Integrated Dose to Crossover of Specific Activity (From Radial to Constant) for 3 Mt – Short Range

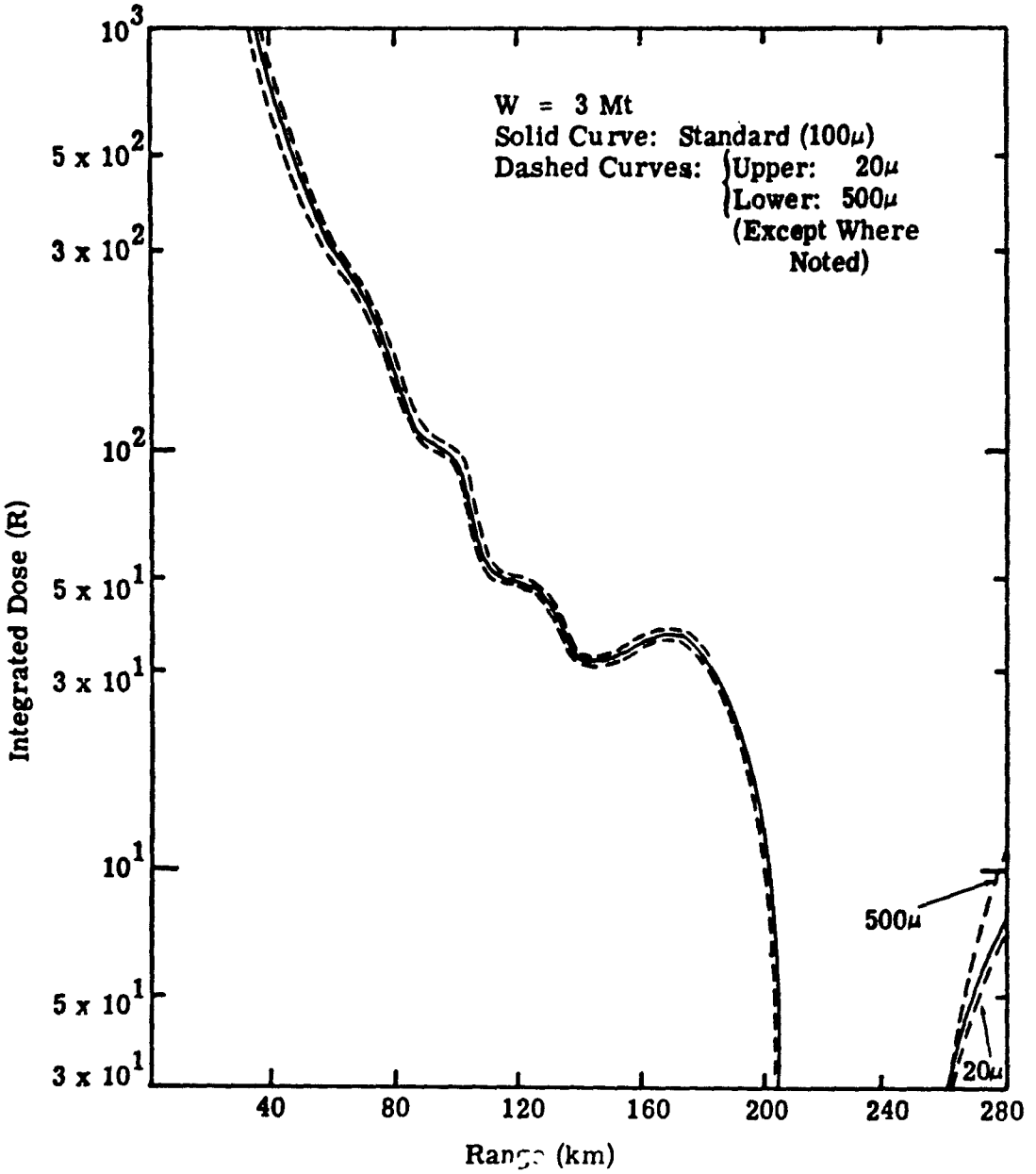

Figure 6.7. Sensitivity of Hotline Integrated Dose to Crossover of Specific Activity (From Radial to Constant) for 3 Mt – Intermediate Range

is the 500μ curve which is the highest. At 30 kt, the same insensitivity to the choice of the crossover point is apparent as indicated in Figures 6.8 and 6.9.

6.2 COMPARISON OF FREILING MODEL WITH SIMPLE DISTRIBUTIONS

There is a substantial amount of uncertainty associated with the distribution of fission activity with particle size. As discussed in the previous section, for example, the Freiling model has to be modified because it does not agree with the observed independence of particle size above a few hundred microns insofar as specific activity is concerned. In addition to the thermodynamic effects involved, there must also be a separate mechanism that is not modeled, which results in the collection of fission debris by the dust with a size-dependent efficiency factor.

As a further investigation of the sensitivity of the predicted dose to model assumptions, modifications were made to the PAM so that the radial component of the activity distribution was first purely volatile (surface distributed) and second purely refractory. In the latter case, then, the entire distribution would be refractory. Figure 6.10 shows the integrated dose along the hotline at 3 Mt for short ranges while Figure 6.11 is for intermediate ranges. The three curves shown are for the standard DELFIC calculation and for these two simpler assumptions. Predictions of the 30 kt hotline dose are shown in Figures 6.12 and 6.13. At both yields, the assumption that the specific activity is independent of particle size (i.e., all of the decay chains are purely refractory) is on the average 20 percent higher while taking the radial component to be volatile (and therefore the specific activity varies with particle

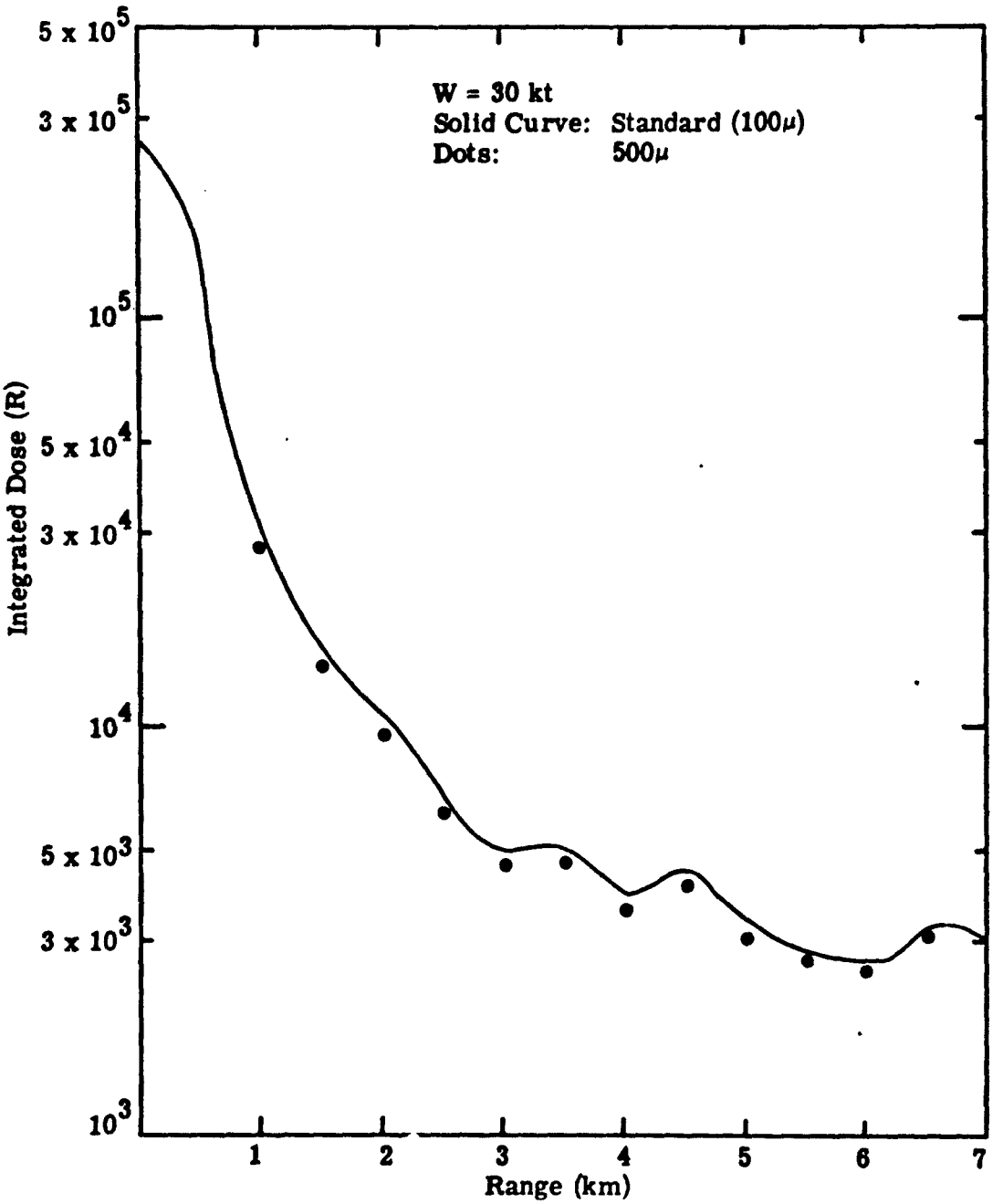

Figure 6.8. Sensitivity of Hotline Dose to Crossover of Specific Activity (From Radial to Constant) for 30 kt – Short Range

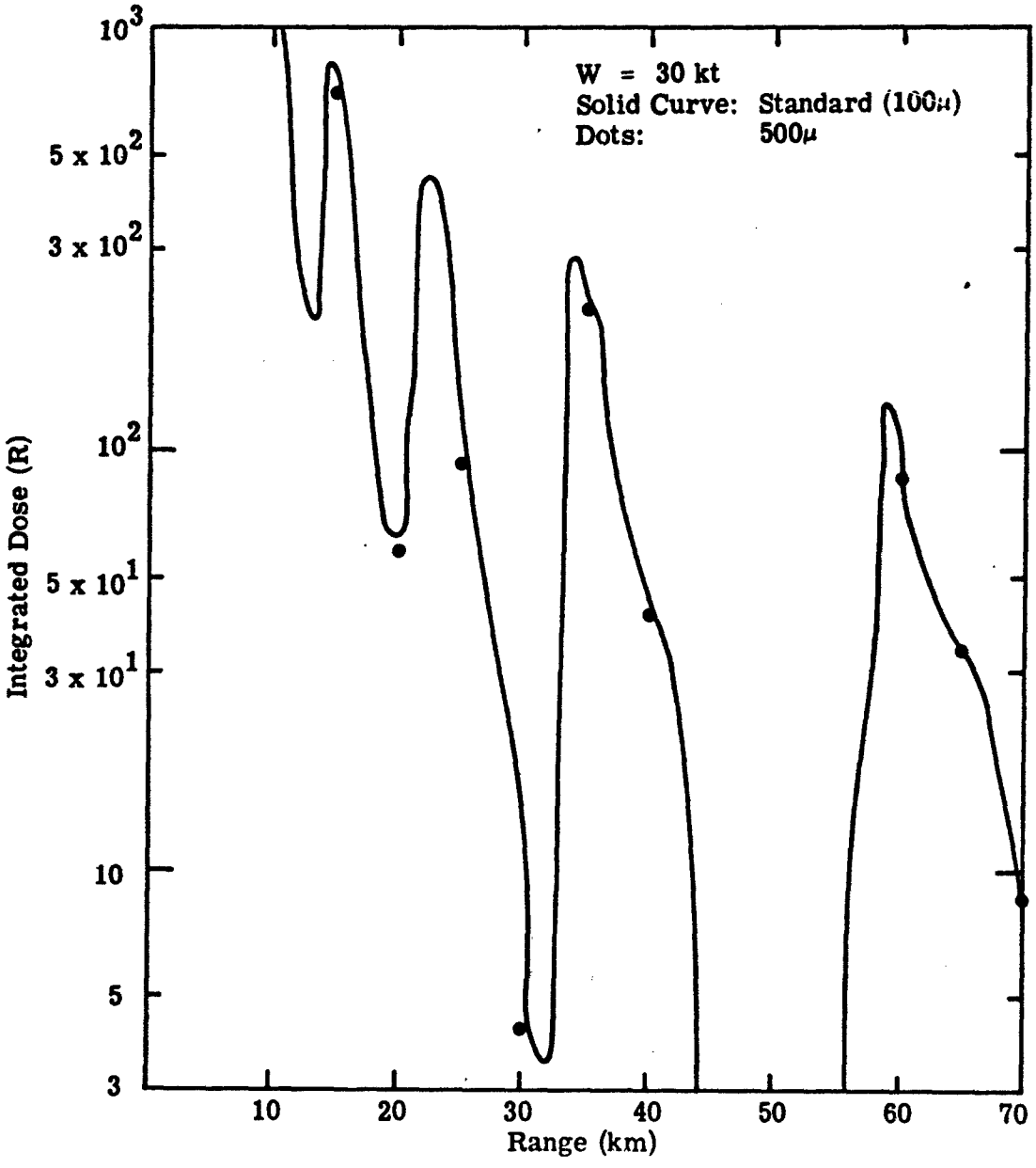

Figure 6.9. Sensitivity of Hotline Dose to Crossover of Specific Activity (Radial to Constant) for 30 kt – Intermediate Range

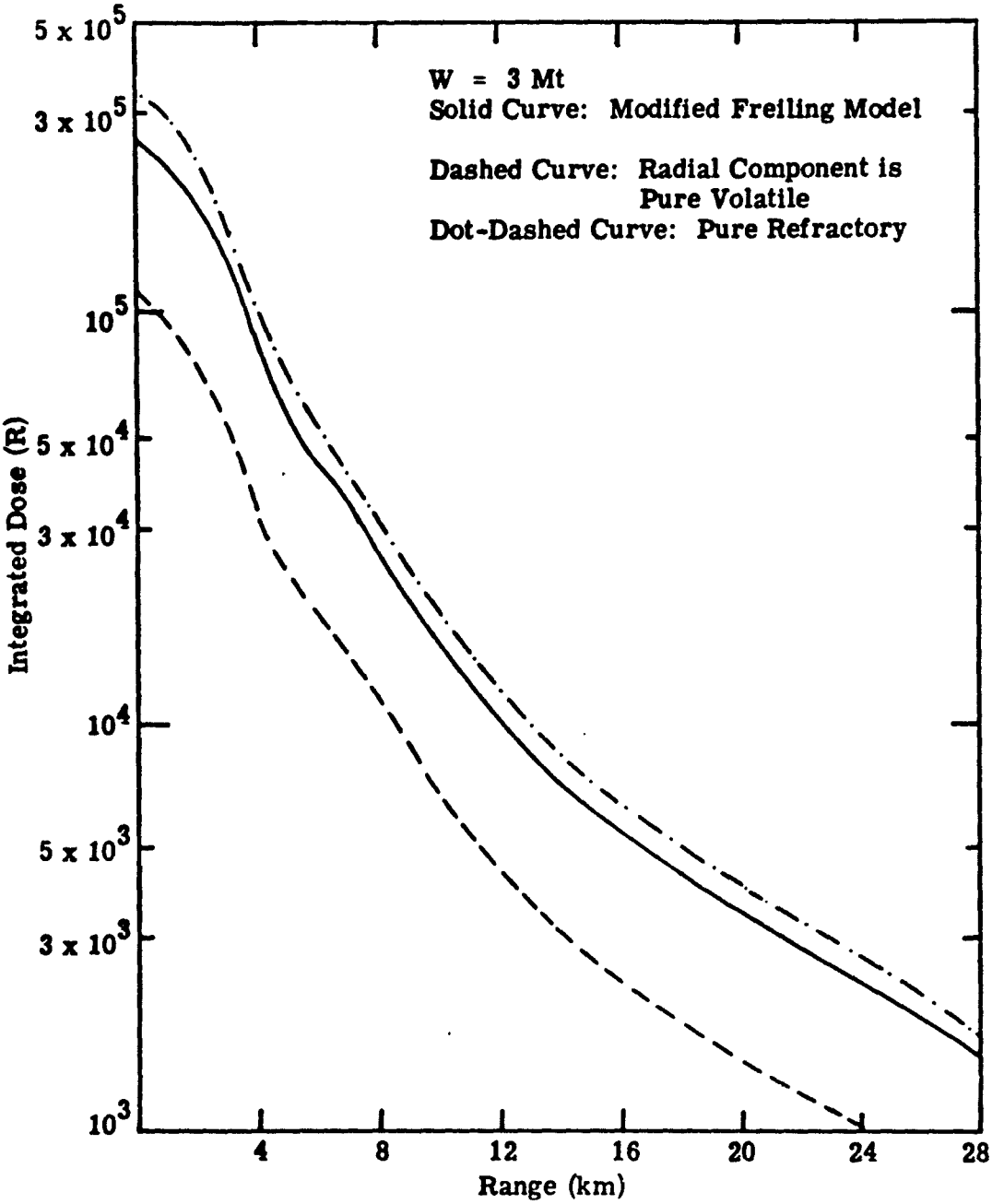

Figure 6.10. Comparison of Freiling Model with Assumptions of Volatile and Refractory Radial Components for 3 Mt Hotline Dose – Short Range

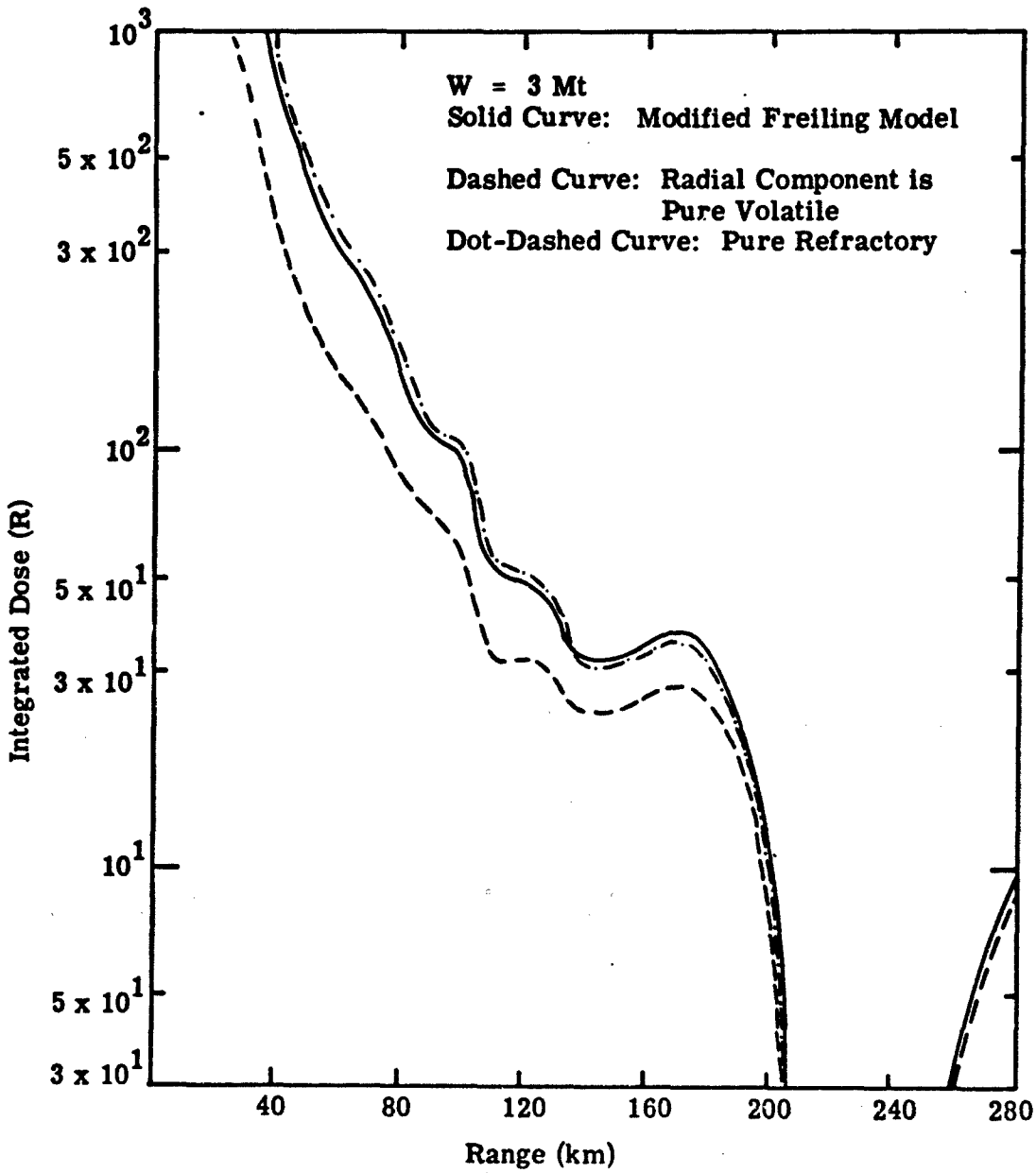

Figure 6.11. Comparison of Freiling Model with Assumptions of Volatile and Refractory Radial Components for 3 Mt – Intermediate Range

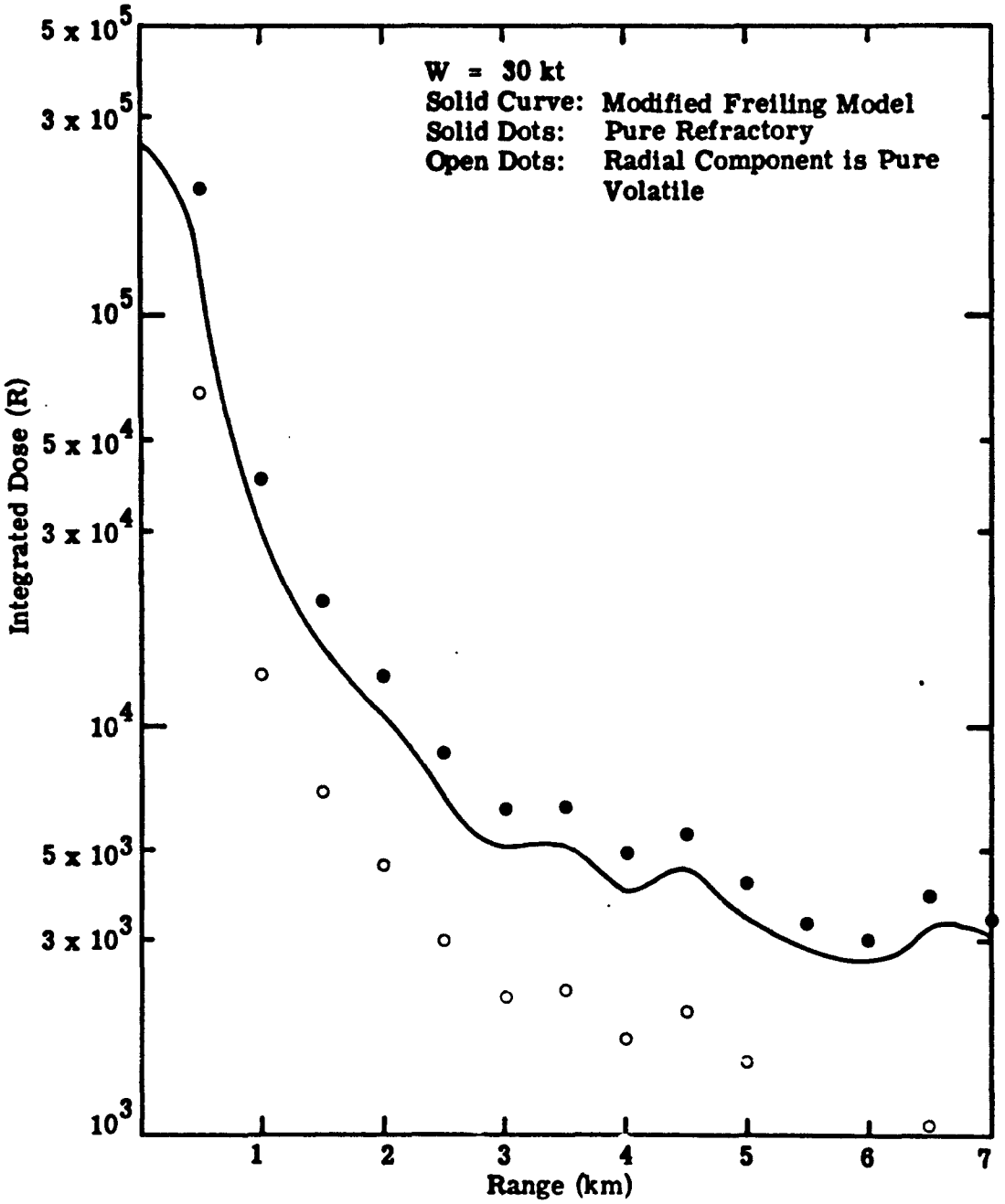

Figure 6.12. Comparison of Freiling Model with Assumptions of Volatile and Refractory Components for 30 kt Hotline Dose – Short Range

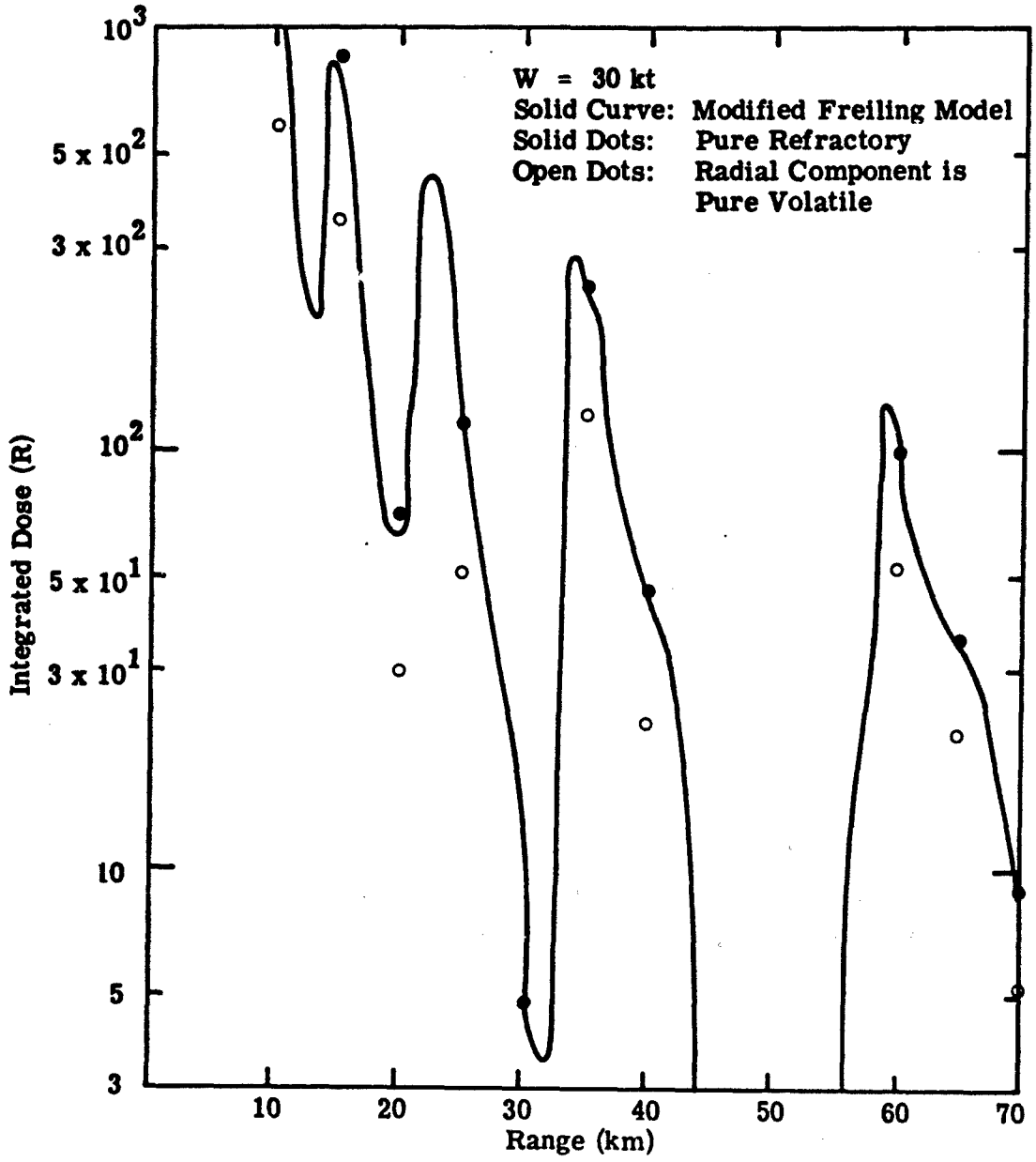

Figure 6.13. Comparison of Freiling Model with Assumptions of Volatile and Refractory Components for 30 kt Hotline Dose – Intermediate Range

diameter (d) as d^{-1} results in an underestimate of the dose by 50 percent. The conclusion to be drawn here is that for short and intermediate ranges, the simple assumption that all mass chains are purely refractory reproduces satisfactorily the more complex Freiling model. It is quite possible, however, that this agreement is significantly influenced by the choice of the particle number distribution, which for this study was a power-law (Section 2).

6.3 REFERENCES

1. R.C. Tompkins, "Department of Defense Land Fallout Prediction System, Volume V, Particle Activity," DASA-1800-V, U.S. Army Nuclear Defense Laboratory, Edgewood Arsenal, Maryland, 1968.

Section 7

SENSITIVITY TO UNCERTAINTIES IN INDUCED SOIL ACTIVATION

Even though the induced activity is not a significant component of the fallout unless the fission fraction is less than perhaps 50 percent, it is one of the most difficult to model. This section is devoted to a discussion of the uncertainties associated with the model of induced activity that is presently employed in the Particle Activity Module.

According to Reference 1, the three basic assumptions are:

a. all neutrons entering the soil are thermalized, and then captured

b. only those neutrons that are seen by the apparent crater contribute

c. all significant soil components are refractory in the fractionation scheme.

In addition, only NTS soil is provided for.

7.1 COMPARISON WITH FISSION ACTIVITY

For a surface burst, DELFIC assumes 17 percent of the emitted neutrons are captured independent of yield and neutron energy spectrum. For comparison, we have the work of Lessler and Guy (Reference 2). Using a Monte Carlo technique, they were able to determine the fraction of neutrons captured versus radius when a mono-energetic neutron source was placed on the surface of dry NTS

soil. A not-too-surprising result of their study was that high- and low-energy neutrons behave differently. Table 7.1 lists the cumulative fraction of neutrons that are captured versus distance (along the surface) from the source and Figure 7.1 is a schematic of the zones used in the calculation. Practically all of the neutrons which were captured outside the 5 m zone were transported indirectly through the air.

Table 7.1 Fraction of Neutrons Captured

Distance From Source (m)	Cumulative Fraction	
	14 Mev	0.5 Mev
5	0.256	0.101
15	0.267	0.121
30	0.279	0.141
45	0.292	0.160
900	0.461	0.386

These numbers, which include the effects of secondary scattering in air, were determined assuming ambient air and soil temperatures. If there is pre-heating, then the fractions would be lower.

Table 7.2 lists the radius[3] of the apparent crater for various yields and the fraction of neutrons captured within the crater boundary for surface bursts. These fractions were obtained by interpolation in Table 7.1 which was derived for dry NTS soil and the assumption is made in this analysis that the values derived are valid for other soils. Note the energy dependence on the fraction captured, particularly at low yields.

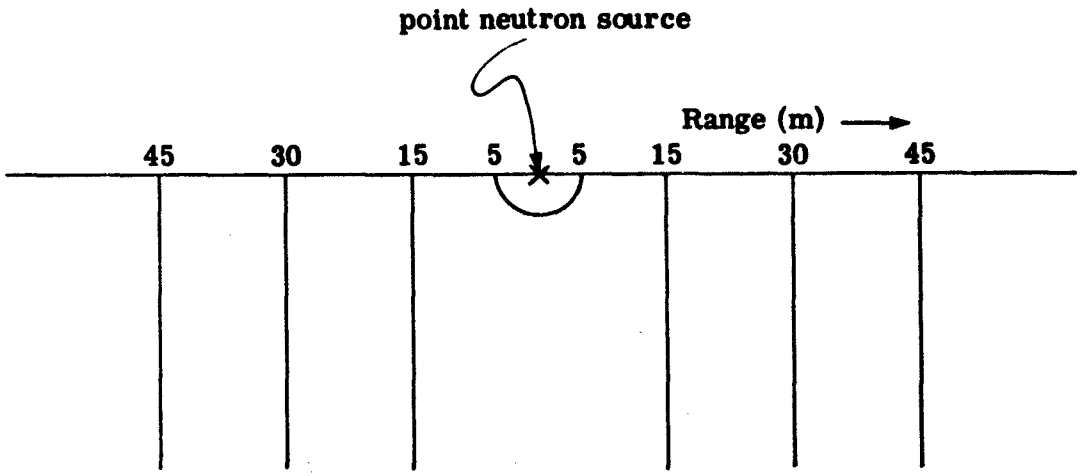

Figure 7.1. Schematic of Zones Used in Monte Carlo Calculations of Neutron Capture in Soil

Table 7.2 Fraction of Neutrons Captured Within Apparent Crater

Yield (Mt)	Radius (m)	Fraction	
		14 Mev	0.5 Mev
.01	36	0.29	0.15
.10	70	0.31	0.18
1.0	136	0.34	0.23
10.	368	0.40	0.31

Studies of the soil burden in the stabilized cloud of a surface burst have shown it to be only a fraction of the mass removed in the cratering process. Consequently the fraction of captured neutrons that contribute to the fallout activity is going to be less than indicated in Table 7.3. For example, at 1 Mt, the soil burden of the stabilized cloud is on the order of 0.3 Mt[4] while the apparent crater mass is about 5 Mt. While no model presently exists for the overall cratering and entrainment process, it has been observed[5] that the soil that is ejected and not entrained tends to originate away from the burst point. On the basis of this, a simple assumption about the original position of the entrained soil is that it occupied a volume centered on the burst point, which when multiplied by an average bulk density for soil of 2.5 gm/cc equals the stabilized cloud loading. A further assumption is made that the region is a paraboloid with depth equal to half the radius. Table 7.3 lists the fraction of neutrons activating the soil in the stabilized cloud. It is these fractions that are to be used in determining the contribution of neutron-induced soil activity to fallout following a surface burst.

Table 7.3 Fraction of Neutrons Activating the Soil Burden of the Stabilized Cloud

W (Mt)	Fraction	
	14 Mev	0.5 Mev
.01	0.26	0.11
.10	0.28	0.13
1.0	0.30	0.16
10.	0.33	0.21

The use of these fractions versus those in Table 7.2 results in only a 10 to 20 percent decrease in the estimate of activated soil in the cloud. However, as will be discussed below, the original location of the activated soil may have important consequences for its size distribution.

As an example of the relative contributions of fission debris and activated soil, consider a 300 kt surface burst with 50 percent fission. Using hypothetical neutron output spectra[6] (in which the fission spectrum is normalized to a total of 2.0×10^{23} neutrons/kt) the number of neutrons per kt emitted above and below 4 Mev is 2.64×10^{22} and 2.32×10^{23} respectively. This partition is justified, since below 4 Mev, capture cross sections are roughly energy independent. In this analysis, we use the 14 Mev fractions for the neutrons above 4 Mev and the 0.5 Mev fractions for the remainder of the spectrum. The fraction in each energy bin which activate entrained soil can be found by interpolation in Table 7.3; the values are 29 percent in the high energy bin and 14 percent in the low energy bin. Figure 7.2 shows the dose that would result from the fission debris and the high and low energy neutrons. The ordinate is a normalized dose in units of R kt^{-1} mi^2 where the dose rate was integrated from time of arrival to H+48 hours. To facilitate the comparison, it was assumed first that the size distribution of the neutron-induced activity was the same as that for the fission debris and second that the fission decay rate was proportional to $T^{-1.2}$ where T is time in hours after burst. This calculation was done for dry NTS soil. Reference 1 provides the decay rate per mole of neutrons (14 Mev and 0.5 Mev) both individually for each soil element and collectively. Thus the curves in Figure 7.2 required only the number of neutrons in each energy bin. Note that although the number of high energy neutrons emitted is only 10 percent of the total, they contribute over 20 percent of the total induced activity.

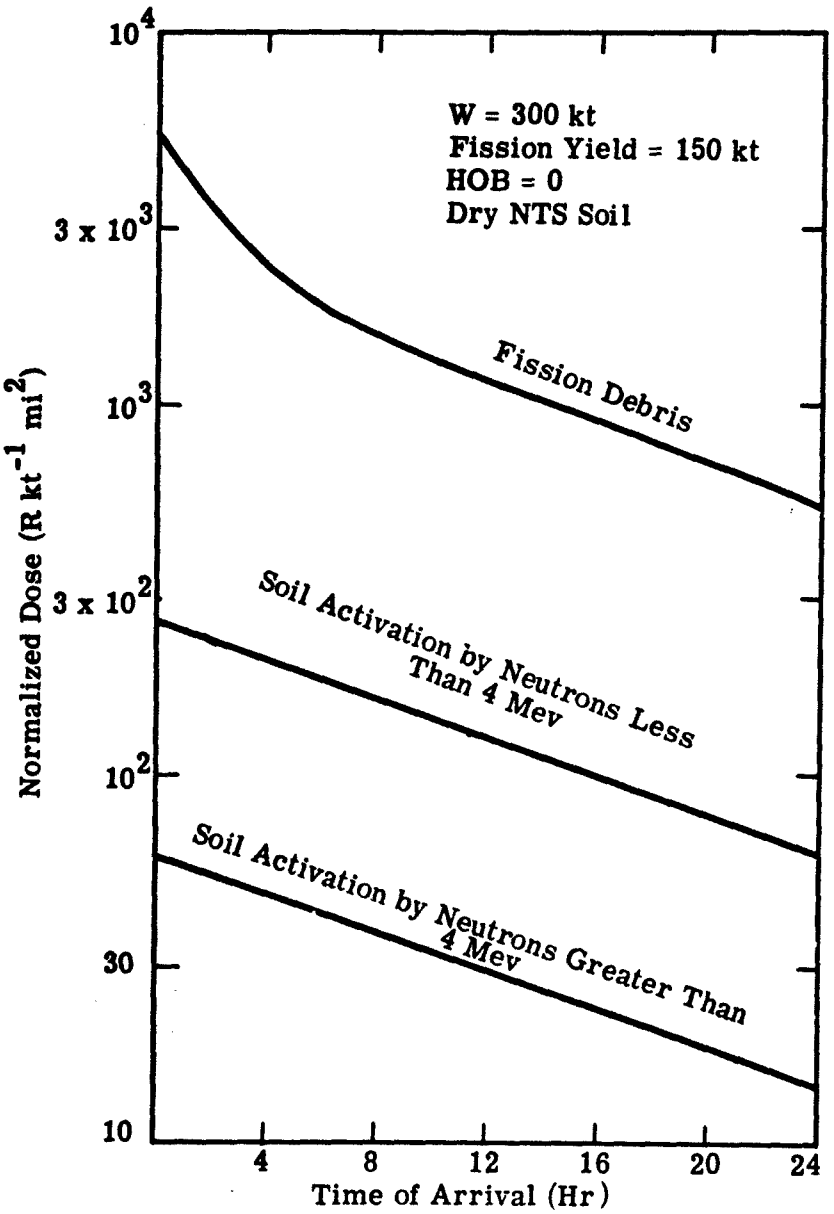

Figure 7.2 Comparison of Fission and Neutron-Induced Soil Activity

The foregoing analysis has not been based on neutron energy spectra from actual weapons, hence caution should be exercised in attempting to draw generalized conclusions.

7.2 SOIL VARIATION EFFECT ON INDUCED ACTIVITY

The Particle Activity Module is presently set up only to handle NTS soil. However, the chemical composition is substantially different than that reported for NTS soil in Lessler and Guy's report (Reference 2). The DELFIC profile is much higher in hydrogen (with an atomic fraction of 0.42 versus 0.16 in Reference 2) and conversely a lower proportion of Na and Al. The discussion to follow assumes the NTS profile of Reference 2.

In addition to the NTS soil, four average profiles[5] have been considered and are the following:

a. Chernozem — an average of five samples of this soil group from the USSR

b. Podzol — an average of two samples of this soil group from the USSR

c. USSR — average of all samples in USSR

d. PRC — average of five Peoples Republic of China samples.

The data given in Reference 5 are only for certain elements and are in terms of weight fractions and are listed in Table 7.4. In particular the water fraction is omitted. In order to make a comparison with the NTS calculation of Reference 2, the following has been assumed:

a. the same weight fraction (0.06) of water as for dry NTS soil

b. the same weight fraction (0.003) for other hydrogen

c. a mean atomic weight determined from the data of Reference 2 for NTS, Chester and Dade soils.

Table 7.4. Weight Fractions for Representative Soils

Element	Chernozem	Podzol	USSR	PRC	NTS
Na	0.0086	0.0188	0.0116	0.0029	0.0134
Al	0.0698	0.0842	0.0769	0.0864	0.0763
Si	0.3014	0.3084	0.3036	0.3119	0.2756
K	0.0175	0.0200	0.0161	0.0069	0.0296
Ti	0	0	0.0002	0.0058	0.0024
Mn	0.0002	0.0011	0.0006	0.0004	0.0003
Fe	0.0335	0.0313	0.0350	0.0486	0.0112
Mg	0.0090	0.0009	0.0073	0.0046	0.0044
Ca	0.0293	0.0144	0.0220	0.0030	0.0866

This latter factor is determined as follows:

$$\overline{A^{-1}} = 0.94 \sum_i \frac{FW_i}{A_i} + 0.06/18$$

where A_i is the atomic weight of the i^{th} element and FW_i is its weight fraction. The second term represents the water contribution and the summation in the first term is renormalized since the weight fractions were determined with the water removed. The mean value of $\overline{A^{-1}}$ was found to be 5.21×10^{-2}. Using this, the atomic fractions were determined as follows:

$$FA_i = 0.94\ FW_i/(\overline{A^{-1}} \times A_i)$$

and are listed in Table 7.5. Figure 7.3 compares the ratio of the induced activity for each soil relative to the fission activity for a 300 kt surface burst with 50 percent fission fraction. The fission and fusion neutron spectra are those of EM-1 and are not intended to be typical of modern weapons. The activity is an integral of the dose rate from time of arrival to H+48 hrs. In determining the relative contribution made by the activated soil, it was assumed to be constant over the dust particle size spectrum. The Podzol soil has the largest effect while the PRC soil is lowest — being only 20 percent of the Podzol-induced activity. Thus, there is a factor of five variation but even the largest is less than 20 percent of the fission activity for this particular case of 50 percent fission fraction.

Table 7.5. Atomic Fractions for Representative Soils

Element	Soil Type				
	Chernozem	Podzol	USSR	PRC	Dry NTS
Na	0.00675	0.0147	0.00910	0.00230	0.0105
Al	0.0466	0.0563	0.0514	0.0577	0.0510
Si	0.193	0.199	0.196	0.201	0.177
K	0.00810	0.00925	0.00745	0.00320	0.0137
Ti	0	0	0.000075	0.00218	0.0009
Mn	0.000066	0.00036	0.00020	0.00013	0.000098
Fe	0.0108	0.0101	0.0113	0.0157	0.0036
Mg	0.00677	0.00068	0.0055	0.00346	0.0033
Ca	0.0132	0.0065	0.0099	0.0013	0.0390

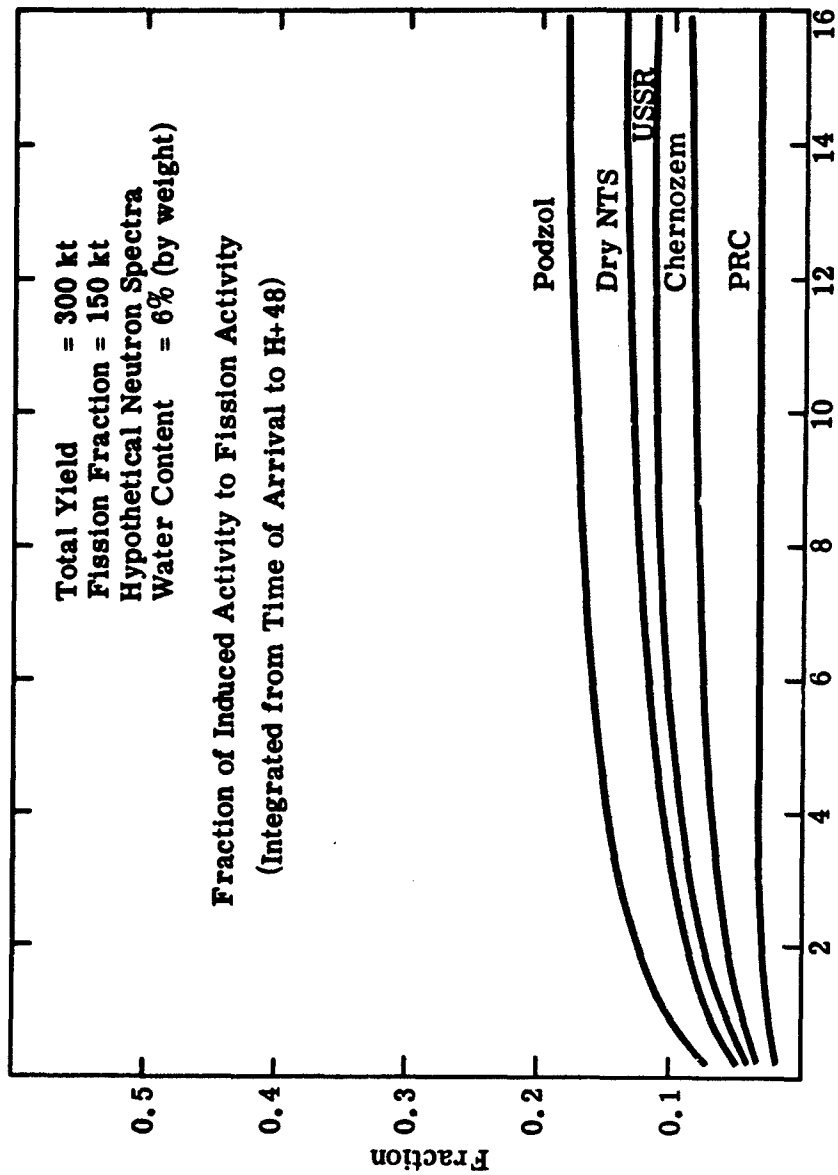

Figure 7.3. Soil Variation of Induced Activity

An important factor in assessing the importance of induced activity to fallout is the percent of water in the soil. As pointed out in Reference 2, hydrogen has a capture cross section that is approximately three times higher than that for the other soil constituents. Consequently, it serves to diminish the number of neutrons that would activate other elements. In the preceding comparison among various soils, it was assumed that each had the same fraction of water (6 percent) as in the dry NTS soil used in Reference 2. Thus, in estimating the number of activated atoms, all that was necessary was to multiply the values supplied in Reference 2 using dry NTS by the ratio of atomic fractions of a given soil to that for the dry NTS soil.

7.3 VARIABLE WATER CONTENT

A comparison of wet versus dry NTS soil by Lessler and Guy indicated that an increase of the water content from 6 to 17 percent by weight decreased the activation by 35 percent. The following shows the mathematics of this effect and indicates how a variable water content would affect the soil activation. The baseline is water content of 6 percent by weight.

It is first necessary to determine the dependence of the hydrogen atomic fraction due to water. Following the above methodology, the mean atomic weight inverse is given by:

$$\overline{A^{-1}} = (1 - FW_{H_2O}) \sum_i \frac{FW_i}{A_i} + FW_{H_2O}/18$$

where FW_{H_2O} is the weight fraction of water and the summation is over the elements listed in Table 7.4. For the baseline case, $\overline{A^{-1}}$ was found to be 5.21×10^{-2} which implies that the summation in the above expression is 5.19×10^{-2}. Thus, for other water weight fractions,

$$\overline{A^{-1}} = (1 - FW_{H_2O})(5.19 \times 10^{-2}) + FW_{H_2O}/18.$$

The atomic fraction of water (H_2O) is then

$$FA_{H_2O} = FW_{H_2O}/(\overline{A^{-1}} \times 18).$$

Consequently the atomic fraction of the hydrogen in the water is

$$FA_H = 2/3(FA_{H_2O}) = (2/3)\, FW_{H_2O}/(\overline{A^{-1}} \times 18)$$

where $\overline{A^{-1}}$ is dependent on FW_{H_2O}. For the baseline case, FA_H is .043, while for wet NTS soil it is equal to .120. If the water content by weight were 30 percent, FA_H would be .209.

The total number of activated soil atoms can be expressed as:

$$f_c \sim 1 - x \cdot FA_H$$

where x is the ratio of the absorption cross-section by hydrogen to the activation cross-sections of the other soil elements. To determine x, the fact that wet versus dry NTS soil reduces f_c by 35 percent is used, i.e.,

$$f_c^{WET} = 0.65\, f_c^{DRY}, \text{ or}$$

$$0.65 = \frac{1 - .120\, x}{1 - .043\, x}$$

which results in x being equal to 3.8. For any other water content, then, the decrease in activation from the baseline case is given by:

$$\frac{f_c}{f_{c_{DRY}}} = \frac{1 - 3.8\ FA_H}{1 - (3.8)(.043)}$$

$$= 1.20\ (1 - 3.8\ FA_H) \quad .$$

For water contents of 10, 20 and 30 percent by weight, this fraction is 0.88, 0.56 and 0.25 respectively. Figure 7.4 shows the dependence on water content using Podzol soil.

7.4 HEIGHT-OF-BURST EFFECTS ON INDUCED ACTIVITY

The Particle Activity Module accounts for HOB variations by calculating the fraction of total solid angle intersected by the apparent crater. Relative to a surface burst, the dependence is given by

$$F = 1 - \frac{HOB_s}{\sqrt{4.24\ HOB_s^2 - 234\ HOB_s + 4225}},$$

$$0 < HOB_s < 36\ ft$$

$$= 0, \quad HOB_s > 36\ ft$$

where HOB_s is the actual height of burst scaled to 1 kt by the conventional cube-root of yield scaling. However, an examination of the HOB dependence in Reference 3 of apparent crater dimensions indicated the log of the apparent crater volume to fall off linearly with HOB_s up to 10 feet with the volume at HOB_s = 10 ft being 0.01 of the crater volume from a surface burst. If it is assumed that both the crater radius and its depth have the same exponential dependence on HOB, then

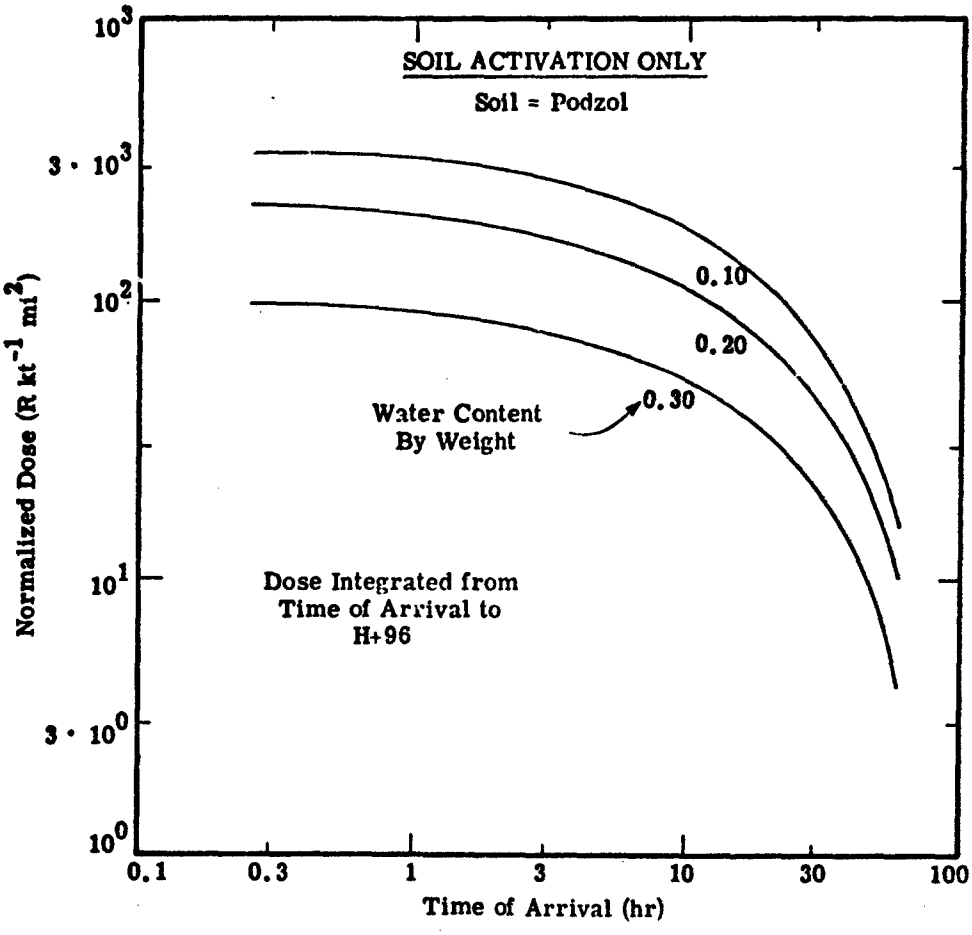

Figure 7.4. Dependence of Induced Activation in Soil on Water Content

$$Ra(HOB_s) = Ra(HOB_s = 0) \cdot \exp(-HOB_s/6.6)$$

where Ra is apparent crater radius and all dimensions are in feet. Furthermore, above a scaled height of burst of approximately 15 feet the crater formation mechanism changes from ejection to compaction. Thus the HOB dependence of the induced activity should go to zero at HOB_s = 15 feet. Using the same rationale as presently contained in the PAM, the formulation of F should be

$$F = 1. - \frac{HOB_s}{\sqrt{HOB_s^2 + (Ra\ W^{-1/3})^2}}$$

$$0 < HOB_s < 15 \text{ feet}$$

$$F = 0, \quad HOB_s > 15 \text{ feet}$$

where Ra has the dependence on HOB_s given above and W is the yield in kt. Figure 7.5 compares the DELFIC formulation with this calculation for a 1 Mt yield. It is apparent that DELFIC is presently overestimating the correction factor above a few scaled feet.

Not considered in the above analysis is the induced activity in the surface layer of dust part of which will be entrained even at HOB_s for which no crater is formed. However, this dust was originally located down to a depth of only a few millimeters. A simple calculation of the transmission of neutrons through soil indicates that less than five percent are captured in the first 5 mm. Consequently, the induced activity in the surface layer has not been considered. However further calculations should be performed.

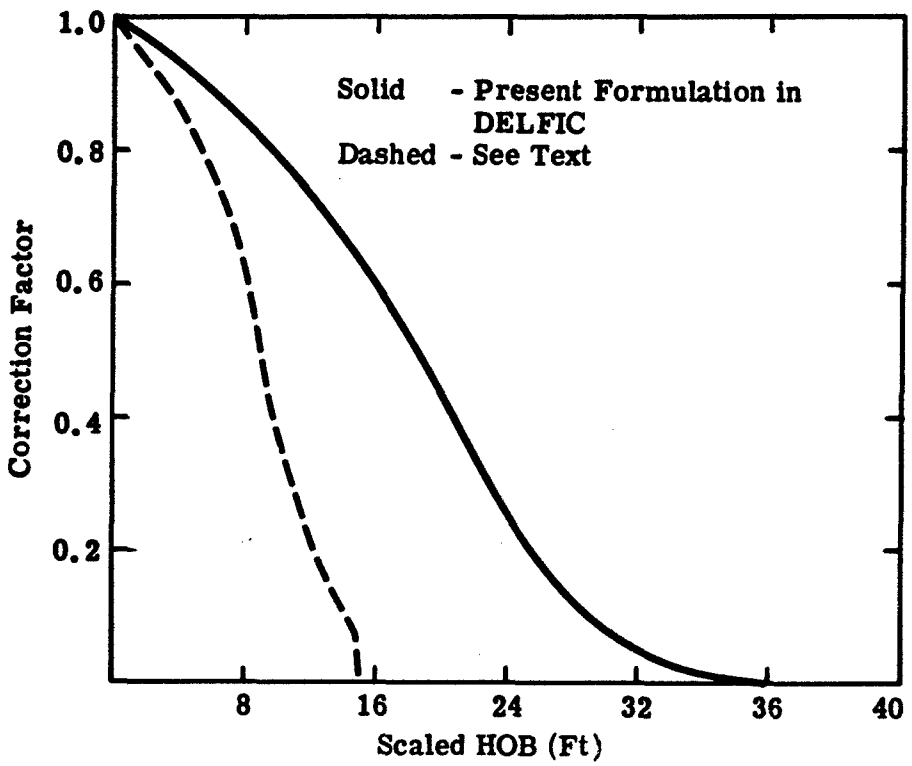

Figure 7.5 HOB Correction Factor for Induced Activity

7.5 SIZE DISTRIBUTION EFFECTS ON INDUCED ACTIVITY

DELFIC assumes that the activated soil is refractory, meaning that it is volume distributed throughout the fallout material. However, as has been pointed out in Section 7.1, most of the neutrons are captured close to the burst point. Crater material that experiences a peak stress greater than a megabar can be expected to be vaporized, while outside this region the dominant effect is to break up the material mechanically. For a 1 Mt surface burst on rock, the 1 megabar point occurs at a range of about 13 meters within which occur 80 to 90 percent of the neutron captures that contribute to fallout. The fraction of entrained material originating in this region is only on the order of 2 percent. The remainder may be subjected to some degree of melting as it is ejected into the fireball but there is probably little vaporization occurring in the fireball. Consequently, it would appear that a reasonable alternative to the DELFIC assumption is that the activated soil is volatile, i.e., it is preferentially area distributed on the fallout particles. To determine the sensitivity to this assumption, the Particle Activity Module was modified in the following manner for the 3 Mt case:

a. the fission activity was set to zero

b. the induced activity was changed to a volume distribution with size below 100μ and area distribution above 100μ.

Figure 7.6 shows the comparison with the current DELFIC assumption. The curves are for integrated dose versus range along the hotline as defined in Section 2. At close-in distances, the DELFIC prediction for the contribution of induced activity is higher as would be expected since the assumption that the activated soil can be treated as

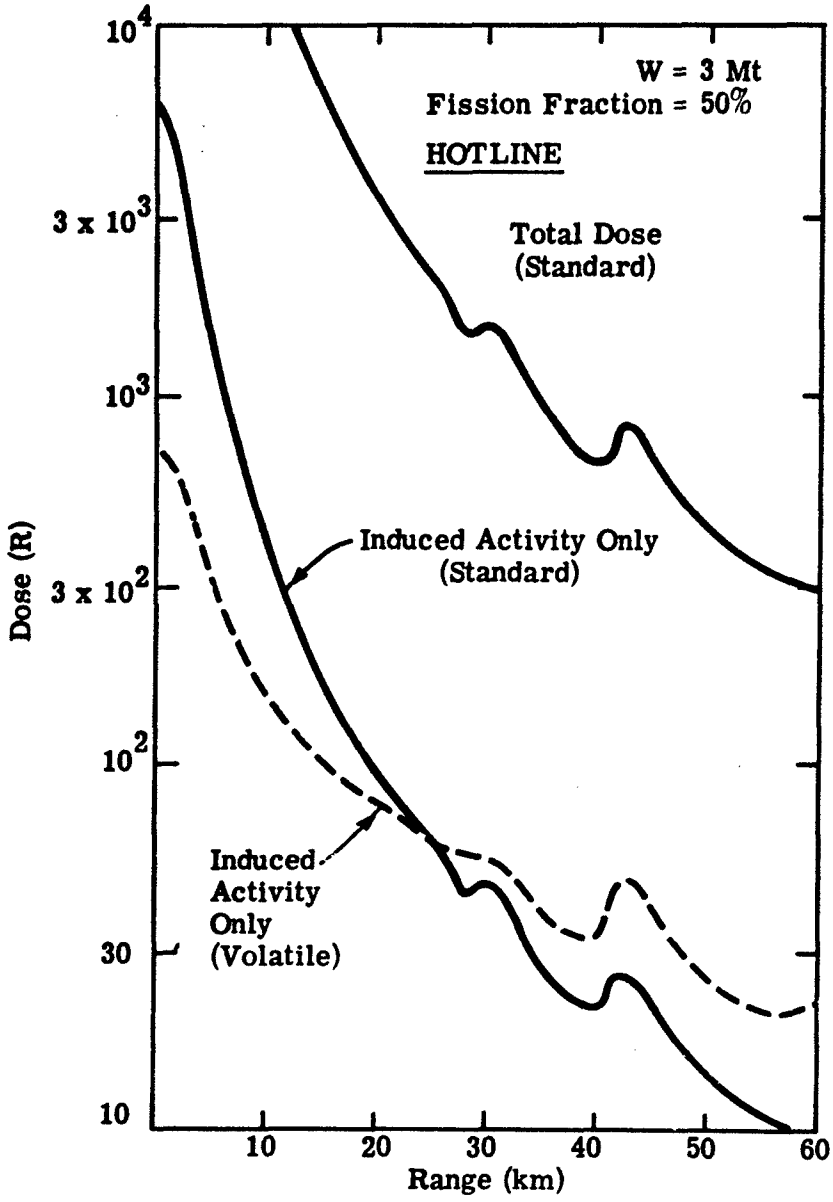

Figure 7.6 Comparison of Alternative Fractionation Assumptions for Induced Activity at Close-In Ranges

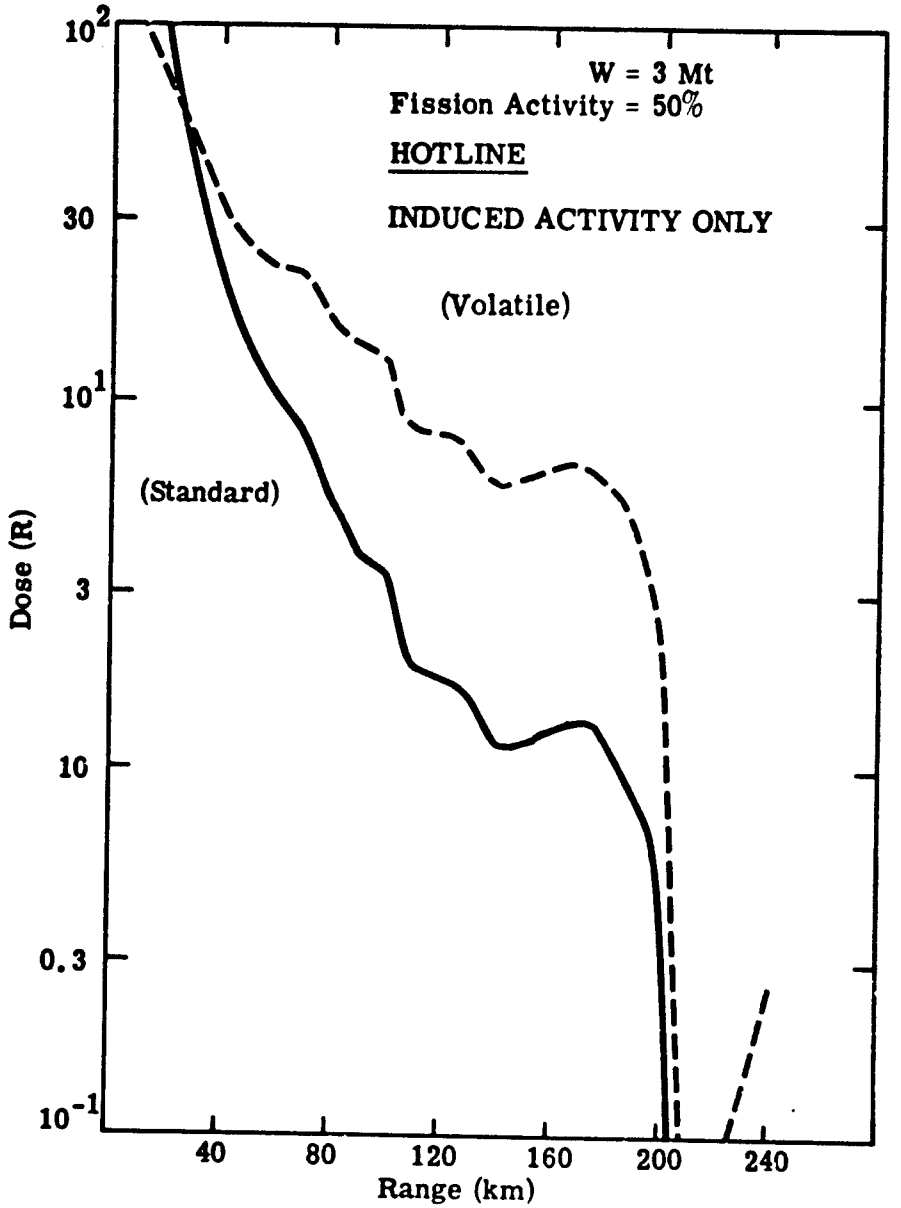

Figure 7.7 Comparison of Alternative Fractionation Assumptions for Induced Activity at Intermediate Ranges

refractory places a higher fraction of this component of the total activity on the larger particles. At zero range, the DELFIC prediction is an order of magnitude higher with the two crossing at about 25 km. The total activity is also shown on Figure 7.3. At ranges beyond 25 km, the model described above results in a higher prediction as shown with less resolution on range in Figure 7.7. However, at ranges greater than 100 km, the induced activity contribution predicted either way is below 10 R for this particular weapon configuration.

7.6 REFERENCES

1. R.C. Tompkins, "Department of Defense Land Fallout Prediction System, Volume V — Particle Activity," DASA-1800-V, U.S. Army Nuclear Defense Laboratory, Edgewood Arsenal, Maryland, 1968.

2. R. M. Lessler and R. W. Guy, "Neutron-Induced Activity in Earth and Sea Water from Buried and Surface Neutron Sources," UCRL-12407, Lawrence Radiation Laboratory, University of California, Livermore, California, 1965.

3. Private communications, W. Layson, Science Applications, Inc., McLean, Virginia, 1974.

4. Private communication, J. E. Mansfield, Science Applications, Inc., McLean, Virginia, 1974.

5. Private communications, Cpt. J. Phillips, Defense Nuclear Agency, 1974.

6. "Chemical Composition and Neutron-Induced Radioactivity Potential of Selected Rocks and Soils," Engineer Intelligence Notes, No. 32, U.S. Army Corps of Engineers, 1959.

Appendix A

USE OF THE STABILIZED CLOUD TAPE FROM SUBROUTINE RSXP IN THE CLOUD RISE MODULE

According to DASA-1800-III (Revised), the RSXP debug printout gives properties of the cloud wafers before they are sectioned in the horizontal plane. The printout column headings and their definitions are given in Table A.1.

Table A.1. Printout Explanation

TIM	Time (sec)
ALT	Altitude of wafer center of mass (m above msl)
RAD	Radius (m)
DIAM	Particle size class midrange diameter (μm)
MASS	Total particulate mass in the wafer (kg)
DZ	Wafer thickness (m)
ZLOW	Wafer bottom altitude (m above msl)
VOL	Wafer volume (m^3)
MBT	(Always = 1) signifies that both wafer top and bottom have been processed
IFLAG	A parameter that signifies whether a wafer is part of the cloud cap or stem. If it is totally or partially in the stem, further vertically subdivided wafers are printed out next. IFLAG = 1 no further subdivision required IFLAG = 2 further subdivision required

A typical example of an RSXP printout is the section of the 3 Mt data shown as Table A.2. First, note that all the volumes are 0.000. Secondly, the height of the cloud at stabilization is given as 2.2098+04 m, which means that ALT is the wafer top height, not the wafer middle height since DZ is given as 2.059+02 and ALT is given as 2.210+04 in the last row of the table. Thirdly, and most importantly, the values of DZ, ZLOW, and VOL seem to be retarded one row in the table. It appears the dotted line shown follows the correct values. Using the values outlined,

$$\text{ALT} - \text{ZLOW} = 2.190+04 - 2.169+04 = 0.021+04 = \text{DZ}.$$

This is more apparent in prior sections of the printout where DZ varies over the particle size class. And finally, the particle size listed is the lower boundary diameter of each size class, not the midrange diameter.

Table A.2. RSXP Debug Printout for 3 Mt

TIM	ALT	RAD	DIAM	MASS	DZ	ZLOW	VOL	MBT	IFLAG
8.480E+02	1.724E+04	3.430E+04	1.519E-01	5.280E+05	2.050E+02	1.683E+04	0.000	1	2
8.480E+02	1.744E+04	3.430E+04	1.519E-01	5.280E+05	2.050E+02	1.703E+04	0.000	1	1
8.480E+02	1.744E+04	3.430E+04	1.519E-01	5.280E+05	2.050E+02	1.703E+04	0.000	1	2
8.480E+02	1.764E+04	3.430E+04	1.519E-01	5.280E+05	2.050E+02	1.723E+04	0.000	1	1
8.480E+02	1.764E+04	3.430E+04	1.519E-01	5.280E+05	2.050E+02	1.723E+04	0.000	1	2
8.480E+02	1.785E+04	3.430E+04	1.519E-01	5.280E+05	2.050E+02	1.743E+04	0.000	1	1
8.480E+02	1.785E+04	3.430E+04	1.519E-01	5.280E+05	2.050E+02	1.743E+04	0.000	1	2
8.480E+02	1.805E+04	3.430E+04	1.519E-01	5.280E+05	2.050E+02	1.764E+04	0.000	1	1
8.480E+02	1.805E+04	3.430E+04	1.519E-01	5.280E+05	2.050E+02	1.764E+04	0.000	1	2
8.480E+02	1.825E+04	3.430E+04	1.519E-01	5.280E+05	2.050E+02	1.784E+04	0.000	1	1
8.480E+02	1.825E+04	3.430E+04	1.519E-01	5.280E+05	2.050E+02	1.784E+04	0.000	1	2
8.480E+02	1.845E+04	3.430E+04	1.519E-01	5.280E+05	2.050E+02	1.804E+04	0.000	1	1
8.480E+02	1.845E+04	3.430E+04	1.519E-01	5.280E+05	2.050E+02	1.804E+04	0.000	1	2
8.480E+02	1.866E+04	3.430E+04	1.519E-01	5.280E+05	2.050E+02	1.825E+04	0.000	1	1
8.480E+02	1.866E+04	3.430E+04	1.519E-01	5.280E+05	2.050E+02	1.825E+04	0.000	1	2
8.480E+02	1.886E+04	3.430E+04	1.519E-01	5.280E+05	2.050E+02	1.845E+04	0.000	1	1
8.480E+02	1.886E+04	3.430E+04	1.519E-01	5.280E+05	2.050E+02	1.845E+04	0.000	1	2
8.480E+02	1.906E+04	3.430E+04	1.519E-01	5.280E+05	2.050E+02	1.865E+04	0.000	1	1
8.480E+02	1.906E+04	3.430E+04	1.519E-01	5.280E+05	2.050E+02	1.865E+04	0.000	1	2
8.480E+02	1.926E+04	3.430E+04	1.519E-01	5.280E+05	2.050E+02	1.886E+04	0.000	1	1
8.480E+02	1.926E+04	3.430E+04	1.519E-01	5.280E+05	2.050E+02	1.886E+04	0.000	1	2
8.480E+02	1.947E+04	3.430E+04	1.519E-01	5.280E+05	2.050E+02	1.906E+04	0.000	1	1
8.480E+02	1.947E+04	3.430E+04	1.519E-01	5.280E+05	2.050E+02	1.906E+04	0.000	1	2
8.480E+02	1.967E+04	3.430E+04	1.519E-01	5.280E+05	2.050E+02	1.926E+04	0.000	1	1
8.480E+02	1.967E+04	3.430E+04	1.519E-01	5.280E+05	2.050E+02	1.926E+04	0.000	1	2
8.480E+02	1.987E+04	3.430E+04	1.519E-01	5.280E+05	2.050E+02	1.946E+04	0.000	1	1
8.480E+02	1.987E+04	3.430E+04	1.519E-01	5.280E+05	2.050E+02	1.946E+04	0.000	1	2
8.480E+02	2.007E+04	3.430E+04	1.519E-01	5.280E+05	2.050E+02	1.967E+04	0.000	1	1
8.480E+02	2.007E+04	3.430E+04	1.519E-01	5.280E+05	2.050E+02	1.967E+04	0.000	1	2
8.480E+02	2.028E+04	3.430E+04	1.519E-01	5.280E+05	2.050E+02	1.987E+04	0.000	1	1
8.480E+02	2.028E+04	3.430E+04	1.519E-01	5.280E+05	2.050E+02	1.987E+04	0.000	1	2
8.480E+02	2.048E+04	3.430E+04	1.519E-01	5.280E+05	2.050E+02	2.007E+04	0.000	1	1
8.480E+02	2.048E+04	3.430E+04	1.519E-01	5.280E+05	2.050E+02	2.007E+04	0.000	1	2
8.480E+02	2.068E+04	3.430E+04	1.519E-01	5.280E+05	2.050E+02	2.027E+04	0.000	1	1
8.480E+02	2.068E+04	3.430E+04	1.519E-01	5.280E+05	2.050E+02	2.027E+04	0.000	1	2
8.480E+02	2.088E+04	3.430E+04	1.519E-01	5.280E+05	2.050E+02	2.048E+04	0.000	1	1
8.480E+02	2.088E+04	3.430E+04	1.519E-01	5.280E+05	2.050E+02	2.048E+04	0.000	1	2
8.480E+02	2.109E+04	3.430E+04	1.519E-01	5.280E+05	2.050E+02	2.068E+04	0.000	1	1
8.480E+02	2.109E+04	3.430E+04	1.519E-01	5.280E+05	2.050E+02	2.068E+04	0.000	1	2
8.480E+02	2.129E+04	3.430E+04	1.519E-01	5.280E+05	2.050E+02	2.088E+04	0.000	1	1
8.480E+02	2.129E+04	3.430E+04	1.519E-01	5.280E+05	2.050E+02	2.088E+04	0.000	1	2
8.480E+02	2.149E+04	3.430E+04	1.519E-01	5.280E+05	2.050E+02	2.109E+04	0.000	1	1
8.480E+02	2.149E+04	3.430E+04	1.519E-01	5.280E+05	2.050E+02	2.109E+04	0.000	1	2
8.480E+02	2.170E+04	3.430E+04	1.519E-01	5.280E+05	2.050E+02	2.129E+04	0.000	1	1
8.480E+02	2.170E+04	3.430E+04	1.519E-01	5.280E+05	2.050E+02	2.129E+04	0.000	1	2
8.480E+02	2.190E+04	3.430E+04	1.519E-01	5.280E+05	2.050E+02	2.149E+04	0.000	1	1
8.480E+02	2.190E+04	3.430E+04	1.519E-01	5.280E+05	2.050E+02	2.149E+04	0.000	1	2
8.480E+02	2.210E+04	3.430E+04	1.519E-01	5.280E+05	2.050E+02	2.170E+04	0.000	1	1
8.480E+02	2.210E+04	3.430E+04	1.519E-01	5.280E+05	2.050E+02	2.170E+04	0.000	1	2

ENTERING WNDSFT

Appendix B

DISCREPANCIES IN THE GROUNDED PARTICLES TAPE

According to DASA-1800-IV, the grounded particles tape contains the X and Y coordinates of each grounded particle, time of impact, particle diameter, mass per unit area, and an area factor associated with the particle. The wind hodograph used with each yield is shown as Table B.1.

Table B.1. Wind Field Data

Vector Altitude, ZV(J)	VX(J)	VY(J)
0.00000	4.55700+00	-8.19000-01
3.04800+03	4.55700+00	-8.19000-01
6.09600+03	6.75800+00	-2.45800+00
9.14400+03	1.00860+01	-1.79200+00
1.21920+04	1.20320+01	-4.40300+00
1.52400+04	1.20320+01	-4.40300+00
1.82880+04	1.51040+01	-2.66200+00
2.13360+04	1.74080+01	-3.12300+00
2.43840+04	2.04800+01	0.00000
2.74320+04	2.30400+01	0.00000
3.04800+04	2.56000+01	0.00000

A planar topography was assumed, and there were no updrafts or other localized wind phenomena input. Consequently, an increasing value of X and a decreasing value of Y correspond to an increasing time of impact. Tables B.2 and B.3 are reproductions of a listing of the 3 Mt grounded particles tape. Various rows of

Table B.2. Section of 3 Mt Tape IPOUT

X (m)	Y (m)	T (sec)	P. Size (wm)	M/A (kg/m^2)	Radius of Wafer Multiplier
[illegible]	[illegible]	[illegible]	[illegible]	[illegible]	[illegible]

Table B.3. Section of 3 Mt Tape IPOUT

X (m)	Y (m)	T (sec)	P. Size (wm)	M/A (kg/m^2)	Radius of Wafer Multipliers
9.9855194E+04	-2.4002480E+05	1.4956660E+00	1.1260171E+01	1.7883298E-05	666
9.8261830E+04	-2.3654900E+05	1.4619180E+00	1.1260171E+01	9.3177758E-05	777
9.8773065E+04	-2.3748320E+05	1.4667080E+00	1.1260171E+01	1.0509778E-04	777
9.8113523E+04	-2.3514882E+05	1.4487480E+00	1.1260171E+01	1.7271518E-05	666
9.7747461E+04	-2.3688368E+05	1.4620010E+00	1.1260171E+01	1.5768810E-05	666
9.8968807E+04	-2.3779075E+05	1.4680056E+00	1.1260171E+01	1.6230977E-05	666
9.9153454E+04	-2.3874800E+05	1.4856708E+00	1.1260171E+01	1.6230977E-05	666
9.9501005E+04	-2.4320077E+05	1.4897452E+00	1.1260171E+01	1.6230977E-05	666
9.9714145E+04	-2.4715229E+05	1.4920052E+00	1.1260171E+01	1.6230977E-05	666
9.9793485E+04	-2.5060565E+05	1.4974740E+00	1.1260171E+01	1.6230977E-05	666
9.9739667E+04	-2.5356321E+05	1.5060200E+00	1.1260171E+01	1.6230977E-05	666
9.9810890E+04	-2.5666197E+05	1.5020010E+00	1.1260171E+01	1.6230977E-05	666
9.9739655E+04	-2.5925807E+05	1.5070661E+00	1.1260171E+01	1.6230977E-05	666
9.9524612E+04	-2.6134034E+05	1.5013078E+00	1.1260171E+01	1.6230977E-05	666
9.9164234E+04	-2.6202756E+05	1.5332605E+00	1.1260171E+01	1.6230977E-05	666
9.8656041E+04	-2.6390834E+05	1.5180078E+00	1.1260171E+01	1.6230977E-05	666
9.8309644E+04	-2.6556367E+05	1.5205785E+00	1.1260171E+01	1.6230977E-05	666
9.8015562E+04	-2.6669068E+05	1.5283211E+00	1.1260171E+01	1.6230977E-05	666
9.7503377E+04	-2.6736530E+05	1.5661620E+00	1.1260171E+01	1.6230977E-05	666
9.7060700E+04	-2.6748215E+05	1.5477080E+00	1.1260171E+01	1.6230977E-05	666
9.6890330E+04	-2.6734007E+05	1.5221605E+00	1.1260171E+01	1.6230977E-05	666
9.3236362E+04	-2.6133604E+05	1.1817601E+00	1.1260171E+01	1.6230977E-05	666
9.2565502E+04	-2.6111806E+05	1.1687017E+00	1.1260171E+01	1.6230977E-05	666
9.1782061E+04	-2.6050200E+05	1.1467078E+00	1.1260171E+01	1.6230977E-05	666
9.0885065E+04	-2.5948212E+05	1.1277087E+00	1.1260171E+01	1.6230977E-05	666
9.0257004E+04	-2.5912472E+05	1.1126784E+00	1.1260171E+01	1.6230977E-05	666
8.9532650E+04	-2.5861200E+05	1.0967208E+00	1.1260171E+01	1.6230977E-05	666
8.8710676E+04	-2.5737426E+05	1.0709825E+00	1.1260171E+01	1.6230977E-05	666
8.7790872E+04	-2.5507635E+05	1.0621057E+00	1.1260171E+01	1.6230977E-05	666
8.6772411E+04	-2.5422670E+05	1.0434176E+00	1.1260171E+01	1.6230977E-05	666
8.9256730E+04	-2.6244120E+05	1.0667625E+00	1.1260171E+01	1.6230977E-05	666
9.1576877E+04	-2.7021352E+05	1.0817005E+00	1.1260171E+01	1.6230977E-05	666
9.3721015E+04	-2.7750132E+05	1.1137704E+00	1.1260171E+01	1.6230977E-05	666
9.5677225E+04	-2.8426198E+05	1.1306592E+00	1.1260171E+01	1.6230977E-05	666
9.7433470E+04	-2.9065240E+05	1.1460706E+00	1.1260171E+01	1.6230977E-05	666
9.3413670E+04	-2.7073946E+05	1.0837707E+00	1.1260171E+01	1.6230977E-05	666
8.9469900E+04	-2.6839181E+05	1.0700183E+00	1.1260171E+01	1.6230977E-05	666
8.5735343E+04	-2.6570336E+05	8.8603867E+00	1.1260171E+01	1.6230977E-05	666
8.1965933E+04	-2.6431017E+05	8.7000181E+00	1.1260171E+01	1.6230977E-05	666
7.8172711E+04	-2.5074946E+05	8.8352505E+00	1.1260171E+01	1.6230977E-05	666
1.2467977E+06	-3.5540688E+05	1.4400026E+05	1.1260171E+01	1.6230977E-05	666
1.3359807E+06	-3.7817488E+05	1.5312028E+05	1.1260171E+01	1.6230977E-05	666
1.3852310E+06	-3.8947008E+05	1.5750026E+05	1.1260171E+01	1.6230977E-05	666
1.4236837E+06	-3.9764885E+05	1.6078014E+05	1.1260171E+01	1.6230977E-05	666
1.4577063E+06	-4.0461336E+05	1.6366033E+05	1.1260171E+01	1.6230977E-05	666
1.4830692E+06	-4.0912340E+05	1.6574660E+05	1.1260171E+01	1.6230977E-05	666
1.5083652E+06	-4.1361027E+05	1.6785785E+05	1.1260171E+01	1.6230977E-05	666
1.5336166E+06	-4.1809832E+05	1.6854784E+05	1.1260171E+01	1.6230977E-05	666
1.6577166E+05	-3.8224894E+04	2.6005680E+04	6.7561028E+01	8.8152237E-05	55
1.6693653E+05	-3.8432604E+04	2.6131827E+04	6.7561028E+01	2.4779015E-05	49
1.6306907E+05	-3.7660121E+04	2.5663384E+04	6.7561028E+01	1.9868685E-05	91
1.6630402E+05	-3.8598307E+04	2.5674080E+04	6.7561028E+01	7.4523641E-06	133
1.6743710E+05	-3.8800357E+04	2.5728701E+04	6.7561028E+01	8.1037902E-06	154
1.6426132E+05	-3.8010261E+04	2.5221862E+04	6.7561028E+01	9.9258865E-05	399
1.6536717E+05	-3.8204760E+04	2.5311105E+04	6.7561028E+01	1.2511058E-04	399
1.6647302E+05	-3.8403210E+04	2.5401746E+04	6.7561028E+01	6.2182177E-05	644
1.6757[illegible]E+05	-3.8599[illegible]E+04	2.5500[illegible]E+04	6.7561028E+01	9.0182177E-05	644

data are marked with symbols (*, *, +) to illustrate pairs of data which are inconsistent. Each pair is for a different particle size, and yet each pair has the same error. For an increasing X and decreasing Y, T is decreasing instead of increasing.

Also, the arrow symbol (→) on Table B.3 shows where the X, Y, and T coordinates all increase by a factor of 10 for no obviously apparent reason.

And finally, also on Table B.3, the symbol ○ shows two rows of data which not only exhibit the increasing X-decreasing Y-decreasing T error, but also shows a wafer with a larger radius hitting the ground before a wafer with a smaller radius. By the logic of the Cloud Rise Module, this is impossible.

It appears that there is an error associated with the time of impact calculations. Similar errors were discovered in the 10 Mt data. These errors were not observed in the 30 kt data, nor were they observed in the 3 Mt or 10 Mt data for wafer radii multipliers much less than 886. The 30 kt data contain very few wafer radii multipliers of 886. Either the time error is yield dependent, or wafer radii dependent.

Appendix C

FORTRAN LISTING OF PROGRAM LINTAP

```
      PROGRAM LINTAP(INPUT,INPUT,TAPE1=INPUT,TAPE2=OUTPUT,TAPE3,TAPE4)
C     LINTAP/73/74/
C        IN          ,ISKIT        ,IRISE        ,JPARIN       ,IPARIN
C        IOUT        ,IO=(W)       ,INTAPO       ,IPOUT        ,IPAROT
C        TAPE        ,NUMTAP(15)   ,IFREC        ,LGO          ,LTHRU
C        NT
      COMMON /A/ PRNT
      PRNT=.TRUE.
      DO    I=1,15
      NUMTAP(I)=0
      NUMTAP(1)=1
      NUMTAP(2)=2
      ISKIP=1
      ISKIP=2
      NUMTAP(5)=5
      CALL OFFSET
      CALL LINOUT
      STOP
      END
```

```
      SUBROUTINE BATMAN
C     VERSION 1
C     R C TOMPKINS -- US ARMY NUCLEAR DEFENSE LABS
C     AUGUST 1968
C     REVISED BY R W JONES -- FEBRUARY 1969
C   THIS VERSION REPLACES SUBROUTINES INGEN, BATMAN, DECAY, AND DOSE OF
C   THE INITIAL VERSION OF DELFIC
C
C
C   THE FUNCTION OF THIS SUBROUTINE IS TO COMPUTE RADIOACTIVE DECAY
C   CHAINS BY MEANS OF THE BATEMAN EQUATION
CALLED BY FRATIO, GRNSR, AND MCNEP
C
C  *  *  *  *  *  *  *  *  *  GLOSSARY  *  *  *  *  *  *  *  *  *  *  *  *
C   AMEGA(700)     INITIAL FISSION PRODUCT ABUNDANCES IN ATOMS/10000
C                  FISSIONS (PARALLEL TO NUCLID)
C   ABUNDO(700)    FISSION PRODUCT ABUNDANCES PER 10000 FISSIONS
C                  ATOMS AT TMSO IN FRATIO
C                  DISINTEGRATIONS/SEC AT TIME (JD=1)
C                  DISINTEGRATIONS FROM TENTER TO TEXIT
C                  OR INFINITY (JD=2)
C   H(15)          CONTRIBUTION OF ONE SUBCHAIN TO ABUNDO
C   CNEJ(480)      BATEMAN COEFFICIENTS FOR ONE SUBCHAIN
C   IHR            COUNTER TO KEEP PLACE IN BRANCHING RATIO TABLE WHILE
C                  SCANNING NUCLIDE TABLE
C   IFIGO          ASSIGNED GOTO PARAMETER CORRESPONDING TO IGO
C   IFJD           ASSIGNED GOTO PARAMETER CORRESPONDING TO JD
C   IGO            (LOGICAL) TRUE GIVES ACTIVITY,
C                  FALSE GIVES ATOMIC ABUNDANCES
C   INFORM(11)     TABLE OF DAUGHTER RETRIEVAL INFORMATION FOR EACH
C                  MEMBER OF A SUBCHAIN, OBTAINED BY TRUNCATING NUCLID
C                  FROM THE LEFT
C   JD             (LOGICAL) TRUE COMPUTES EXPOSURE RATE,
C                  FALSE COMPUTES DOSE
C   KDOS           (LOGICAL) TRUE COMPUTES DOSE FROM TENTER TO TEXIT,
C                  FALSE COMPUTES DOSE FROM TENTER TO INFINITY
C   KFJD           SEE IFJD
C   LIM(11)        SUBCHAIN TABLE OF INDICES FOR MULT TO FIND CURRENT
C                  BRANCHING PATH
C   LSUB           COUNTER FOR SUBCHAIN MEMBERS
C   NUC(11)        CROSS REFERENCE OF SUBCHAIN MEMBERS TO INDEX IN NUCLID
C   SBR(11)        SUBCHAIN BRANCHING RATIOS
C   SCA(15)        FISSION YIELDS OF SUBCHAIN MEMBERS
C   SDC(15)        DISINTEGRATION CONSTANTS OF SUBCHAIN MEMBERS
C   TENTER         ENTRY TIME (SEC) FOR DOSE CALCULATION WITH JD = FALSE
C   TEXIT          EXIT TIME (SEC) FOR DOSE CALCULATION
C                  WITH JD = FALSE, KDOS = TRUE
C   TIME           TIME (SEC) AT WHICH EXPOSURE RATE OR MASS CHAIN
C                  COMPOSITE IS CALCULATED WITH JD = TRUE
C
C

      COMMON /PAM/
     *    AMEGA(700)  ,ABUNDO(700) ,ALAFON      ,ABRANCH(130) ,BSUBK(90)
     *   ,CAPTS       ,DCON1(700)  ,ICF(90)     ,IHR(185)     ,FAC(7,18)
     *   ,FISNUM      ,FMASS(200)  ,FOGANY(7,18),FP(700)      ,FW
     *   ,IBRA        ,IGO         ,INUC        ,ISO(18)      ,ITAB
     *   ,JGO         ,JRM(185)    ,KDOS        ,KOUT         ,KRK
```

```
     *   .LMAX        .MASCHN      .MAXNUC      .MULT(11)    .NPRNT(15)
     *   .NUCLID(700) .PACT(200)   .PSIZE(200)  .TENTER      .TEXIT
     *   .TIME        .FLAM(7.1M)  .JD
      LOGICAL IGO.JD.KDOS.NPRNT
      DIMENSION  EFAC  (11)  .KBR   (11)
     1           .INFORM(11)  .LIM   (11)  .NUC   (11)  .SBR   (11)
     2           .SCA   (11)  .SDC   (11)
C
      LOGICAL FLAG
C
CC  SET INITIAL VALUES
      DO 1 I = 1.INUC
    1 AMINDO(I) = 0.0
      IHR = 0
C
CC  BEGIN MAIN LOOP THROUGH THE NUCLIDE TABLE
C
   10 DO 500 IN = 1.INUC
C   FIND THE NEXT NUCLIDE THAT BEGINS A SUBCHAIN
      IF (NUCLID(IN))11.500.490
C
C   SET PARAMETERS FOR BEGINNING OF A SUBCHAIN
C         MEMBERSHIP COUNTER
   11 LSUB = 1
C         BRANCHING RATIO COUNTER
      LHR = IRR
      KBR(1) = LHR
C         STARTING INDEX
      NUC(1) = IN
   12 LIM(LSUB) = 0
C   PROCESS A SUBCHAIN MEMBER
   13 KP = NUC(LSUB)
      IM = LIM(LSUB)
      INFO = MOD(IABS(NUCLID(KP)).MULT(5))
      INFORM(LSUB) = INFO
      INC = 1
C   SET UP SUBCHAIN DISINTEGRATION CONSTANTS
      SDC(LSUB) = DCON(KP)
CHECK FOR END OF SUBCHAIN
      IF (INFO.EQ.0) GO TO 21
CHECK FOR BRANCHING
      IF (MOD(INFO.MULT(1)).LT.0) GO TO 14
      SBR(LSUB) = 1.0
      GO TO 15
C   SET UP SUBCHAIN BRANCHING RATIOS
   14 LR = LHR + 5 - IM
      SBR(LSUB) = BRANCH(LR)
C   EXTRACT THE DAUGHTER INCREMENT
   15 ID = MOD(INFO.MULT(IM+1))/MULT(IM)
C   SEE IF THIS INCREMENT SHOULD BE NEGATIVE
      IF (MOD(INFO.MULT(2))/MULT(1).EQ.IM)GO TO 16
C   SET PARAMETER TO LOOK AHEAD FOR BRANCHING RATIO OF DAUGHTER
      KI = KP
      GO TO 17
C   SET PARAMETER TO LOOK BEHIND FOR BRANCHING RATIO OF DAUGHTER
   16 KI = -1
      LHR = 0
```

```
      INC = -INC
COMPUTE DAUGHTER INDEX
   17 NDAUT = NP + INC*ID
      NDA = NDAUT - 1
C   STEP THROUGH THE NUCLIDE TABLE TO ESTABLISH THE CORRECT INDEX FOR
C   THE BRANCHING RATIO OF THE DAUGHTER
      DO 20 K = 1,NDA
   20 LAR = LHR + 4 - IABS(MOD(NUCLID(K),MULT(1)))
      KAR(LSUR+1) = LHR
C
C   ACCEPT THE DAUGHTER FOR MEMBERSHIP IN THE SUBCHAIN AND RECYCLE
      LSUM = LSUM + 1
      IF (LSUR.GT.11) GO TO 1301
      NUC(LSUR) = NDAUT
      GO TO 12
C
CC  A SUBCHAIN HAS NOW BEEN SET UP AND CAN BE STUDIED IN TOTO
C   ELIMINATE UNI-MEMBERED SUBCHAIN
   21 IF (LSUR.EQ.1) GO TO 500
C   RUN BACK THROUGH THE SUBCHAIN TO ACCUMULATE BRANCHING RATIOS
      ASSIGN 23 TO LGO
      JL = 0
      SCA(LSUR) = 1.0
      LAST = LSUR + 1
      DO 22 L = 2,LSUR
      LBACK = LAST - L
      SCA(LBACK) = 1.0
      GO TO LGO,(22,23)
C   FIND THE LAST BRANCH IN THE SUBCHAIN
   23 IN = LIM(LBACK)
      IF (MOD(INFORM(LBACK)*MULT(IN))/MULT(IN-1))22,22,24
   24 JL = LBACK
      ASSIGN 22 TO LGO
   22 SCA(LBACK) = SNR(LBACK)*SCA(LBACK+1)
      SCA(LSUR) = 0.0
CORRECT FISSION YIELDS FOR BRANCHING
      FLAG = .FALSE.
      DO 25 J = 1,LSUM
      JN = NUC(J)
      SCA(J) = SCA(J)*ABEGN(JN)
      IF (FLAG) GO TO 25
C   MAKE A NOTE IF AT LEAST ONE VALUE OF SCA IS NONTRIVIAL
      IF (SCA(J))25,25,27
   27 FLAG = .TRUE.
   25 CONTINUE
C
C   OMIT COMPUTATIONS FOR TRIVIAL SUBCHAIN
      IF (.NOT.FLAG) GO TO 30
C
CC  THE CENTRAL COMPUTATIONS BEGIN AT THIS POINT
C
      DO 200 N=1,LSUR
      IF(ID) TENTFR=TIME
      EFAC(N)=EXP(-SDC(N)*TENTFR)
      IF(NINS) EFAC(N) = EFAC(N)-EXP(-SDC(N)*TEAIT)
      A=0.0
      DO 193 K=1,N
```

```
      CNIJ=1.0
      Q=0.0
      DO 162 K=1,N
      K2=N-K+1
      IF(K2.NE.N) CNIJ=CNIJ*SDC(K2)
      IF(K2.EQ.K1) GO TO 162
      FACTC=SDC(K2)-SDC(K1)
      IF(ABS(FACTC).LT.1.E-15) FACTC=SIGN(1.E-15,FACTC)
      CNIJ=CNIJ/FACTC
  162 IF(K2.LE.K1)Q=Q+CNIJ*SCA(K2)
      IF(JD) GO TO 163
      IF(SDC(K1).LE.0.0) GO TO 163
      Q=Q/SDC(K1)
  163 R=R+Q*EFAC(K1)
      IF(R.LE.0.0) GO TO 200
      IF(IGO) R=R*SDC(N)
      NK=NUC(N)
      ABUNDO(NK)=ABUNDO(NK)+R
  200 CONTINUE
C
C   SET UP A NEW SUBCHAIN STARTING FROM DEEPEST UNEXPLORED BRANCH
   90 IF (K1)500,499,91
   91 LSUB = K1
      LIM(LSUB) = LIM(LSUB) - 1
      LAR = KHR(LSUB)
      GO TO 11
C
C
 1301         WRITE (KOUT,1351) NUCLID(IN)
C
C   STEP UP BRANCH COUNTER IN MAIN LOOP
  400 IHR = IHR + 4 - MOD(IABS(NUCLID(IN)),4)*MULT(1)
  500 CONTINUE
      IF (NPRNT(9)) WRITE (KOUT,1000) (NUCLID(I),ABUNDO(I),I=1,NUC)
      RETURN
 1000 FORMAT (1H1,10HOUTPUT OF BATMAN//8X,6HNUCLID,11X,6HABUNDO/
     1    (5X,A12,5X,1PE12.4))
 1351 FORMAT (25H0SUBCHAIN BEGINNING WITH A12,8H TOO A16)
      END
```

```
      SUBROUTINE FRATIO
     1    (SLOTMP,TMSO,MCHN)
C
C     W. J. COMPTON -- US ARMY NUCLEAR DEFENSE LABS
C     SEPTEMBER 1986
C
      COMMON /PAM/
     *     AHFGN(700)   ,ARUNDO(700) ,ALAFON      ,BRANCH(130) ,BSUBK(90)
     *    ,CAPFIS       ,DCON(700)   ,ECF(90)      ,ENN(185)    ,FAC(7,18)
     *    ,FISNUM       ,FMASS(200)  ,FOGNNY(7,18) ,FP(200)     ,FW
     *    ,IMPA         ,IGO         ,INUC         ,ISO(18)     ,ITAR
     *    ,JGO          ,JPN(185)    ,KDOS         ,KOUT        ,KRN
     *    ,LMAX         ,MASCHN      ,MAXNUC       ,MULT(11)    ,NPRNT(15)
     *    ,NUCLID(700)  ,PACT(200)   ,PSIZE(200)   ,TENTER      ,TEXIT
     *    ,TIME         ,XLAM(7,18)  ,JD
      LOGICAL IGO,JD,KDOS,NPRNT
      DIMENSION FP(90)
      DIMENSION HOIL(40)
C
      EQUIVALENCE (FP,RSUBK)
C
      LOGICAL NOTO
C
      DATA HOIL//3173.0,2907.0,3000.0,2976.0,1764.0,1010.0,1026.0,331.8
     1,1[illegible],1855.0,3497.0,4495.0,4808.0,3300.0,1351.0,583.0,4505.0,6149
     2,0.,436.0,2451.0,1832.0,2123.0,2247.0,1832.0,1534.0,457.4,165.9,15
     355.0,3093.0,4604.0,4367.0,4252.0,4464.0,4348.0,5*4300.0/
C
      TMS = TMSO
      IGO = .FALSE.
      JD = .TRUE.
      KDOS = .FALSE.
      MAXCHN = 90
      DO 40 I = 1,MAXCHN
   40 FP(I) = 0.0
C
      CALL BATMAN
C
      MCHN = 0
      RFRC = 0.0
      CHN = 0.0
      LAST = IABS(NUCLID(1))/MULT(9)
      NOTO = .FALSE.
C
      DO 10 MA = 1,INUC
      NAME = IABS(NUCLID(MA))/MULT(6)
      MASS = NAME/MULT(3)
      NAT = MOD(NAME,MULT(3))
      IF (NAT.GE.27.AND.NAT.LE.66) GO TO 1
      WRITE (KOUT,51) NAT,MASS
      ABU = 0.0
      GO TO 10
    1 IF (MASS.EQ.LAST)GO TO 3
      MCHN = MCHN + 1
      IF (NOTO) FP(MCHN) = RFRC/CHN
      RFRC = 0.0
```

```
      CHN = 0.0
      NOTO = .FALSE.
    3 ABUND = ABUNDO(NR)
      MASS = MASS
      IF (ABUND)10,10,4
    4 NOTO = .TRUE.
      IF (ROIL(NAT=26).GE.SLOTMP) RFRC = RFRC + ABUND
      CHN = CHN + ABUND
   10 CONTINUE
      MCHN = MCHN + 1
      IF (NOTO) FR(MCHN) = RFRC/CHN
C
      IF (NPRNT(6)) GO TO 22
   19 DO 12 L = 1,MCHN
      RSUBK(L) = SQRT(FR(L)) - 1.0
      POWER = RSUBK(L)
      SUM = 0.0
      DO 20 M = 1,ITAR
   20 SUM = SUM + FMASS(M)*PSIZE(M)**POWER
   12 FO(L) = 1.0/SUM
      IF (NPRNT(7)) GO TO 23
   21 IPU = .TRUE.
      RETURN
   22 WRITE (KOUT,501)
      WRITE (KOUT,502) (J,FR(J),J=1,MCHN)
      GO TO 19
   23 WRITE (KOUT,503)
      WRITE (KOUT,502) (K,RSUBK(K),K=1,MCHN)
      GO TO 21
  501 FORMAT (1H1, 40HOUTPUT OF FRATIO// 5(6X, 4HMCHN, 9X, 2HFR, 3X))
  502 FORMAT ( 5(7X, I2, 1PE12.4))
  503 FORMAT(////63X,4HCHN9X5HRSUBK//)
  513 FORMAT (66H0BOILING POINT IS NOT AVAILABLE FOR ELEMENT I3,
     1  4H(MASS I3,1H))
      END
```

```
SUBROUTINE GXPSR      73/74   OPT=1                FTN 4.0+P357     04/04/74  23.47.31.     PAGE     1

      SUBROUTINE GXPSR
C
C     CASSIDY - NNDL / TOMPKINS - NDL
C
C     NOVEMBER 1966
CALLED BY PAM2
      COMMON /PAM/
     *     AMEIGN(700)   *AMUNDO(700) *ALHPOM       *MMANCH(130) *BSUBK(90)
     *    *CAPFIS        *DCON(700)   *ECF(90)      *ERM(185)    *FAC(7,18)
     *    *FISNUM        *FMASS(700)  *FOGMNT(7,18) *FP(200)      *FW
     *    *IHRA          *IGO         *INDIC        *ISO(18)     *ITAB
     *    *JGO           *JRM(185)    *KDOS         *KOUT        *KRM
     *    *MAX           *MASCHN      *MAXNUC       *MULT(11)    *NPRNT(15)
     *    *NUCLID(700)  *PACT(700)   *PSIZE(200)   *TENTER      *TEXIT
     *    *TIME          *XLAM(7,18)  *JD
      LOGICAL IGO,JD,*KDOS,*NPRNT
C
      DIMENSION ART(90)
C
      DATA CROSS,UNIT/100.0,1.0/
C
  901 FORMAT
     1    (1H1,OUTPUT OF GXPSR/5X13HPARTICLE SIZE7X24HFISSION PROCUCT AC
     2TIVITY)
  902 FORMAT
     1    (6X7HNICHON,16X1)H(N*M**2)/MR//)
  903 FORMAT
     1    (5X1PE12.4,1X,E12.4)
  904 FORMAT
     1    (6X7HNICHON,14X6HM**N**2///)
C
      CALL MATMAN
      MAXNCH = 90
      NCH = 0
      DO 1 I = 1,MAXNCH
    1 ART(I) = 0.0
C
      DO 10 J = 1,KRM
      K = IRM(J)
      IF (ERM(J))11,10,12
   11 NCH = NCH + 1
C*****PASS CHAIN NORMALIZATION FACTOR
C
   12 ART(NCH) = ART(NCH) + ARUNDO(K)*ABS(ERM(J))
C
   10 CONTINUE
C
      DO 20 LC = 1,NCH
      IF (ART(LC))20,20,21
   21 ANEX = FISNUM(LC)
      CRISS = CROSS**ANEX
      RADIAL = ECF(LC)/(UNIT * CRISS*FCF(LC))
      STRAIT = RADIAL*CRISS
      TNEX = FISNUM*ART(LC)
      DO 40 LD = 1,ITAB
   40 FP(LD) = FP(LD) + (RADIAL*PSIZE(LD)**ANEX + STRAIT)*TNEX*FMASS(LD)
   20 CONTINUE
```

```
C
C
      IF (.NOT.WPRNT(10)) RETURN
C
      WRITE (KOUT,901)
      IF (J0) GO TO 101
      WRITE (KOUT,912)
      GO TO 102
  101 WRITE (KOUT,902)
  102 CONTINUE
      DO 103 I=1,ITAB
      WRITE (KOUT,903) PSIZE(I),FP(I)
  103 CONTINUE
C
      RETURN
      END
```

```
SUBROUTINE INUC02                                                    FTN 4.0+P357     04/04/74 23.47.34.     PAGE     1

      SUBROUTINE INUC02
C
C     COMMON /BANK/
     *     SMEGN(700)   *ARUNXX(700) *ALRFON      *BRANCH(130) *BSUBK(90)
     *    *CAPFIS       *DCON(700)   *FCF(90)     *EHH(185)    *FAC(7,18)
     *    *FISHUM       *FMASS(200)  *FOGRNY(7,18) *FP(200)     *FW
     *    *IGHA         *IGO         *INUC        *ISO(18)     *ITAB
     *    *JGO          *JRM(185)    *KDOS        *KOUT        *KRM
     *    *LMAX         *MASCHN      *MAXNUC      *MULT(11)    *NPRNT(15)
     *    *NUCLID(700) *PACT(200)   *PSIZE(200)  *TENTEN      *TEXIT
     *    *TIME         *XLAM(7,18)  *JD
      LOGICAL IGO,JD,KDOS,NPRNT
C
 1000 FORMAT
     1    (17H1OUTPUT OF INUC02/5X53HINDUCED ACTIVITY IN THE TRANSPORTED
     2 SOIL CONTRIBUTES 1PE12.4,23H TO EACH PARTICLE SIZE.)
C
      SDRE = 0.0
C
      DO 20 L = 1,LMAX
      IS = ISO(L)
C
      DO 22 I = 1,IS
      DLA = XLAM(I,L)
      IF (.NOT. JD) GO TO 12
      DKI = XFAC(I,L)*DLAM*FOGRNY(I,L)*EXP(DLAM*TIME)
      GO TO 22
C
   12 IF (.NOT.KDOS) GO TO 14
      DKI = FAC(I,L)*FOGRNY(I,L)*(EXP(DLAM*TENTEN) - EXP(DLAM*TEXIT))
      GO TO 22
C
   14 DKI = FAC(I,L)*FOGRNY(I,L)*EXP(DLAM*TENTEN)
C
   22 SDRE = SDRE + DKI
   20 CONTINUE
C
C
      SDRE = SDRE*ALRFON*FISHUM
C
      DO 24 MA = 1,ITAB
   24 FP(MA) = FP(MA) * SDRE*FMASS(MA)
C
      IF (NPRNT(11)) WRITE (KOUT,1000) SDRE
      RETURN
      END
```

```
      SUBROUTINE INDCD2
C
C     ROUTINE FOR LIBR
      COMMON /PARAM/
     *    ADPGN(760)   ,ARUNIN(780) ,ALHFOM      ,AMANCH(130) ,BSUBK(90)
     *   ,CAPFIS       ,DCON(700)   ,FCF(90)      ,EHN(185)    ,FAC(7,18)
     *   ,FISHRM       ,FMASS(280)  ,FOGMNY(7,18) ,FP(280)     ,FW
     *   ,IGNA         ,IGO         ,INUC         ,ISO(18)     ,ITAB
     *   ,KO           ,JRM(185)    ,KDOS         ,KOUT        ,KRM
     *   ,LMAX         ,MASCMP      ,MAXNUC       ,MULT(11)    ,NPRNT(15)
     *   ,PARCLID(700) ,PACT(280)   ,PSIZE(280)   ,TENTEN      ,TEXIT
     *   ,TIME         ,ALAM(7,18)  ,JO
      LOGICAL IGO,JO,KDOS,NPRNT
C
 1000 FORMAT
     1    (17H1OUTPUT OF INDCD2/5X53HINDUCED ACTIVITY IN THE TRANSPORTED
     2 SOIL CONTAINUTS (PE12.4,23H TO EACH PARTICLE SIZE.)
C
      SOME = 0.0
C
      DO 22 L = 1,LMAX
      IS = ISO(L)
C
      DO 22 I = 1,IS
      DLAM = -ALAM(I,L)
      IF (.NOT. JO) GO TO 12
      DMI = -FAC(I,L)*DLAM*FOGMNY(I,L)*EXP(DLAM*TIME)
      GO TO 22
C
   12 IF (.NOT.KDOS) GO TO 14
      DMI = FAC(I,L)*FOGMNY(I,L)*(EXP(DLAM*TENTER) - EXP(DLAM*TEXIT))
      GO TO 22
C
   14 DMI = FAC(I,L)*FOGMNY(I,L)*EXP(DLAM*TENTEN)
C
   22 SOME = SOME + DMI
   24 CONTINUE
C
C
      SOME = SOME*ALHFOM*FISHRM
C
      DO 26 MA = 1,ITAB
   26 FP(MA) = FP(MA) + SOME*MASS(MA)
C
      IF (.NOT.IGO) WRITE (KOUT,1000) SOME
      RETURN
      END
```

```
      SUBROUTINE MCHDEP
C
C       # C TOMPKINS - US ARMY NUCLEAR DEFENSE LABS
C     NOVEMBER 1968
CALLED BY PAM2
C
      COMMON /PAM/
     *    AMINON(700)  ,ARUNDO(700) ,ALAMOM       ,ARANCH(130) ,ASUBK(98)
     *   ,CAPFIS       ,NCON(700)   ,ECF(98)      ,EPH(185)    ,FAC(7,18)
     *   ,FISNUM       ,FMASS(200)  ,FOGAMY(7,18) ,FP(200)     ,FW
     *   ,IHNA         ,IGO         ,INUC         ,ISO(18)     ,ITAB
     *   ,JGO          ,JNM(185)    ,KOOS         ,KOUT        ,KRM
     *   ,LMAX         ,MASCHN      ,MAXNUC       ,MULT(11)    ,NPRNT(15)
     *   ,NUCLID(700)  ,PACT(200)   ,PSIZE(200)   ,TENTER      ,TFXIT
     *   ,TIME         ,XLAM(7,18)  ,JD
      LOGICAL IGO,JD,KOOS,NPRNT
C
      DIMENSION FMTA(12),FMTB(18),UNITC(2),UNITF(2)
C
      LOGICAL TZERO,TMINUS
C
      DATA (FMTA(I),I=1,18)/6H(/14X3,4HIH TOT,4HAL AMI,6HNDANCE,6H OF HA
     1,6HSS CHA,4HIN ,3(,6H4H WAS,6HIPE12.,6H4, 9H/
     /,(FMTB(I),I=1,15)/6H(17H10,6HUTPUT ,6HOF MCH,6HDEP///,6H5X13HP
     3,4HNTICL,6HE SIZE,6H6X22HA,4HCTIVIT,4HY OF M,4HASS CH,6HAINI4/
     4,6HH,7H1,6HCRONS),6H9X 9H/
     5,(UNITC(I),I=1,2)/4H CURIE,4HS /) /
     6,(UNITF(I),I=1,2)/4H FISSI,6HONS/) /
      DATA CROSS,UNIT/100.0,1.0/
C
  903 FORMAT
     1    (5X1PE12.4,14(E12.4))
C
      TZERO = .FALSE.
      TMINUS = .FALSE.
      FMTA(11) = UNITC(1)
      FMTA(12) =  NITC(2)
      FMTB(16) = UNITC(1)
      FMTB(17) = UNITC(2)
      IF (TIME)11,1,2
    1 TZERO = .TRUE.
COMPUTE EQUIVALENT FISSIONS
      AMINOM = 1.0
      FISNUM = FISNUM*1.E4
      FMTA(11) = UNITF(1)
      FMTA(12) = UNITF(2)
      FMTB(16) = UNITF(1)
      FMTB(17) = UNITF(2)
    2 IF (NPRNT(13)) WRITE (KOUT,FMTB) MASCHN
      IF (TZERO) GO TO 10
COMPUTE ACTIVITY IN CURIES
      CALL BATMAN
      AMINOM = 0.0
      DO 220 K1=1,INUC
      IF(MASCHN.NE.IABS(NUCLID(K1))/MULT(9)) GO TO 220
C     SUM THE ACTIVITIES IN ONE MASS CHAIN AND CONVERT TO CURIES
      AMINOM = AMINOM + AMINDO(K1)
```

```
      SUBROUTINE MCHDEP
C
C        M C TOMPKINS - US ARMY NUCLEAR DEFENSE LABS
C      NOVEMBER 1966
CALLED BY PAM
C
      COMMON /PAM/
     *    AMUON(100)   ,AMUNKN(706) ,ALAMDM       ,AWANCH(130) ,ASUBK(90)
     *   ,CAMPIS       ,DCON(700)   ,ECF(90)       ,ERM(185)    ,FAC(7,18)
     *   ,FISNUM       ,FMASS(200)  ,FOGRNY(7,18) ,FPI(200)    ,FM
     *   ,INMA         ,IGO         ,IMUC          ,ISO(18)     ,ITAB
     *   ,JGO          ,JNM(185)    ,KDOS          ,KOUT        ,KRM
     *   ,LMAX         ,MASCHN      ,MAXNUC        ,NULT(11)    ,NPRNT(35)
     *   ,NUCLID(700)  ,PACT(200)   ,PSIZE(200)    ,TENTER      ,TEXIT
     *   ,TIME         ,WLAM(7,18)  ,JO
      LOGICAL IGO,JO,KDOS,NPRNT
C
      DIMENSION FMTA(12),FMTB(18),UNITC(2),UNITF(2)
C
      LOGICAL IZERO,TMINUS
C
      DATA (( FMTA(I),I=1,18)/6H(/14X3,6HIN TOT,6HAL AMU,6HNDANCE,6H OF MA
     1,6HSS CHA,6HIN I3,,6HGM WAS,6HIPE12.,6H6,  9H/
     /,(FMTB(I),I=1 15)/6H(17H10,6HUTPUT ,6HOF NCH,6HDEP///,6H5X13HP
     *,6HARTICL,6HE SIZE,6HA22HA,6HCTIVIT,6HY OF M,6HASS CH,6HAININ4/
     *,6HH57H4),6HCRONS),6H9X  9H/
     *,(UNITC(I),I=1,2)/4H CURIE,4HS  /) /
     *,(UNITF(I),I=1,2)/4H FISSI,6HONS/) /
      DATA CROSS,UNIT/130.0,1.0/
C
  903 FORMAT
     1    (5X1PE12.4,1X,E12.4)
C
      IZERO = .FALSE.
      TMINUS = .FALSE.
      FMTA(11) = UNITC(1)
      FMTA(12) = UNITC(2)
      FMTB(16) = UNITC(1)
      FMTB(17) = UNITC(2)
      IF (TIME)1,1,2
    1 IZERO = .TRUE.
COMPUTE EQUIVALENT FISSIONS
      AMUON = 1.0
      FISNUM = FISNUM*1.E6
      FMTA(11) = UNITF(1)
      FMTA(12) = UNITF(2)
      FMTB(16) = UNITF(1)
      FMTB(17) = UNITF(2)
    2 IF (KMAS)3,3,33) WRITE (KOUT,FMTB) MASCHN
      IF (IZERO) GO TO 10
COMPUTE ACTIVITY IN CURIES
      CALL MATMAN
      AMUON = 0.0
      DO 220 I=1,INUC
      IF(MASCHN,NUCLID(I))220,220,9
C     SUM THE ACTIVITIES IN ONE MASS CHAIN AND CONVERT TO CURIES
      AMUON = AMUON + AMUNDD(I)
```

```
      SUBROUTINE CONTINUE
      COMMON /ALLOC/ A(7F10
C
      IF (ISWTCH(9,9,1)
C     THE CALL IS AN ARRIVAL OF GAPSR
      NMAX = NSIMX(NASCHN-7))
      CRISS = CWOSS**NNFX
      RADIAL = FLOAT(MACHN-7))/(UNIT * CWISS**ECF(NASCHN-7)))
      STRAIT = RADIAL**CRISS
      AHNDM = ARNDM**FISHRM
      DO 130 LD = 1,TIAB
      DSR = (RADIAL**SIZF(LD)**NNFX + STRAIT)*AHNDM*PMASS(LD)
  130 FP(LD) = FP(LD) + DSR
      IF (.NOT.WPRNT(17)) GO TO 9
      WRITE (IOUT,98))
   98    (PSIZ(I),FP(I),I=1,TIAH)
    9 WRITE (IOUT,FM(4) MASCHN,AHNDM
      RETURN
C  * * * * * * * CODE INSERTION POINT * * * * * * * * *
C
   11 THIS = .TRUE.
      RETURN
C
C  * * * * * * * * * * * * * * * * * * * * * * * * * *
      END
```

```
      SUBROUTINE PAN2
C
C     * * * * * * * * * * * * GLOSSARY * * * * * * * * * * * *
C
C     FA(I,J)         ACTIVITY DENSITY IN EACH PARTICLE SIZE FRACTION
C     ITAB            NUMBER OF PARTICLE SIZE CLASSES
C     MASCHN(I)       MASS NUMBER REQUESTED FOR OUTPUT WITH JGO = 2
C     SA(I,J)         FRACTION OF TOTAL SURFACE IN EACH PARTICLE SIZE CLASS
C                     DIVIDED BY FRACTION OF TOTAL VOLUME
C
C     * * * * * * * * * * * * * * * * * * * * * * * * * * * *
C
      COMMON /PAN/
     *    A(700)    *AHUNDO(700) *ALMFOM      *BRANCH(130) *BSUNK(90)
     *   *CAMFIS    *CHCON(700)  *CCF(90)     *ENH(185)    *FAC(7,18)
     *   *FISSION   *FMASS(200)  *FOGHNY(7,18) *FP(200)      *FW
     *   *H.A       *IGO         *INUC        *ISO(18)     *ITAB
     *   *JD        *JPM(185)    *KDOS        *KOUT        *KRM
     *   *LAST      *MASCHN      *HARMNC      *MULT(11)    *NPHNT(15)
     *   *PHICI(700) *PACT(200)  *PSIZE(200)  *TENTER      *TEXIT
     *   *TIME      *TLAM(7,18)  *JD
      LOGICAL IGO,JD,KDOS,NPHNT
C
      WRITE(6,8)
    8 FORMAT(1H1,'TOTAL PAN OUTPUT/9X5HPSIZE7X2HFP)
      WRITE(6,9)
    9 FORMAT(5(F12.4,1X,F12.4))
C
      DO 10 I = 1,ITAB
   10 FA(I) = 0.0
C
      GO TO (1,2,3),JGO
C
    1 CALL PANSN
      IF (IGO .EQ. 3) GO TO 4
      CALL PANS
      IF (LAST) GO TO 6
      CALL PANCUT
      IF (.NOT.NPHNT(11)) RETURN
      WRITE (KOUT,100)
      WRITE (KOUT,101) (PSIZE(I),FP(I),I=1,ITAB)
      RETURN
    2 CALL PANDEP
      GO TO 5
      END
```

```
      SUBROUTINE UWAN
C
C     W C CONPKINS - US ARMY NUCLEAR DEFENSE LABS
C     MAY 1966
CALLED BY MAM2
C
C   DLAM          DISINTEGRATION CONSTANT OF NP239
C   PLAM          DISINTEGRATION CONSTANT OF U239
C
      COMMON /PAM/
     *     AHERR(700)   ,ARUNDO(700) ,ALREON      ,BRANCH(130) ,BSUNK(90)
     *    ,CAPFIS       ,DCON(700)   ,ECF(98)      ,ERM(185)    ,FAC(7,18)
     *    ,FISNUM       ,FMASS(200)  ,FOGHNY(7,18) ,FP(200)     ,FW
     *    ,IHPA         ,IGU         ,INRIC        ,ISO(1A)     ,ITAB
     *    ,JJO          ,JRM(185)    ,KDOS         ,KOUT        ,KRM
     *    ,LMAX         ,MASCM       ,MAXNUC       ,MULT(11)    ,NPRNT(15)
     *    ,NUCLID(700) ,PACT(200)   ,PSIZF(200)   ,TENTER      ,TEXIT
     *    ,TIME         ,XLAM(7,18)  ,JO
      LOGICAL IGO,JO,KDOS,NPRNT
C
COMPUTE U239 DISINTEGRATION CONSTANT
      PLAM = 0.693147/(23.5*60.0)
COMPUTE NP239 DISINTEGRATION CONSTANT
      DLAM = 0.693147/(56.0*3600.0)
C
      A=CAPFIS*1.54*PLAM
      GLIMP = DLAM/(DLAM - PLAM)
      GLUMP = A/EXP(PLAM*TENTER)
C
      IF (.NOT.JO) GO TO 3
      AMPAN = AZERO*EXP (-PLAM*TIME)
      AMPUN = GLUMP*AMPAN - GLIMP*EXP (-DLAM*TIME)
      GO TO 7
C
    3 IF (.NOT.KDUS) GO TO 4
      AMPAN = AZERO/PLAM*(EXP (-PLAM*TENTER) - EXP (-PLAM*TEXIT))
      AMPUN = GLUMP*AMPAN -
     1(GLIMP*(EXP (-DLAM*TENTER) - EXP (-DLAM*TEXIT))/DLAM
      GO TO 7
C
    4 AMPAN = AZERO/DLAM*EXP (-PLAM*TENTER)
      AMPUN = GLUMP*AMPAN - GLIMP/DLAM*EXP (-DLAM*TENTER)
C
    7 ANEP = (AMPAN*.127E-6 + AMPUN*.946E-4)*FISNUM
      DO 8 J=1,ITAB
    8 FP(J) = FP(J) + ANEP*FMASS(J)
C
      IF (PRNT(12)) WRITE (KOUT,100) ANEP
  100 FORMAT
     1    (15H1OUTPUT OF UWAN/5X21HMASS 239 CONTRIBUTES 1PE12.4,
     2    23H TO EACH PARTICLE SIZE.)
      RETURN
      END
```

```
      SUBROUTINE PAM1
     1          (IMAX    ,KMAX    ,FN
     2           ,INPUT  ,NAMTAB  ,SIGMA)
C
C     A.F. JONES -- US ARMY NUCLEAR DEFENSE LABS
C     FACILESS VERSION   FEBRUARY 1970
C     MODIFIED 1980
C
C     ***** DRIVER PROGRAM FOR TIME-INDEPENDENT PART OF PARTICLE-ACTIVITY
C     ******
C
C     CALLED BY GEISET
C
C  * * * * * * * * * * * * * GLOSSARY * * * * * * * * *
C
C     ******          CAPTURE-TO-FISSION RATIO
C     ****            NUMBER OF NEUTRONS EMITTED PER FISSION
C     ****            SIX CHARACTER IDENTIFIER OF FISSION TYPE
C     INTAPE(10)      LOGICAL ARRAY TO CONTROL FILE MANIPULATION
C                     (1) TRUE  = SET INTP NOT EQUAL TO ISIN
C                         FALSE = SET INTP = ISIN
C                     (2) TRUE  = SET KRD = INTP
C                         FALSE = SET KRD = ISIN
C                     (3) TRUE  = WRITE FILE IPAM
C                     (4) TRUE  = READ FILE IPAM INTO MEMORY AND RETURN
C                     (5-10) = SPARES
C     ****            RESTART FILE OF PAM1 OUTPUT FOR RESTARTS
C     ****            INPUT FILE (RCD) USED BY OTHER DELETE MODULES
C     ****            RCD FILE OF PAM OUTPUT FOR PERIPHERAL PRINTING
C     ******          INPUT FILE (RCD) CONTAINING SOIL PARAMETERS
C     KOUT(20)        LOGICAL ARRAY TO CONTROL WRITING OF KOUT, TRUE = WRITE
C                     (1)  SETUP = TRANSITION CARDS (WARNING - PRODUCES SOME
C                                  700 PAGES)
C                     (2)  SETUP = INTERMEDIATE FORM OF NUCLIDE TABLE (OCTAL
C                     (3)  SETUP = FINAL FORM OF NUCLIDE TABLE (OCTAL)
C                     (4)  YIELD = FISSION YIELD TABLE
C                     (5)  EXPOSURE RATE MULTIPLIERS
C                     (6)  FRACTN = REFRACTORY FRACTIONS (FN)
C                     (7)  FRACTQ = SQUARE ROOT OF FN (HSUNK)
C                     (8)  INDCOM = INFORMATION STORED FOR USE BY INDCOP
C                     (9)  MATDSN = NUCLIDE ANNIHILATORS (WARNING - THIS
C                                   OPTION COMBINED WITH KO = FALSE WILL HURT YOU
C                                   IN SPEED)
C                     (10) GRAM = FISSION PRODUCT ACTIVITY VS PART SIZE
C                          (WARNING - SEE (9))
C                     (11) INDUCD = INDUCED ACTIVITY (SOIL) VS PART SIZE
C                          (WARNING - SEE (9))
C                     (12) U238 = INDUCED ACTIVITY (MASS 239) VS PART SIZE
C                          (WARNING - SEE (9))
C                     (13) MCHAIN = SELECTED MASS CHAIN ACTIVITY VS PART SIZE
C                     (14) SPARE
C                     (15) PART = TOTAL ACTIVITY VS PART SIZE (WARNING-SEE 9
C                     (16-20) SPARES
C     ****  (17)      RUN IDENTIFICATION FOR PARTICLE-ACTIVITY MODULE
C  * * * * * * * * * * * * * * * * * * * * * * * * * * * *
C
      COMMON /CPAM/
```

```
*    EMEGA(700)  *ARUNDO(700)  *ALMEAN      *BRANCH(130)  *HSURK(90)
*    *CAPE(5)    *DCON(700)    *ECF(90)     *EHM(185)     *FAC(7*18)
*    *FSHOW      *FMASS(200)   *FRANNY(7*18) *FP(200)      *FW
*    *HWA        *IGO          *INRC        *ISU(18)      *ITAM
*    *JGO        *JRM(185)     *KDOS        *KOUT         *KRM
*    *LMAX       *MASCMN       *MARNUC      *MULT(11)     *NPRNT(15)
*    *PUELIU(700) *PALI(700)   *PSIZE(200)  *TENTER       *TEXIT
*    *TIMF       *TLAM(7*18)   *JM
 LOGICAL IGO,JD,KDOS,NPRNT
 DIMENSION PAMID(12),NUMTAP(15),TYPE(12)
 PUBLIC TYPE,FI,SID
 LOGICAL IFTAPE(19)
 DATA TYPE      /8HP239FI8,8HP239ME8,8HP239TM8,8HU233FI8,8HU233ME8,
1HU233TM8,8HU235FI8,8HU235ME8,8HU235TM8,8HU238FI8,8HU238ME8,8HU238TM8/
 DATA (AMEGA (I),I=1,95   )/
$ 0.000000    * 0.000000    * 0.000000    * 0.000000    * 0.000000    *
$ 0.000000    * 0.000000    * 0.000000    * 0.000000    * 0.000000    *
* 0.000000    * 0.000000    * 0.000000    * 0.000000    * 1.470000E-1*
* 4.770000E-1* 1.260000E+0* 7.620000E-1* 6.700000E-3* 0.000000    *
* 1.000000E-2* 7.260000E-1* 1.950000E+0* 1.230000E+0* 9.040000E-2*
$ 5.000000E-2* 0.000000    * 0.000000    * 5.770000E-1* 2.470000E+0*
$ 2.000000E+0* 6.380000E-1* 0.000000    * 0.000000    * 0.000000    *
$ 3.000000E-1* 2.130000E+0* 4.150000E+0* 8.490000E-1* 4.495000E-1*
* 3.000000E-2* 0.000000    * 0.000000    * 3.280000E-2* 1.720000E+0*
$ 5.000000E+0* 3.430000E+0* 3.670000E-1* 1.830000E-1* 0.000000    *
$ 0.000000    * 1.210000E+0* 6.040000E+0* 7.680000E+0* 2.230000E+0*
* 2.000000E-2* 2.150000E-2* 0.000000    * 0.000000    * 3.550000E-1*
$ 6.000000E+0* 9.450000E+0* 5.120000E+0* 6.260000E-1* 0.000000    *
$ 0.000000    * 3.830000E+0* 1.090000E+1* 1.010000E+1* 1.106800E+0*
$ 5.000000E-1* 0.000000    * 0.000000    * 1.700000E+0* 1.160000E+1*
* 1.000000E+1* 7.730000E+0* 3.040000E-1* 0.000000    * 0.000000    *
* 1.000000E-1* 1.750000E+1* 5.140000E+1* 1.637700E+1* 1.085450E+1*
* 2.000000E+0* 0.000000    * 0.000000    * 0.000000    * 9.910000E+0*
* 5.000000E+1* 7.460000E+1* 2.400000E+1* 4.960000E-1* 0.000000    /
 DATA (AMEGA (I),I=96,190 )/
* 1.000000E+0* 1.220000E+1* 9.750000E+1* 6.360000E+1* 9.929000E+0*
* 0.000000    * 0.000000    * 0.000000    * 2.330000E+1* 9.680000E+1*
$ 1.000000E+2* 2.480000E+1* 6.000000    * 0.000000    * 0.000000    *
$ 0.000000    * 0.000000E+0* 0.120000E+1* 1.500000E+2* 3.505000E+1*
$ 2.000000E+0* 0.000000    * 0.000000    * 7.480000E-1* 5.050000E+1*
* 1.000000E+2* 6.000000E+1* 1.385000E+1* 0.000000    * 0.000000    *
* 2.000000E+1* 1.300000E+2* 9.950000E+1* 3.405000E+1* 0.850000E-1*
$ 0.000000    * 0.000000    * 0.000000    * 5.440000E+0* 9.260000E+1*
* 2.000000E+2* 1.220000E+2* 1.640000E+1* 0.000000    * 0.000000    *
* 0.000000    * 5.330000E+1* 1.970000E+2* 1.484969E+2* 4.730000E+1*
$ 0.000000    * 0.000000    * 0.000000    * 0.000000    * 2.030000E+1*
* 1.000000E+2* 2.130000E+2* 9.970000E+1* 5.090000E+0* 0.000000    *
* 0.000000    * 1.430000E+0* 7.970000E+1* 2.280000E+2* 1.653000E+2*
$ 2.000000E+1* 0.000000    * 0.000000    * 0.000000    * 0.000000    *
* 3.730000E+1* 1.410000E+2* 2.180000E+2* 6.810000E+1* 9.690000E-1*
$ 0.000000    * 1.950000E+1* 1.150000E+2* 2.360000E+2* 1.250000E+2*
* 1.000000E+1* 0.000000    * 0.000000    * 0.000000    * 0.000000    *
$ 5.000000E-1* 6.130000E+1* 2.120000E+2* 1.430000E+2* 4.310000E+1*
* 0.000000    * 0.000000    * 0.000000    * 0.000000    * 2.850000E+1/
 DATA (AMEGA (I),I=191,285)/
* 1.700000E+2* 2.540000E+2* 4.823590E+1* 2.411795E+1* 3.310000E+0*
* 0.000000    * 9.250000E-1* 6.490000E+1* 2.150000E+2* 1.770000E+2*
```

```
$ 1.7434760E+1, 1.7434780E+1, 0.000000   , 0.000000   , 1.4200000E+1,
$ 1.4400000E+2, 2.4300000E+2, 1.4400000E+2, 7.5200000E+0, 0.000000   ,
$ 0.000000   , 0.000000   , 0.000000   , 4.9400000E+1, 1.9200000E+2,
$ 1.4400000E+2, 4.4100000E+1, 0.000000   , 0.000000   , 0.000000   ,
$ 7.4920000E+0, 9.3500000E+1, 1.4600000E+2, 1.8400000E+2, 1.3000000E+1,
$ 0.000000   , 0.000000   , 5.1400000E+0, 4.7300000E+1, 1.4400000E+2,
$ 1.4400000E+2, 1.5124100E+1, 1.5128100E+1, 0.000000   , 0.000000   ,
$ 2.4810000E+1, 1.2000000E+2, 1.5400000E+2, 5.1200000E+1, 8.4300000E-1,
$ 0.000000   , 0.000000   , 0.000000   , 1.9900000E+0, 4.7500000E+1,
$ 1.1700000E+2, 7.3700000E+1, 1.1200000E+1, 0.000000   , 0.000000   ,
$ 0.000000   , 0.000000   , 0.4900000E-1, 2.7000000E+1, 7.4900000E-1,
$ 0.000000E+1, 9.9100000E+0, 0.000000   , 0.000000   , 0.000000   ,
$ 0.000000   , 2.8500000E-1, 2.1000000E+1, 6.8200000E+1, 5.7100000E+1,
$ 1.1400000E+1, 0.000000   , 0.000000   , 0.000000   , 0.000000   ,
$ 1.5700000E+1, 5.9400000E+1, 5.4200000E+1, 1.3300000E+1, 0.000000   ,
$ 0.000000   , 0.000000   , 0.000000   , 0.000000   , 0.0800000E+0,
$ 0.000000E+1, 6.5000000E+1, 2.5400000E+1, 1.2000000E+0, 0.000000   /
 DATA (AMISN (I),I=246,300)/
$ 0.000000   , 5.4000000E-1, 2.1100000E+1, 5.9300000E+1, 6.2500000E+1,
$ 3.2200000E+0, 1.4100000E+0, 0.000000   , 0.000000   , 0.000000   ,
$ 0.000000   , 0.000000   , 9.0400000E+0, 6.4300000E+1, 5.1600000E+1,
$ 1.5000000E+1, 2.3300000E-1, 0.000000   , 2.2900000E+0, 2.7100000E+1,
$ 5.5000000E+1, 3.0200000E+1, 1.7497000E+0, 8.7500000E-1, 0.000000   ,
$ 0.000000   , 0.000000   , 1.1300000E-1, 1.2500000E+1, 6.6430000E+1,
$ 0.000000E+1, 9.9100000E+0, 0.000000   , 0.000000   , 0.000000   ,
$ 0.000000E-1, 3.6500000E+1, 5.2400000E+1, 2.1300000E+1, 6.1090000E-1,
$ 0.000000E-1, 0.000000   , 0.000000   , 5.6400000E-1, 1.2300000E+1,
$ 6.4400000E+1, 3.6300000E+1, 5.9400000E+0, 0.000000   , 0.000000   ,
$ 6.4700000E+0, 3.9100000E+1, 6.5100120E+1, 6.3513300E+0, 3.1750000E+0,
$ 2.6200000E-2, 2.6200000E-2, 0.000000   , 0.000000   , 0.000000   ,
$ 0.000000   , 2.6400000E+0, 2.6400000E+1, 5.0800000E+1, 2.6000000E+1,
$ 2.4200000E+0, 0.000000   , 1.3100000E-1, 1.2400000E+1, 6.6800000E+1,
$ 6.3400000E+1, 6.7100000E+0, 2.3500000E+0, 0.000000   , 0.000000   ,
$ 0.000000   , 0.000000   , 0.000000   , 5.6200000E+0, 1.3300000E+1,
$ 6.3400000E+1, 1.9200000E+1, 3.2720000E-1, 3.2720000E-1, 0.000000   ,
$ 0.000000   , 6.6600000E-1, 1.9300000E+1, 5.0000000E+1, 1.6191600E+1,
$ 1.6191600E+1, 1.3291500E+0, 1.3291500E+0, 0.000000   , 0.000000   /
 DATA (AMISN (I),I=341,375)/
$ 0.000000   , 9.1400000E+0, 4.2300000E+1, 4.7600000E+1, 1.3800000E+1,
$ 1.5000000E-1, 0.000000   , 1.0200000E+0, 2.9200000E+1, 5.8600000E+1,
$ 1.6113100E+1, 1.6113100E+1, 1.6597000E+0, 7.2985000E-1, 0.000000   ,
$ 0.000000   , 1.2300000E+1, 4.9700000E+1, 4.9700000E+1, 1.2300000E+1,
$ 0.000000   , 0.000000   , 0.000000   , 6.000000   , 6.6400000E+0,
$ 1.4100000E+1, 2.8032900E+1, 2.8032900E+1, 1.0538650E+1, 5.2682500E+0,
$ 6.7400000E-1, 0.000000   , 6.1400000E-1, 2.3400000E+1, 5.9100000E+1,
$ 2.0312000E+1, 2.0312000E+1, 2.0312000E+0, 2.0312000E+0, 0.000000   ,
$ 0.000000   , 1.1200000E+1, 5.0400000E+1, 2.7259600E+1, 2.7259300E+1,
$ 6.3000000E+0, 4.1100000E-2, 6.2200000E-2, 0.000000   , 5.0500000E+0,
$ 6.6400000E+1, 6.7400000E+1, 2.1214000E+1, 2.1214000E+1, 6.3000000E+0,
$ 0.000000   , 3.2300000E-1, 2.4300000E+1, 0.000000   , 9.7100000E+1,
$ 6.2250000E+1, 6.3654500E+0, 2.1749750E+0, 0.000000   , 0.000000   ,
$ 2.5400000E+1, 1.0900000E+2, 5.5542400E+1, 5.5542400E+1, 3.0130000E+1,
$ 0.000000   , 0.000000   , 0.000000   , 2.1300000E+1, 1.1100000E+2,
$ 1.6600000E+2, 2.3200000E+1, 1.1666150E+1, 3.0599867E-1, 0.000000   ,
$ 0.000000   , 0.000000   , 1.5900000E+1, 1.0700000E+2, 0.000000   ,
$ 1.7100000E+2, 7.1200000E+1, 3.1900000E+0, 0.000000   , 0.000000   ,
$ 7.5000000E+0, 9.5400000E+1, 2.0300000E+2, 5.3100000E+1, 2.0500000E+1/
```

```
      DATA (ABS(I),I=471,570)/
     * [illegible]  0.000000  , 0.000000  , 0.000000  , 5.570000E-1,
     * 5.[illegible]  2.140000E+2, 1.410000E+2, 4.400000E+1, 0.000000  ,
     * 0.[illegible]  2.720000E+1, 1.680000E+2, 1.208313E+2, 6.041565E+1,
     * 1.[illegible]  5.316667E-1, 2.658333E-1, 0.000000  , 0.000000  ,
     * 7.[illegible]  7.020000E+1, 2.470000E+2, 2.240000E+2, 4.870000E+1,
     * 0.[illegible]  0.000000  , 0.000000  , 0.000000  , 1.370000E+1,
     * 1.[illegible]  2.700000E+2, 6.021500E+1, 3.410780E+1, 7.500000E+0,
     * 3.[illegible]  0.000000  , 4.430000E+1, 1.940000E+2, 2.170000E+2,
     * [illegible]  5.[illegible]  0.000000  , 1.520000E+1, 1.240000E+2,
     * 1.[illegible]  5.000000E+1, 1.599403E+0, 3.199600E+0, 0.000000  ,
     * 1.[illegible]  4.470000E+1, 1.690000E+2, 8.450000E+1, 3.610000E+1,
     * 0.[illegible]  0.000000  , 0.000000  , 3.030000E+1, 1.670000E+2,
     * 2.[illegible]  7.440000E+1, 1.700000E+0, 0.000000  , 5.450000E+0,
     * 9.[illegible]  2.160000E+2, 1.280000E+2, 1.740000E+1, 0.000000  ,
     * 3.[illegible]  4.[illegible]  1.790000E+2, 1.740000E+2, 4.320000E+1,
     * 0.[illegible]  0.000000  , 0.000000  , 1.600000E+1, 1.160000E+2,
     * 1.[illegible]  8.300000E+1, 4.630000E+0, 0.000000  , 1.480000E+0,
     * 4.[illegible]  1.770000E+2, 1.270000E+2, 2.270000E+1, 0.000000  ,
     * 0.[illegible]  0.000000  , 2.410000E+1, 1.190000E+2, 1.430000E+2/
      DATA (ABS(I),I=571,665)/
     * [illegible]  [illegible]  5.420000E-1, 0.000000  , 0.000000  , 6.500000E+0,
     * [illegible]  1.420000E+2, 7.400000E+1, 8.440000E+0, 0.000000  ,
     * [illegible]  [illegible]  3.030000E-1, 2.910000E+1, 1.110003E+2, 9.110000E+1,
     * 2.[illegible]  0.000000  , 0.600000  , 1.650000E+1, 6.370000E+1,
     * [illegible]  [illegible]  1.[illegible]  1.130000E+0, 0.000000  , 0.000000  ,
     * [illegible]  [illegible]  [illegible]  2.490000E+1, 6.440000E+1, 4.280000E+1,
     * [illegible]  0.[illegible]  0.000000  , 0.000000  , 0.000000  , 4.310000E+0,
     * [illegible]  [illegible]  2.[illegible]  7.090000E+0, 9.050000E-2, 0.000000  ,
     * [illegible]  3.[illegible]  8.240000E+0, 1.490000E+1, 7.850000E+0,
     * 4.[illegible]  0.000000  , 0.000000  , 1.970000E+0, 8.210000E+0,
     * [illegible]  2.210000E+0, [illegible]  0.000000  , 0.000000  , 0.000000  ,
     * [illegible]  [illegible]  3.770000E+0, 7.380000E+0, 3.690000E+0, 3.61[illegible]E-1,
     * [illegible]  0.[illegible]  0.000000  , 0.000000  , 9.350000E-2,
     * 1.[illegible]  5.[illegible]  4.[illegible]  9.800000E-1, 0.000000  ,
     * [illegible]  4.[illegible]  2.[illegible]  4.230000E+0, 1.620000E+0,
     * [illegible]  [illegible]  [illegible]  [illegible]  1.400000E+0,
     * [illegible]  2.[illegible]  3.[illegible]  0.000000  , 0.000000  ,
     * [illegible]  2.140000E+0, 2.260000E+0, 6.000000E-1, 0.000000  ,
     * [illegible]  1.[illegible]  1.190000E+0, 2.070000E+0, 9.030000E-1/
      DATA (ABS(I),I=666,760)/
     * [illegible]  0.000000  , 9.500000E-3, 4.[illegible]E-1, 1.390000E+0,
     * 1.[illegible]  1.950000E-1, 0.000000  , 1.510000E-1, 7.440000E-1,
     * [illegible]  2.[illegible]  4.300000E-3, 0.000000  , 0.000000  ,
     * [illegible]  0.000000  , 0.000000  , 0.000000  , 0.000000  ,
     * [illegible]  0.000000  , 0.000000  , 0.000000  , 0.000000  ,
     * 0.[illegible]  0.000000  , 0.000000  , 0.000000  , 0.000000  ,
     * [illegible]  0.[illegible]  0.000000  , 0.000000  , 0.000000  /

      DATA (BRANCH(I),I=1,95  )/
     * [illegible]  4.000000E-1, 3.600000E-1, 6.400000E-1, 5.000000E-1,
     * [illegible]  4.600000E-2, 9.400000E-1, 4.400000E-1, 5.600000E-1,
     * 1.[illegible]  [illegible]  1.400000E-1, 8.100000E-1, 3.000000E-2,
     * [illegible]  7.000000E-2, 9.300000E-1, 1.140000E-1, 8.820000E-1,
     * 1.[illegible]  8.500000E-1, 6.000000E-1, 4.000000E-1, 2.500000E-1,
     * [illegible]  2.000000E-2, 9.800000E-1, 9.600000E-1, 4.000000E-2,
     * [illegible]  1.300000E-1, 5.000000E-1, 5.000000E-1, 9.950000E-1,
```

```
     $ 5.000000E-3, 2.000000E-1, 7.940000E-1, 5.000000E-1, 5.000000E-1,
     $ 5.000000E-1, 5.000000E-1, 5.000000E-1, 5.000000E-1, 1.600000E-2,
     $ 9.400000E-1, 6.000000E-1, 1.200000E-1, 5.000000E-1, 5.000000E-1,
     $ 9.000000E-1, 1.000000E-1, 5.000000E-1, 5.000000E-1, 7.200000E-1,
     $ 1.000000E-1, 1.400000E-1, 9.600000E-2, 9.100000E-1, 9.500000E-1,
     $ 5.000000E-2, 5.000000E-1, 5.000000E-1, 6.000000E-1, 1.000000E-1,
     $ 1.000000E-1, 2.100000E-1, 7.800000E-1, 1.000000E-3, 5.000000E-1,
     $ 5.000000E-1, 5.000000E-2, 5.000000E-1, 4.500000E-1, 5.000000E-1,
     $ 5.000000E-1, 3.000000E-2, 9.700000E-1, 5.000000E-1, 5.000000E-1,
     $ 5.000000E-1, 5.000000E-1, 2.150000E-1, 7.850000E-1, 9.900000E-1,
     $ 1.000000E-2, 5.000000E-1, 5.000000E-1, 2.200000E-1, 7.800000E-1,
     $ 9.400000E-1, 2.000000E-2, 9.700000E-1, 3.000000E-2, 6.500000E-2/
      DATA (WBARCM(I),I=96,110 )/
     $ 9.150000E-1, 1.710000E-1, 8.270000E-1, 6.800000E-1, 3.200000E-1,
     $ 9.000000E-1, 1.000000E-1, 1.500000E-1, 8.500000E-1, 2.000000E-1,
     $ 8.000000E-1, 8.000000E-3, 9.920000E-1, 7.200000E-1, 2.800000E-1,
     $ 1.100000E-1, 8.700000E-1, 2.600000E-2, 9.700000E-1, 3.000000E-1,
     $ 7.000000E-1, 4.300000E-2, 9.600000E-1, 9.200000E-1, 8.000000E-2,
     $ 1.000000E-2, 9.700000E-1, 9.000000E-2, 9.000000E-1, 7.500000E-1,
     $ 2.500000E-1, 7.400000E-1, 2.700000E-1, 0.000000    , 0.000000    /
      DATA (DCON  (I),I=1,35   )/
     $ 6.931470E+1, 1.448420E-1, 6.931470E-2, 4.140686E-6, 1.365518E-5,
     $ 0.000000    , 6.931470E+1, 3.465735E-1, 9.902100E-2, 5.776225E-3,
     $ 4.011497E-5, 1.437825E+0, 0.000000    , 6.931470E+1, 4.620980E-1,
     $ 1.732867E-1, 2.567211E-3, 1.481083E-3, 0.000000    , 6.931470E+1,
     $ 6.931470E+1, 2.772588E-1, 7.249284E-2, 5.776225E-3, 1.414580E-2,
     $ 1.404545E-4, 0.000000    , 6.931470E+1, 3.465735E-1, 8.664337E-2,
     $ 2.310490E-2, 0.000000    , 7.265492E-4, 0.000000    , 6.931470E+1,
     $ 4.620980E-1, 1.448420E-1, 4.620980E-2, 1.241860E-2, 1.703301E-5,
     $ 4.975215E-4, 0.000000    , 6.931470E+1, 6.931470E+1, 2.772588E-1,
     $ 4.664137E-2, 9.154811E-5, 1.925540E-3, 1.264500E-4, 0.000000    ,
     $ 6.931470E+1, 4.620980E-1, 1.540327E-1, 2.772588E-2, 1.241860E-3,
     $ 2.969741E-3, 3.600750E-13, 0.000000    , 6.931470E+1, 4.620980E-1,
     $ 2.310490E-1, 2.772588E-2, 1.925540E-2, 0.000000    , 6.931470E+1,
     $ 6.931470E+1, 3.465735E-1, 9.902100E-2, 2.100465E-2, 2.026746E-4,
     $ 6.418624E-4, 0.000000    , 6.931470E+1, 4.620980E-1, 1.386294E-1,
     $ 3.450817E-2, 0.000000    , 5.361254E-4, 0.000000    , 6.931470E+1,
     $ 6.931470E+1, 3.465735E-1, 9.902100E-2, 1.004561E-2, 4.620980E-4,
     $ 8.022535E-5, 1.013373E-4, 0.000000    , 6.931470E+1, 4.620980E-1,
     $ 1.732867E-1, 3.450817E-3, 3.610141E-4, 0.000000    , 6.931470E+1/
      DATA (DCON  (I),I=96,190 )/
     $ 6.931470E-1, 1.411970E+0, 1.777300E-2, 3.450817E-3, 4.375928E-5,
     $ 2.072173E-4, 0.000000    , 6.931470E+1, 3.465735E-1, 4.332169E-2,
     $ 1.155245E-2, 0.000000    , 1.110812E-2, 4.313141E-7, 0.000000    ,
     $ 6.931470E+1, 4.620980E-1, 4.332169E-2, 1.271824E-2, 1.481083E-4,
     $ 1.000511E-15, 0.000000    , 6.931470E+1, 6.931470E+1, 2.772588E-1,
     $ 4.252435E-2, 6.876456E-5, 4.618028E-4, 0.000000    , 6.931470E+1,
     $ 3.465735E-1, 1.575314E-1, 3.610141E-3, 7.501591E-4, 1.584621E-7,
     $ 4.332169E-2, 0.000000    , 6.931470E+1, 6.931470E+1, 4.332169E-1,
     $ 2.100465E-2, 6.278695E-3, 7.846465E-10, 2.994414E-4, 0.000000    ,
     $ 6.931470E+1, 3.465735E-1, 6.931470E-2, 9.627042E-3, 1.984957E-4,
     $ 2.310490E-4, 1.343146E-7, 0.000000    , 6.931470E+1, 4.620980E-1,
     $ 2.310490E-1, 1.407825E-1, 7.131142E-4, 5.348356E-5, 0.000000    ,
     $ 6.931470E+1, 6.931470E+1, 1.465735E-1, 1.237762E-1, 1.444655E-1,
     $ 1.425600E-3, 2.412853E-14, 5.943652E-3, 0.000000    , 6.931470E+1,
     $ 6.451650E-1, 2.410649E-1, 8.865500E-3, 5.776225E-4, 0.000000    ,
     $ 6.931470E+1, 6.931470E+1, 1.465735E-1, 1.712867E-2, 1.155245E-3,
```

```
 * 1.[illegible]E-7, 2.139140E-6, 2.242153E-7, 0.000000 , 6.931470E+1,
 * 6.[illegible]E+1, [illegible], 6.931470E+1, [illegible], 0.000000 ,
 * [illegible], 0.000000 , 6.931470E+1, 6.931470E+1, 4.620980E-1/
 DATA (DCON (I),I=141,285)/
 * 1.[illegible]E-1, 1.132[illegible]E-5, 1.155245E-2, 1.482527E-4, 0.000000 ,
 * 6.[illegible]E+1, 6.931470E+1, 6.931470E-1, 2.772588E-1, 1.155245E-2,
 * 2.[illegible], 5.776225E-3, 0.000000 , 6.931470E+1, 6.931470E-1,
 * 4.[illegible], [illegible], [illegible], 2.695351E-6, 3.209014E-5,
 * 1.[illegible], 0.000000 , 6.931470E+1, 4.620980E-1, 1.980420E-1,
 * 3.[illegible], 0.000000 , 4.332169E-2, 0.000000 , 6.931470E+1,
 * 6.[illegible], 2.772588E-1, 1.155245E-2, 7.912637E-4, 8.251750E-4,
 * 0.[illegible], 6.931470E+1, 6.931470E+1, 3.465735E-1, 9.902100E-2,
 * 1.[illegible], 2.567211E-3, 1.386294E-1, 0.000000 , 6.931470E+1,
 * 4.[illegible], 1.732867E-1, 2.772588E-2, 9.627042E-3, 2.020790E-7,
 * 2.[illegible], 0.000000 , 6.931470E+1, 6.931470E+1, 2.310490E-1,
 * [illegible], 2.418028E-4, 0.000000 , 2.625557E-3, 1.650350E-2,
 * 0.[illegible], 6.931470E+1, 6.931470E+1, 3.465735E-1, 5.776225E-3,
 * 1.[illegible], 4.375428E-5, 1.824071E-2, 5.348356E-6, 0.000000 ,
 * 6.[illegible], 6.931470E+1, 6.620980E-1, 1.732867E-1, 7.701633E-2,
 * 2.[illegible], 2.751458E-5, 2.310490E-2, 0.000000 , 6.931470E+1,
 * 6.[illegible], 2.772588E-1, 1.155245E-2, 2.511402E-3, 1.540327E-2,
 * 5.[illegible], 1.137748E-15, 0.000000 , 6.931470E+1, 6.931470E+1,
 * 3.[illegible], 1.155245E-2, 2.686616E-3, 3.850817E-2, 0.000000 /
 DATA (DCON (I),I=286,380)/
 * 6.[illegible], 6.931470E+1, 6.620980E-1, 2.772588E-1, 4.332169E-2,
 * 1.[illegible], 2.310490E-2, 2.457268E-3, 1.375292E-5, 1.777300E-2,
 * 0.[illegible], 6.931470E+1, 6.931470E-1, 3.465735E-1, 6.931470E-2,
 * 1.[illegible], 0.000000 , 6.931470E+1, 6.931470E+1, 4.620980E-1,
 * 1.[illegible], 5.776225E-2, 1.500742E-5, 5.022804E-4, 9.366851E-3,
 * 1.[illegible], 0.000000 , 6.931470E+1, 6.620980E-1, 2.310490E-1,
 * 9.[illegible], 2.168611E-6, 6.016901E-5, 0.000000 , 6.931470E+1,
 * 5.[illegible], 3.465735E-1, 1.732867E-1, 8.251750E-3, 9.627042E-3,
 * 3.[illegible], 0.000000 , 6.931470E+1, 6.931470E+1, 4.620980E-1,
 * 2.[illegible], 2.418028E-3, 1.386294E-1, 0.000000 , 6.931470E+1,
 * 6.[illegible], 2.772588E-1, 1.540327E-2, 3.465735E-2, 5.501167E-4,
 * 1.[illegible], 3.632866E-6, 4.269198E-5, 1.000000E-15, 0.000000 ,
 * [illegible], [illegible], [illegible], [illegible], [illegible],
 * 0.[illegible], 6.931470E+1, 6.931470E+1, 4.620980E-1, 1.386294E-1,
 * 1.[illegible], 2.418028E-5, 2.310490E-4, 9.627042E-5, 2.567211E-4,
 * 5.[illegible], 0.000000 , 6.931470E+1, 6.620980E-1, 1.540327E-1,
 * 2.[illegible], 2.310490E-4, 2.567211E-3, 1.386294E-1, 0.000000 ,
 * 6.[illegible], 6.620980E-1, 2.310490E-1, 4.077335E-2, 4.278685E-3,
 * 1.[illegible], 2.418028E-4, 5.776225E-3, 3.274504E-8, 0.000000 /
 DATA (DCON (I),I=381,475)/
 * 6.[illegible], 3.465735E-1, 1.155245E-1, 9.627042E-4, 1.386294E-2,
 * 0.[illegible], 6.931470E+1, 6.620980E-1, 1.732867E-1, 6.931470E-2,
 * 3.[illegible], 2.310490E-2, 8.785401E-10, 7.131142E-6, 0.000000 ,
 * 4.[illegible], 2.310490E-1, 1.732867E-2, 1.540327E-2, 0.000000 ,
 * 2.[illegible], 3.465735E-6, 0.000000 , 6.931470E+1, 2.772588E-1,
 * 7.[illegible], 1.925408E-2, 6.931470E-2, 6.418028E-8, 2.817671E-4,
 * 0.[illegible], 6.931470E+1, 3.465735E-1, 6.931470E-2, 3.465735E-2,
 * 0.[illegible], 5.501167E-4, 8.886500E-3, 1.337089E-7, 0.000000 ,
 * 1.[illegible], 1.386294E-1, 4.620980E-2, 1.190974E-3, 8.534611E-7,
 * [illegible], 1.383196E-7, 0.000000 , 6.931470E+1, 2.310490E-1,
 * 9.[illegible], 1.098225E-13, 4.080237E-4, 6.418028E-7, 0.000000 ,
 * 6.[illegible], 6.620980E-1, 2.310490E-1, 2.750583E-3, 8.557370E-5,
 * 2.[illegible], 7.640509E-8, 2.070332E-5, 0.000000 , 6.931470E-1,
```

```
$ 3.4657356-1, 2.0267466-4, 1.0502236-3, 2.2386476-5, 0.000000    ,
$ 6.9314706+1, 0.000000    , 6.9314706+1, 6.6209866-1, 1.0696716-4,
$ 4.1856706-5, 1.4567146-7, 1.6065076-4, 1.3727816-15, 1.0024176-6,
$ 0.000000    , 6.9314706+1, 6.6209806-1, 6.4432506-3, 1.9256086-3,
$ 3.1222446-4, 0.000000    , 1.5403276-5, 0.000000    , 6.9314706+1,
$ 6.9314706-1, 1.0502236-2, 5.9568716-4, 6.6180246-6, 4.8135216-4,
 DATA (DCON  (I),I=476,570)/
$ 9.9653426-7, 6.4485466-7, 0.000000    , 6.9314706+1, 6.9314706+1,
$ 1.1462466-2, 1.6304796-3, 7.4664726-6, 8.3713606-5, 0.000000    ,
$ 6.9314706+1, 1.7773036-2, 6.3759226-3, 2.3104906-4, 9.2413606-4,
$ 9.2567716-6, 3.6486596-6, 1.5223036-6, 0.000000    , 6.9314706+1,
$ 6.9314706+1, 6.6209806-1, 2.7505836-4, 2.1797306-6, 0.000000    ,
$ 6.6334196-5, 6.9413656-9, 0.000000    , 6.9314706+1, 3.6481426-1,
$ 8.2517506-3, 2.8737466-5, 7.5506216-4, 2.0924156-5, 1.0982256-14,
$ 0.000000    , 2.4110496-1, 1.1552456-1, 8.3511906-4, 0.000000    ,
$ 6.1711806-7, 0.000000    , 6.9314706+1, 2.3104906-1, 2.4407666-2,
$ 2.9824176-3, 7.5220986-10, 4.4432506-3, 0.000000    , 6.9314706+1,
$ 1.6057156-1, 1.1006776-1, 8.2517506-4, 1.5877176-4, 0.000000    ,
$ 1.0902506-15, 0.000000    , 6.9314706+1, 1.4657356-1, 1.6490026-2,
$ 1.2164976-3, 1.3594176-4, 0.000000    , 6.9314706+1, 6.6209806-1,
$ 4.3321696-2, 1.0582206-2, 6.2677606-7, 6.7495736-6, 0.000000    ,
$ 6.9314706+1, 6.9771356-1, 2.7725886-2, 6.6180246-4, 5.0656046-5,
$ 2.4311716-7, 0.000000    , 6.9314706+1, 6.6209806-1, 8.0061176-2,
$ 1.1552456-3, 1.3752926-4, 0.000000    , 6.9314706+1, 6.9314706-1,
$ 1.4657356-1, 5.3319006-2, 6.6180246-4, 5.8365716-6, 5.8130116-7,
$ 0.000000    , 6.9314706+1, 6.6209806-1, 1.9804706-1, 6.6209806-2,
 DATA (DCON  (I),I=571,665)/
$ 2.4144246-6, 6.6777176-4, 0.000000    , 6.9314706+1, 6.9314706-1,
$ 3.4657356-1, 7.7019336-2, 3.8508176-3, 3.7197466-5, 0.000000    ,
$ 6.9314706+1, 6.9314706+1, 6.6209806-1, 1.7326476-1, 8.3111156-4,
$ 6.7346116-4, 0.000000    , 6.9314706+1, 6.9314706+1, 3.4657356-1,
$ 9.6272426-3, 9.6270426-4, 7.2275096-7, 8.4478866-9, 0.000000    ,
$ 6.9314706+1, 6.9314706-1, 3.4657356-1, 1.7326476-2, 5.9243336-3,
$ 0.000000    , 3.4850556-4, 0.000000    , 6.9314706+1, 6.6209806-1,
$ 1.9804706-1, 2.3110496-2, 9.6270426-5, 3.6260066-4, 0.000000    ,
$ 6.9314706+1, 6.6209806-1, 2.7725886-1, 6.6209406-2, 0.000000    ,
$ 7.1111426-5, 0.000000    , 6.9314706-1, 3.4657156-1, 9.9021006-2,
$ 8.4885506-4, 6.7750076-6, 2.7455036-10, 0.000000    , 6.9314706+1,
$ 6.6209806-1, 1.3862946+1, 3.8508176-3, 1.9256086-3, 0.000000    ,
$ 2.0706126-5, 1.6895776-9, 0.000000    , 6.9314706+1, 6.6209806-1,
$ 2.3110496-1, 3.8508176-2, 2.1004456-3, 6.0986136-6, 0.000000    ,
$ 6.9314706+1, 3.4657356-1, 5.7762256-2, 6.6209406-4, 0.000000    ,
$ 1.3727416-9, 0.000000    , 6.9314706+1, 3.4657156-1, 1.3862946-1,
$ 1.1552456-2, 6.9135216-4, 1.2920306-9, 0.000000    , 6.6209806-1,
$ 1.5602276-1, 2.7725886-2, 1.9254036-5, 5.2094146-7, 0.000000    ,
$ 6.9314706+1, 2.3110496-1, 5.3119006-2, 2.3104906-2, 1.2833066-5/
 DATA (DCON  (I),I=666,760)/
$ 0.000000    , 6.9314706+1, 3.4657356-1, 1.1552456-1, 7.7016336-4,
$ 1.9254036-4, 0.000000    , 6.6209806-1, 1.9804706-1, 6.9510506-2,
$ 5.7762256-4, 1.0689716-5, 0.000000    , 6.9314706+1, 2.7725886-1,
$ 6.6209406-2, 6.6209806-3, 0.000000    , 1.0989776-7, 0.000000    ,
$ 6.9314706+1, 1.9804706-1, 1.7326476-1, 3.1502506-4, 3.1222446-4,
$ 1.1552456-6, 0.000000    , 0.000000    , 0.000000    , 0.000000    ,
$ 0.000000    , 0.000000    , 0.000000    , 0.000000    , 0.000000    /
 DATA (DCON  (I),I=761,855)/
$-4.4000006-7, 1.1700006-6,-1.0000006-6, 7.4900006-7,-3.5000006-7,
$ 1.4000006-5,-1.0300006-7, 1.9900006-7,-2.1000006-6,-4.0400006-7,
```

```
 $ 3.2400000E-6, 1.1400000E-8,-2.4400000E-6, 2.7100000E-6, 6.2400000E-6,
 $-1.  00000E-7,-1.1500000E-7,-1.4400000E-5,-6.8600000E-7, 1.4900000E-5,
 $ 2.7000000E-7, 2.4200000E-7,-4.1700000E-6,-9.0900000E-7, 2.7700000E-8,
 $-2.  00000E-6, 4.7500000E-7,-4.1000000E-6,-7.6800000E-6, 3.1200000E-6,
 $-1.  00000E-5, 1.1000000E-5,-4.9400000E-6,-4.1400000E-6, 2.8200000E-6,
 $ 1.2400000E-6,-5.4800000E-6, 1.2200000E-6,-1.1400000E-6, 4.8800000E-7,
 $ 1.  00000E-7,-1.4400000E-6,-3.7800000E-6, 1.3300000E-6, 3.9100000E-6,
 $-1.  00000E-5,-2.3300000E-7, 3.8200000E-6, 3.5000000E-6,-8.5600000E-7,
 $ 7.  00000E-7,-5.0700000E-6,-7.9200000E-6, 1.9300000E-6,-5.3400000E-6,
 $-2.  00000E-6, 1.2200000E-7,-2.1500000E-7, 3.0000000E-6,-3.8400000E-6,
 $ 4.  00000E-7, 1.7500000E-7,-8.6800000E-6, 1.6800000E-6,-1.2200000E-6,
 $ 1.  00000E-6,-2.4500000E-7, 2.3600000E-6,-6.3700000E-7, 6.9100000E-7,
 $ 1.  00000E-7, 8.0500000E-8,-3.4000000E-7, 8.9000000E-7, 3.7700000E-7,
 $ 1.  00000E-7,-1.2500000E-7, 1.2400000E-6,-1.7700000E-7, 1.0400000E-6,
 $ 1.  00000E-6,-2.4300000E-6,-7.0400000E-6, 5.2500000E-7, 3.8500000E-6,
 $ 1.  00000E-6,-1.1400000E-6,-2.6900000E-7, 4.0700000E-6, 1.4700000E-7,
 $-2.  00000E-6,-4.9000000E-6,-4.8400000E-7, 2.0200000E-6,-5.3500000E-6/
 DATA (F49    (I),I=96,185 )/
 $ 1.  00000E-7, 4.4200000E-7,-4.9600000E-6,-1.4600000E-6, 3.9800000E-7,
 $ 2.  00000E-6, 1.2700000E-7,-4.3600000E-6,-2.7100000E-6, 2.6300000E-6,
 $ 5.  00000E-7, 2.1400000E-8,-2.3900000E-6, 9.2800000E-6, 4.9000000E-7,
 $-5.  00000E-6, 1.4300000E-7, 1.2500000E-5, 4.3000000E-7,-7.8400000E-6,
 $-1.  00000E-5, 9.3000000E-6, 2.1300000E-6, 2.2100000E-6, 1.9800000E-7,
 $-1.  00000E-5, 1.1200000E-5,-1.1200000E-5, 7.8400000E-6, 3.1400000E-6,
 $ 3.  00000E-7, 3.0600000E-7,-4.8400000E-6, 1.2200000E-5, 7.5400000E-7,
 $-4.  00000E-6,-1.0600000E-5, 2.3900000E-6, 1.4900000E-6,-1.2100000E-5,
 $ 1.  00000E-5,-1.1300000E-6,-4.4100000E-6, 9.7900000E-6,-1.4600000E-6,
 $ 1.  00000E-6, 2.4500000E-7,-3.2300000E-6, 1.1600000E-6, 1.1400000E-5,
 $-3.  00000E-6, 1.2700000E-7, 4.6700000E-7,-4.9500000E-6, 6.0100000E-6,
 $-2.  00000E-6,-2.0000000E-6,-1.2300000E-7, 1.4000000E-7,-1.6500000E-6,
 $ 4.  00000E-6,-1.0000000E-6, 6.5300000E-6,-9.6000000E-7,-5.2400000E-6,
 $-1.  00000E-5, 2.4000000E-6,-4.0400000E-6,-5.6000000E-6, 1.2400000E-6,
 $-3.  00000E-6, 1.9200000E-6, 5.8000000E-6,-8.0400000E-7, 1.8600000E-7,
 $-5.  00000E-6,-2.2600000E-7, 2.8400000E-7,-3.0200000E-6,-3.3800000E-6,
 $-2.  00000E-6, 5.3000000E-6,-1.9500000E-7,-2.0200000E-6,-2.0300000E-6,
 $ 2.  00000E-7, 4.0000000    , 0.0000000    , 0.0000000    , 0.0000000    /
 DATA (F49C   (I),I=1,7),J= 1,13)/
 $ 1.  00000E-7, 1.4459453E-1, 1.2444480E-3, 2.1547688E-4, 0.0000000    ,
 $ 0.  00000    , 0.0000000    , 0.0000000    , 0.0000000    , 0.0000000    ,
 $ 0.  00000    , 0.0000000    , 0.0000000    , 0.0000000    , 4.8289050E-2,
 $ 8.  00000E-4, 1.2250000E-3, 0.0000000    , 0.0000000    , 0.0000000    ,
 $ 0.  00000    , 0.9971408E-2, 8.1494028E-4, 3.3244078E-3, 0.0000000    ,
 $ 0.  00000    , 0.0000000    , 0.0000000    , 2.7141578E-3, 0.0000000    ,
 $ 0.  00000    , 0.0000000    , 0.0000000    , 0.0000000    , 0.0000000    ,
 $ 7.  00000E-4, 0.0000000    , 0.0000000    , 0.0000000    , 0.0000000    ,
 $ 0.  00000    , 0.0000000    , 2.8499111E-4, 7.5613748E-4, 3.6044578E-2,
 $ 8.  00000E-4, 4.5555334E-5, 0.0000000    , 0.0000000    , 5.7790018E-1,
 $ 1.  00000E-7, 0.0000000    , 0.0000000    , 0.0000000    , 0.0000000    ,
 $ 0.  00000    , 1.1660258E-2, 1.5402064E-2, 8.6756748E-4, 1.1912518E-4,
 $ 0.  00000    , 0.0000000    , 0.0000000    , 1.9695338E-2, 8.1197598E-5,
 $ 0.  00000    , 0.0000000    , 0.0000000    , 0.0000000    , 0.0000000    ,
 $ 0.  00000    , 0.0000000    , 0.0000000    , 0.0000000    , 0.0000000    ,
 $ 0.  00000    , 0.0000000    , 8.0258078E-3, 0.0000000    , 0.0000000    ,
 $ 0.  00000    , 0.0000000    , 0.0000000    , 0.0000000    , 1.3465568E-3,
 $ 1.  00000E-3, 1.9111868E-4, 0.0000000    , 0.0000000    , 0.0000000    ,
 $ 0.  00000    /
 DATA (F49AC  (I,J),I=1,7),J=14,14)/
```

```
     $ 0.000000    • 0.000000    • 0.000000    • 0.000000    • 0.000000    •
     * 0.000000    • 0.000000    • 0.000000    • 0.000000    • 0.000000    •
     * 0.000000    • 0.000000    • 0.000000    • 0.000000    • 1.884[illegible]E-4•
     * 1.708[illegible]E-4• 4.141[illegible]E-4• 2.304[illegible]E-6• 0.000000    • 0.000000    •
     $ 0.000000    • 4.870690E-4• 0.000000    • 0.000000    • 0.000000    •
     * 0.000000    • 0.000000    • 0.000000    • 4.538654E-4• 0.000000    •
     * 0.000000    • 0.000000    • 0.000000    • 0.000000    • 0.000000    /
      DATA ((PHONY(I,J),I=1,7),J=1,13 )/
     * 0.000000    • 0.000000    • 0.000000    • 5.862700E-6• 0.000000    •
     * 0.000000    • 0.000000    • 0.000000    • 0.000000    • 0.000000    •
     * 0.000000    • 0.000000    • 0.000000    • 0.000000    • 0.000000    •
     * 0.000000    • 4.722400E-4• 0.000000    • 0.000000    • 0.000000    •
     * 0.000000    • 7.170000E-7• 0.000000    • 1.225100OE-6• 0.000000    •
     * 0.000000    • 0.000000    • 0.000000    • 7.750000E-6• 0.000000    •
     * 0.000000    • 0.000000    • 0.000000    • 0.000000    • 0.000000    •
     * 1.710000E-5• 0.000000    • 0.000000    • 0.000000    • 0.000000    •
     $ 0.000000    • 0.000000    • 0.000000    • 0.000000    • 0.000000    •
     * 0.000000    • 1.[illegible]23000E-4• 0.000000    • 0.000000    • 0.000000    •
     * 0.000000    • 0.000000    • 0.000000    • 0.000000    • 1.000000    •
     * 0.000000    • 0.000000    • 0.000000    • 0.000000    • 1.061075E-5•
     * 0.000000    • 0.000000    • 0.000000    • 0.000000    • 6.405800E-6•
     * 0.000000    • 0.000000    • 0.000000    • 0.000000    • 0.000000    •
     * 0.000000    • 0.000000    • 0.000000    • 0.000000    • 0.000000    •
     * 0.000000    • 0.000000    • 8.626750E-6• 0.000000    • 0.000000    •
     * 0.000000    • 0.000000    • 0.000000    • 0.000000    • 0.000000    •
     * 0.000000    • 6.[illegible]090E-6• 0.000000    • 0.000000    • 0.000000    •
     * 0.000000    /
      DATA ((PHONY(I,J),I=1,7),J=14,18)/
     * 0.000000    • 5.643800E-7• 0.000000    • 0.000000    • 0.000000    •
     * 0.000000    • 0.000000    • 0.000000    • 6.620000E-6• 0.000000    •
     * 0.000000    • 0.000000    • 0.000000    • 0.000000    • 1.575000E-7•
     * 0.000000    • 0.000000    • 0.000000    • 0.000000    • 0.000000    •
     * 0.000000    • 0.000000    • 0.000000    • 0.000000    • 0.000000    •
     * 0.000000    • 0.000000    • 0.000000    • 0.000000    • 0.000000    •
     * 0.000000    • 0.000000    • 0.000000    • 0.000000    • 0.000000    /
      DATA ((FLAM  (I,J),I=1,7),J=1,13 )/
     * 7.418[illegible]E-9• 7.[illegible]1246E-19• 6.93000E-31• 1.743656E-7• 0.000000    •
     * 0.000000    • 0.000000    • 6.[illegible]7319E-6• 6.93000E-31• 6.93000E-31•
     * 6.93000E-31• 6.93000E-31• 1.0[illegible]644E-5• 3.20[illegible]33E-3• 6.93000E-31•
     * 6.93000E-31• 7.747324E-5• 0.000000    • 0.000000    • 0.000000    •
     * 0.000000    • 1.[illegible]9213E-17• 6.93030E-31• 1.552619E-5• 0.000000    •
     * 0.000000    • 0.000000    • 0.000000    • 5.021734E-3• 0.000000    •
     * 0.000000    • 0.000000    • 0.000000    • 0.000000    • 0.000000    •
     * 1.243333E-5• 0.000000    • 0.000000    • 0.000000    • 0.000000    •
     * 0.000000    • 0.000000    • 6.93000E-31• 6.93000E-31• 6.93000E-31•
     * 6.93000E-31• 1.[illegible]1379E-3• 0.000000    • 0.000000    • 6.93000E-31•
     * 1.770[illegible]E-9• 0.000000    • 0.000000    • 0.000000    • 0.000000    •
     * 0.000000    • 6.93000E-31• 6.93000E-31• 5.276864E-8• 1.354424E-3•
     * 0.000000    • 0.000000    • 0.000000    • 7.129870E-14• 3.090000E-4•
     * 0.000000    • 0.000000    • 0.000000    • 0.000000    • 0.000000    •
     * 2.[illegible]52[illegible]E-4• 6.[illegible]000E-31• 6.93000E-31• 6.93000E-31• 6.93000E-31•
     * 4.[illegible]957E-5• 6.[illegible]2590E-4• 7.461240E-5• 0.000000    • 0.000000    •
     * 0.000000    • 0.000000    • 0.000000    • 0.000000    • 1.281[illegible]3E-34•
     * 6.[illegible]10[illegible]E-31• 1.215[illegible]4E-3• 0.000000    • 0.000000    • 0.000000    •
     * 0.000000    /
      DATA ((FLAM  (I,J),I=1,7),J=14,18)/
     * 6.93000E-31• 7.[illegible]0000E+1• 0.000000    • 0.000000    • 0.000000    •
```

```
$ 0.000000    , 0.000000    , 6.93000E-31, 3.07180HF-3, 0.000000    ,
$ 0.000000    , 0.000000    , 0.000000    , 0.000000    , 2.985142E-7,
$ 6.93000E-31, 6.93000E-31, 1.204133E-3, 0.000000    , 0.000000    ,
$ 0.000000    , 5.608974E-7, 0.000000    , 0.000000    , 0.000000    ,
$ 0.000000    , 0.000000    , 0.000000    , 6.93000E-31, 0.000000    ,
$ 0.000000    , 0.000000    , 0.000000    , 0.000000    , 0.000000    /
 DATA ALHFOM/ 1.499949E+3 /
 DATA (JHH    (I),I=1,95    )/
$        4.        5.        11.       12.       17.
$       18.       25.        26.       33.       39.
$       40.       41.        47.       48.       49.
$       56.       70.        78.       84.       85.
$       86.       87.        93.      100.      101.
$      104.      109.       115.      122.      123.
$      128.      129.       136.      145.      146.
$      147.      153.       154.      160.      161.
$      163.      169.       176.      177.      178.
$      186.      192.       193.      194.      209.
$      210.      218.       224.      225.      232.
$      240.      241.       249.      250.      257.
$      258.      259.       267.      268.      274.
$      275.      283.       284.      291.      293.
$      294.      295.       308.      309.      310.
$      311.      317.       318.      341.      342.
$      343.      350.       357.      359.      360.
$      361.      369.       377.      378.      379.
$      384.      392.       401.      402.      408/
 DATA (JHH    (I),I=96,185 )/
$      409.      410.       419.      424.      425.
$      425.      427.       434.      440.      441.
$      442.      443.       447.      448.      451.
$      455.      457.       458.      460.      468.
$      473.      474.       475.      476.      477.
$      484.      486.       489.      490.      491.
$      492.      493.       498.      499.      501.
$      502.      507.       508.      509.      514.
$      516.      523.       528.      529.      535.
$      535.      537.       542.      543.      544.
$      549.      550.       551.      556.      557.
$      563.      564.       571.      572.      574.
$      576.      595.       600.      593.      602.
$      604.      609.       616.      621.      622.
$      624.      631.       632.      638.      639.
$      646.      652.       653.      659.      665.
$      670.      671.       677.      686.      690.
$      691.        0.         0.        0.        0/
 DATA (ISO    (I),I=1,18   )/
$        4.        0.         0.        0.        0.
$        0.        0.         0.        0.        0.
$        0.        0.         0.        0.        0.
$        0.        0.         0/
 DATA (HHFCTO(I),I=1,95    )/
$ -9670700004. 9671020148. 9671282692. 9671544836. 9671806980.
$ 9872065024. -9804974132. 9805238276. 9805500420. 9805762564.
$ 9806024708. 9806319620. 9806282756. -9939193860. 9939456204.
$ 9939718148. 9939980292. 9940242436. 9940500484.-10073411588.
$ 10073673732. 10073935876. 10074198020. 10074460164. 10074755076.
```

```
      DATA (NUCLID(I),I=571,665)/
     1 1934625E12*, 1934742E24*, 1936388E47*,-1936757E36*, 1937599E80*,
     2 1937E79E67*, 1937A51E88*, 1937A779E12*, 1937781E58*, 1937799E04*,
     3-1938094E58*, 1938107E08*, 1938107E52*, 1938107E58*, 1938109E60*,
     4 1938112E88*, 1938113E12*,-1938662E03*, 1938690E58*, 1938695E24*,
     5 1938721E88*, 1938736E12*, 1938737E56*, 1938800E08*, 1938825E84*,
     6-1938836E56*, 1938840E28*, 1938840E52*, 1938840E88*, 1938840E92*,
     7 1938841E08*,-1938842E28*, 1938847E56*,-2001312E36*, 2001334E80*,
     8 2001E09E92*, 2001E12E08*, 2001417E12*, 2001461E36*, 2001609E60*,
     9-2014736E36*, 2014780E50*, 2014786E52*, 2014812E36*, 2014834E84*,
     A-2014836E48*, 2014891E12*,-2028182E36*, 2028203E80*, 2028234E24*,
     B 2028280E88*, 2028284E12*, 2028313E96*, 2028334E04*,-2041804E64*,
     C 2041830E08*, 2041836E52*, 2041842E36*, 2041870E40*, 2041734E88*,
     D-2041786E30*,-2041791E68*, 2041787E78*,-2055025E92*, 2055052E36*,
     E 2055075E48*, 2055104E12*, 2055130E28*, 2055156E12*, 2055182E60*,
     F-2068467E88*, 2068500E78*, 2068526E52*, 2068552E96*, 2068578E44*,
     G-2081E86E48*, 2081E97E12*,-2081E97E12*,-2081954E32*, 2081921E36*, 2081E48E88*,
     H 2091974E72*, 2092008E88*, 2092026E12*, 2092052E80*,-2095161E64*,
     I-2095161E48*, 2095179E04*, 2095222E56*, 2095244E72*, 2095247E28*,
     J-2104726E42*, 2104741E04*, 2104761E36*, 2104774E40*, 2104787E84*/
      DATA (NUCLID(I),I=666,760)/
     K 2108E00E16*,-2112147E28*, 2122213E64*, 2122234E80*, 2122265E52*,
     L 2122290E04*, 2122317E24*,-2135A35E92*, 2135A61E36*, 2135A75E80*,
     M 2135E13E24*, 2135E40E88*, 2135E58E16*,-2149056E28*, 2149083E64*,
     N 2149103E50*, 2149135E52*, 2149161E00*,-2149187E40*, 2149213E88*,
     O-2149247E48*, 2149250E32*, 2162531E36*, 2162557E40*, 2162584E24*,
     P 2162600E88*, 2162635E16*,          0*,          0*,          0*,
     Q          0*,          0*,          0*,          0*,          0/
      DATA (MULT   (I),I=1,91   )/
     R          0*,          0*,        512*,       4096*,       3276*,
     S      20216*,      20971*,    16777216*,    13421772*,  10737418*,
     T  858993*,5*/
      DATA I=84,NUC=94,LMAX,MAXNUC/
     U        12*,        692*,        181*,         18*,         780/
    1 FORMAT (12A6/10L1/20L1)
    2 FORMAT (2F10.3/4A)
    3 FORMAT (1H1   50(1H* ) * * * * * * * * *//12X10HT H E   D E P A R
     1T M E N T   O F   D E F E N S E   F A L L O U T   P R E D I C T I
     20 N   S Y S T E M //53X1(3H* ) * * * * * * * * *////6HX-RAYPARTICLE ACT
     1IVITY MODULE///55X11HPREPARED BY/43X36HHQ ARMY NUCLEAR DEFENSE LAB
     4ORATORY/47X26HEDGEWOOD ARSENAL, MARYLAND////20X12A6)
    4 FORMAT (////49X,13HCONTROL VARIABLE ARRAYS//48X9HIFTAPE(I)/38X10L5/
     1//49XHHMPPWT(I)//23X15L5)
    5 FORMAT (////60X,3HCAPTURE - TO - FISSION RATIO IS,F10.3)
    6 FORMAT (///15X,43HNUMBER OF NEUTRONS EMITTED PER FISSION IS,F10.3)
    7 FORMAT (///47X,19HTYPE OF FISSION IS A6)
    8 FORMAT (///20X55HTHE CLOUD REACHED THE SOIL CONDENSATION TEMPERATUR
     1E OF F7.1,4H AT F4.2,5H SEC.)
    9 FORMAT (///,21H0TOTAL YIELD IS,1PE12.4,10H KILOTONS.)
   10 FORMAT (///61X15HFISSION YIELD IS,1PE12.4,10H KILOTONS.)
   11 FORMAT (///32X9HTHERE ARE,I4,36H PARTICLE CLASSES WITH SIGMA OF,
     1    F7.4,1H.)
   12    FORMAT (///41X, 20HTHE HEIGHT OF BURST IS , F9.1, 8H METERS. )
C
C*****************************************************************
C*****************************************************************
C
```

```
S= 3311 A 2341        73/74   OPT=1                                FTN 4.8+P357     84/04/74  23.47.43.     PAGE    14

      PRINT = [5000]
      TAPE = [6000]
      DATA CAPFIS/2HFI/
      REWIND [5000]
      READ (5000,2)
     1    CAPFIS,EMITN,FISSID
    2 FORMAT (K000[0,4)
     1    (NAME(I),I=1,12)
      WRITE (K000[0,4)
     1    (IFTAPE(J),J=1,10),(NPRNT(K),K=1,15)
      WRITE (K000[0,5) TM
      WRITE (K000[0,10) E4
      WRITE (K000[0,7) FISSID
      WRITE (K000[0,12) MOM
      WRITE (K000[0,3) CAPFIS
      WRITE (K000[0,4) EMITN
      WRITE (K000[0,6) SLOTNO,TMSO
      WRITE (K000[0,11) ITAB,SIGMA
      IF (FISSID.EQ.ITYPE(6))GO TO 335
      WRITE (K000[0,100) FISSID
A220  FORMAT (2H0,20X,20HERROR,20X,20H/* FISSION DATA FOR *,
     1    45H* TYPE FISSION IS NOT AVAILABLE.*)
      STOP
  335 CONTINUE=6.33333333
      IF (EMITN.LE.0.0) GO TO 100
C
C     * CONVERT MOM FROM METERS TO FEET.
C
      MOM=3.28084
      CONTINUE=3.33333333
      IF (MSCI.LT.3.0) GO TO 274
      E04=3.0
      GO TO 247
  274 IF (MSCI)276,277,275
  275 E04=MSCI/(2.24*MSCI*MSCI-234.*MSCI+6225.)
      GO TO 246
  276 IF (MSCI.LT.-2.0) GO TO 278
  277 E04=0
      GO TO 246
  278 E04 = 1.E4
      GO TO 247
  246 E04 = ALBEDO*E04
  247 E04 = ALBEDO*EMITN
      GO TO 101
  100 E04= 0
  101 CONTINUE
      CALL PWAIT0
     1    (SLOTNO ,TMSO   ,MCHN   )
      RETURN
      END
```

```
      7 FORMAT(* OUTPUT ALONG A LINE BEGINNING AT R (M) = *F10.3*  Y (M)
     * *F10.3* WITH AN ANGLE (DEG) = *F10.4* TO THE HORIZONTAL *)
        IF(LDIS.NE.0)WRITE(4) RMIN,YMIN,ALPHA,RMAX
        ALPHA=ALPHA*DEGRAD
        READ 1,KKK
        IF(LDIS.NE.0)WRITE(4) KKK
        DO 8 JJJ=1,KKK
        READ 9,NREQ,T1,T2,MASCHN
      9 FORMAT(I4,2F10.3,I4)
        IF(LDIS.NE.0)WRITE(4) NREQ,T1,T2,MASCHN
        PRINT 101,NREQ,T1,T2,MASCHN
    101 FORMAT(*NREQ = *I4*  T1 = *F10.3*  T2 = *F10.3*  MASCHN = *I4)
        IF(NREQ.NE.10)MASCHN=0
        IF(MASCHN.EQ.0.AND.NREQ.NE.10)GO TO 1A
        IF(MASCHN.GT.71.AND.MASCHN.LT.162)GO TO 16
        PRINT 100
    100 FORMAT(* MASCHN LT 71 OR GT 162*)
        STOP
     1A DO 17 I=1,NMAX
     17 QMAP(I)=0.
        REWIND IPOUT
        READ(IPOUT)TST
        READ(IPOUT)(TST,J=1,15)
        READ(IPOUT)(DETID(J),J=1,7),(DETID(J),J=1,12),(DETID(J),J=1,12),
       *(DETID(J),J=1,12),(DETID(J),J=1,12)
        READ(IPOUT)NPS
        READ(IPOUT)(TST,TST,TST,TST,J=1,NPS)
        READ(IPOUT)(DETID(J),J=1,12)
        FISNUM=FW*1.45E15
        RUFSAM=SSAM/GRUFF
        JGO=1
        ITAR=NPS
        IF(NREQ.EQ.15.OR.NREQ.EQ.1A)GO TO 26
        T1=TIMSEC(T1,3,0)
        T2=TIMSEC(T2,3,0)
     2A TIME=T1-TGZ
        TENTEN=TIME
        KDOS=.FALSE.
        IF=(T+T2-TGZ
        JD=.TRUE.
        GO TO (12,27,31,10,28,32,12,29,30,29,32,32,32,32,32,27,32,32,32,32
       *),NREQ
     27 TIME=3.00.
        GO TO 31
     28 KDOS=.TRUE.
        GO TO 30
     29 JGO=2
        FISNUM=FISNUM*1.E+4
        RUFSAM=SSAM
        GO TO 31
     30 JD=.FALSE.
        FISNUM=FISNUM/3.00.
     31 IF(NREQ.EQ.6.OR.NREQ.EQ.5)GO TO 501
        CALL PAM2
        GO TO 12
    501 TENTEN =0.
        KD=1=1
```

```
      ROW = 5
      I = 1
      DIJ = 7680.
  501 DO 2 KO=2,KO[A]-ONE
      B(KO+ONE)=B(KO)
      IF(.NOT.(KO=5))GO TO 503
      IF(ITEM.LE.IF)IT)GO TO 503
      MASC=MASC+CM(I)
      GO TO 502
  503 CALL PAM2
      DO 504 KO=CAN=1,ITAM
  504 B(KO+ONE)=B(KO)+FP(KO+CAN)
  502 IF(I.EQ.IF(IT(MOD))IEN
      IF(I.EQ.3).GT.1)GO TO 511
      IF(I.EQ.CM(1.GT.0)GO TO 511
      I=I-2
      KONE=KO+2+1
      M=S=TL)Y(IT/7200.
      IF(I.EQ.0).EQ.0)GO TO 511
      I=I=KO+KONE-1
      T=I=7200.
      DIJ=7200.
      GO TO 512
  511 M=O=KO+2=MASCM(
      IF(I.EQ.2).GT.2)GO TO 32
      IF(I.EQ.1)GO TO 505
      I=I-1
  505 F.M=I(* IMPROPER TIME SPECIFICATION *)
      GO TO 4
   32 IF=I=IF)IT/2.
      KO=2
      CALL PAM2
      B(KO)=IF(IT+M
      I=I-(KO+CAN+2)+ITAM
  503 FOR=KO+CAN+2)=B(KO+CAN)
      M=772=78.5
      DO 301 I=I,NIJ
      IF(I.EQ.1.OR.I.EQ.NIJ)GO TO 301
      DO 2 I=I,NIJ
      B=B(IROUT)F(I)+Y(I)+T(I)+PS(I)+FMAS(I)+INRZ(I)
      IF(I.EQ.IZ(I).EQ.MAG)GO TO 33
      M=Z(I)=Z(I)
      B=Z=-M2Z*B6.)*M=Z2
      GO TO 34
   33 M=Z=Z2
   34 B=Z=.5*(I(I)-XMIN)**2+(Y(I)-YMIN)**2)
      RSM=SQZ=M=Z
      IF(I.EQ.MAG(A))GO TO 302
      B=M=(M=M=M)
      BETA=ATAN((Y(I)-YMIN)/(X(I)-AMIN))
      IF(X(I).GT.XMIN.AND.BETA.LT.0.)GO TO 40
      IF(Y(I).GT.YMIN.AND.BETA.LT.0.)GO TO 41
      IF(Y(I).LT.YMIN.AND.BETA.GT.0.)GO TO 41
      GO TO 42
   40 BETA=IMOP)+BETA
      GO TO 42
   41 BETA=PI+BETA
```

```
SUBROUTINE LINOUT     72/74   OPT=1                    FTN 4.8+P357     04/04/74  21.48.08.     PAGE     4

      42 PHI=ABS(ALPHA-META)
         RTF=R*RGZF*SIN(PHI)
         ZTF=R*RGZF*COS(PHI)
         IF(RMZ.GE.RGZF)GO TO 35
         THETA=ASIN(RMZ/RGZF)
         THETA1=META-THETA
         THETA2=META+THETA
         IF(ALPHA.GE.THETA1.AND.ALPHA.LE.THETA2)GO TO 36
         GO TO 342
      36 ZTEMP=SQRT(RMZ**2-RTF**2)
         ZIST=ZTEMP-ZTEMP
         KIST=ZIST/DGR+2.
         GO TO 37
      35 KIST=1
         ZTEMP=SQRT(RMZ**2-RTF**2)
      37 ZZND=ZTEMP+ZTEMP
         KZND=ZZND/DGR+1.
         IF(KIST.GT.KMAX)GO TO 382
         IF(KIST.GT.KZND)GO TO 382
         IF(KZND.GT.KMAX)KZND=KMAX
         NOSD=3
         PARSIZ=PS(I)
         DO 90 IM=1,ITAR
         IF(PSIZE(IM).LE.PARSIZ)GO TO 91
      90 CONTINUE
         PRINT 92
      92 FORMAT(' ERROR IN LINOUT, PARSIZ NEQ ANYTHING ')
         STOP
      91 IPS=IM
         GO TO (401,414,402,403,403,410,411,414,414,414,416,414,419,421,422
        *,423,427,427,427,427),NNEW
     401 F=1.0
         GO TO 428
     402 IF(T(I)-TI)414,414,382
     403 IF(T(I)-TI)404,404,405
     404 TEMP=TI-TGZ
         GO TO 413
     405 TEMP=T(I)-TGZ
         GO TO 411
     406 IF(T(I)-TZ)407,382,382
     407 IF(T(I)-TI)409,404,404
     408 TEMP=T(I)-TGZ
         GO TO 414
     409 TEMP=TI-TGZ
         GO TO 413
     410 F=F45(I)
         GO TO 424
     411 IF(T(I)-TZ)412,382,382
     412 IF(T(I)-TI)402,382,410
     413 WCAN=WCAN+1
         DO 508 MCAN=1,WCAN
         IF(T(I)-(TOTEM+DELT).AND.TENTEM.LE.TOUT(KJUN+1))GO TO 509
     508 CONTINUE
         IF(TFO(WCAN).LE.0.)TFO(WCAN)=1.
         TMAJ1=ALOG(TFO(WCAN))
         TMAJ=ALOG(TEMP+DELT)
         QMAJ1=ALOG(FCAN(IJS,WCAN))
```

```
      C  ...42=ALOG(FCAN(IPS,KFOW))
         GO TO 410
  405 IF(TFD(KJEN),LT.0.)TFD(KJEN)=1.
      T...2)=ALOG(TFD(KJEN))
      D...W2=ALOG(TFD(KJEN+1))
      C...A2)=ALOG(FCAN(IPS,KJEN))
      C...32=ALOG(FCAN(IPS,KJEN+1))
  410 A...2=(C...A2-C...A2)/(TMAX-TMAX2)
      T...23=ALOG(TINTER)
      F...(IPS)=EXP(C...A2-XMAX*(TMAX-TMAX3))
  414 F...2(IPS)=FMASS(I)/(FMASS(IPS)*DUMFSAM)
      GO TO 428
  416 K...0=1
  417 F=F(I)
      GO TO 428
  418 K...0=2
      GO TO 417
  419 N...0=1
  420 F...ANS17
      GO TO 428
  421 K...0=2
      GO TO 420
  422 IF(PARSIZ.GE.T).AND.PARSIZ.LE.T2)GO TO 410
      GO TO 402
  423 IF(PARSIZ.GE.T').AND.PARSIZ.LE.T2)GO TO 414
      GO TO 422
  427 C... TINUE
      N...0=1
      GO TO 401
  428 C... TINUE
C     ...SHEILDING FUNCTION SHOULD BE INSERTED HERE
      DO 305 IE0=KISI,K2ND
      DM...=DMAP(IE0)
      GO TO (454,455),NOWD
  454 IF(ABS(DM...).LT.1.E-20)GO TO 456
      D...P(IE0)=AMIN1(DM...,F)
      GO TO 305
  455 D...P(IE0)=AMAX1(DM...,F)
      GO TO 305
  456 D...P(IE0)=DMAP(IE0)*F
  305 C... TINUE
  402 C... TINUE
      GO TO 304
  301 R...PHE=DGA
      IF(DIS.EQ.0)GO TO 309
      DO 410 I=1,NMAX
      R...PHE=ALPHA*F...
  410 A...IF(A) EALPHA*DMAP(I)
      IF(DIS.LT.0)GO TO 8
      R...PHE=DGA
  309 DO 406 I=1,NMAX
      A...PHE=ALPHA*F...
  406 P...RINT 4,7,A...ALPHA,DMAP(I)
  307 F... MAT(' RANGE (M) = ',F15.6,'   VALUE = ',F15.6)
    8 C... TINUE
    2 C... TINUE
      RETURN
```

```
SUBROUTINE LAYOUT   71/76   OPT=1                    FTN 4.0+336   06/04/76  23.48.08.   PAGE   6

      END
```

```
      SUBROUTINE GETSET
C
C     FIRST HALF OF THE OUTPUT PROCESSOR
C     THIS PROGRAM INITIALIZES AND WRITES HEADINGS FOR THE OUTPUT
C     PROCESSOR.  THEN IT CALLS THE FIRST PART OF THE PARTICLE ACTIVITY
C     MODULE (PART1) TO PRECOMPUTE DATA USED BY THE SECOND PART OF THE
C     PARTICLE ACTIVITY MODULE WHICH WILL BE CALLED DURING THE
C     EXECUTION OF LIMPO.
C
C ***********************************************************************
C
      COMMON /SET3/
     *     AZ          ,BZZ         ,BZZZ        ,BZZZZ       ,DELTAX
     *    ,DGX         ,DGY         ,DIFCON      ,DIFADJ      ,EMAS(2500)
     *    ,ESUM        ,IC(18)      ,ICON        ,ICTR        ,IH
     *    ,IOT(18)     ,IP          ,ITT(18)     ,IV          ,JC(18)
     *    ,JIN         ,JOUT        ,JPOUT       ,KTR(2500)   ,KTAPE
     *    ,LAST        ,MAPRUN      ,MAPRAY      ,MIN         ,MAREQ
     *    ,NA          ,NAZX        ,NBZX2       ,NBZY
     *    ,NCL         ,NE          ,NF          ,NIJ         ,NMAP
     *    ,NMAX        ,NOX         ,NP(21)      ,NREQ        ,NS
     *    ,NTAPES      ,NTAPET      ,NTASK       ,NXMAP       ,NYMAP
     *    ,PS(2500)    ,RADMAX      ,RUFSAM      ,RMIN        ,NOPART
     *    ,SCLOMM      ,T(2500)     ,T1          ,T2          ,TGZ
     *    ,TLIMIT      ,X(2500)     ,X1          ,X2          ,X3
     *    ,XA          ,XF          ,XGZ         ,XMAX        ,XMIN
     *    ,XNMAP       ,XO          ,Y(2500)     ,YF          ,YGZ
     *    ,YMAX        ,YMIN        ,YO          ,SUBRAD
      COMMON /TAPE/
     *     ISIN        ,ISOUT       ,INISE       ,JPARIN      ,IPAMIN
     *    ,IOTOPO      ,IOxIND      ,IHTOPO      ,IPOUT       ,IPAROT
     *    ,NSTAPE      ,NUMTAP(15)  ,IEXEC       ,LGO         ,LTHRU
     *    ,NPRT
      COMMON /CODE2/ OPTID(12), SSAM
      COMMON /BAA/
     *     ABFAC(700)  ,ABUNDO(700) ,ALMFOM      ,BRANCH(130) ,BSUHK(90)
     *    ,CAPFES      ,DCONT(700)  ,FCF(90)      ,FRM(185)    ,FAC(7,18)
     *    ,ISTOM       ,FMASS(200)  ,FOUNNY(7,18) ,FP,200)      ,FN
     *    ,IHPA        ,IGO         ,INUC         ,ISO(18)     ,ITAB
     *    ,JGO         ,JRM(185)    ,KOOS         ,KOUT        ,KRM
     *    ,LMAX        ,MASCH       ,MAXNUC       ,MULT(11)    ,NPRNT(15)
     *    ,OCCLUD(700) ,PACT(700)   ,PSIZE(200)   ,TENTER      ,TEXIT
     *    ,TIME        ,XLAM(7,18)  ,JD
      COMMON / ROMOD / RHZ(2500)
      LOGICAL IGO,JD,xOOS,NPRNT
C
C     DIMENSIONS PECULIAR TO GETSET.
C
      DIMENSION CHID(12),OPID(12),PSFID(12),TOPID(12),WID(12),TID(12)
C
C ********** ********** ********** GLOSSARY **********
C
C     DIFCON              ATMOSPHERIC DIFFUSION CONSTANT
C     DIFADJ              ADJUSTMENT FACTOR TO ALLOW FOR DIFFUSIVE GROWTH
C                         OF CLOUD SUBDIVISIONS.
C     RUFSAM IS A GROUND ROUGHNESS FACTOR
C     OPID( )             OUTPUT PROCESSOR IDENTIFICATION
```

```
C     WIND( )              WIND FIELD IDENTIFICATION
C     TOPID( )             TOPOGRAPHY IDENTIFICATION
C     HZ                   WIDTH OF CLOUD WHEN AS FIRST READ
C     HZ2 = HZ/2 IS THE WIDTH OF THE BUFFER ZONE BETWEEN MAP ZONES.
C     S222                 SQUARE OF HALF THE CLOUD SUBDIVISION LENGTH
C     DELTAX               MAP ZONE WIDTH EXCLUSIVE OF BUFFER ZONES
C     DX&. DY = LENGTHS OF GRID INTERVALS IN X AND Y DIRECTIONS
C          RESPECTIVELY
C     MTST.DTST.MOUT       TEMPORARY STORAGE
C     IC(J)                OVERALL CONTROL VARIABLES
C     IC(17) = POSITIVE MEANS STOP WITHOUT ENTERING OUTPUT PROCESSOR
C     IC(17) = 0 MEANS PROCEED WITH JOB
C     IC(18) POSITIVE MEANS PRINT TAPE IPOUT BEFORE EXECUTION
C     IC(18) = 0 MEANS DO NOT PRINT TAPE IPOUT
C     IPOUT = JMOUT = TAPE ON WHICH PARTICLE PARAMETERS ARE WRITTEN BY
C          THE TRANSPORT PROGRAM.
C     ISOUT                SYSTEM OUTPUT TAPE NUMBER
C     ISIN                 SYSTEM INPUT TAPE NUMBER
C     IOT(J)               ID NUMBERS OF AVAILABLE TAPE UNITS
C     ITT(J)               ID NUMBERS OF AVAILABLE TAPE UNITS
C     IERROR               ERROR STOP TRACE WORD
C     IH.IV                HORIZONTAL AND VERTICAL CHARACTER SPACINGS FOR
C                          THE PRINTER IN TERMS OF CHARACTERS PER INCH
C     ICON                 A ROUTE CONTROL PARAMETER
C     ICTR                 A CONTROL PARAMETER
C     JC(J)                LOCAL CONTROL VARIABLES
C     JC(1) ... OUTPUT FORMAT CONTROL VARIABLE
C        =1      2-LINE E-FORMAT PRINTER MAP
C        =2      2-LINE F11.3 FORMAT PRINTER MAP
C        =3      MULTIPLE BURST BINARY TAPE
C        =4      A SORT RUN (SEE JC(4) )
C        =5      COMBINATION OF 1) AND #3
C        =6      COMBINATION OF 2 AND #3
C     JC(4) ... NUMBER OF AREAS OF INTEREST (NAOI) USED IN SORT
C     JC(8) ... CONTROL FOR REWINDING THE MULTIPLE BURST TAPE
C        =0      REWIND MSTAPE BEFORE WRITING MAP
C        #0      DON#T REWIND MNTAPE BEFORE WRITING MAP
C     JC(10) ... PRINTER MARGIN CONTROL
C        =0      LEAVE PAGE MARGINS AS SET
C        #0      SET FOR NO MARGIN AT TOP AND BOTTOM OF PAGE
C     JC(14) ... IF SET =0. CALLS PAM2 ONLY
C     JC(15) ... CONTROL FOR USE OF ATMOSPHERIC DIFFUSION MODEL
C        =0      DON#T USE DIFFUSION MODEL
C        #0      USE DIFFUSION MODEL
C     JC(16) ... MAP GRID INTERVAL CONTROL
C        =0      ADJUST GRID INTERVALS TO YIELD AN UNDISTORTED MAP
C        #0      DISTORTED MAP ALLOWED
C     JC(18) ... MAP ADJUSTMENT OPTION
C        =0      ADJUSTMENT OF GRID INTERVALS PERMITTED
C        =1      NO ADJUSTMENT OF GRID INTERVALS PERMITTED
C     JR.NI                TEMPORARY STORAGE
C     LAST                 =1 INDICATES A SUBSEQUENT SORT IS REQUIRED
C     MIP                  NUMBER OF CLASSES USED FOR PARTICLE SORT
C     MAXWAY = MAXIMUM NUMBER OF WAFERS THAT CAN BE CONSIDERED AT ONE
C          TIME
C     MAPNUM = 0     ...   MAP CALLED FOR FIRST TIME
C     MAPNUM = #0    ...   MAP HAS PREVIOUSLY PRINTED N STRIPS OF A MAP
```

```
C      MP(10)              MAXIMUM NUMBER OF PROCESSING REQUEST TYPES
C                          ALLOWED FOR IN THE CODE
C      NZ                  NUMBER OF MAP ZONES RIGHT OF 1ST MAP
C      NPTS0, NMAP = NUMBER OF OUTPUT GRID POINTS ON ENTIRE MAP
C      NPTS = MAXIMUM NUMBER OF WAFERS THAT SHOULD BE WRITTEN IN ONE
C           BLOCK ON THE TAPE CONTAINING WAFERS THAT HAVE YET TO BE
C           SWEPT).
C      NMAX = NUMBER OF GRID POINTS IN X DIRECTION IN THE CORE-LOAD MAP
C           COUNTING 2 BUFFER ZONES
C      NOX                 SMALLEST X INDEX OF A MAP POINT TO THE RIGHT OF
C                          THE LEFT BOUNDARY OF THE CLOUD SUBDIVISION
C      NOX = NUMBER OF GRID POINTS IN X DIRECTION IN THE CORE-LOAD MAP
C           WITHOUT BUFFER ZONES.
C      NYSW = NUMBER OF GRID POINTS IN Y DIRECTION IN THE CORE-LOAD MAP
C      NXX = NUMBER OF GRID POINTS IN X DIRECTION OF WAFER
C      NXX2 = (NX/2)/2 = NUMBER OF GRID POINTS IN X DIRECTION OF THE
C           BUFFER ZONE.
C      NIT=K               A SEQUENTIAL COUNTER FOR SPECIFICATIONS OF MAP
C                          COORDINATES AND GRID INTERVALS
C      NPT                 NUMBER OF PARTICLE CLASSES
C      NTAPES              THE NUMBER OF AVAILABLE TAPE UNITS
C      NTAPST              THE NUMBER OF AVAILABLE TAPE UNITS
C      NPT                 NUMBER OF PARTICLE DESCRIPTIONS IN THE CURRENT
C                          PARTICLE BLOCK
C      NST                 TEMPORARY STORAGE OF A DATA BLOCK COUNT
C      NTYP                COMPUTATION TYPE CODE
C      NMP                 A COUNTER FOR MAP REQUESTS
C      NDX                 THE NUMBER OF GRID INTERVALS IN DELTAX
C      OMAP(J)             THE MAP ARRAY
C      DX                  THE FLOATING EQUIVALENT OF NDX
C      TI,TF               REQUEST TIME ARGUMENTS
C      XP,YP,ZP(I)         PARTICLE DESCRIPTION VARIABLES (INDEXED)
C      XMAX,XMIN           MAXIMUM AND MINIMUM X COORDINATES OF THE MAP
C      XLIM,YLIM,XB        LIMITING MAP COORDINATES TAKING INTO ACCOUNT
C                          THE BOUNDARY BUFFER ZONES
C      YMAX,YMIN           MAXIMUM AND MINIMUM Y COORDINATES OF THE MAP
C
C
C ***********************************************************************
C
C
C ********** BEGINNING OF PROGRAM **********
C
      [illegible] HIST,OUT,PROGRAM
      [illegible] SWEEP,OUT
      [illegible] (P,X(2500))
      DA[illegible]T/6HGETSET,6HIPOUT /
      [illegible]
      DT[illegible]
      [illegible]
      [illegible]
      MA[illegible]
      MA[illegible]
      [illegible]
      [illegible]
      [illegible]
```

```
      NTASK=0
C
C     CHECK IDENTIFICATION OF IPOUT
C
      REWIND IPOUT
      READ (IPOUT) IPOUT
      IF (IPOUT.EQ.NISI) GO TO 1
      IF (PRINT) WRITE (ISOUT,27) IPOUT
      STOP
1     READ (IPOUT) FM,SSAM,SLOTM,TMSD,SIGMA,TW,HOR,NCL,TLIMIT,BZ,POPANT
     1,BZ,TW,TW,TW,RADMAX
      SIGMAS=SIGMA*SIGMA*0.5
C
C     PRECOMPUTATION FOR DIFFUSION MODEL
C
      SUMRAD=RADMAX
      RADMAX=RADMAX**2
C
      READ (IPOUT) (DETID(J),J=1,12),(CRID(J),J=1,12),(PSEID(J),J=1,12),
     1(TID(J),J=1,12),(ID(J),J=1,12)
      READ (IPOUT) NPS
      READ (IPOUT) (PSI(F(J),FMASS(J),PACT(J),SV,J=1,NPS)
      ITAPENS
      READ (IPOUT) (TOPID(J),J=1,12)
C
C     READ IDENTIFIER FOR OUTPUT PROCESSOR BIN
C
      READ (ISIN,25) (OPID(J),J=1,12)
C
C     READ LIST OF AVAILABLE TAPES
C
      READ (ISIN,32) (IOT(J),J=1,18)
C
C     TEST TO REMOVE OTHER PROGRAM TAPES
C
      NTAPES=18
      DO 8 J=1,18
      IF (IOT(J)) 6,7,2
2     IF (IOT(J)-IPOUT) 3,6,3
3     IF (IOT(J)-ISOUT) 4,6,4
4     IF (IOT(J)-ISIN) 8,5,8
5     IF (IOT(J)-MITAPE) 8,6,8
6     IOT(J)=0
7     NTAPES=NTAPES-1
8     IT(J)=0
      NTAPET=NTAPES
      IF (NTAPES.EQ.0) GO TO 11
C
C     NOW CONSOLIDATE IN THE ARRAY
C
      JM=1+NTAPES
      DO 12 J=1,ITAPES
      IF (IOT(J)) 12,9,12
9     IF (IOT(JM)) 11,11,10
10    IOT(J)=IOT(JM)
      JM=JM+1
```

```
      GO TO 12
   11 I=I+1
      GO TO 9
   12 IC(I)=IOUT(J)
C
C     READ CONTROL VARIABLE ARRAY
C
   13 READ (ISIN,12) (IC(J),J=1,IN)
      READ (ISIN,28) DIFCON
C
C     THIS PART OF THE CODE DUMPS TAPE IPOUT IF REQUIRED
C     IC(14) POSITIVE MEANS DUMP TAPE IPOUT BEFORE EXECUTION
C
      SETP=.TRUE.
C
C     IC(14) = 0 MEANS DO NOT DUMP TAPE IPOUT
C
      IF (IC(14) ) 14,26,15
   14 REWIND 101
  101 FORMAT(* ERROR IN GETSET, IC(12) .LT. 0 *)
      STOP
   15 SETP=.FALSE.
      WRITE (ISCRT,3)
      WRITE (ISCRT,4)
      WRITE (ISCRT,101) (TITD(J),J=1,12)
   16 NIJ=0
   17 READ (IPOUT) NIJ
      NST=NST+1
      IF (NIJ) 18,20,19
   18 BACKFILE 102
  102 FORMAT(* ERROR IN GETSET, NIJ .LT. 0 *)
      STOP
   19 READ (IPOUT)(X(I),Y(I),T(I),PS(I),FMAS(I),IRBZ(I),I=1,NIJ)
      IF (NST-1) 20,20,17
      WRITE (ISCRT,6) NST
      WRITE (ISCRT,6) NIJ
      WRITE (ISCRT,7)
      WRITE(ISCRT,205)(X(I),Y(I),T(I),PS(I),FMAS(I),IRBZ(I),I=1,NIJ)
  205 FORMAT(5E12.5,I12)
      GO TO 17
   20 CONTINUE
C
C     IC(17)  POSITIVE MEANS STOP WITHOUT ENTERING OUTPUT PROCESSOR
C     IC(17) = 0 MEANS PROCEED WITH JOB
C
      IF (IC(17)) 21,24,23
   21 REWIND 103
  103 FORMAT(* ERROR IN GETSET, IC(17) .LT. 0 *)
      STOP
   23 WRITE (ISCRT,6)
      STOP
C
C     END OF TAPE IPOUT DUMP
C
   24 CONTINUE
C
C     READ PRINTER INSCRIPTION = CHAR/INCH HORIZONTAL,VERTICAL
```

```
C
      READ (ISIN,12) IM,IV
C
C     PRINT A HEADING TO IDENTIFY PRINTED OUTPUT
C
      WRITE (ISHOUT,3H)
      WRITE (ISHOUT,29) (OPID(J),J=1,12),(DETID(J),J=1,12),(CRID(J),J=1,
     12),(PSEID(J),J=1,12),(TID(J),J=1,12),(WID(J),J=1,12),(TOPID(J),J=1
     2,12)
      WRITE (ISHOUT,31)
      WRITE (ISHOUT,33)
      WRITE (ISHOUT,2A) (IC(J),J=1,18)
      WRITE (ISHOUT,34)
      WRITE (ISHOUT,2A) (IDIC(J),J=1,18)
      WRITE (ISHOUT,35)
      WRITE (ISHOUT,3A) IM,IV
C
C     DIFFUSION RECOMPUTATION FOR DIFFUSION MODEL
C
      DIFCON=3.3*DIFCON
C
      CALL PAM1 (HOR,SETHR,THSD,TW,ISIN,ISHOUT,IPOUT,NUMTAP,SIGMA)
      RETURN
C
 24   FORMAT (12A6)
 25   FORMAT (15A,18I4)
 27   FORMAT (29HO WRONG TAPE REEL ON DRIVE   I2)
 28   FORMAT (6E10.3)
 29   FORMAT (////29X,43H****  SUMMARY OF INPUT IDENTIFIERS AND INITIAL
     1CONDITIONS  ****////25X,43H****  OUTPUT PROCESSOR IDENTIFICATION  **
     2**//25X,12A6///25X,56H****  INITIAL CONDITIONS (FIREBALL) IDENTIFICA
     3TION  ****//25X,12A6///25X,37H****  CLOUD RISE IDENTIFICATION  ****//
     425X,12A6///25X,49H****  PARTICLE SET EXPANSION IDENTIFICATION  ****
     5//25X,12A6///25X,36H****  TRANSPORT IDENTIFICATION  ****/25X,12A6///
     625X,31H****  WIND IDENTIFICATION  ****//25X,12A6///25X,37H****  TOPO
     7GRAPHY IDENTIFICATION  ****/25X,12A6)
 30   FORMAT (///1X,24HTRANSPORT IDENTIFICATION///25X,12A6)
 31   FORMAT (///25X,24H****  OTHER INPUTS  ****)
 32   FORMAT (1H1)
 33   FORMAT (/1X,77H****  THE CONTROL VARIABLE ARRAY, IC(J), WAS GIVEN
     1THE FOLLOWING VALUES  ****)
 34   FORMAT (///1X,56HTHE FOLLOWING LOGICAL TAPES ARE AVAILABLE FOR SORT
     1ING.)
 35   FORMAT (///1X,63HPRINTER DESCRIPTION  -  CHARACTERS PER INCH)
 36   FORMAT (14X,10HHORIZONTAL IS,I3,10HVERTICAL  I3)
 37   FORMAT (1X,1HX,19X,1HY,19X,1HT,1X,2HPS,14X,4HMASS)
 38   FORMAT (1H1,50X,19H* * * * * * * * * *///12X,101HT H E  D E P A R T M
     1E N T  O F  D E F E N S E  F A L L O U T  P R E D I C T I O N
     2  S Y S T E M///31X,19H* * * * * * * * *////44X,23HOUTPUT PROCE
     3SSOR MODULE///55X,11HPREPARED BY/43X,34HTECHNICAL OPERATIONS RESEA
     4RCH,INC.//52X,17HHUNTSVILLE,ALABAMA.)
 39   FORMAT (////45X,29HLISTING OF GROUNDED PARTICLES)
 41   FORMAT (///1X,6HBLOCK I4)
 42   FORMAT (1X,6HNO. OF PARTICLES IN THIS BLOCK IS  I4)
 43   FORMAT (1X,6H NO RE), THIS JOB, JUST TAPE DUMP)
      END
```

Appendix D

FORTRAN LISTING OF SIZE DISTRIBUTION CHANGE PROGRAM

```
      PROGRAM DIAM(INPUT,OUTPUT,TAPE1,TAPE2)
      DIMENSION PSIZE(60),D(61),F(60),AA(12),BB(12),CC(12),DD(12),EE(12)
      DIMENSION X(2500),Y(2500),T(2500),PS(2500),FMAS(2500),IRBZ(2500)
      REWIND 1
      REWIND 2
      READ(1) TST
      WRITE(2)TST
      READ(1) X1,X2,X3,X4,X5,X6,X7,N1,Y1,Y2,Y3,Y4,Y5,Y6,Y7
      WRITE(2)X1,X2,X3,X4,X5,X6,X7,N1,Y1,Y2,Y3,Y4,Y5,Y6,Y7
      READ(1) (AA(J),J=1,12),(BB(J),J=1,12),(CC(J),J=1,12)
     *,(DD(J),J=1,12),(EE(J),J=1,12)
      WRITE(2)(AA(J),J=1,12),(BB(J),J=1,12),(CC(J),J=1,12)
     *,(DD(J),J=1,12),(EE(J),J=1,12)
      READ(1) NPS
      WRITE(2)NPS
      XNPS=NPS
      READ(1) (PSIZE(J),F(J),D(J),SV,J=1,NPS)
      D(NPS+1)=PSIZE(NPS)**2/D(NPS)
      PRINT 5
    5 FORMAT(*1*)
      DO 4 I=1,NPS
    4 PRINT 2,D(I),PSIZE(I),D(I+1)
    2 FORMAT(4F10.4)
      PRINT 5
      READ 2,U,SIG
      PRINT 2,U,SIG
      NPS1=NPS+1
      U=ALOG(U)
      SIG=ALOG(SIG)
      U=U+3.*SIG**2
      SUM=0.
      DO 6 I=1,NPS1
    6 D(I)=(ALOG(D(I))-U)/SIG
      PRINT 5
      DO 9 I=1,NPS1
    9 PRINT 104,I,D(I)
  104 FORMAT(I5,F15.8)
      PRINT 5
      Y1=P(D(1))
      DO 7 I=1,NPS
      Y2=P(D(I+1))
      F(I)=Y1-Y2
      PRINT 2,Y1,Y2
      SUM=SUM+F(I)
      Y1=Y2
    7 PRINT 103,I,F(I)
      PRINT 5
      DO 8 I=1,NPS
      F(I)=F(I)/SUM
    8 PRINT 103,I,F(I)
  103 FORMAT(I5,F10.8)
      DO 200 I=1,NPS1
  200 D(I)=EXP(SIG*D(I)+U)
      WRITE(2)(PSIZE(J),F(J),D(J),SV,J=1,NPS)
      DO 200 I=1,NPS
  200 F(I)=F(I)*XNPS
      READ(1) (AA(J),J=1,12)
```

```
PROGRAM DIAM      73/74   OPT=1                FTN 4.0+P357     06/04/74  21.00.20.     PAGE   2

      WRITE(2)(AA(J),J=1,12)
  204 READ(1) NIJ
      WRITE(2)NIJ
      POINT 5
      PRINT 205,NIJ
  205 FORMAT(I10)
      IF(NIJ)201,201,202
  202 READ(1) (X(I),Y(I),T(I),PS(I),FNAS(I),IRBZ(I),I=1,NIJ)
      DO 203 I=1,NIJ
      DO 204 J=1,NPS
      IF(PS(I)-LT.D(J).AND.PS(I).GT.D(J-1))FNAS(I)=FNAS(I)+F(J)
  204 CONTINUE
  203 CONTINUE
      DO 207 I=1,NIJ
  207 WRITE(2) X(I),Y(I),T(I),PS(I),FNAS(I),IRBZ(I)
      PRINT 2070,(X(I),Y(I),T(I),PS(I),FNAS(I),IRBZ(I),I=1,NIJ)
 2070 FORMAT(5E15.8,110)
      GO TO 206
  201 STOP
      END
```

```
FUNCTION P              73/74   OPT=1                    FTN 4.0+P357      04/04/74  21.00.26.      PAGE    1

      FUNCTION P(X)
      T(Z)=1./(1.+.2316419*Z)
      IF(X.GE.0.)GO TO 1
      Y=-X
      P=       1./SQRT(2.*3.1415926536)*EXP(-.5*Y**2)*(.319381530*T(Y)
     1-.356563782*T(Y)**2+1.781477937*T(Y)**3-1.821255978*T(Y)**4
     2+1.330274429*T(Y)**5)
      RETURN
    1 P    =1.-1./SQRT(2.*3.1415926536)*EXP(-.5*X**2)*(.319381530*T(X)
     1-.356563782*T(X)**2+1.781477937*T(X)**3-1.821255978*T(X)**4
     2+1.330274429*T(X)**5)
      RETURN
      END
```

Best Available Copy